AES 2023 Torremolinos - Spain

The 9th International Conference on Antennas and Electromagnetic Systems

June 5 Ð 8, 2023
Torremolinos - Spain

Proceedings

ISSN 2491-2417

aesconference.org

AES 2023 Torremolinos - Spain

The 9th International Conference on Antennas and Electromagnetic Systems

Edited by

Enrique M‡rquez Segura | University of Malaga, Spain
Said Zouhdi | Paris-Saclay University, France

TABLE OF CONTENT

ORGANIZATION I COMMITTEES

Conference Chairs

Enrique M‡rquez Segura
University of Malaga, Spain

Said Zouhdi
ParisÐSaclay University, France

International Advisory Committee

Yahia Antar, Canada
Christos Christopoulos, UK
Tie Jun Cui, China
Peter de Maagt, Netherlands
Apostolos Georgiadis, Spain
D. V. Giri, USA
Xun Gong, USA
Lixin Guo, China
Yang Hao, UK
Nathan Ida, USA
Koichi Ito, Japan
Ahmed Kishk, Canada
Kwai Man Luk, Hong Kong
Andrea Massa, Italy
Alain Sibille, France
Ari Sihvola, Finland
Paul Smith, Australia
J(Yiannis) C. Vardaxoglou, UK
Junhong Wang, China

Technical Program Committee

Christos Argyropoulos, USA
Silvio Ernesto Barbin, Brazil
Xavier Begaud, France
Yangjian Cai, China
Pai-Yen Chen, USA
Christophe Craeye, Belgium
Tian Sen Jason Horng, Taiwan
Zhirun Hu, UK
Ruey-Bing Hwang, Taiwan
Sungtek Kahng, Korea
Ali Khenchaf, France
Sebastien Lallechere, France
Allen M. Larar, USA
Howard Lee, USA
Jensen Li, Hong Kong
Jean-Marc Lopez, France
Ozlem Ozgun, Turkey
Oscar Quevedo-Teruel, Sweden
Eva Rajo-Iglesias, Spain
Blaise Ravelo, China
Junsuk Rho, Korea
Josaphat T. Sri Sumantyo, Japan
Van Yem Vu, Viet Nam
Amir I. Zaghloul, USA
Kuang Zhang, China
Qi-Jun Zhang, Canada
Linjie Zhou, China
Arkady Zhukov, Spain

Special Sessions Organizers

Jeremy Barton, Canada
Mario Ferraro, Italy
Angelo Freni, Italy
Yongxin Guo, Singapore
Enrique M‡rquez Segura, Spain
Paola Pirinoli, Italy
Vaibhav Thakore, Canada
Maxim Zhadobov, France
Arkady Zhukov, Spain

Sponsors

UniversitŽ Paris-Saclay is a research university based in Paris, France. UniversitŽ Paris-Saclay offers a comprehensive and varied range of Undergraduate, MasterÕs and PhD degrees, renowned internationally thanks to the UniversityÕs reputation for research excellence and the commitment of its academic staff. The UniversityÕs constituent faculties, institutes and component institutions all contribute to the curricula with cutting-edge specialised courses in Science and Engineering, Life Sciences and Health, and Social Sciences and Humanities.
UniversitŽ Paris-Saclayis ranked 1st in France and 16th in the world according to the Academic Ranking of World Universities (ARWU).

AEM - Advanced Electromagnetics is a free, peer-reviewed, Gold Open Access journal. It covers recent international research results in the general Þeld of Electromagnetic Waves, Antennas and Propagation. Authors of articles published in Advanced Electromagnetics retain the copyright of their articles and are free to reproduce and disseminate their work (under a Creative Commons Attribution License). AEM is widely indexed and has a Scopus CiteScore of 2.2 (2021).

PLENARY SPEAKERS

Shanhui Fan

Stanford University, USA

Electromagnetics for Energy Applications

Shanhui Fan is the Joseph and Hon Mai Goodman Professor in the School of Engineering, a Professor of Electrical Engineering, a Professor of Applied Physics (by courtesy), and a Senior Fellow of the Precourt Institute for Energy, at the Stanford University. He received his Ph. D in 1997 in theoretical condensed matter physics from the Massachusetts Institute of Technology (MIT). His research interests are in fundamental studies of solid state and photonic structures and devices, especially photonic crystals, plasmonics, and meta-materials, and applications of these structures in energy and information technology applications. He has published over 600 refereed journal articles, has given over 380 plenary/keynote/invited talks, and holds over 70 US patents. He has cofounded two companies aiming to commercialize high-speed engineering computations and radiative cooling technology respectively. Prof. Fan received a National Science Foundation Career Award (2002), a David and Lucile Packard Fellowship in Science and Engineering (2003), the U. S. National Academy of Sciences W. O. Baker Award for Initiatives in Research (2007), the Adolph Lomb Medal from the Optical Society of America (2007), a Vannevar Bush Faculty Fellowship from the U. S. Department of Defense (2017), a Simons Investigator in Physics (2021), and the R. W. Wood Prize from Optica (2022). He is a Web of Science Highly Cited Researcher since 2015, and a Fellow of the IEEE, the American Physical Society, the Optical Society of America, and the SPIE.

Electromagnetics for Energy Applications
Electromagnetic Þelds represent one of the most important carriers of energy. The ability to control electromagnetic Þelds therefore play an essential role in the generation, transport, and utilization of energy. In this talk, we review our efforts in advancing electromagnetic technology for energy applications. Examples include radiative cooling, nighttime power harvesting, and the use of non-reciprocity to reach the ultimate efÞciency limit of solar energy harvesting.

Yongxin Guo

National University of Singapore, Singapore

EfÞcient Wireless Power Transfer for IoTs and Biomedical Applications

Yongxin Guo is currently a Full Professor at the Department of Electrical and Computer Engineering, National University of Singapore (NUS). Concurrently, He is Director, Center for Peak of Excellence on Smart Medical Technology at NUS Suzhou Research Institute and Co-Director, Center for Smart Sensing and ArtiÞcial Intelligence, NUS Chongqing Research Institute. He has authored or co-authored over 500 international journal and conference papers and 4 book chapters. He holds over 50 granted/Þled patents in USA, China and Singapore. His current research interests include RF sensing, antennas and electromagnetics in medicine ; wireless power for biomedical applications and internet of things ; wideband and small antennas for wireless communications ; and RF and microwave circuits and MMIC modelling and design. He has graduated 19 PhD students at NUS.

Dr. Guo is a Fellow of IEEE and a Fellow of Academy of Engineering, Singapore. He is serving as Editor-in-Chief, IEEE Journal of Electromagnetics, RF and Microwave in Medicine and Biology for the term of 2020-2023. He served as the IEEE Fellow Evaluation Committee for IEEE Engineering in Medicine and Biology Society (2019-2020). Dr Guo was the Chair for IEEE AP-S Technical Committee on Antenna Measurement in 2018-2020. He served as Associate Editor for IEEE Antennas and Propagation Magazine (2018-2020), IEEE Journal of Electromagnetics, RF and Microwave in Medicine and Biology (2017 Ð 2020), Electronics Letters (2015-2019), IEEE Antennas and Wireless Propagation Letters (2013-2018), and IET Microwaves, Antennas & Propagation (2014-2017). He has served as General Chair/Co-Chair for a number of international conferences. He was the recipient of 2020 IEEE Microwave and Wireless Components Letters Tatsuo Itoh Prize of the IEEE Microwave Theory and Techniques Society. He was elected as a Distinguished Lecturer of IEEE Antennas and Propagation Society for the term of 2022-2024.

EfÞcient Wireless Power Transfer for IoTs and Biomedical Applications

Wireless power transfer (WPT) plays an increasingly important role in internet of things (IoTs) and biomedical applications. With the rapid development of 5G and IoTs, the dense deployment of sensor nodes become more popular. Various wireless power application scenarios will be introduced. Our recent research progress on near-Þeld inductive and capacitive WPT and far-Þeld WPT will be reported. Adaptive rectiÞer design and reconÞgurable diode topology will be explained. Waveform-optimized WPT together with reconÞgurable diode topology will be further illustrated.

Yahya Rahmat-Samii

University of California - Los Angeles, USA

Yahya Rahmat-Samii is a Distinguished Professor, a holder of the Northrop-Grumman Chair in electromagnetics, a member of the U.S. National Academy of Engineering (NAE), a Foreign Member of the Chinese Academy of Engineering (CAE) and the Royal Flemish Academy of Belgium for Science and the Arts, the winner of the 2011 IEEE Electromagnetics Field Award, and the Former Chairman of the Electrical Engineering Department, University of California at Los Angeles (UCLA), Los Angeles, CA, USA. He was a Senior Research Scientist with the Caltech/NASAÕs Jet Propulsion Laboratory. He has authored or coauthored more than 1100 technical journal and conference papers and has written over 36 book chapters and six books and is the holder many patents. He has more than 20 cover-page IEEE publication articles.

Prof. Rahmat-Samii is a fellow of IEEE, AMTA, ACES, EMA, and URSI. He was a recipient of the Henry Booker Award from URSI, in 1984, which is given triennially to the most outstanding young radio scientist in North America, the Best Application Paper Prize Award (Wheeler Award) of the IEEE Transactions on Antennas and Propagation in 1992 and 1995, the University of Illinois ECE Distinguished Alumni Award in 1999, the IEEE Third Millennium Medal and the AMTA Distinguished Achievement Award in 2000. In 2001, he received an Honorary Doctorate Causa from the University of Santiago de Compostela, Spain. He received the 2002 Technical Excellence Award from JPL, the 2005 URSI Booker Gold Medal presented at the URSI General Assembly, the 2007 IEEE Chen- To Tai Distinguished Educator Award, the 2009 Distinguished Achievement Award of the IEEE Antennas and Propagation Society, the 2010 UCLA School of Engineering Lockheed Martin Excellence in Teaching Award, and the 2011 campus-wide UCLA Distinguished Teaching Award. He was also a recipient of the Distinguished Engineering Educator Award from The Engineers Council in 2015, the John Kraus Antenna Award of the IEEE Antennas and Propagation Society and the NASA Group Achievement Award in 2016, the ACES Computational Electromagnetics Award and the IEEE Antennas and Propagation S. A. Schelkunoff Best Transactions Prize Paper Award in 2017. Rahmat-Samii was the recipient of the prestigious Ellis Island Medal of Honor in 2019. The medals are awarded annually to a group of distinguished U.S. citizens who exemplify a life dedicated to community service. These are individuals who preserve and celebrate the history, traditions, and values of their ancestry while exemplifying the values of the American way of life and are dedicated to creating a better world. Among the receipts of this honor are seven US presidents to name the few. He is listed in WhoÕs Who in America, WhoÕs Who in Frontiers of Science and Technology and WhoÕs Who in Engineering. He has been a plenary and millennium session speaker at numerous national and international symposia. He has been the organizer and presenter of many successful short courses worldwide. Many of his students have won major theses and conference paper awards.

He has had pioneering research contributions in diverse areas of electromagnetics, antennas, measurements and diagnostics techniques, numerical and asymptotic methods, satellite and personal communications, human/antenna interactions, RFID and implanted antennas in medical applications, frequency-selective surfaces, electromagnetic band-gap and meta-material structures, applications of the genetic algorithms and particle swarm optimizations. He was the 1995 President of the IEEE Antennas and Propagation Society and 2009Ð2011 President of the United States National Committee (USNC) of the International Union of Radio Science (URSI). He has also served as an IEEE Distinguished Lecturer presenting lectures internationally.

The Art, Science and Engineering of Modern Antenna Measurements and Diagnostics : From MarconiÕs First Measurements to TodayÕs Incredible Advances
Starting with MarconiÕs Þrst antenna pattern measurements, we then discuss modern planar near-Þeld antenna measurements as a novel paradigm linking electromagnetic theory, sampling techniques, back projection and FFT. Based on the fundamental electromagnetic principles, the underlying concepts governing simulations, designs and operations of planar-near Þeld measurements and diagnostics techniques will be highlighted. Modern measurement systems such as plane-polar, bi-polar and robotics

scanning systems will be presented. Representative measurement results of reßector, array, reßectarray and lens antennas will be presented for diverse applications including planetary missions, radars for remote sensing, and Cubesats. Finally, the topics of diagnostics and phaseless antenna measurement techniques and algorithms will be touched upon..

Eva Rajo-Iglesias

University Carlos III of Madrid, Spain

Eva Rajo-Iglesias was born in Monforte de Lemos, Spain, in 1972. She received the M.Sc. degree in telecommunication engineering from the University of Vigo, Spain, in 1996, and the Ph.D. degree in telecommunication engineering from the University Carlos III of Madrid, Spain, in 2002. She was a Teacher Assistant with the University Carlos III of Madrid from 1997 to 2001. She joined the Polytechnic University of Cartagena, Cartagena, Spain, as a Teacher Assistant, in 2001. She joined University Carlos III of Madrid as a Visiting Lecturer in 2002, where she has been an Associate Professor with the Department of Signal Theory and Communications since 2004. Since 2018 she is Full Professor in the same department. She visited the Chalmers University of Technology, Gšteborg, Sweden, as a Guest Researcher, in 2004, 2005, 2006, 2007, and 2008, and has been an AfÞliated Professor with the Antenna Group, Signals and Systems Department, since 2009 to 2016. She has co-authored more than 75 papers in JCR international journals and more than 120 papers in international conferences. Her current research interests include microstrip patch antennas and arrays, metamaterials, artiÞcial surfaces and periodic structures, gap waveguide technology and MIMO systems. Dr. Rajo-Iglesias was the recipient of the Loughborough Antennas and Propagation Conference Best Paper Award in 2007, the Best Poster Award in the Þeld of Metamaterial Applications in Antennas, at the conference Metamaterials 2009, the 2014 Excellence Award to Young Research Staff at the University Carlos III of Madrid and the Third Place Winner of the Bell Labs Prize 2014. She is currently an Associate Editor of the IEEE Antennas and Propagation Magazine and has served as Associate Editor of the IEEE Antennas ans Wireless Propoagation Letters (2011-2017).

Designing Antennas with Gap Waveguide Technology : Exploring New Trends

A brief introduction to the foundational principles of gap waveguide technology, followed by an overview of traditional designs of directive antennas using corporate fed arrays will be presented. Subsequently, novel applications of this technology in the millimeter frequency bands will be explored, which include the implementation of alternate periodic structures replacing the conventional bed of nails. Finally, the potential of combining this technology with established technologies like microstrip, as well as the design of other types of antennas as leaky wave antennas, will be discussed. In this way, an overview of different on going research lines connected to this technology will be presented.

Wen Tong

Huawei Wireless, Canada

cmWave-MIMO : towards the 1K-element-array paradigm

Wen Tong is the CTO, Huawei Wireless. He is the head of Huawei wireless research. In 2011, Dr. Tong was appointed the Head of Communications Technologies Labs of Huawei, currently, he is the Huawei 5G chief scientist and leads HuaweiÕs 10-year-long 5G wireless technologies research and development.

Prior to joining Huawei in 2009, Dr. Tong was the Nortel Fellow and head of the Network Technology Labs at Nortel. He joined the Wireless Technology Labs at Bell Northern Research in 1995 in Canada.

Dr. Tong is the industry recognized leader in invention and standardization of advanced wireless technologies, he is the key contributor to 3GPP since its inception. Dr. Tong was elected as a Huawei Fellow and an IEEE Fellow. He was the recipient of IEEE Communications Society Industry Innovation Award for Òthe leadership and contributions in development of 3G and 4G wireless systemsÓ in 2014, and IEEE Communications Society Distinguished Industry Leader Award for Òpioneering technical contributions and leadership in the mobile communications industry and innovation in 5G mobile communications technologyÓ in 2018. He is also the recipient of R.A. Fessenden Medal. For the past three decades, he had pioneered fundamental technologies from 1G to 5G wireless and Wi-Fi with more than 450 granted US patents.

Dr. Tong is a Fellow of Canadian Academy of Engineering, Fellow of Royal Society of Canada, and he serves as Board of Director of Wi-Fi Alliance, he is the committee member for ÒIEEE Fellow CommitteeÓ.

cmWave-MIMO : towards the 1K-element-array paradigm

In this talk, we present the development of massive MIMO antenna technologies for the emerging 6G and associated challenges. The overall system performance and antenna design-choice in terms of spectrum and channel propagation properties are discussed. We explore the centimeter wave spectrum for the 6G massive MIMO. The candidate frequency range is from 7GHz to 15GHz, we discuss the new propagation properties and ultra-large antenna element array architecture, namely, the 1K-element-array paradigm for both base-station and user-equipment.

KEYNOTE SPEAKERS

Andrea Fratalocchi

KAUST, Saudi Arabia

Universal light encoders : artiÞcial intelligent optical hardware for real-time hyperspectral imaging and ultrasensitive detection

Andrea Fratalocchi is a Full Professor (from Jan 2023) in the Computer, Electrical, and Mathematical Sciences and Engineering Division at KAUST University. He joined KAUST in January 2011 as Assistant Professor and was promoted to Associate Professor in July 2016. Before joining KAUST, Andrea Fratalocchi was a Research Fellow at the Sapienza University of Rome under a KAUST Fellowship Award. From 2007 to 2009, Andrea Fratalocchi worked as a post-doctoral researcher at Sapienza University under a "New Talent" Award from the research center "Enrico Fermi." In 2012 he was appointed as Editor of Nature ScientiÞc Report. In 2017, he won the Middle East GCC Enterprise Award as the best electrical engineer of the year. In 2019, he became a Fellow of the Institute of Physics (IOP), a Senior Member of the IEEE, and a Fellow of the Optical Society of America (OSA) : "For pioneering innovations in the use of complex optical systems and the development of creative technologies in clean energy harvesting, bio-imaging, and advanced optical materials". According to the standardized citations index collected by Plos (https ://doi.org/10.1371/journal.pbio.3000918).

Andrea Fratalocchi is in the top 2% of Optics worldwide. Andrea Fratalocchi authored more than 200 publications, including three books and six patents. Andrea Fratalocchi is the co-founder of Pixeltra (www.pixeltra.com), a startup company implementing a revolutionary artiÞcial intelligent hardware and software hyperspectral technology for security, food safety, and biomedical applications.

Universal light encoders : artiÞcial intelligent optical hardware for real-time hyperspectral imaging and ultrasensitive detection

I will summarize present and future research in the Þeld of universal light encoders (ULEs), which represent artiÞcial intelligent optical hardware implementing arbitrary user-deÞned functionalities in ultrathin metasurfaces. ULEs process information at the speed of light and can be integrated into any conventional monochrome camera for machine vision, transforming the system into an optical neural network processor. I will discuss applications of ULEs in the implementation of HyplexTM, a high-resolution hyperspectral imaging camera and a universal platform for ultrasensitive detection.

Mona Jarrahi

University of California Los Angeles, USA

Hyperspectral Terahertz Imaging Using Plasmonic Detectors

Mona Jarrahi is a Professor of Electrical and Computer Engineering at the University of California Los Angeles. She has made signiÞcant contributions to the development of ultrafast electronic and optoelectronic devices and integrated systems for terahertz, infrared, and millimeter-wave sensing, imaging, computing, and communication systems by utilizing novel materials, nanostructures, and innovative plasmonic concepts. Her scientiÞc achievements have been recognized by several prestigious awards including the Presidential Early Career Award for Scientists and Engineers; Friedrich Wilhelm Bessel Research Award from Alexander von Humboldt Foundation; Moore Inventor Fellowship from the Gordon and Betty Moore Foundation; Kavli Fellowship by the USA National Academy of Sciences, Grainger Foundation Frontiers of Engineering Award from the USA National Academy of Engineering; Breakthrough Award from Popular Mechanics Magazine; Research Award from Okawa Foundation; Early Career Award in Nanotechnology from the IEEE Nanotechnology Council; Outstanding Young Engineer Award from the IEEE Microwave Theory and Techniques Society; Booker Fellowship from the USA National Committee of the International Union of Radio Science; Lot Shafai Mid-Career Distinguished Achievement Award from the IEEE Antennas and Propagation Society; Early Career Award from the USA National Science Foundation; Young Investigator Awards from the USA OfÞce of Naval Research, the Army Research OfÞce, and the Defense Advanced Research Projects Agency. Prof. Jarrahi is a Fellow of IEEE, OSA and SPIE societies and has served as a distinguished lecturer of IEEE, traveling lecturer of OSA, and visiting lecturer of SPIE societies.

Hyperspectral Terahertz Imaging Using Plasmonic Detectors
This talk gives an overview of advancements in hyperspectral terahertz imaging systems, which utilize plasmonic photoconductive terahertz detectors to provide signiÞcantly higher signal-to-noise ratio levels.

Maria Kafesaki

University of Crete, Greece

Cylinder- and multi-coated-cylinder-systems as multifunctional metamaterials : An Effective Medium description

Maria Kafesaki is Associate Professor in the Dept. of Materials Science and Technology of the University of Crete and Adjunct Researcher at the Institute of Electronic Structure and Laser (IESL) of Foundation for Research and Technology Hellas (FORTH). She obtained her Ph.D. in 1997, at the Physics Department of the University of Crete, Greece, on elastic wave propagation in complex media. She has worked as a post-doctoral researcher in the Consejo Superior de Investigaciones CientiÞcas in Madrid, Spain, and in IESL of FORTH (1997-2001). Her current research is on the area of electromagnetic wave propagation in periodic and random media, with emphasis on photonic crystals and metamaterials, where she has large theoretical and computational experience. She has more than 110 publications in refereed journals (with more than 6500 citations and h-index=42, according to Web of Science), and more than 70 invited talks at international conferences and schools. She has participated in many European projects as well as in the organization of many international conferences and schools. She is a Fellow of the Optical Society of America. Figure : A simple PT-symmetric chiral bi-layer. Under oblique incidence of circularly polarized (CP) waves the bi-layer eigenvalues ! indicate the existence of a mixed phase and two exceptional points, highly tunable by the incidence angle.

Cylinder- and multi-coated-cylinder-systems as multifunctional metamaterials : An Effective Medium description

We discuss an effective medium approach for analyzing metamaterials composed of cylindrical scatterers/meta-atoms, either simple or coated/multi-coated. We demonstrate the potential of this approach in THz systems made of polaritonic cylinders as well as in graphene-based nanotubes. In both cases we demonstrate a reach palate of optical responses, including negative index and hyperbolic metamaterial response.

Enrica Martini

University of Siena, Italy

Recent advances in metasurface antennas design and modelling

Enrica Martini received the Laurea degree (cum laude) in telecommunication engineering from the University of Florence, Italy, in 1998. From 1998 to 1999 she worked at the University of Florence under a one-year research grant from the Alenia Aerospazio Company, Rome, Italy. In 2002, she received the PhD degree in informatics and telecommunications from the University of Florence and the Ph.D. degree in electronics from the University of Nice-Sophia Antipolis, under joint supervision. In 2002, she was appointed Research Associate at the University of Siena, Italy. In 2005, she received the Hans Christian ¯rsted Postdoctoral Fellowship from the Technical University of Denmark, Lyngby, Denmark, and she joined the Electromagnetic Systems Section of the ¯rsted DTU Department until 2007. From 2007 to 2017 she was a Postdoctoral Fellow at the University of Siena, Italy. In 2012, she co-founded the start-up Wave Up Srl, Siena, Italy, of which she was the CEO from 2016 to 2018. From 2019 to 2021 she was an assistant professor at the University of Siena, Italy. She is currently an Associate Professor with the Department of Information Engineering and Mathematics, University of Siena, Siena, Ital Dr. Martini coordinated tasks of various research projects funded by national and international governmental institutions, as well as by industry. Her research interests include metasurfaces and metamaterial characterization, metasurface-based antennas and microwave devices, electromagnetic scattering, antenna measurements and tropospheric propagation. Dr. Martini was a co-recipient of the 2016 Schelkunoff Transactions Prize Paper Award, of the Best Paper Award in Antenna Design and Applications at the 11th European Conference on Antennas and Propagation in 2017, of the Best Poster Award at the Metamaterials Congress in 2019 and of the Best Paper Award in Electromagnetics at the 15th European Conference on Antennas and Propagation in 2021.

Recent advances in metasurface antennas design and modelling

This contribution provides an overview of the recent advances in the Þeld of modulated metasurface antennas. After reviewing the most advanced analytical and numerical models, different designs and realizations will be presented, including antennas with shaped pattern, dual polarized, multibeam and beam scanning antennas.

Taiichi Otsuji

Tohoku University, Japan

Graphene-based van der Waals 2D heterostructure materials and devices for terahertz wireless communications

Taiichi Otsuji is a Full Professor at the Research Institute of Electrical Communication (RIEC), Tohoku University, Sendai, Japan. He received the Dr. Eng. degree in electronic engineering from Tokyo Institute of Technology, Tokyo, Japan in 1994. From 1984 to 1999 he worked for NTT Laboratories, Kanagawa, Japan. In 1999 he joined Kyushu Institute of Technology as an associate professor, being a professor in 2002. He joined RIEC, Tohoku University, in 2005. His current research interests include terahertz electronic, photonic and plasmonic materials/devices and their applications. He has authored and co-authored 300 peer-reviewed international journal papers and more than 600 international conference proceedings including 210 invited presentations, and holds 13 Japanese and 8 US patents. He is the recipient of the Outstanding Paper Award of the 1997 IEEE GaAs IC Symposium in 1998, the Prizes for Science and Technology in Research Category, the Commendation for Science and Technology by the MEXT, Japan, in 2019, and the 59th Achievement Award of the IEICE (Institute of Electronics, Information, and Communication Engineers), Japan, in 2022. He has served as an IEEE Electron Device Society Distinguished Lecturer since 2013. He is a Fellow of IEEE, OPTICA (former OSA, Optical Society of America), and JSAP (Japan Society of Applied Physics).

Graphene-based van der Waals 2D heterostructure materials and devices for terahertz wireless communications

This paper reviews recent advances in the research and development of graphene-based van der Waals 2D heterostructure materials and devices for terahertz wireless communications.

Willie J. Padilla

Duke University, USA

Physics Informed Deep Learning In Metamaterials

Willie J. Padilla is a professor at Duke University with a masterÕs degree and doctorate in physics. He received a Young Investigator Award from the OfÞce of Naval Research and a Presidential Early Career Award for Scientists and Engineers. Padilla is a fellow of the American Physical Society, Optical Society of America and Kavli Frontiers of Science. He is also a Web of Science Highly Cited Researcher in physics for 2018 and 2019. He heads a group working in the area of metamaterials with a focus on machine learning, computational imaging, spectroscopy and energy, and has published more than 200 peer-reviewed journal articles.

Physics Informed Deep Learning In Metamaterials

Deep learning has had profound impacts in electromagnetic metamaterials, however there are several,drawbacks including. Through incorporation of prior knowledge, physics informed deep neural networks (PINNs),have the capability to solve many of the outstanding problems in deep learning and may additionally learn new,physics of systems under study. We discuss three different studies using physics informed deep learning and,describe the future of the Þeld is also given.

Atif Shamim

KAUST, Saudi Arabia

On-Chip Antennas - The Last Barrier to True RF System-on-Chip

Atif Shamim received his MS and PhD degrees in electrical engineering from Carleton University, Canada in 2004 and 2009 respectively. He was an NSERC Alexander Graham Bell Graduate scholar at Carleton University from 2007 till 2009 and an NSERC postdoctoral Fellow in 2009-2010 at Royal Military College Canada and KAUST. In August 2010, he joined the Electrical and Computer Engineering Program at KAUST, where he is currently an Associate Professor and principal investigator of IMPACT Lab. He was an invited researcher at the VTT Micro-Modules Research Center (Oulu, Finland) in 2006. His research work has won best paper awards in IEEE ICMAC 2021, IEEE IMS 2016, IEEE MECAP 2016, IEEE EuWiT 2008, Þrst prize in IEEE IMS 2019 3MT competition and IEEE AP-S Design Competition 2022, Þnalist/honorable mention prizes in IEEE AP-S Design Competition 2020, IEEE IMS 2017 (3MT competition), IEEE IMS 2014, IEEE APS 2005. He has been selected as the Distinguished Lecturer for IEEE AP-S (2022-2024). He has won the Kings Prize for the best innovation of the year (2018) for his work on sensors for the oil industry. He was given the Ottawa Centre of Research Innovation (OCRI) Researcher of the Year Award in 2008 in Canada. His work on Wireless Dosimeter won the ITAC SMC Award at Canadian Microelectronics Corporation TEXPO in 2007. Prof. Shamim also won numerous business-related awards, including 1st prize in CanadaÕs national business plan competition and was awarded OCRI Entrepreneur of the year award in 2010. He is an author/co-author of around 300 international publications, an inventor on more than 40 patents and has given close to 100 invited talks at various international forums. His research interests are in innovative antenna designs and their integration strategies with circuits and sensors for ßexible and wearable wireless sensing systems through a combination of CMOS and additive manufacturing technologies. He is a Senior Member of IEEE, founded the Þrst IEEE AP/MTT chapter in Saudi Arabia (2013) and served on the editorial board of IEEE Transactions on Antennas and Propagation (2013-2019), and as a Guest Editor for IEEE AWPL Special issue (2019), and is currently serving as an Associate Editor for IEEE Journal of Electromagnetics, RF and Microwaves in Medicine and Biology. He serves on numerous IEEE committees such IEEE Technical committees on Antenna Measurements (AP-S), Microwave Controls (MTT-S 13), and Additive Manufacturing (CRFID). Find out more details at (https ://cemse.kaust.edu.sa/impact).

On-Chip Antennas - The Last Barrier to True RF System-on-Chip

In the last decade, the increased level of integration provided by silicon technologies and emerging applications at millimeter wave frequencies has helped to achieve true System-on-Chip solutions bringing the antennas on the chip. This is because antenna sizes at these frequencies become small enough for practical on-chip realization. However, there are a number of challenges to overcome, for instance dealing with silicon substrate high conductivity and permittivity, metal stack-up and layout restrictions, and on-chip characterization through delicate probes, etc.

Fredrik Tufvesson

Lund University, Sweden

Channel modelling and characterization for communication and sensing in a 6G era

Fredrik Tufvesson received his Ph.D. in 2000 from Lund University in Sweden. After two years at a startup company, he joined the department of Electrical and Information Technology at Lund University, where he is now professor of radio systems. His main research interests is the interplay between the radio channel and the rest of the communication system with various applications in wireless systems such as massive MIMO, mm wave communication, vehicular communication and radio based positioning. Fredrik has authored around 90 journal papers and 140 conference papers, he is fellow of the IEEE and recently he got the Neal Shepherd Memorial Award for the best propagation paper in IEEE Transactions on Vehicular Technology and the IEEE Communications Society best tutorial paper award.

Channel modelling and characterization for communication and sensing in a 6G era

6G is expected to be based on distributed and co-located ultra-massive MIMO at frequencies ranging from one or a few GHz to hundreds of GHz. It will support both communication and sensing applications and should at the same time offer extreme reliability, enormous data rates, and ultra-low latencies. In this talk, we discuss channel characteristics, channel models, and the implications on 6G. Based on measurement examples, we point out possible directions and limitations and what we really can expect from the various frequency bands.

Ventsislav K. Valev

University of Bath, UK

Chiroptical harmonic scattering : predicted in 1979 and demonstrated four decades later

Ventsislav K. Valev is a Full Professor and a Research Fellow of the Royal Society, in the Physics Department of the University of Bath, where he serves as the Head of Department. He is also an Associate Fellow of Homerton College, in the University of Cambridge.

Valev was born in Bulgaria. He studied physics at the University of Western Brittany (France), with a Þnal year at the University of Cardiff (Wales), as an Erasmus student. He received his PhD in 2006, from the Radboud University Nijmegen (the Netherlands). Subsequently, he was a post-doc and a Research Fellow at the KU Leuven University (Belgium). In 2012, he became a Research Fellow in the Cavendish Laboratory at the University of Cambridge and, in 2013, he joined Homerton College, as a Research Associate. Since 2014, he has been working at the University of Bath, where he arrived as a Reader and a Research Fellow of the Royal Society. In 2019, he was promoted to professor and in 2021 he became the Director of Research for the Department of Physics. He was appointed Head of Department in 2022.

ValevÕs research group focuses on the interaction between powerful laser light and nanostructured materials. He builds laser experiments to study novel materials, such as plasmonic nanostructures, metamaterials, 2D materials and quantum optical materials. He explores the physics of photons, electrons and magnetism conÞned to tiny volumes of space Ð nanoparticles or 2D sheets. He aims to discover new properties and to test theoretical predictions, seeking out new and useful intersections between classical electromagnetism and quantum mechanics. His investigations are both fundamental and applied, with potential beneÞts for the pharmaceutical, food, perfume, and agrochemical industries.

Chiroptical harmonic scattering : predicted in 1979 and demonstrated four decades later
Chiroptical harmonic scattering (CHS) was predicted in 1979, but an experimental observation of this effect remained elusive for 40 years. A Þrst form of CHS was reported in 2019 ; it was demonstrated that light scattered at the second-harmonic from Ag nanohelices dispersed in water could reveal the chirality of the nanohelices. Observations in other systems (metal and semiconductor) and at the third-harmonic quickly followed. Now, we show the effect in high refractive index dielectrics.

TUTORIALS

Prof. Willie J. Padilla

Duke University, USA

Tuesday 6th June
15:00 - 16:00 Ñ Playamar

Introduction to Deep Learning Techniques for ArtiÞcial Electromagnetic Materials

Willie J. Padilla is a professor at Duke University with a masterÕs degree and doctorate in physics. He received a Young Investigator Award from the OfÞce of Naval Research and a Presidential Early Career Award for Scientists and Engineers. Padilla is a fellow of the American Physical Society, Optical Society of America and Kavli Frontiers of Science. He is also a Web of Science Highly Cited Researcher in physics for 2018 and 2019. He heads a group working in the area of metamaterials with a focus on machine learning, computational imaging, spectroscopy and energy, and has published more than 200 peer-reviewed journal articles.

Introduction to Deep Learning Techniques for ArtiÞcial Electromagnetic Materials
Deep neural networks (DNNs) have enhanced and transformed traditional research methods and are driving scientiÞc advance. Deep learning has shown immense potential in the Þeld of artiÞcial electromagnetic materials (AEM) research, with applications spanning electromagnetic metamaterials, metasurfaces, photonic crystals, and plasmonics. In this brief tutorial we review the status of the Þeld with a focus on recent advances, key limitations, and future directions. Strategies, guidance, evaluation, and limits of using deep networks for both forward and inverse AEM problems are presented.

GUIDELINES FOR PRESENTERS I IN-PERSON

In-person Oral Presentations

Each session room is equipped with a stationary computer connected to a LCD projector. Presenters must load their presentation Þles in advance onto the session computer. Technician personnel will be available to assist you.

Scheduled time slots for oral presentations are 15 mn for regular, 20 mn for invited presentations, 30 mn for keynote talks and 35 mn for plenary talks, including questions and discussions. Presenters are required to report to their session room and to their session Chair at least 15 minutes prior to the start of their session.

The session chair must be present in the session room at least 15 minutes before the start of the session and must strictly observe the starting time and time limit of each paper.

In-person Poster Presentations

Presenters are requested to stand by their posters during their session. One poster board, A0 size (118.9 x 84.1 cm), in portrait orientation, will be available for each poster. Pins or thumbtacks are provided to mount your posters on the board. All presenters are required to mount their papers 30mn before the session and remove them at the end of their sessions. Posters must prepared using the standard AES poster template (available on the conference website).

GUIDELINES FOR PRESENTERS I ONLINE

All Oral presentations will be in person with option for remote viewing via Zoom.

Poster sessions will be hybrid, consisting of both in person and virtual presentations. Instructions for virtual poster presenters can be found here : guidelines).

USEFUL INFORMATION

Venue

AES 2023 will be held at :
Palacio de Congresos y Exposiciones de la Costa del Sol
3 Calle Mexico, 29620 Torremolinos (Spain)

https://palacio-congresos.es

Opened in October 1970, the Palacio de Congresos y Exposiciones de Torremolinos (Congress and Exhibition Centre) was the result of a project designed in 1967 by the architects Rafael de la Hoz and Gerardo Olivares James. The building, which became the state heritage property in 1971.

The complex is built on an estate of 70,000 square meters, of which 18,000 square meters are gardens. Situated in a privileged location in the municipality of Torremolinos and located in the upper area of the town on a hill overlooking the sea, the Congress Center is an icon of MalagaÕs coastal landscape.

The building is arranged in a circular format around which the various auditoriums, meeting rooms, administrative ofÞces and annexed buildings are distributed. The central hall is presided over by its most iconic visual symbol, an emblem of convention and business tourism in Spain : a large translucent dome with an unprecedented crystal lamp hanging from the center of the exposed radial roof, falling like drops in a waterfall spilling over the center of the composition.

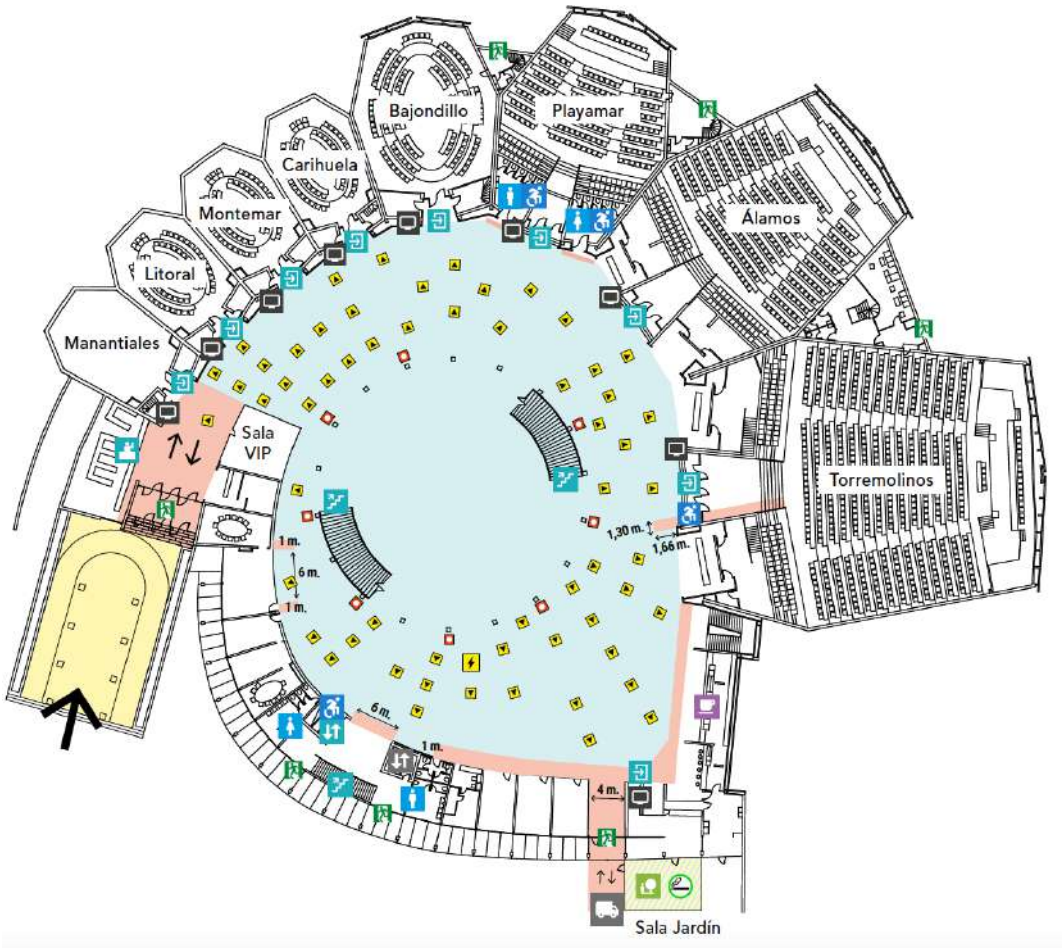

Getting to Venue

Getting to Torremolinos from Malaga Airport

Torremolinos is around 8km away from Malaga international airport. You can go from the airport to the city center by taxi, by train or by bus.

Taxi

The airport has a well-signposted taxi rank outside the arrivals area of Terminal T3. Make sure that the taxi driver has started the taximeter at the beginning of the journey (minimum fare). We recommend requesting a receipt for any complaint or claim.

Train

The new suburban train station in the new Terminal T3 building links the airport with Torremolinos city centre and other cities like Benalmadena and Fuengirola in one direction, and it links Malaga city center in the other direction.

The train station is situated underground and accessed via escalators. It is well signposted and can be reached via the square outside arrivals or outside departures. Before the station entry barriers you will see several self-service tickets machines on your right where you can buy your tickets.

The Þrst train to Torremolinos leaves the airport at 05 :32, leaving every 20-30 minutes until the last train at 23.42. Line : C1. Estimated travel time : 10 minutes.

Bus

You will Þnd the bus stop straight in front of you outside the arrivals area of Terminal T3 on the side of the road where there are a couple of shelters with seats. You will also see a ticket ofÞce in the left hand corner of the arrivals forecourt where you should purchase your tickets for the journey. Line : Torremolinos-Benalmadena-Airport. Estimated travel time : 30 minutes.

Getting to Torremolinos from Malaga train station

There are two train stations in the centre of Malaga : Maria Zambrano and Centro Alameda. Maria Zambrano station provides high-speed (AVE) and long-distance links to many Spanish cities like Barcelona, Cordoba, Madrid, Santiago de Compostela, Seville, etc, as well as local and regional routes.

You can take Line C1 from any of the two stations to reach Torremolinos. The estimated travel time is 20 minutes. You can check the timetables on the website of the national rail company RENFE

Getting to Torremolinos from Malaga bus station

Malaga bus station is located at the street "Paseo de los Tilos" very near Maria Zambrano train station. So it will be very easy to take a bus or a train from this station. You can take bus line Malaga-Torremolinos. Estimated travel time : 20 minutes.

TABLE OF CONTENTS

Plenary presentation

Keynote presentation

Tutorial

Spatiotemporal effects in multimode optical fiber

Additive manufacturing for electromagnetic devices

Antennas, EM and Smart Sensing Technologies for Biomedical and Healthcare Applications

Advances in Sensor Technologies Involving Electrodynamics and Magnetism

Smart Electromagnetic Skins and their Applications

Nanoscale Electrodynamics

Antenna theory and design

Array antennas, active, adaptive and reconfigurable antennas

Analytical, Computational and numerical techniques

Imaging, inverse scattering and remote sensing

Metamaterials, metasurfaces, FSS and EBG

Nanophotonics, plasmonics and quantum optics

Optics and Photonics

Optoelectronics, Photonic Materials and Devices

Scattering and diffraction

Propagation theory

Material Characterization and non-destructive testing

Plenary presentation

Keynote presentation

!"# $%&%()*++",*-./*# $1!./ ($456/" $%&$$$$$$$$$$$

!"#$%&'()*)#+,-*%"./0%&'1*(&-#2#.#()*#"-%))#+%"-*/3-#.()*,(&04(&%5#6%&%()
,73%&'3%.-&()*#6(+#"+*("0*8)-&('%'"#-#$%*0%-%.-#/"

$

!" ! #$%&%'())*+#,

!"#$%&#'()*+,-./012+34+506.178.-0+-9:+;3<=/167+59>8966789>*+?89>+%@:/00-A+B98C67D812+34+E.869.6+-9:+)6.A93
F?%BE)G*+)A/H-0+IJKMLKOO*+E-/:8+%7+@8-
+%9:76-47-1-03..A8QR-/D1P6:#PD-

$

!"#$%&'$)!"#$%%"&'(()*$+,"-*,&,./").0"1'/*,"*,&,)*23"$."/3,"1$,%0"41"'.$5,*&)%"%$63/",.240,*&"789:&;<"#3$23"
,-,&,./")*/$1$2$)%"$./,%%$6,./"4-/$2)%"3)*0#)*,"$(-%,(,./$.6")*=$/*)?0,1&,,*0"1'.2/$4.)%$/$,&"$."'%$3"
(,/)&' *1)2,&@" 89:&" -*42,&&" $.14*()/$4.")/" /3," &-,,0" 41" %$63/").0" 2)." =," $./,6*)/,0" $./4").>" 24.5,./$4.)%"
(4.423*4(,"2)(,*)"14*"()23$.,"5$&$4.<"/*).&14*($.6"/3,"&>&/,("$./4").".4-/$2)%"..,'*)%"../#4*A"-*42,&&4*@"!"#$%%"
0$&2'&&")--%$2)/$4.&" 41" 89:&" $." /3," $(-%,(,./$4." 41" B>-%,C<")" 3$63,&4%'/$4." 3>-,*&-,2/*)%" $()6$.6"
2)(,*)").0")"'.$5,*&)%"-%)/14*("14*"'%/*)&,.&$/$5,"0,/,2/$4.@
"

8.$5,*&)%"%$63/",.240,*&"789:;-*,&,./")"2%)&&"41"),2)%"$./,%%$6,./"3)*0#)*,"/*)$.,0"/4"$(-%,(,./").>"
'&,*?0,1$.,0" $.-'/ ?4'/-'/" 1'.2/$4.@" D3,&," 24(-4.,./&" 24(-*$&," .).4&/*'2/'*,0" (,/)&'*1)2,&" #$/3" &'$/)=%>"
,.6$.,,*,0".).4*,&4.)/4*&"#$/3"24./*4%%)=%,"1,)/'*,&"41"(E&2)%,@"D3,"-3>&$2)%41".).4&/*'2/'*,&")2/&")&"
).",G'$5)%,./"3$00,."%)>,*'"41")*/$1$2$)%"..,'*)%"../#4*A&H"'.$5,*&)%")--*4C$()/4*&<"#3$23"-*42,&&"$.14*()/$4.")
/3," &-,,0" 41" %$63/" #$/34'/" *,G'$*$.6" ,%,2/*@"$2&,&," &>&/,(&" $(-%,(,./" =)&$2" 4-/$2)%" 2$*2'$/*>").0" (4*,"
)05).2,0"&>&/,(&"/3)/"-,*14*("()23$.,"%,)*.$.6"1'.2/$4.)%$/$,&"0$*,2/%>"$."3)*0#)*,@
"

!."/3$&"'>.4/, "/)%A<"!"#$%%"0$&2'&&"-*,&,./").0"1'/*,"*,&,)*23"$."/3$&"1$,%0"41"&2$,.2,@"!"#$%%"=,6$."=>"0$
4-/$2)%"89&J'(4/$5)/$4.").0"1'.0)(,./)%"0,&$6.").0"/3,$*"/*)$.$.6"#$/3"=4/3"&41/#)*,").0"()23$.,"%,)*.$.6"
3)*0#)*,")--*4)23,&@"!"#$%%"=3$,1%>"&'(()*$+,"/3,"*,2,./")--%$2)/$4.&"41"/3$&"/,23.4%46>"$."3>-,*&-,2/*)%"
$()6$.6"7B!;").0"=$4&,.&$.6'@
" " " "

!."B!<"!"#$%%"0$&2'&&"/3,"$(-%,(,./)/$4."41")"2)(,*)"14*")2G'$*$.6").0"-*42,&&$6,"3%,*&-,2/*)%"5$0,4&"
$."3$63"*,&4%'/$4.")/"K)T,"1*-,*"&,24.0" 14*()23$.,"5$&$4."&,6(,./)/$4.").0"4=L,2/?*)2A$.6$."6*4'.0").0"
)$*=4.,")--%$2)/$4.&@"!."/3,"1$,%0"?41,"&$4<"!"#$%%"0$&2'&&"/3,"1'.0)(,./)%&").0")--%$2)/$4.&"41"89:
$(-%,(,./$.6")."$./,6*)/,0"-%)/14*("/,23.4%46>"/3)/"4-,.&"/4"'%/*)&,.&$/$5,"0,/,2/$4."=,%4#"MNTNFPM"Q4%@
" "
"

*+ ,+%+-'+)#

78 R,/().<"S <"Q)A)*,.A4<"Q<"T'*6',/, ?94-,+<"U<"S*)/)%42238$U<"T'*4)0=).0"5,2/4*$)%"'%/*)/3$6./$2&"#$/3"
,C-,*$(,./)%" ,11$2$,.2>" '-" /4" WW$X" /3," 5$&$=%," *,6$4." 5$)" '.$5+,*&)%C$()/4*&Y<" 9$63/Z" [2$,.2," \"
U--%$2)/$4.&<"54%@"NF<".4@"N<"+@"]^<"EFEN@

%8 Q)A)*,.A4<" Q@ _).6<" ` @?T'*6',/, ?94-,+<" U@R,/().<" S @S*)/)%42238$U<@"Va4='&/").0" [2)%)=%,"
S%)b-/$2&"4."S%,C$=%,"[')/&"5$)":54%'/$4.)*>"c,'*)%c,/#4*A&Y<"U05).2,0"!./,%%$6,./"[>&/,(&<@"
ENFFNFP<"E@EN

'8! Q)A)*,.A4<"Q@T'*6',/, ?94-,+<'U@<).6< "`@'<R,/().< "S<R$).24%)[@'<T,*.)*0 <" R<'S*)/)%42238$U@<"
Va,)%?$(," B>-,*&-,2/*)%" !()6$.6" $." B)*0#)*," 5$)" D*)$.,0" Q,/)&'*1)2,+: .240,*&Y<"d4.1,*,.2," 4."
d4(-'/,*"e$&$4.").0"f)//,*. "a,246.$/$4."defa ;<"g'%E@EE=@

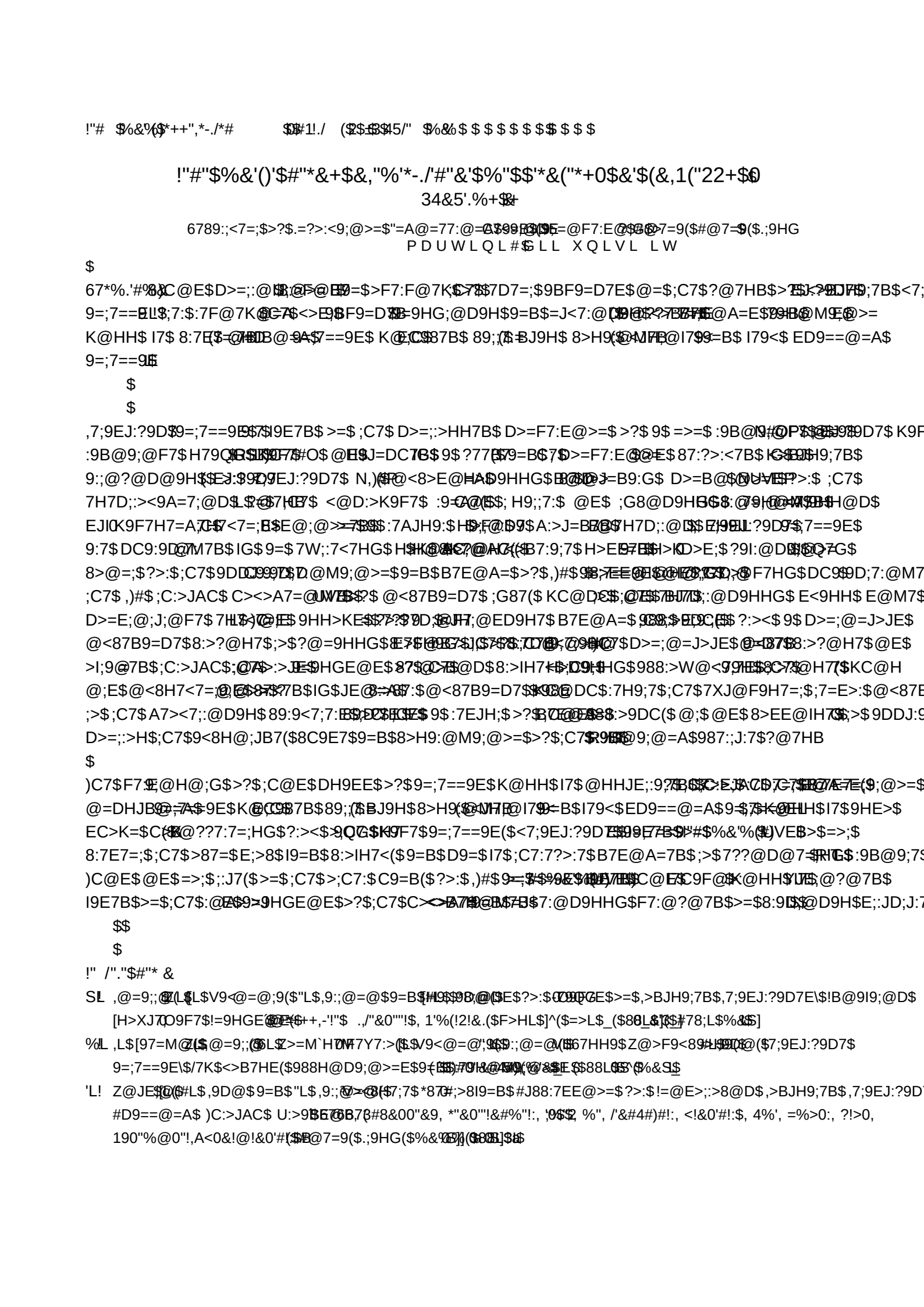

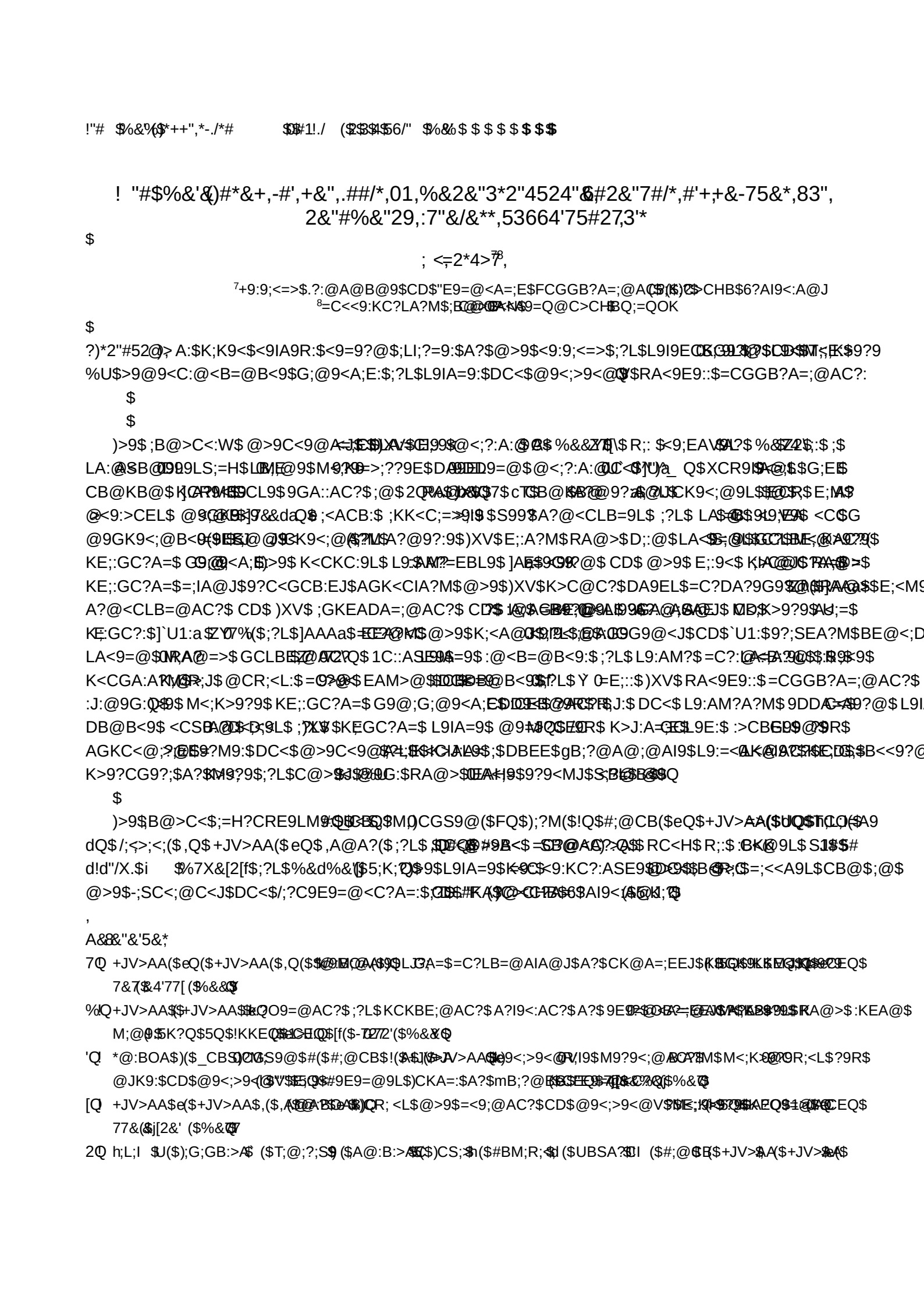

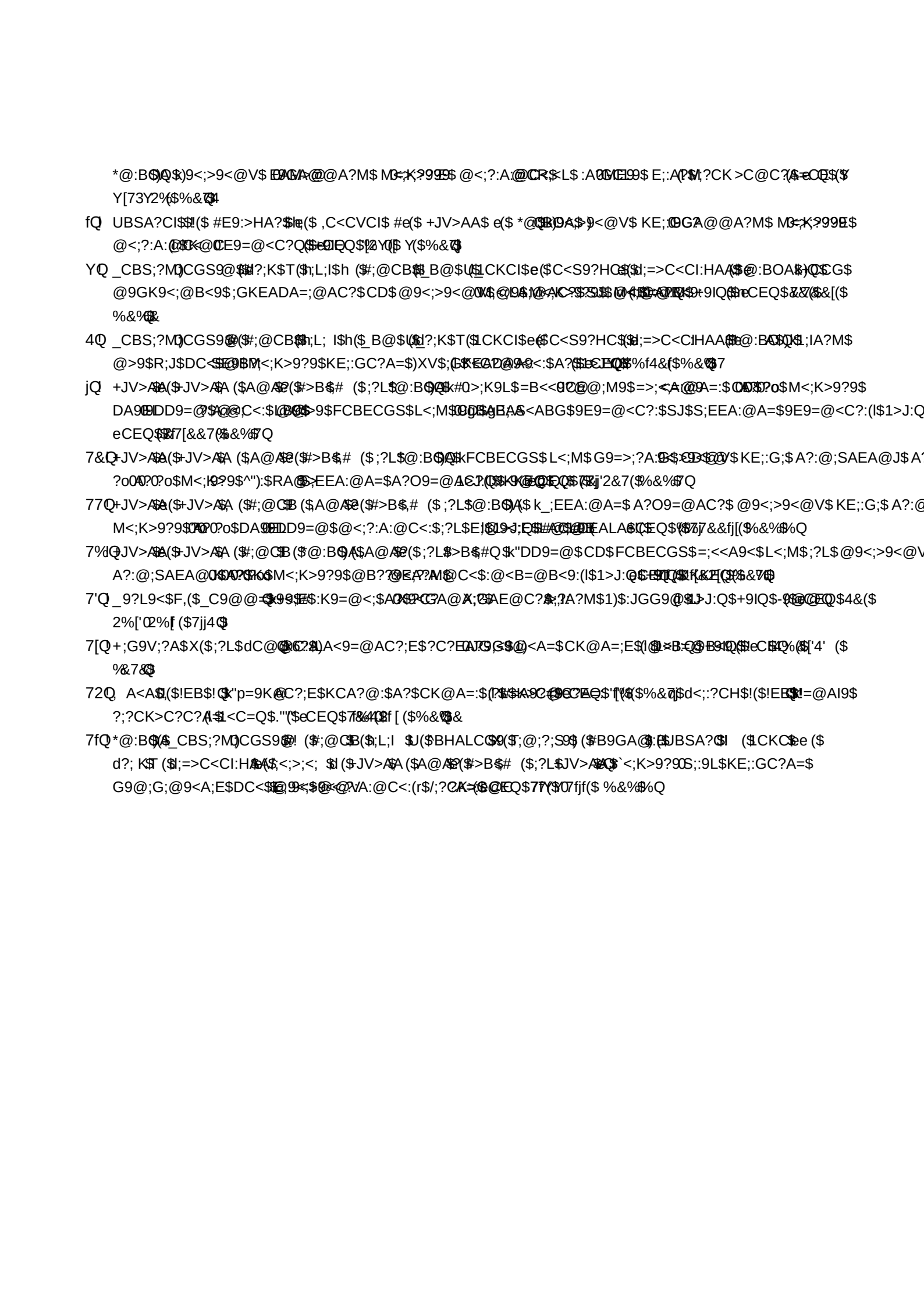

!"#$%&%'($)*++",*-./*#0#1!./($2$3$4$56/"$%&%'$ $ $ $ $ $ $ $ $ $ $

!

"#$%&'()*!+&'!,-$.%*/0+.('*/#$%&'()*1#1.(, 1!+1!,-$.%2-&/.%0&+$!,(.+,+.()%+$13!4&!

522(/.%6(!7('%-,!'(1/)%8.%0&$

$

"9:!7+6%'%1<=<!4:!>+10$+,8)0-; <! ! 7:!?+2(1+@%

7$89:;<=>?9;$@9A$+BCB=ADE$=;<$)BDE;9F9GH$IBFF=C$J8*+)IK($.;C>?>:>B$9@$"FBD>A9;?D$#>A:D>:AB$=;<$-=CB

M&&7'$IBA=NF?9;($OAB>B($PABBDB$

%$6;?QBAC?>H$9@$OAB>B($RBS>L$9@$,=>BA?=FC$#D?B;DB$=;<$)BDE;9F9GH($M&&7'$IBA=NF?9;($OAB

TD9AABCS9;<?;G$=:>E9AU$N=@BC=N?V?BCFL@9A>ELGA$

$

4A1.)+/.3! WB$ <?CD:CC$ =;$ B@@BD>?QB$ XB<?:X$ =SSA9=DE$ @9A$ =;=FHY?;G$ XB>=X=>BA?=FC$ D9X

CD=>>BABACZXB>=0=>9XC($B?>EBA$C?XSEB$9A$DWB$<ZBX9;C9A=>B$>EB$S9>B;>?=F$9@$>E?C$=

)IY$ CHC>BXC$ X=<B$ 9@$ S9F=A?>9;?D$ DHF?;<BAC$ =C$ [BFF$ =C$?;$ GA=SEB;B0\=CB<$;=;9>:\BCL

<BX9;C>A=>B$=$AB=DE$S=F=>B$9@$9S>?D=?;$ABCS9;QB$?;BF$<;<$EHSBA\9F?D$XB>=X=>BA?=F$ABC

$ $

.;$ ABDB;>$ HB=AC($ E?GE0?;<B]$ <?BFBD>A?D$ XB>=X=>BA?=FC$ =;<$ XB>=X=>BA?=FC$ X=<B$ 9@$

SE9;9;0S9F=A>?9;$X=>BA?=FCK$E=QB$G=?;B<$C?G;?@?D=;>$=>>B;>?9;$<:B>9>EB?A$=\?F?>H$>9$

C:\[=QBFB;G>E$ABC9;=;DBC$=Q9?<?;G$>EB$E?GE9XB>=X=>BA?=FCL$)EB$=DD:A=>B$<E

9@$C:DE$XB>=X=>BA?=FC$=C$B@@BD>?QB$XB<?=$AB^:?ABC$=SSA9=DEBC$=SSF?D=\FB$\BH9;<$>

ABG?XBC$[EBAB$>EB$[=QBFB;G>E$?;C?<B$>EB$XB>=0=>9XC$?C$D9XS=A=\FB$>9$>EB?A$C?YBL$)EB

XB<?:X$ =SSA9=DEBC($C:DE$ =C$,=][BFF0P=A;B>>$ =SSA9=DE$ E=QB$ \BB;$ <BQBF9SB<$ @9

WE?FB$ <?@@BAB;>$ B]>B;C?9;C$ 9@$ >EB$,=][BFF0P=A;B>>$ =SSA9=DE$ E=QB$ \BB;$ <BCDA?\B$ [=QB$ SA9S=G=>?9;$?;$ >E?C

CD=>>BABAC$_7`($;9;B$C:DE$=SSA9=DE$ $ B]?C>C$@9A$CHC>BXC$9@$DHF?;<A?D=F$CD=>>BABAC($

.;$>E?C$C>:<H($[B$?;>A9<:DB$=;$B@@BD>?QB$XB<?:X$=SSA9=DE$>E=>$=DD:A=>BFH$<BCDA?\

XB>=X=>BA?=FC$ X=<B$ 9@$ DHF?;<A?D=F$ CD=>>BABAC$ \BH9;<$ >EB$ ^:=C?0C>=>?D$ ABG?XBL$ *:A$

O9EBAB;>$19>B;>?=F$!SSA9]?X=>?9;$JO1!K$XB>E9<($[E?DE$?C$[BFF0N;9[;$?;$>EB$#9F?<$#>=>B$1EH

WB$\:?F<$9;$>EB$[9AN$9@$a:$B>$=FL$_%`$=;<$B]>B;<$>EB$=SSA9=DE$>9$D9=>B<$=;<$X:F>?0D9=>

S9>B;>?=F>9?;D9AS9A=>B$=$XB>=C:A@=DB$=>$B=DE$?;>BA@=DBL$)EB$DHF?;<BAC$D=;$\B$X=<B

X=>BA?=F($?;DF:<?;G$<?BFBD>A?D($XB>=FC($=;<$S9F=A?>9;?D$X=>BA?=FC($[E?FB$>EB$XB>=C:A@=

=;<$BFBD>A?D$C:A@=DB$?XSB<=;DB$(SSA9=DE$E=QB$\BB;$<BCDA?\B$[=QB$SA9S=G=>?9;$?;$>E?C$

!SSF?D=>?9;$9@$9:A$O1!0\=CB<$=SSA9=DE>9Q=A?9:C$DHF?;<BA0\=CB<$CHC>BXC$E=C$CE9[;$=

XB>=X=>BA?=F$ABCS9;CBL$!C$=;$B]=XSFB($[B$<BX9;C>A=>B$>E?C$ABCS9;CB$?;$>EB$D=CB$9@$#?0

?;$CHC>BXC$9@$GA=SEB;B0\=CB<$;=;9>:\BC$_b`L$.;$\9>E$CHC>BXC$[B$ABQB=F$=$QBAH$A?DE$ABC

EHSBA\9F?D$<?SBAC?9;$ABF=>?9;($;BG=>?QB$A$ABQA?DBBAQB$B]A0YBA9$SBAX?>>?Q?>H$9A$SBAXE

$

WB$=DN;9[FB<GB$@:;<?;G$\H$>EB$"6$SA9cBD>C$1I*)*,")!($/!/*1*-a($d.#*+#6+8($=C$[BFF$=C$@A9X$

IBFFB;?D$89:;<=>?9;$@9A$+BCB=ADE$=;<$.;;9Q=>?9;L$

$

B(2()(&/(1!

!

7Ll +L$+:SS?;($e"Q=F:=>?9;$9@$B]>B;<B<$,=][BFF0P=A;B>>$>EB9A?BC(f$*S>?DC$O9XX:;L($d9FL$74%($%M'($%&&&

%&L aL$W:($5L$-?($gL0hL$gE=;G($=;<OL)L$OE=;($e"@@BD>?QB$XB<?:X$>EB9AH$@9A$X=G;B>9<?BFBD>A?D$
F9;G0[=QBFB;G>E$F?X?>f($ $ 1EH[illegible]4277($%&72L$

'L! OEL$1L$,=Q?<?C($!L$OL$)=C9F=XSA9:($"L$/L$"D9;9X9:(O,L$#9:N9:F?C($=;<$,$j=@BC=N?($e19F=A?>9;?D$DHF
X:F>?@:;D>?9;=F$XB>=X=>BA?=FCU$#?;GFB$CD=>>BA?;G$=;<$B@@[illegible]
%&%&L$

bL OEL$,=Q?<?C($!LOL)=C9F=XSA9:($,L$j=@BC=N?($e"@@BD>?QB$XB<?:X$<BCDA?S>?9;$@9A$D9=>B<$=;<$
E>>SUZZ=A]?QL9AGZ=\CZ[illegible]9$1EHCL$+BQLi

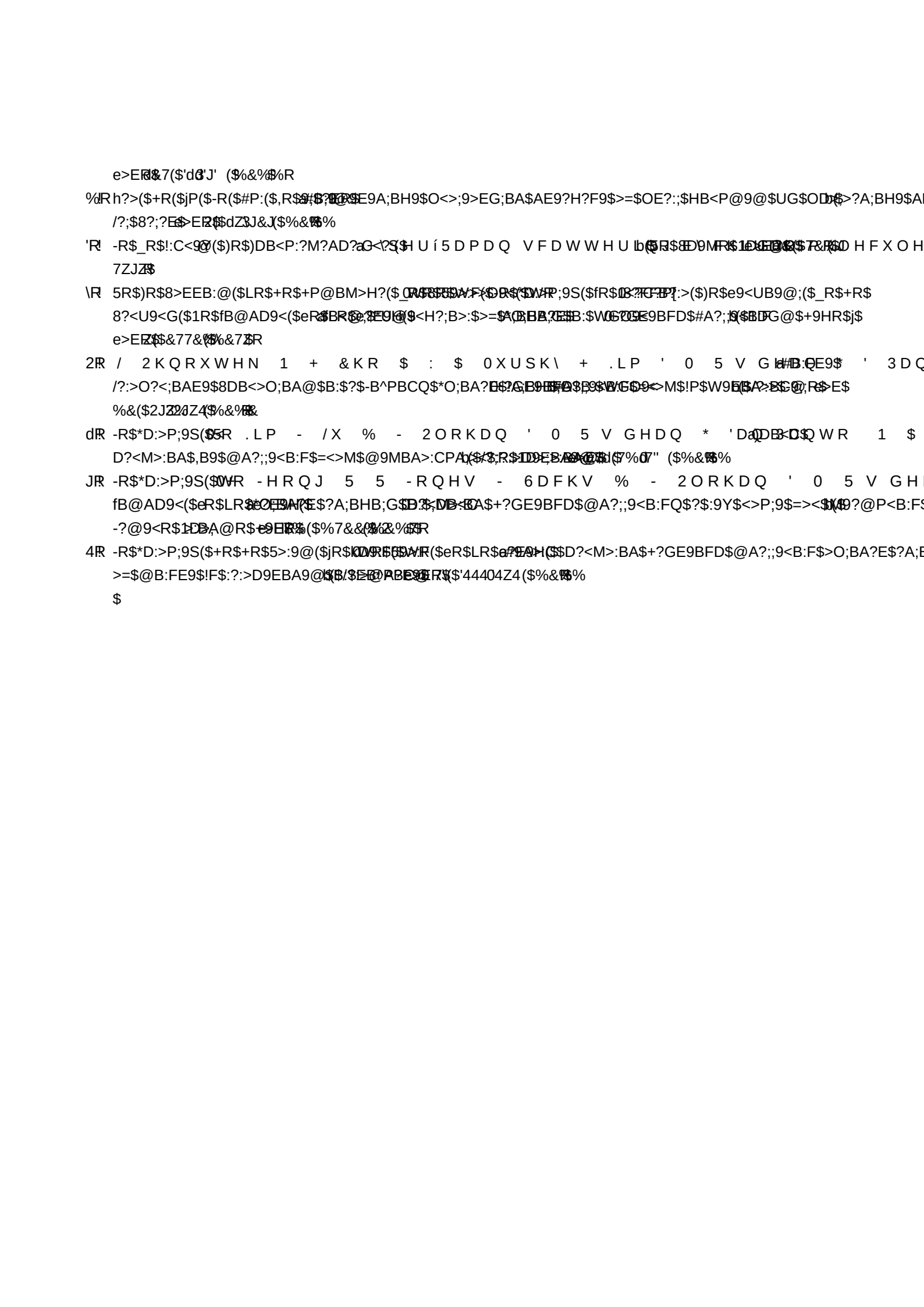

!"# $%&%($*++",*-./*# $%#1./ ($%&$$$

$

)N:$<H>NA=L$<DJ@APC:FI:$LH;;A=>$B=A?$>N:$$

*BBED:AB#DE:@D:$T9"#G&&7]`%UQ

@.*.,.)&.$ '

7Q /<F:CG

F:LEI@

%QfN<>E

-A=:@>Y$/:H=<C$/:>PA

Hyperspectral Terahertz Imaging Using Plasmonic Detectors

(Invited talk)

Mona Jarrahi

University of California, Los Angeles, USA
PMDUUDKL#XFOD HGX

Abstract: This talk gives an overview of advancements in hyperspectral terahertz imaging systems, which utilize plasmonic photoconductive terahertz detectors to provide significantly higher signal-to-noise ratio levels.

Terahertz waves have unique specifications that enable unprecedented sensing functionalities useful for personal health monitoring, environmental monitoring, and security screening as well as pharmaceutical, industrial, and agricultural product quality control. This is because most molecules have unique spectral signatures in the terahertz frequency range and many optically opaque materials are relatively transparent to terahertz waves. $GGLWLRQDOO\ WHUDKHUW] SKRWRQV DUH VXIILFLHQWO\ ORZ H especially for biomedical sensing applications. Although unique potentials of terahertz waves have been recognized for quite a while, the low efficiency, higher costs, and bulky nature of traditional terahertz systems has impeded their usage in practical applications. In this talk, I will give an overview of advancements in hyperspectral terahertz imaging systems, which utilize plasmonic photoconductive terahertz detectors [refs] to provide several orders of magnitude higher signal-to-noise ratio levels compared to the state-of-the art.

References

1. 1 7 <DUGLPFL ' 7XUDQ 0 -DUUDKL ³(IILFLHQW 3KRWRFRQGXFWL 1DQRFDYLWLHV ´ $3/ 3KRWRQLFV
2. 3 ./X ' 7XUDQ 0 -sensitivity Dekomm-Jarrahi compatible photoconductive terahertz detection WKURXJK FDUULHU WUDQVLW WLPH-638E5,2020 WLRQ ´ 2SWLFV ([SUHVV
3. ' 7XUDQ 1 7 <DUGLPFL 0 -enhanced photoconductive terahertz detector pumped by Ytterbium-GRSHG ILEHU ODVHU ´ 23E45,2020 ([SUHVV
4. N. Wang, S. Cakmakyapan, -Y. /LQ + -DYDGL 0-temperature heterodyne terahertz detection with quantum-OHYHO VHQVLWLYLW\ 97 1982,2019 H $VWURQRP\
5. 1 7 <DUGLPFL ' 7XUDQ 6 &DNPDN\DSDQ Broadband photoconductive terahertz 'HWHFWRU %DVHG RQ D 3ODVPRQLF 1DQRFDYLW\ ´ $SSOLHG 3K\VLFV /H
6. 1 7 <DUGLPFL 0 structure-DQKL ³E RQ 3KRWRFRQGXFWLYH 7HUDKHUW] (PLV 1802437, 2018
7. 1 7 <DUGLPFL 0 -DUUDKL ³+LJK 6HQVLWLYLW\ Plasmonic Nano-Pillar Based Photoconductive Terahertz Detector Arrays´ Scientific Reports, 7, 42667, 2017
8. C. W. Berry, N. Wang, M. R. Hashemi, M. Unlu, and M. Jarrahi, "Significant performance enhancement in photoconductive terahertz optoelectronics by incorporating plasmonic contact electrodes," Nature Communications, 4, 1622, 2013

!"# $%&%($*++",*-./*# $0#1!./ ($2$3$4$56/" $%&$ $ $ $ $ $ $ $ $ $ $ $ $

!"#$$%&'()*%&&+$,'#$*'-"#.#-/%.+0#/+)$'1).'-)((2$+-#/+)$ ' '
#$*'3%$3+$,'+$'#'45'%6$#

$

!"#$%&'())*+#

!"#$%&'(&)*"'+$,-+.*&./0&1/(',2.$-'/&3"+4/'*'567&89/0&:/-;'',<-$=6?&??@7&BC?&DD&8?&AE"0"&
+',,"<#'/0-/5&.9$4',F&(,"0,-G%$9(;"<<'/H"-$%*$4%<"

$

$

!"#$%&'$()!"#$%#&'(&)*&+#*,#-&#-.%&+#,/#+$%*0$-1*2$)#*&+#),13*4.%%$5&#6768#.*#90&:1&/)$&%#0./;$/;#
90,4#,/&#,0#.#9&<#"=>#*,#?1/+0&+%#,9#"=>@#7*#<$33#%1((,0*#-,*?#),441/$).*$,/#./+#%&/%$/;#.((3$).*$,/%#
%?,13+#.*#*?&#%.4&#*$4&#,99&0#&3$&4#&/,04,1%#+.*.#0.*&%B#./+#*?&#$(3$).*$,/%#,/#!"@#D.%&+#,/#4&.%10&4&/*#&'.4(3&'
+$%)1%%#)?.//&3#)?.0.)*&0$%*$)%#4#)+&/&%B#./+#*?&#$(3$).*$,/%#,/#!"@#D.%&+#,/#4&.%10&4&/*#&'.4(3&'
<&#(,$/*#,1*#(,%%$-3&#+$0&)*$,/%#./+#3$4$*.*$,/%#./+#<?.*#<&#0&.334#)*&#5(&$*,1%#90&:1&/)A##/+%@

Tutorial

!"# $%&'()$*++",*-./*# $$#1!./ ($2334$56/" $%&$ $ $ $ $ $ $ $ $ $ $ $

!"#$%&'(#)%"*#%*+,,-*.,/$")"0*1,(2")3',4*5%$*6$#)5)()/7*87,(#$%9/0",#)(*:/#,$)/74 *

$

!"##"$%&'%()*"##)

!"# $%&'()*+,-%*!"#$%&'#().*!/0 *

*

! 12&&%'32"4#"5*6,(7&8#%;364#::6<4,-%;%4,

$

$

!"#$%&'$)!""#$%"&'()$%"*+,'-.$/!00.1$2(3"$"%2(%4"5$(%5$*'(%.6,'7"5$*'(58*8,%()$"'."('42$7"*2,5.$
(%5$('"$5'838%9$.48"%*8684$(53(%4":$!""#$)"('%8%9$2(.$.2,+%$877"%."$#,*"%86(5*8%42(6$8"
")"4*',7(9%"*84$7(*"'8().$/;<=1$"'."('42>$+8*2$(##)84(*8,%.$.#(%%8%9$")"4*',7(9%"*84$7"*(7(*"'8().>$
7"*(.&'6(4".>$#2,*,%84$4'?.*().>$(%5$#)(.7,%84.:$@%$*28.$A'8"6$*&*,'8()$+"$"'38"+$*2"$.*(*&.$,6$*2
+8*2$($6,4&.$,%$"'4"%*$(53(%4"$)>$78*(*8,%.>$(%5$6&*&"'$58"'4*8,%.:$B*'(*"98".>$9&85(%4">$"3()&(*
(%5$)878*.$,6$&.8%9$5""#$%"*+,'-.$6,'$A,*2$6,'+('5$(%5$8%3"'."$;<=$#',A)"7.$("'$#$'."%*"5:

!

!

*

Spatiotemporal effects in multimode optical fiber

Light by light manipulation in multimode fibers

T. Mansuryan[1], A. Tonello[1], Y. Arosa Lobato[3], M. Ferraro[2], M. Zitelli[2], F. Mangini[2], Y. Sun[2], B. Wetzel[1], K. Krupa[4], S. Wabnitz[2], V. Couderc[1]

[1]UniversitŽ de Limoges, XLIM, UMR 7252, 123 Avenue Thomas, 87060 Limoges, France

[2]DIET, Sapienza University of Rome Via Eudossiana, 00184 Rome, Italy

[3]University of Santiago de Compostela, Praza do Obradoiro S/N, Santiago de Compostela, 15782 Coru–a, Spain

[4]Institute of Physical Chemistry, Polish Academy of Sciences, ul. Kasprzaka 44/52, 01-224 Warsaw, Poland

*corresponding author: Vincent.couderc@xlim.fr

Abstract: We demonstrate that a low-intensity beam can be severely cleaned or distorted by a high-energy pump beam copropagating in a multimode optical fibre at different wavelengths. Thus, the M! coefficient of the weak beam is either enhanced or degraded relative to the pump intensity, allowing an ultra-fast light-by-light control. This unconventional development extends the concept of the self-cleaning process where a single beam undergoes a significant brightness improvement inside its own peak power.

Providing additional degrees of freedom, a multimode beam propagation has been attracting a great interest as it allows unveiling various new processes based on its highly complex dynamics [1-4]. Among others, Kerr-induced beam self-cleaning is one of the most debating phenomenon recently discovered. It permits changing a speckled structure into a quasi-single mode beam by using the light intensity itself. Such self-transformation can be explained in terms of four-wave-mixing interactions, so far, demonstrated only at a single wavelength due to a nonlinear non-reciprocity of the mode coupling process [4]. This behaviour arises from a presence of self-phase-modulation different impacting high-order and low-order modes. However, up to now this process seems resulting only in particular Rayleigh-Jeans, energy distribution without allowing an on-demand control of the energy distribution over the guided modes [5].

In this paper, we demonstrate experimentally that incoherent speckled propagation of a weak beam can be controlled by means of a cross-phase-modulation enabled by an additional high power pump beam at a different wavelength, instead. We show that the change in modal energy distribution leading to the brightness enhancement (i.e. M! decrease) (see figure 1(a)), can be controlled and properly adapted. Interestingly, we notice a monotone evolution of the entropy while improving M! coefficient. Differently from previous studies we also show that by modifying the initial modal structure of the pump wave it is possible to obtain the opposite effect, observed as a beam defocusing or a beam degradation (i.e. M! increase) (see figure 1(b)), due to a change of the energy distribution to the benefit of high-order modes. Our findings allow to generalise the concept of light control by light in multimode optical fibers. Numerous applications ranging from ultrafast focus control for nonlinear imaging or beam quality control for lidar can be addressed. A further extension of the light self-organization approach to the time domain can also be envisaged while allowing to control, for instance, multimode laser dynamics based on amplifying fibers or supercontinum generation in passive fibers. We believe that our results may also lead new building blocks and strengthen the research activity on thermodynamic-based description of beams propagation in complex media since a large number of modes may lead to averaging approach, as well [6].

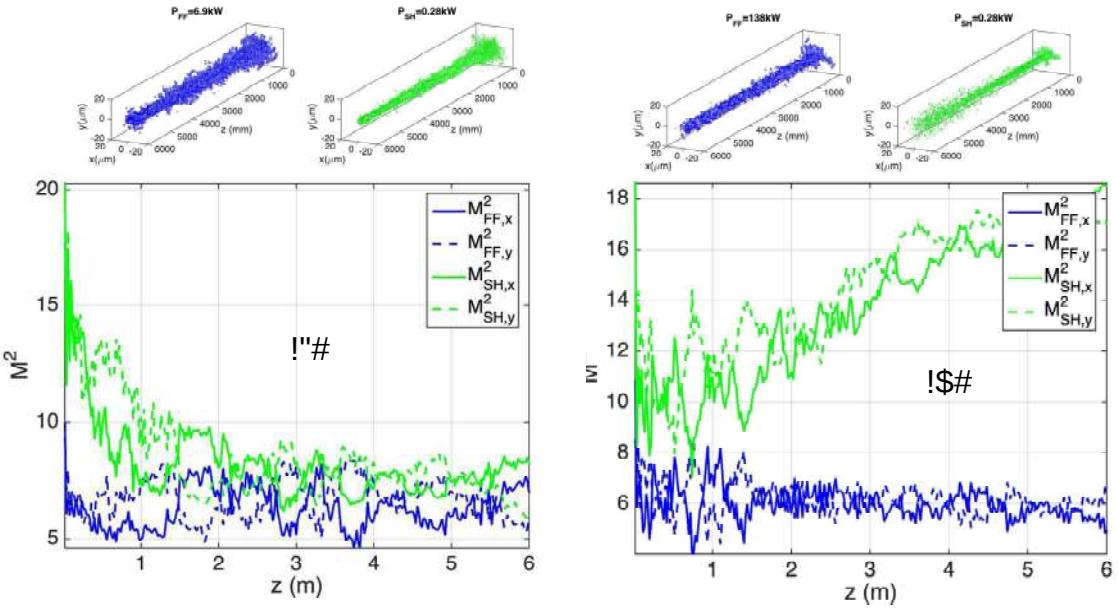

Figure 1: Numerical simulations of the M! coefficient evolution of a weak and a strong beams (pump) copropagating in a graded index optical fiber for two different cases. (a) cross-cleaning of the weak beam because of the pump beam intensity; (b) cross-defocusing of the weak beam because of the pump beam intensity

References

1. A. Picozzi, G. Millot, and S. Wabnitz, ÒNonlinear virtues of multimode fibre,Ó Nat. Photonics 9, 289-291, 2015.

2. L. G. Wright, W. H. Renninger, D. N. Christodoulides, and F. W. Wise, ÒSpatiotemporal dynamics of multimode optical solitons,Ó Opt. Express 23, 3492-3506, 2015.

3. K. Krupa, A. Tonello, A. Barthelemy, V. Couderc, B. M. Shalaby, A. Bendahmane, G. Millot, and S. Wabnitz, ÒObservation of geometric parametric instability induced by the periodic spatial self-imaging of multimode waves,Ó Phys. Rev. Lett. 116, 183901v, 2016.

4. K. Krupa, A. Tonello, B. M. Shalaby, M. Fabert, A. Barthelemy, G. Millot, S. Wabnitz, and V. Couderc, ÒSpatial beam self-cleaning in multimode fibres,Ó Nat. Photonics 11, 237-241, 2017.

5. Hamed Pourbeyram, Pavel Sidorenko, Fan O. Wu, Nicholas Bender, Logan Wright, Demetrios N. Christodoulides, and Frank Wise, ÒDirect observations of thermalization to a Rayleigh-Jeans distribution in multimode optical fibres,Ó Nat. Physics, 18, 685-690, 2022.

6. M. Ferraro, F. Mangini, F. O. Wu, M. Zitelli, D. N. Christodoulides, and S. Wabnitz, ÒCalorimetry of photon gases in nonlinear multimode optical fibers,Ó arXiv:2212.12177 [physics.optics] (2022).

$$\frac{dU_n}{dz} + J_n(z)U_{n+1} + J_{n-1}(z)U_n + |U_n|^2 U_n = 0$$

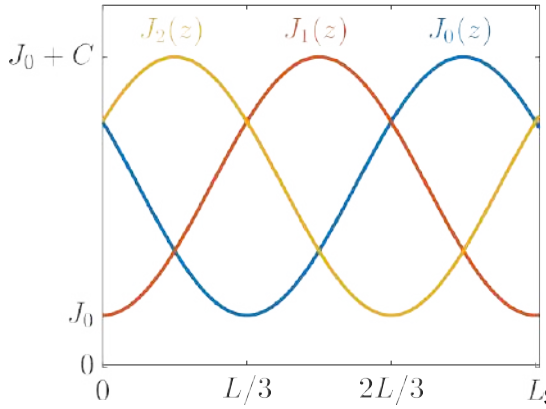

a9$RCJJ$:<9E9?=$GCAA9<9?=$<9MC>9E$@A$D@B9<9?=$E=<FD=F<9E$:<@:;M;=C@?$]GCED<9=9$E@J
]J@D;JC\9G^$;?G$=<;H$9JC?MP$

$

$

!P!$;DV?@RJ9GM9E$BCE$D@JJ;Q@<;=@<E$@?$=BCE$9AA@<=0\$;H9E$E;$1G$V9<(@59EE$D$M<9MCEGCEP$
U9$B;E$Q99?$EF::@<=9G$QI$=B9$/#_$D<&?2$8$

$

=2-2+2(32$&

7!P +P$9<;H;$($`PbP-P$a@?M($,PUP$_<@E\(KP,PKC$;?G$1PERC?GEE9C$MFCG;?D9$C?$D@<9J9EE$:B@=
D<IE=;J$ACQ9<N$!$B9JCD;J$DB;?$D9E$%($%&7g

%!P 5h<M9?E9$,P($,FVB9<i99($#$+9DB=E>;?($,P$;?=C\9G$?@?JC?9;<$)B@FJ9EE$:<9$cg($gk($
%&%&7P$5h<M9?E9?$,$;?G$+9DB=E>;?$,PW($eWB9<?$?F>Q9<$M@H9<?E$E@JC=@?$>@=C@?$C?$?@?JC?9;<$
1BIEP$+9HP$-9==P$7%4($%&7

'P! 1;<V9$+($D9H9E$ ($WF9H;E<;H9<$5E$?G$b9H<9VCGCE$1P?G$ eJ@SF9=$E@JC=@?E$C?$ESF;<9$J;==CD9EN$"TCE=9?D
;?G$GI?;>CD(E1BIEP$+9HP$?'@&ZZ%(%&%$%

ZP 1;<V9<$ +($ WF9H;E<;H9<$ 5E$b9H<9VCGCE$1P?G$!D9H9E$ #($?GC?M$;?G$)<;H9JC?M$ a;H9E$ C?$;$,@G9J$ @
19<C@GCD;JJI$,@GFJ;9G$9?EC@?;J$a;H9MFCG$E$E<QC==9G$A@<$:FQJCD$=C@?($%&%'P
$

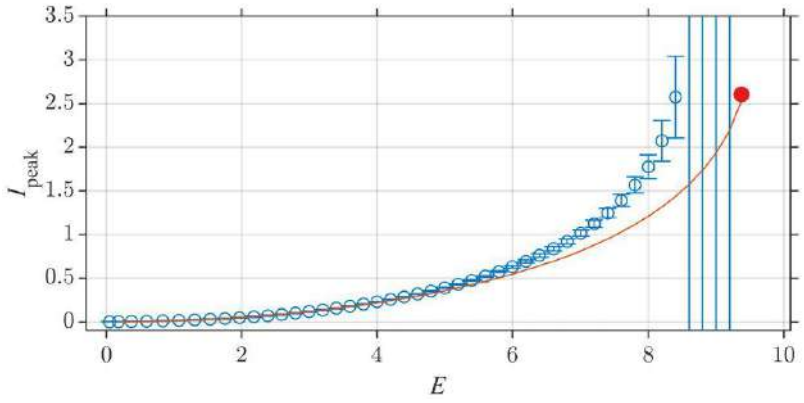
3.5
3
2.5
2
1.5
1
0.5
0
I_{peak}
0
2
4
6
8
10
E

AES 2023, TORREMOLINOS - SPAIN, 5 – 8 JUNE 2023

Random lasing in multimode diode-pumped graded-index fiber with fs-inscribed 3D refractive-index structures

A.G.Kuznetsov[1], A.A.Wolf[1], Zh.Munkueva[1,2], A.V.Dostovalov[1], S.A. Babin[1,2]

[1]Institute of Automation and Electrometry SB RAS, 1 Koptyug Ave., Novosibirsk, Russia, 630090
[2]Novosibirsk State University, Novosibirsk, Russia, 630090
[*]corresponding author: babin@iae.nsk.su

Abstract: We review our recent results on the random Raman lasing based on femtosecond (fs) pulse written randomly spaced scattering points (Rayleigh mode) and random array of fiber Bragg gratings (FBGs) in multimode graded-index (GRIN) fiber directly pumped by multimode laser.

Raman fiber lasers (RFLs) based on multimode graded-index (GRIN) fibers allow for direct pumping by laser diodes (LDs) in all-fiber scheme [1], see also [2] for a review. An attractive feature of such lasers is a possibility to efficiently convert a highly multimode pump radiation into a Stokes beam generation, the quality of which turns out to be much better than that for the original pump beam, thanks to the Raman beam cleanup effect [8] treated as the main reason. The use in the laser cavity of output couplers based on a fiber Bragg grating (FBG) inscribed by femtosecond pulses in the on-axis area of the GRIN fiber core, corresponding to the fundamental mode, makes it possible to further enhance the effect of beam cleaning for the generated Stokes radiation. So, in a single-stage resonator consisting of FBG pair resonantly reflecting Stokes beam at a wavelength of 976 nm at ~100 W pumping by multimode LD with beam quality M^2 ~ 34 at 940 nm, high-quality (M^2 ~ 2) Stokes beam has been obtained in 1-km GRIN fiber with record pump-to-Stokes brightness enhancement factor of 73 [3]. For a random lasing of the 1st Stokes wave in multimode GRIN fiber with low-quality pumping much higher pump power is required. So, more than 300 W power of random lasing at the first Stokes wavelength of 1120 nm has been obtained in ~1 km GRIN fiber at ~700 W multimode pumping by fiber combined Yb-doped fiber lasers at 1070 nm [4], however the threshold pump power for such Raman laser is as high as ~500 W.

Here we review our recent results on the random Raman lasing based on femtosecond (fs) pulse written randomly spaced scattering points (artificial Rayleigh reflector) or random array of short fiber Bragg gratings (FBGs) in graded-index (GRIN) fiber which is directly pumped by multimode laser diode. The artificial random structures help to reduce the pumping threshold for random lasing and allow for the quality improvement, similarly to regular FBG with spatial filtering properties [3]. Note that much better output characteristics of random lasing are achieved in the latter case (random grating array). The fabricated 1-3D random arrays form a half-open cavity together with the input high-reflective regular FBG. Above the threshold pump power of ~100W from a multimode 940-nm laser diode with beam quality M^2 ~ 34, random lasing of the 1st-order Stokes beam was obtained with output power reaching ~30 W at maximum pumping. The output beam quality parameter varies with FBG distribution in the fiber cross-section and its best value amounts to M^2 ~ 2, while the linewidth narrows to 0.1-0.2 nm. The main mechanisms of spatio-spectral beam narrowing in this configuration will be discussed.

The authors acknowledge financial support of Russian Science Foundation (grant-72-30024).

References

1. Wolf, A.A., Nemov, I.N, Dostovalov, A. V., Tyrtyshnyy, V.A, Myasnikov, D. V, Babin, S.A. ³ * H Q H U D W L Q J high-quality beam in a multimode LD-pumped all-fiber 5 D P D Q O D V, Vol. 25, 1850125 (2017).
2. Babin, S.A., Zlobina, E.A, Kablukov, S.I. ³ 0 X O W L P R G H) L E H U 5 D P D Q / D V H U V ' L U H F W O \ 3 X P Sel. Top. Quantum Electron., Vol. 24, 1–10, 2018.
3. Kuznetsov, A.G., Kablukov, S.I., Podivilov, E.V., % D E L Q 6 $ ³ % U L J K W Q H V V H Q K D Q F H P H Q W LD-pumped graded-index fi E H U 5 D P D Q O D V H U ´ 2 4, 103422 (2021).
4. Chen, Y, Fan, C., Yao, T., Xiao, H., Leng, J., Zhou, P., Nemov, I.N., Kuznetsov, A.G. % D E L Q 6 $ ³ % U L J K W enhancement in random Raman fiber laser based on a graded-index fiber with high- S R Z H U P X O W L P R G H S X P S L Lett. Vol. 46, 1185, 2021.

Reduced model for nonlinear multimode dynamics in photonic crystal structures

F. R. Talenti[1,2*], A. De Rossi[1], and S. Wabnitz[2]

[1]Thales Research and Technology, Campus Polytechnique, 1 Avenue Augustin Fresnel, 91767 Palaiseau, France
[2]Dipartimento di Ingegneria dell'Informazione, Elettronica e Telecomunicazioni, Sapienza University of Rome, 00184 Rome, Italy
[*]corresponding author: francescorinaldo.talenti@uniroma1.it

Abstract: We recently introduced a novel technique for the systematic design of multimode photonic crystal (PhC) cavities with a prescribed dispersion curve, based on a well established 1D reduced model. This is particularly interesting in the view of miniaturizing parametric generators of nonclassical light, optical nanocombs, and mode-locked laser sources. Here we apply our model to the study of nonlinear multimode interactions.

Introduction

The route towards the demonstration of optical frequency comb (OFC) generation in PhC structures [1] has been paved since a few years. The main interest comes from the minimal footprint of PhCs, resulting in ultra-low operational power levels, possibly leading to nonlinear quantum sources. The optical parametric oscillator (OPO), which can be seen dynamically as the very first stage of an OFC, has been reported recently [2]. Nevertheless, the residual nonzero dispersion of real fabricated samples, leading to largely unequally spaced neighboring cavity modes, makes the demonstration of PhC-OFC – which is composed of equally spaced frequency components – particularly challenging [3]. Both fabrication tolerances and intrinsic geometrical characteristics are responsible for this shortcoming. In a recent paper [4], we presented a novel self-consistent systematic technique, permitting to efficiently tailor the cavity dispersion management directly at the design stage. In order to do that, we set up a simple 1D reduced model (RM), which approximates a wide class of multimode PhC resonators to a distributed feedback (DFB) mirror. Interestingly, the model is also capable of describing nonlinear parametric interactions between the resonant modes of the resonator, thus describing the overall intra-cavity field evolution. In what follows, we show how we can simulate the PhC-OPO dynamics, which enables us to predict OFC generation under realistic experimental situations.

Nonlinear multimode interactions in PhCs

The RM of ref. [4] can be generalized to embed nonlinear cross (γ_x) and self- ($\gamma_{+,-}$) phase modulation terms:

$$\begin{cases} \partial_t A^+ = (\mathcal{D}_2 \partial_x^2 - i v_g \partial_x) A^+ - \mathcal{K} A^- + i(\gamma_x |A^-|^2 A^+ + \gamma_+ |A^+|^2 A^+) \\ \partial_t A^- = (\mathcal{D}_2 \partial_x^2 + i v_g \partial_x) A^- - \mathcal{K} A^+ + i(\gamma_x |A^+|^2 A^- + \gamma_- |A^-|^2 A^-) \end{cases}, \quad (1)$$

where $A^{+,-}$ are two counter-propagating waves, linearly coupled by means of a DFB mirror ($\mathcal{K}$). v_g and D_2 are the group velocity and the second order dispersion, respectively. Here we highlight nonlinear terms. In Figure 1, we report the cold cavity spectrum (a) and the nonlinear evolution of the field (b). In (a) we colored the three fundamental modes interacting nonlinearly, while grey dashed lines indicate higher-order modes, whose contribution can be neglected for weakly nonlinear systems. Here we report a general physical situation using arbitrary units, by setting $v_g(x)=1$ a.u., and neglecting leading-order dispersion terms. The coupling is chosen in such a way to shape the parabolic potential well, which is depicted in red in panel (a). The field is treated by means of a modal decomposition analysis on the OPO triplet $\Phi_{+,-,0}$. We can see how nonlinear terms work as a tea spoon, mixing the stationary eigen solutions of the system. As the $\gamma_{x,+,-}$ terms increase, the coupling between modes is stronger and, eventually, it is no longer fully described by a pure OPO interaction, since higher-order modes also partecipate in the wave mixing process.

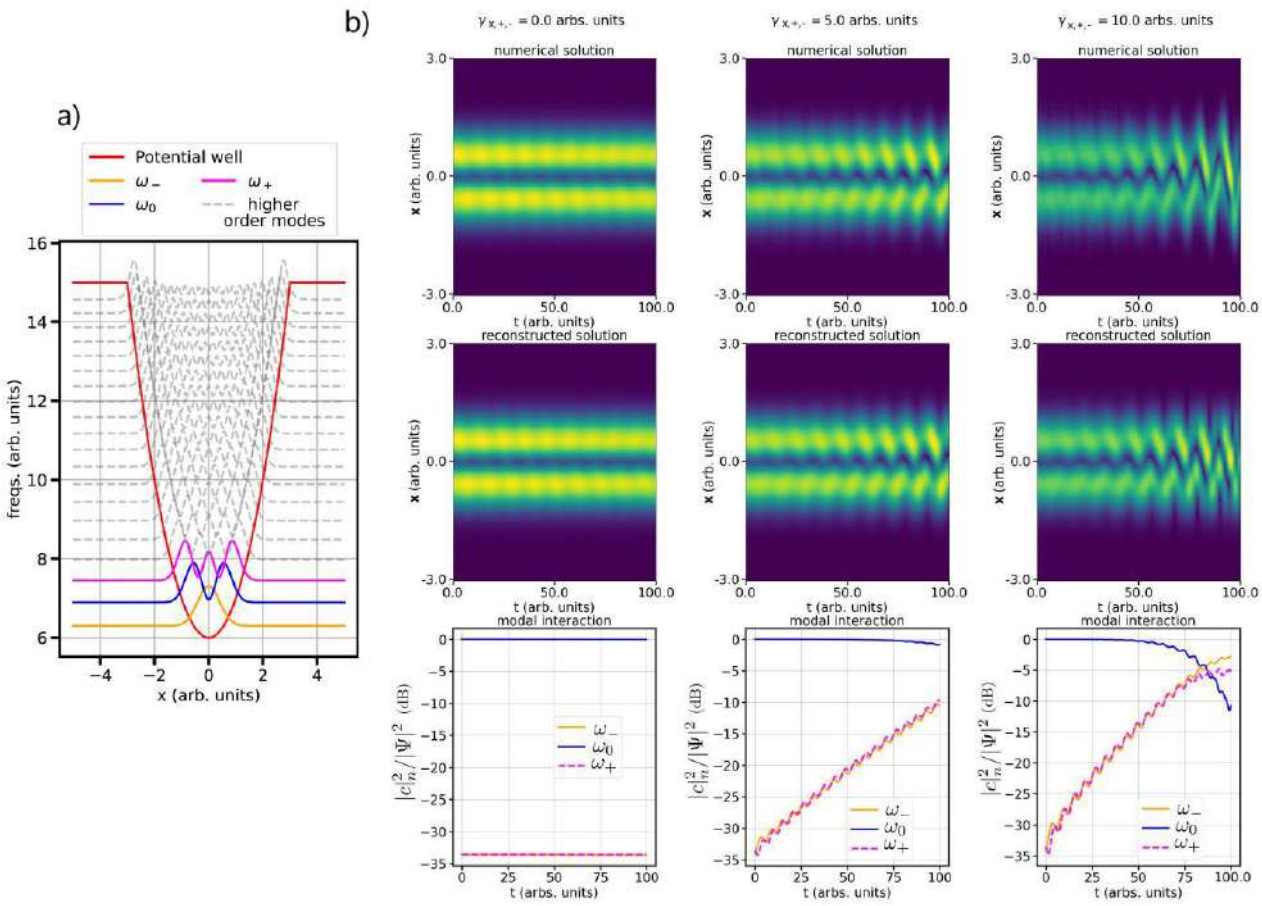

Figure I: a) !"#$% &'!% ()*+,-% ./0(,1234% 5'0% ("#"10$%3"$0%:,01)(,+:;% :":#+:0)1#-4% <+6'01% 3"$0.7% :",% /)1,+(+/),+:;% ,"% ,'0% :":#+:0)1% +:,01)(,+":7%)10% ("#"10$% +:% ;10-7% 0+% ##2,1)% 0% >0(,+*0% /",0:,+)#% =0##4% ?@% A":#+:0)1%>10B20:(-%3+C+:;%$-:)3+(.%">%,'0%D&D%,1+/#0,4%D:%,"/%0%0%01,%(%23.2#,.%">%(,1%./":$ +:;% :":#+:0)1+,-% #0*0#4% 5'0% >+1.,% 1"=% +.%,'0% :2301+()#% ."#2,+":% ">%,'0% $-:)3+()#% 0*"#2,+"1%E>%)#% 0%-.,034% 5'0% 10/10.0:,.%+30%7% ='+#0% ":%%01%+()#%%+%0% .'"=%'0% ./),+)#% (""1$+:),0% 5'0% +:,1)()*+,-% >+0#$% +:,0:.+,-% +.% ("#"1% 3)//0$7% >1"3% ?#20% F("#$7%#"=% +:,0:.+,-@%,"%-0##"=% F=)137% '+;'% +:,0:.+,-@,4,03% +,)1% +:,% 1% +:,0:.+,-% 0% .0(":$%1"=%0%##2.,1)%0% 10(":.,12(,0$%."#2,+":.%>1"3%$)#%$0("3/".+,+":%):)#-.+4%+:)##-7%0%?",,"3%1"=%0% .'"= %0% 3"$)#% 0*"#2,+"=%('%#0)$7%),%0)('%;+*0:%+:.,)"7%0% $0("3/".+,+":% ">%,'0% +:,1)()*+,-% >+1%$0% D&D% ,1+/#0,4

Conclusion

In conclusion, we presented an application of a reduced model recently introduced for the systematic design of PhC structures, and the optimization of their geomtry [1]. Because of its generality, our analysis can also be extended to describe parametric nonlinear interactions in a wide class of multimode PhC resonators.

References

1. & R P E U L p 6 Comb of high-Q resonances in a compact photonic cavity, Laser & Photonics Reviews, 2017.
2. Marty, G et al., "Photonic crystal optical parametric oscillator," Nat. Photonics 15, 53–58 (2021).
3. Chopin, A. et al., "Canonical Resonant Four-Wave-Mixing in Photonic Crystal Cavities: Tuning, Tolerances and Scaling," IEEE Journal of Selected Topics in Quantum Electronics, vol. 29, no. 1: Nonlinear Integrated Photonics, 2023.
4. Talenti, F. R. et al., "Fast dispersion tailoring of multimode photonic crystal resonators," Phys. Rev. A 106, 023505 2022.

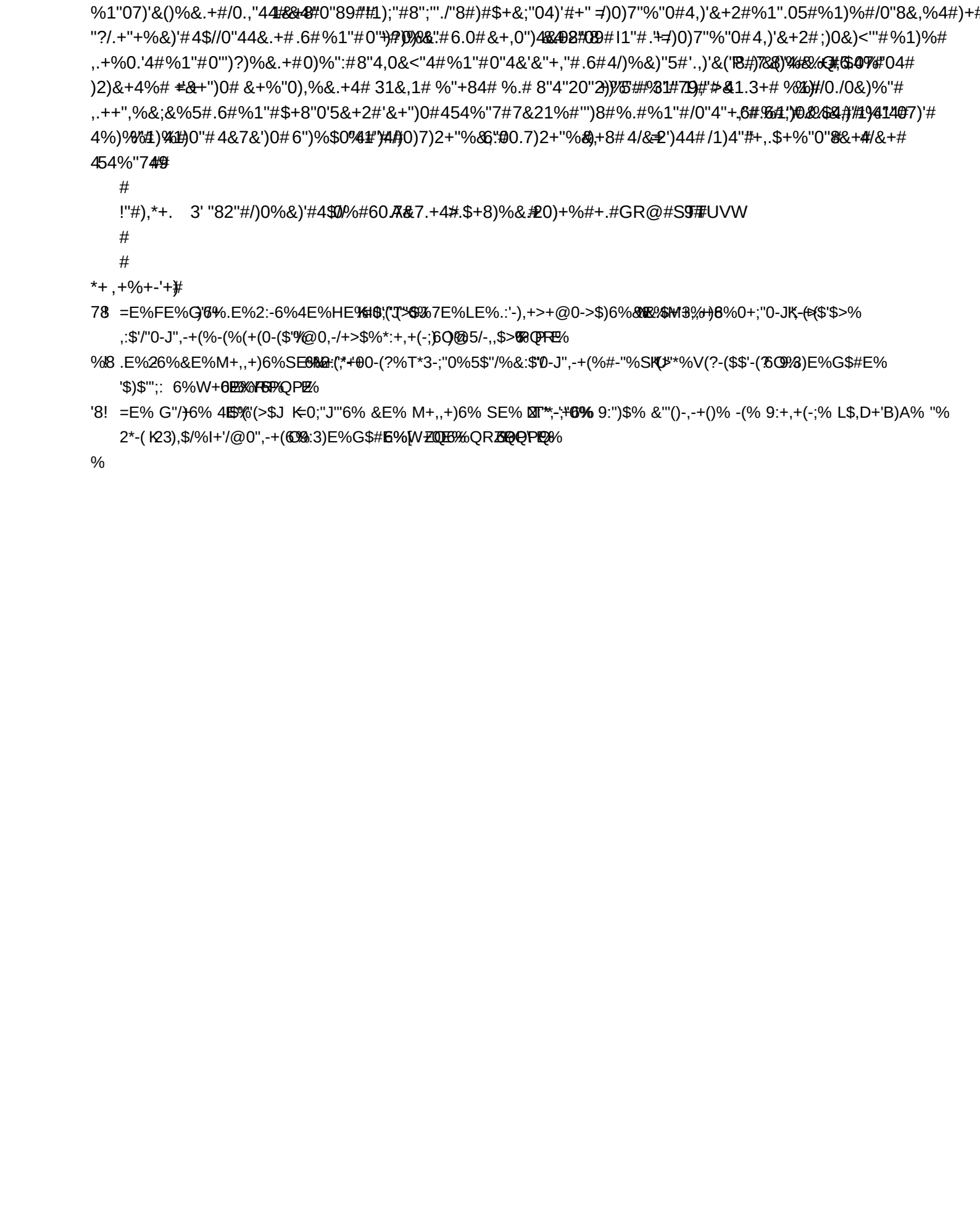

AES 2023, TORREMOLINOS - SPAIN, 5 - 8 JUNE 2023

Two-waves thermalization and calorimetry experiments in nonlinear multimode optical fibers

Mario Ferraro [1,*], Fabio Mangini[1], Fan O. Wu[2], Mario Zitelli [1], Demetrios N. Christodoulides[2], and Stefan Wabnitz[1]

[1]DIET, Sapienza University of Rome, 00184 Roma, Italy

[2]CREOL, University of Central Florida, 32816 Orlando, Florida, USA

[*]corresponding author: mario.ferraro@uniroma1.it

Abstract: We carried out two-waves thermalization and calorimetry experiments in nonlinear multimode optical fibers. Our results extend the thermodynamic description of the beam self-cleaning effect, enabling a new paradigm for the all-optical control of the spatial profile of intense multimode laser beams.

The thermodynamic theory of light propagation in weakly nonlinear multimode optical systems allows for describing laser beams in analogy with a gas of particles [1]. In such a thermodynamic framework, the nonlinearity is responsible of the interaction among the gas of photons, which leads to the establishment of a thermal equilibrium after a sufficiently long propagation distance. Recently, the gas-like representation has been applied to the spatial beam self-cleaning (BSC) effect [2], which consists on the spontaneous formation of a bell-shaped intensity profile at the output of graded-index (GRIN) multimode optical fibers (MMF) [3]. The BSC effect, which is driven by the Kerr nonlinearity can be described as resulting from the thermalization of the multitude of fiber modes, leading to a mode power distribution which obeys the Rayleigh-Jeans (RJ) law.

Hence, BSC is associated with the transformation of a nonequilibrium system at the fiber input (Fig. 1a) into a state of equilibrium, i.e., of maximum entropy, at the fiber output (Fig. 1b). Note that virtually all the experimental demonstrations of BSC use linearly polarized light at the fiber input. At the same time, it is well-known that light progressively loses its degree of polarization upon propagation in a MMF [4]. Therefore, in Fig. 1a,b, we represent the input state as a gas which occupies half of the modal volume, i.e., only the modes with a given polarization are populated at the fiber input. Whereas, at thermal equilibrium, the gas homogeneously occupies the whole modal volume, moreover, it is possible to define thermodynamic parameters such as the gas temperature (T) and chemical potential (μ). Remarkably, the value of thermodynamic parameters is only determined by the injection conditions of the input laser beam. As a consequence, one can somehow associate a temperature even to a nonequilibrium state such as the input state. Note that such a temperature has a pure statistical meaning, i.e., it cannot be measured with a thermometer.

Experimentally, in short fiber spans, i.e., whose typical length is of the order of a few meters, BSC is observed whenever the input power is high enough to ensure that interactions among the gas particles lead to a thermal equilibrium within the limited propagation distance. Typically, one observes a transformation from a speckles (Fig. 1c) into a bell-shaped beam (Fig. 1d), whenever the input peak power of the laser pulses reaches values of the order of few tens of kilowatts.

Here we extend the thermodynamic description of BSC in MMF to two-wave thermalization (for more details, see Ref. [5]). We carried out experiments where two orthogonally polarized infrared beams are simultaneously injected into the core of a standard GRIN MMF. Such an input condition is represented in Fig. 1e in the same fashion as in Fig. 1a,b. In particular, in Fig. 1e, the particles of the two gases are shown with different colors, since the two beams were prepared so that they have different values of T and μ at the fiber

input. In analogy with the single gas system, maximization of entropy of the gas mixture leads to the establishment of a thermal equilibrium, where the system eventually reaches a single temperature. Moreover, being the particles indistinguishable, at thermal equilibrium, the two gases are associated with the same value of the chemical potential. Consequently, the particles are depicted with the same color in Fig. 1f.

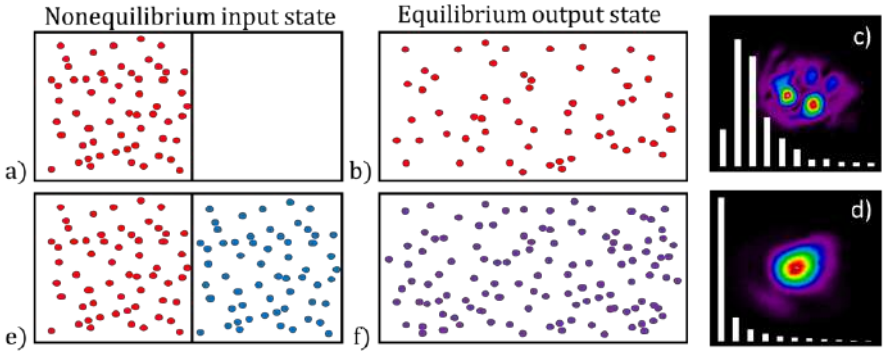

Fig. 1. (a) Representation, in the thermodynamic framework, of a linearly polarized beam at the input of a MMF. (b) Depiction of the equilibrium state corresponding to BSC, which is reached at the fiber output. (c) Intensity profile of the beam at the output of a GRIN MMF when the input peak power is lower than the BSC threshold. (d) Intensity profile of a self-cleaned beam. The histograms in (c) and (d) represent the distribution of the mode powers, sorted by their propagation constants. In (d) the monotonic trend obeys the RJ law. (e) Representation of the fiber input when two orthogonally polarized beams with different values of T and are simultaneously injected. (f) Equilibrium state resulting from two-wave thermalization.

Our experiments verified the theoretical expectation: we found that the experimentally determined temperature and chemical potential of the photon gas mixture are independent of the output polarization direction (i.e., T and are the same in both the left and right sides of the box in Fig. 1f). Moreover, we experimentally verified that the value of entropy of the equilibrium state is grater than that at the fiber input. Finally, we demonstrate that the equilibrium values of T and F D Q E H Y D U L H G laws of Rayleigh-Jeans calorimetry, e.g., by acting on the temperature or mass of any of the two gases at the fiber input. In this regard, our results pave the way for novel signal processing functionalities based on MMFs, such as the all-optical control of the spatial profile of intense multimode laser beams.

We acknowledge the financial support of the European Research Council (740355), Ministero dell'Istruzione dell'Universit^ e della Ricerca (R18SPB8227), and Sapienza University (Avvio alla Ricerca Grants AR2221815ED243A0, AR2221815C68DEBB).

References

1. F. O. Wu, A. U. Hassan, and D. N. Christodoulides, Nat. Photonics 13, 776–782 (2019)
2. F. Mangini et al., Opt. Express 30, 10850–10865 (2022)
3. K. Krupa et al., "Spatial beam self-cleaning in multimode fibres," Nat. Photonics 11, 237–241 (2017)
4. K. Krupa, et al., Optics letters 44, 1171-1174 (2019)
5. Ferraro, M., et al. "Calorimetry of photon gases in nonlinear multimode optical fibers." arXiv 2212.12781 (2022)

Thermodynamic fluctuations in optical nonlinear systems

K. G. Makris [1,2*], G. G. Pyrialakos[3], Fan O. Wu[4] and D. N. Christodoulides[3]

[1]ITCP-Physics Department, University of Crete, Heraklion, 71003, Greece

[2]Institute of Electronic Structure and Laser (IESL) FORTH, Heraklion, 71110, Greece

[3]Ming Hsieh Department of Electrical and Computer Engineering,
University of Southern California, Los Angeles, California 90089, USA

[4]CREOL, College of Optics and Photonics, University of Central Florida, Orlando, FL 32816, USA

[*]corresponding author: makris@physics.uoc.gr

Abstract: In the context of the new area of optical thermodynamics of weakly nonlinear systems, we provide a fluctuation theory based on grand canonical ensemble. Our theory is generic and can be applied to any weakly nonlinear and non-integrable system (for example planar waveguide, optical fiber, photonic lattice) that contains a finite number of supermodes. By employing non-equilibrium statistical mechanics we also study the out-of-equilibrium behaviour.

In recent years, considerable effort has been devoted to the study of nonlinear highly multimoded optical systems [1]. The physical motivation behind these theoretical and experimental efforts has been the search for high power optical sources that has been enabled by a sequence of new developments in multimode technologies pertaining to both guided wave structures and optical cavities. Understanding and predicting the complex nonlinear response of such systems especially when hundreds or thousands of modes are involved, is a challenging task. In the best case, all relevant approaches are mostly based on complicated nonlinear optical simulations, that make the description of realistic multimode fibers a formidable task. Thus a theory that explains and predicts such a complex behavior is still missing.

Quite recently however, a self-consistent theoretical framework has emerged, what we call Optical Thermodynamics [2-6]. In particular, optical thermodynamic theory is capable of describing such complex phenomena by means of thermodynamics of the systemÕs supermodes. A complete set of thermodynamic variables was determined and thus was able to describe and accurately predict the equilibrium behavior of the multimode system. The equation of state, the entropy and the Rayleigh-Jeans modal occupancies distribution was derived axiomatically either on thermodynamical grounds [2-4] or equivalently on statistical mechanical foundations [5, 6]. Such an approach is universal since it can be applied to any weakly nonlinear optical multimode system of finite number of supermodes that involves a finite number of conserved quantities. We can derive the fundamental relations that govern the grand canonical ensemble through maximization of the Gibbs entropy at equilibrium. In this classical picture of statistical phase-mechanics, we obtain analytical expressions for the probability distribution, the grand partition function, and the relevant thermodynamic potentials.

The first part of the talk is devoted to the understanding of the role of equilibrium fluctuations and the second

part to develop a non-equilibrium description of the system. In order to achieve our first goal we are going to rely on the grand canonical formalism [5] and directly calculate the relevant fluctuations based on the grand partition function expression. For states far from equilibrium, we develop a Langevin type of approach for the projection modal coefficients and derive effective stochastic equations that govern every supermode. Our analytical expressions are compared with direct numerical results of system-bath simulations, in all cases, and the agreement is excellent.

In conclusion, by means of statistical mechanics, we have established a solid foundation for the optical thermodynamics for equilibrium and non-equilibrium states. This formulation was carried out in the grand canonical ensemble picture and is applicable to any nonlinear arrangement involving conserved quantities such as the power, Hamiltonian, and a finite set of distinguishable modes. The equilibrium expressions for the fluctuations of power, Hamiltonian and modal occupancy/number were found in excellent agreement with direct bath-system simulations. Even more interestingly, we were able to apply a Langevin type of formalism in order to understand the non-equilibrium behavior of our system. Our results universally apply to any other weakly nonlinear highly multimoded bosonic arrangement.

Acknowledgements: This project was funded by the European Research Council (ERC Consolidator) under the grant agreement No. 101045135 (Beyond Anderson).

References

1. L. G. Wright, D. N. Christodoulides, and F. W. Wise, Nat. Phot. 9, 306 (2015).
2. F. O. Wu, A. U. Hassan, and D. N. Christodoulides, Nat. Phot. 13, 776 (2019).
3. M. Parto, F. O. Wu, P. S. Jung, K. G. Makris, and D. N. Christodoulides, Opt. Lett. 44, 3936 (2019).
4. F. O. Wu, P. S. Jung, M. Parto, M. Khajavikhan, and D. N. Christodoulides, Comm. Phys. 3, 1 (2020).
5. K. G. Makris, Fan. O. Wu, P. S. Jung, and D. N. Christodoulides, Opt. Lett. 45, 1651 (2020).
6. F. O. Wu, Q. Zhong, H. Ren, P. S. Jung, K. G. Makris, and D. N. Christodoulides, Phys. Rev. Lett. 128, 123901 (2022).

Multimode dissipative spatiotemporal solitons in coherently driven passive nonlinear cavities with parabolic potentials

Y. Sun, P. Parra-Rivas, C. Milián, Y. V. Kartashov, M. Ferraro, F. Mangini, M. Zitelli, R. Jauberteau, F. R. Talenti, and S. Wabnitz
DIET, Sapienza University of Rome, Rome, Italy
Institut Universitari de Matemàtica Pura i Aplicada, Universitat Politècnica de València, València, Spain
Institute of Spectroscopy, Russian Academy of Sciences, Troitsk, Moscow, Russia
CNR-INO, Istituto Nazionale di Ottica, Via Campi Flegrei, Pozzuoli, Italy
corresponding author: yifan.sun@uniroma.it

Abstract: We show the presence of stable high order light bullets in a coherently driven passive multimode Kerr cavity with a three dimensional potential. These states have very rich multimode features, which are unveiled by decomposing the nonlinear solutions on the three dimensional linear eigenmodes of the cavity.

[illegible]

In this work, we uncover the existence of a rich variety of LBs of different orders in the context of multimode externally driven Kerr cavities with the added influence of parabolic potential. We examine the stability of various high order LBs and calculate them in terms of their bifurcation diagram. By decomposing the LBs into three dimensional linear eigenmodes, we can obtain the evolution of the modal energies of high order LBs. We attribute the origin of the high order LBs primarily to the corresponding high order modes.

In the mean field approximation, the dynamics of the electric field envelope $A(x, y, \tau, t)$ propagating within the cavity is governed by an extended dimensionless Lugiato Lefever (LLE) equation with a D parabolic potential:

$$\frac{\partial A}{\partial t} = \mathrm{i}\left(\nabla_\perp^2 + \frac{\partial^2}{\partial \tau^2}\right)A - \mathrm{i}\left(x^2 + y^2 + C\tau^2\right)A + \mathrm{i}|A|^2 A - (1 + \mathrm{i}\delta)A + P,$$

where δ is the cavity detuning parameter, P is the pumping rate, $\nabla_\perp^2 = \partial_{xx} + \partial_{yy}$ accounts for diffraction, $\partial_{\tau\tau}$ accounts for dispersion, $(x^2 + y^2)$ is the transverse parabolic index profile or spatial potential, and $C\tau^2$ originates from synchronous phase modulation.

Figure (a) shows the bifurcation diagram of LB energy vs detuning δ. Four examples of LB states for the negative detuning values $\delta = -1, -4, -8, -11.5$ are plotted in Fig. (i)–(iv), respectively. The two shells, i.e., isosurfaces, with different colors represent different field intensities $I_1 = 3$ (red) and $I_2 = 0.1$ (blue). The four states that we consider represent the first high order LBs. They are separated by the three peaks visible in the bifurcation diagram. Apart from these LBs, we also observe wave collapse and three dimensional breathers in the red and blue regions, respectively. Numerical continuation and direct numerical simulation are used to calculate these states. By decomposing these solutions on the three dimensional linear eigenmodes, we obtain modal energy E_n ($n = 1, 2, \ldots$), which is plotted in Fig. (b). As the detuning δ decreases, for each nth order bullet, its modal energy E_n increases until it reaches a peak value, where a phase transition of LB order occurs.

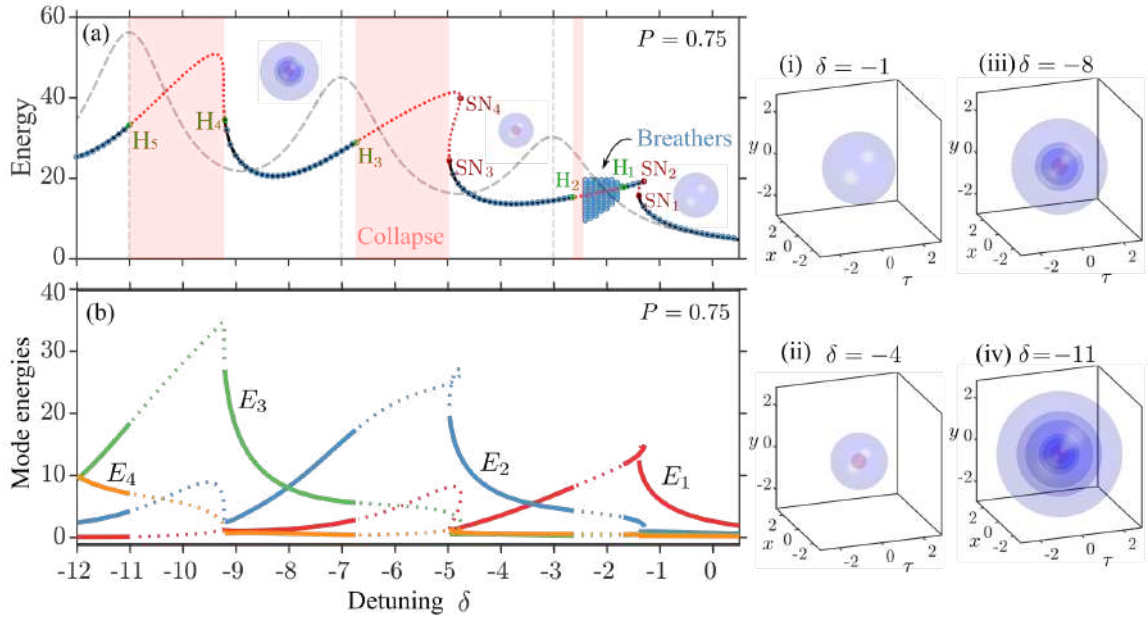

)LJXUH DE %LIXUFDWRQ GLDJUDP V VKRZLQJ WKH ILHOG HQHUJ\ RI WKH EXOBWE$E(t)$ LQ D DQG WKH UMP RGDOHQHUJ\ $E_n(t)$ LQ E YV δ IRUWKH SXPS S$P = 0.75$ LQ D 6RGGEDFN GDVKHG UHG OQHV UHSUHVHQWWDEOH XQWDEOH VROWRQV REWDLQHG E\ QXP HULFDO FRQWLQXDWLRQ %OXH FLUFOHV VXSHUP SRVHG RQ VROG OQHV DUH VRXWRQV IURP GLIIHUHQW HULFDOVP XOWLRQV 7KH FROOSVHUHJLRQ DUH P DUNHG E\ UHGDVKHG DQG EUDWKHUP SDWWHUQV DUH P DUNHG E\ \SDWWHUQV RQ VROG OQHV DUH VRXWRQV IURP GLIIHUHQW VWDWH RI WKH FDYLW\ + HUH $C = 1$

7KLV ZRUN UHYHDOV WKH SUHVHQFH RI DGLYHUVH UDQJH RI / %V ZLWK KLJK RUGHUV LQ PXOWP RGH H[WLQDO GULYHQ . HUFDYLWHV ZLWK SDUDERLF SRWHQWLDO 7KURXJK RXU DQDOVLV ZH HYDOXDWH WKH VWDELOLW RI PXOWSOH KLJK RUGHU / %V DQG FDWHJRUL]H WKH P %\ SURFHVVQJ WKH/ %V LQWR OQH DUWKUH GLP HQVLRQDOLJHQ RGHV ZHWDFHWKHRUJLQRI WKHKLJK RUGHU/ %V WR WKHUFRUHVSRQGLQJ KLJK RUGHUP RGHV

: H DFNQRZOHGJH WKH ILQDQFLDO VXSSRUW RI WKH (XURSHDQ 5HVHDUFK &RXQFLO 0 LQLVWHUR GHO)WUK]LRQH GHO8QLYHUVLW H GHOD5LFHUFD 5 63% 0 DUH6NORGRZVND&XULH $FWLRQV * UDQW3,' 1%& 0 &,1 $(, DQG ³(5') $ ZDL RI P DNLQJ (XURSH DQG 6DSLHQ]D 8QLYHUVLW $YYLR DQG 5LFHUFD * UDQW $5 (' $ $5 & '(%%

5HHUHQFHV

< 6LGHUHJ 2 SW/ HWW
< 9 . DUDVKRY * ($ VWDNKDFKLN % $ 0 DRP HG DQG/ 7RUQ1 DW5HY 3K\ V
& 0 LQ Q< . DUDVKRY DQG/ 7RUQ 3K\ V 5HY / HWW
2 9 6KWULQD 0 3)HGRUN < 6 . LYVKDU DQG6 . 7XUWW Q 3K\ V 5HY $
9 / . DDVKQNRY DQG6 : DEQW / DV-U3K\ V / HWW
$. 7XVQQ $ 0 7LNDQ DQG7 - . LSSHQEHJ 3K\ V 5HY $
1 (QJOEHUW1 * ROP DQ 0 (UNLQWR 1 0 RWDQ 6 3 * RJD) / HR DQG-) DWP H DJ LY
< 6XQ 3 3DUD5LYDV 0) HUDUR) 0 DQJLQL 0 =LWKQ5 -DXEHUWDX) 5 7DPQW DQG6 : DEQW 2 SW/ HWW

< 6XQ 3 3DUD5LYDV & 0 LQ Q< 9 . DUDVKRY 0) HUDUR) 0 DQJLQL 0 =LWKQ5 -DXEHUWDX) 5 7DPQW DQG6 : DEQW DJ LY

Additive manufacturing for electromagnetic devices

,WHUDWLYH FRUUHFWLRQ RI SKDVH HUURUV LQ I XVLQJ IXOO ZDYH PRGHOLQJ

&DUH\ 5DSS DQG 0RUJHQWKDOHU
1RUWKHDVWHUQ 8QLYHUVLW\ %RVWRQ 0$ 86$
UDSSDSRUW#QHX HGX

$EVWUDFW WULEXWHG GLHOHFWULF OHQVHV RIIHU VLJQLILFDQW FRQYHQWLRQDO XQLIRUP GLHOHFWULF OHQV DQWHQQDV EXW R EDVHG GHVLJQ 7KH FXUUHQW LQYHVWLJDWLRQ FRQVLGHUV DQ L ZDYH SURSDJDWLRQ WKURXJK D OHQV WKDW PHDVXUHV WKH SKD SURILOH RI WKH OHQV 7KH GHVLJQ SURFHVV SURFHHGV LWHUDV IRU WKH RSWLPDO OHQV DQWHQQD

'HVLJQ 0HWKRG

$VVXPH WKH GHVLUHG OHQV LV IOD GVDQGLDXDUXDU GLZHLWKF WKQLFRUP *U IHG E\ D SRLQWKVRXUFHG DFDWHGJKQDO,GQHDOHFWU KDYH UHODWLYH GLHFWULF FRQVWDQWV VPDOOHU WKDQ RQH VLPSOLILHG FRQGLWLRQ WKDW UD\ WUDYHO WKHVH RHG HQQRXWKHU WUDFH VWUDLJKW GRZQ WKH RXWHU

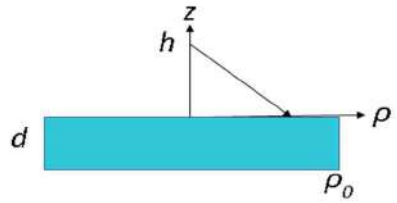

7R JHQHUDWH D SODQH ZDYH RXWSXW ZLWK DOO H[LWLQJ UD\V PXVW EH WKH VDPH (TX OHQJWK6 WKURXJK WKH OHQV VXUIDF FRQVWDQW ZKLFK RFFXUV ZKHQ

$$\frac{\sqrt{\epsilon_{lens}(\rho)}\,h}{\lambda} = \frac{\sqrt{\epsilon_{lens}(\rho)}\,h}{\lambda} + p$$

)LJXUH)ODW FLUFXODU OHQV JHRPHWU\ 1RWH WKDW WKH GLVWD RI WKH OHQV DQG WKH SRLQW

)RU D *+] *U PP GLDPHWHU PLWKLFN OHQVKZLWK PHHWKS RLG GLHOHFWULF FRQVWDQW S ZKHUH WKH [LQLWLDO LQ WKH

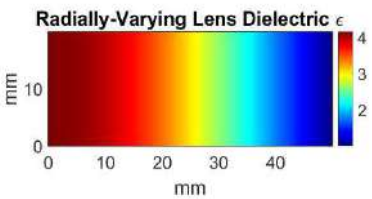

7KH HOHFWULF ILHG SRLQW VRXUFH WKD GLVWULEXWHG GLH PRGHOHG ZLWK 'LIIHUHQFH)UHTXH)')' PHWKRG DQG)LJ 7KHUH LV

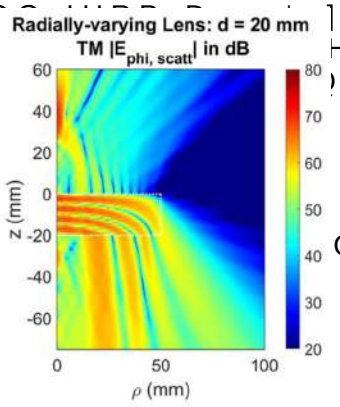

)LJXUH)LHOG VFDWWHUHG EDFNVFDWWHU ZLWK QR OHQV DQG DFFXPXODWHG GLHOHFWULF FRQVWDQW SURILOH

ULJKW

7KH EDFNVFDWWHU FDQ EH DPHOLRUDWHG WKH GLHO WKLFNQHVV DV ZHOO DV GUDZLQJ XS WKH EDFN UD\V WUDFH VWUDLJKW WKURXJK WKH OHQV FXUYDWXUH DFFXPXODWHG

WKH LQGH[RI UHIUDFWLRQ RI WKH OHQV LV K\SRWKHVL]HG WR RSHUDWH ZLWKRXW EHUSDXQG
PDWFKHG DW WKH WRS OHQV VXUIDFH DQG WKH EDVH LPPHUVHG LQ D [PPXHPWULFDO\
XQLW\ DW WKH ERWWRP VXUIDFH DW

s: E: ¿àôë@ í A F(t Ç\ Ç r

¥(:é (; L ^ ' :t

s: E: ¿àôë@ ì F— í A 6 F(Ç\ Ç F(t

7R GHWHUPLQH WKH LQGH[RI UHIUDFWLRQ RQ DQ LQGLYLGXDO GL
IURP 7KH VROXWLRQ WR Eé;:@ 4é 6 7KH UHVXOWLQJ GLVWULEXWL
ZLWK L F y w ¥Eó ý:ŵ DQG PDPLPäSUHVHQWV D PDWFK WR IUHH VSDF
VXUIDFHV ZKLOH NHHSLQJ WKH SKDVH FKDQJH YHUWLFDOO\ VWU
DV WKH SUHYLRXV OHQV

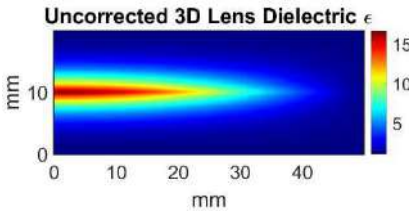

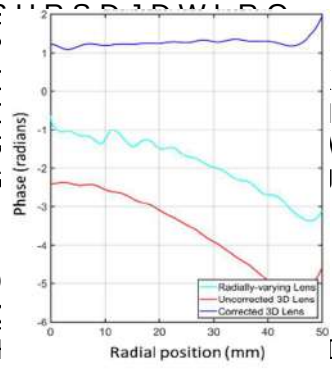

)LJXUH ')ODW FLUFXODU OHQV WR U 8VLQJ
GLHOHFWULF FRQVWDQW SURILOH

7KH)')' PRGHOHG S
WKURXJK WKLV '
LQGLFDWHV QHDU SC DYLRU
RQ H[LWLQJ WKH OHC LV VWL
SKDVH HUURU DFUR WRP
DSHUWXUH 7KH UHG
LQGLFDWHV SKDVHV W
IURP GHWDLOHG SKDVH LQ DEOHV D
FRUUHFWLRQ WR WKH GLHOHFWULF FRC LEXWLRQ
Jàôë LQ)LUVW ILW D IRXUWK RUGHU DO LQ
)LJ WKHQ VHW LW HTXDO WR WKH QXPEHU R3KDVH OHUURUV WKH
DQG VROYH ,WHUDWH WKH PRGHOLQJ ZLWK YDU\LQJ ' XQFRUUHFWHG D
RULJLQDO DQG WKH JHRPHWULF SKDVH YDULDWLRQ LV
PLQLPL]HG VHH)LJ EOXH FXUYH ZLWK UDGLDO SKDQGVH YDU
K U WKH FRUUHFWHG G ñ:E; E ws v äUyus ; F v äU ur :; ZLWK é; JLYHQ LQ

5HVXOWV DQG &RQFOXVLRQV

7KH FRPSXWHG ZDYH SDWWHUQ LQ)LJ VKR
IURQWV EHORZ WKH ERWWRP H[LW VXUIDFH RI
IDUILHOG SDWWHUQV RI WKH WKUHH OHQVHV
' FRUUHFWHG DUH
DORQJ ZLWK WKH
H[FLWHG DSHUWXUH
FLUFXODU GLPHQVLR
7KH SDWWHUQ RI OHQV
EOXH DSSURDFKHV
ZLWK OHVV WKDQ
UHGXFWLRQ EXW ZL REHV

,W KDV EHHQ VKRZQ
ZDYH PRGHOLQJ RI
GLVWULEXWHG GLHC

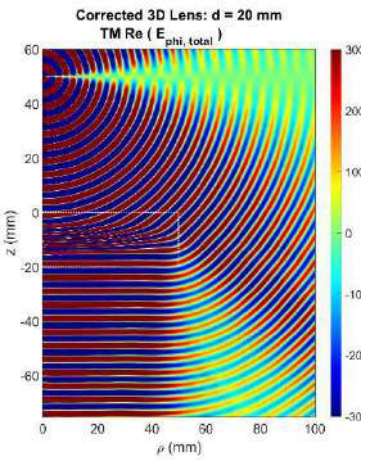

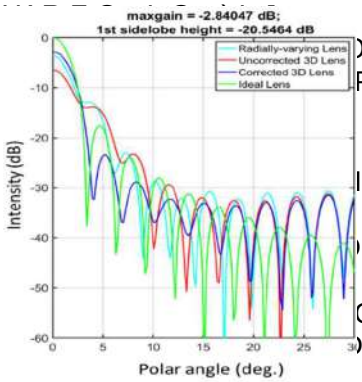

)LJXUH 5HDO SDUW RI)LJXUH QRUPDOL]HG S
ILHOG H[FLWHG E\ DSHUWXUH SUR JKW FLUFXODU SHUWXUE WKH GLHOHFWULF
SRODUL]HG SRQQ VRXUFH DW RP UDGLDOO\ YDU\LQJ XQFRUUH
ZLWK ' SKDVH FRUUHFWHG OHQV ZKLWH FRUUHFWHG DQG L
GLVWULEXWLRQ WR FRUUHFW SKDVH HUURUV
DQG JHQHUDWH QHDU SHUIHFW SDWWHUQV

!"#$%&%'($)*++",*-./*#0#1!./($2$3$4$56/"$%&%' $$$$$$$$$$$

!"#$%&"'()*+,-.$./*%$0(10'&.2*+$3%'./&4()*"'(5*2(155/&/'%.(67%.8'4/4($%" 9'4/3%(*5()*-,0"':;'4*%$.*2(</&2*=$#'()/2&-/.4

>?("'(0$(;-@/$

789:;<:=8><?$@8$,:<8=:<AB:$!9CAB:@:$:$(C"D$$@8$)8C8B?=F>AB:BA?>($6>AG8;DA@:@$1?CA<8B>AB:$@8$,:@;A@ G:C8><A>H@8C:;FIA:JF9=H8D

!@4.2$&A(B8/4(=*2C('"$04(=/.8($(%'=(+'.8*"'*0*37(5*2(&*-,0"':2'4*%$.*2(+/&2*=$#'(&/2&-/.4?(B8' 52'D-'%&7(2'4,*%4'(*5(.8'(/+,'"$%&'(+$.2/E(*5(.8'("'#/&'(-%"'2($%$074/4(/4(*@.$/%"'(/%(,*0':2'4/"-'(5*2+ @7(+'$%4(*5($(5-00:=$#'(4*0#'2F(%$+'07F(.8'(5/%/.'('0'+'%.(+'.8*"'(GH1<IF(=/.8($(+*""0(*2"'2(2"'-&./*% G<J;I(0$7'2(*%(.*,(*5(/.(.*(3'.(.8'(52'D-'%&7(2'4,*%4'(=/.8('$4'? B8/4(/+,'"$%&'(+$.2/E(4.$%"4(5*2('0'&.2*+$3%'./&4F(/?'?F(%*(&/2&-/.($,,2*E/+$./*%(/4(.$C'%(/%.*($&&*-%.(.* 4*0#'(<$E='00K4('D-$./*%4?(L2$,,/%3(.8'(,874/&$0(/%5*2+$./*%(/%&0-"""(/%(.8'(,*0':2'4/"-'(2',2'4'%.$./*% *5(.8'(/+,'"$%&'(+$.2/E(5*2(.8'(+/&2*=$#'(5/0.'2(-%"'2($%$074/4F($(0/%'$2("7%$+/&$0(474.'+(&$%(@' /"'%./5/"'F(=8/&8(,2*#/"'4(#$0-$@0'("'4/3%(/%5*2+$./*%?(B*(4*+'('E.'%.F(/%(.8'(%$22*=@$%"(0/+/.F(.8/4 "7%$+/&$0(474.'+(/4(4/+/0$2(.*($(&/2&-/.(2',2'4'%.$./*%? B8/4(%'=("7%$+/&$0(474.'+(4.$%"4(-,*%('0'&.2*+$3%'./&4F(3/#/%3(2/4'(.*($%('0'&.2*+$3%'./&$007(3'%'2$.'" &*-,0/%3(+$.2/E(5*2(&*-,0"':2'4*%$.*2(+/&2*=$#'(&/2&-/.4?(6'#'2$0($,,0/&$./*%4F(4-&8($4(+/&2*=$#'(5/0.'24F "/,0'E'24($%"($%.'%%$4F(=/00(48*=(.8'(&$,$@/0./'4(*5(.8/4(%'=(.'&8%/D-'?

!"#$%&'()*+#%,$-.%'/)0.1+/#&2,+-.)"" .('/#&+.,+3'&()%,'+.)+/.$'((1+,$)%,'+ %#$4+""*,#-5.6+$&#)-,+*./#2"'0(#+%.'3.%#"'#$'((1+,$)%,'+. -#&7,$#-.,-.1&*,+*.89.,+/1-%&0 %'.$)&&0.'1%.:#%%#&.)+/.:#%%#&.#"'#$%&,$)".'/#-,*+-;.<4#&#.).-,+*"#./#7,$#.,-.+'."'+*#& $'+$#,7#/.%'.2#&3'&(.).-,+*"'#.31+$%,'+)",%0;.:1%.&)%4#&.(1"%,2"'#.%)-=-.)%.%4#.-)(#.%,(#5 >+3'&%1+)%#"0;.(1$4.#"'#$%&,$)".'/#-,*+.)$%,7,%0.,-.-%,"".:)-#/.'+.:&1%#?3'&$# $'(21%)%,'+)".-,(1")%,'+-.%'.2&#/,$%.%4#.)$%1)".240-,$)".:#4)7,'&.'3.#"'#$%&'()*+#%,$.@!AB /#7,$#-5.C4#-#.%,(#?$'+-1(,+*.-,(1")%,'+-.)&#.&#2#)%#/;.$4)+*,+*.%4#./#7,$# $4)&)$%#&,-%,$-.1+%," .-)%,-30,+*.-%&,$%#&.-2#$,D$)%,'+-.'3.#(#&*,+*.,+3'&()%,'+.)+/ $'((1+,$)%,'+-.%#$4+""*,#-5 !E$,#+%.(,$&'<)7#.$,&$1,%.)+/.)+%#++)./#-,*+.,-.-%,"".)+.'2#+.2&':"#(5.F#7#&)".)/? 4'$.%#$4+,G1#-.)&#.)7),"):"#.3'&.#)$4.!A./#7,$#;.('-%.'3.%4#(.:)-#/.'+.)22&'H,()%,'+-5 I'<#7#&;.%4#.$1&&#+%.!A./#-,*+-.)&#.$4)""#+*,+*.#+'1*4.%'.1-#.)22&'H,()%#./#-,*+ (#%4'/""*,#-.)+/.$'-%"'0.31""?<)7#.'2%,(,J)%,'+."'"2-;.%02,$)""0.1-,+*.$'((#&$,)".!A -'3%<)&#;.)&#.#(2"'0#/.,+-%#)/5 6+.%4,-.<'&=.<#.2&'2'-#.%'.1-#.$'(21%)%,'+)".#"'#$%&'()*+#%,$-.@K!AB.)-.)+.)$%1)" /#-,*+.%"";.&)%4#&.%4)+.L1-%.)+.)+)"0-,-.'+#5.C4,-.$)+.:#.)$4,#7#/.:0.-4&,+=,+*.K!A.,+%').-,(2"#.2)&)(#%#&,J#/.#G1,7)"#+%.$,&$1,%.3'&(;.3&'(.<4,$4.)+.#"'#$%&,$)".#+*,+##&.$)+.*#%)$%,'+):"#./#-,*+.,+-,*4%-5 M1(#&,$)".$'/#-;.-1$4.)-.D+,%#?#"#(#+%.)+/.,+%#*&)".#G1)%,'+?:)-#/.-"'7#&-;.2&'7,/#).&#",):"#.)+/.)$$1&)%#.2&#/,$%,'+.'3.#"'#$%&'()*+#%,$-;.:1%.)%.%4#.#H2#+-#.'3.#H%&#(#"'0 ")&*#.$'(21%)%,'+)".%,(#.-,+$#.)+.#H%&#(#"'0.")&*#.()%&,H.-0-%#(.4)-.%'.:#.-"'7#/5.N

('/#"'?'&/#& . &#/1$%,'+ . @AO8B . %#$4+,G1# . ,- . $)2):"# . '3 . -4&,+=,+* . %4#-# . ")&*# . ()%&,H
-0-%#(-.,+%'.).3),&"0.-()""?-,J#.&#/1$#/.()%&,H.-0-%#(;.<4,$4.,-.-()"".#+'1*4./#2#+/,+*
'+.%4#.1+/#&"0,+*.#"#$%&'()*+#%,$.$'(2"#H,%0.'3.%4#.'&,*,+)".-0-%#(5.6+.'%4#&.<'&/-;.%4#
#"#$%&'()*+#%,$.,+3'&()%,'+.,-.$'(2&#--#/.%'.%4#.(,+,(1(.-,J#.:0.(#)+-.'3.AO85.C4,-
,-.).41*#.)/7)+%)*#.)-.%4#.#"#$%&'()*+#%,$.&#-2'+-#.$)+.+'<.:#.':%),+#/.,+.&#)".%,(#5
N+0 . #"#$%&'()*+#%,$. /#7,$#; . &)+*,+* . 3&'(. (,$&'<)7# . $,&$1,%-; .)+%#++)- . %' . -,",$'+
24'%'+,$-.,-.:)-#/.12'+.%4#.12&,-,+*.'3.%4#./'(,+)+%.#"#$%&'()*+#%,$.#,*#+('/#-.PQR
<4,$4; . ,+ . %1&+; .)&# . :1,"% . 12 . :0 .)/#G1)%#"0 . 21%%,+* . '"$)" . &#-'+)%'&- . '& . '"$)" . ('/#-
%'*#%4#&; . <,%4 .) . -2#$,D$. $'12",+* . %'2""*0 . PSR5 . T&,+*,+* .)"" . %4#-# . '"$)" . &#-'+)%'&-
%'*#%4#& . <,%4 . %4# . -2#$,D$. ,+%#&)$%,'+ .)('+* . %4#(. ,- .)% . %4# . 4#)&% . '3 . $)&&0,+* . '1%
#"#$%&'()*+#%,$./#-,*+.PUR5.I)7,+*.$'+%&"'.'7#&.%4#-#.'"$)".&#-'+)%'&-.,-.,+/##/.%4#.=#0
)+/.G1)+%,30,+*.%4#,&.$'12",+*-.,-.).$4)""#+*,+*.2&':"#(.,+.#"#$%&'()*+#%,$-.PVR5
C4,- . <'&= .),(- . %' . D+/ . '1% . +#< . #E$,#+% . -0+%4#-,- .)+/ . /#-,*+ . %#$4+,G1#- . 3'&
(,$&'<)7#.$,&$1,%-.)+/.)+%#++)-.:0.(#)+-.'3.)/7)+$#/.K!A.$'/#-.%'.-"'7#.A)H<#""W-
#G1)%,'+-.+1(#&,$)""0;.3'$1-,+*.'+.$'12"#/?&#-'+)%'&.!A.$,&$1,%-5.M'%.'+"0.%4#.KX>.%,(#
,+.!A.-,(1")%,'+-.+##/-.%'.:#.&#/1$#/;.:1%.)"-'.%4#.+1(:#&.'3.)+)"0-#-.<,%4,+.%4#
'2%,(,J)%,'+.""2.1+%,".)+.!A./#-,*+.,-.':%),+#/5
Y#.-4'<.)+.#"#$%&'()*+#%,$)""0.*#+#&)%#/.$'12",+*.()%&,H.3'&.$'12"#/?&#-'+)%'&
(,$&'<)7#.$,&$1,%-.:0.(#)+-.'3.).-,+*"#.31""?<)7#.-,(1")%,'+5.C4,-.&#-1"%.2&'7,/#-
7)"1):"#./#-,*+.,+3'&()%,'+5.F#7#&)".)22",$)%,'+-;.-1$4.)-.(,$&'<)7#.D"%#&-;./,2"#H#&-
)+/.)+%#++)-;.<,"".-4'<.%4#.$)2):,",%,#-.'3.%4,-.+#<.%#$4+,G1#./1&,+*.%4#.2&#-#+%)%,'+5.

!"#"$"%&'"
KH Z5./#.").81:,).)+/.A5.A&'J'<-=,;.[N.$'(2)$%.:)-,-.3'&.&#",):"#.3)-%.3&#G1#+$0.-<##2.7,).%4#.
&#/1$#/?:)-,-.(#%4'/;\.6!!!.C&)+-5.A,$&'<)7#.C4#'&0.C#$45;.7'"5.]];.+'5.Q^;.225.VU]_`VUaS;.
S^Qa5
%H Z5./#.").81:,);.bc#-$&,2%,'+.'3.A,$&'<)7#.K,&$1,%-.7,).%4#.8#/1$#/?T)-,-.A#%4'/.d,7,+*.
X40-,$)".6+-,*4%;b.,+. 6!!!.C&)+-)$%,'+-.'+.N+%#++)-.)+/.X&'2)*)%,'+ ;.7'"5._^;.+'5.QQ;.225.Q^eeV?
Q^e]a;.M'75.S^SS5
'H Z5./#."). 81:,); . b!A?T)-#/.c#-,*+.'3.A,$&'<)7#.9,"%#&-.)+/.c,2"#H#&-f.91""?Y)7#.K'12",+*
A)%&,H.)+/.6%-.M)&&'<:)+/.K'1+%#&2)&%;b .S^SS.eS+/.!1&'2#)+.A,$&'<)7#.K'+3#&#+$#.@!1AKB ;
A,")+;.6%)"0;.225.]^?]U;.S^SS5
LH Z5./#."). 81:,)5.@S^S UB.91""?<)7#.$'12",+*.()%&,H.&#-1"%-.,+.ANCgNT5.PO+",+#R5.N7),"):"#f
4%%2-fhh/&,7#512(5#-h-h$+Ci#jL&ik-H(:l

Review of patch antennas for wireless applications using inkjet printing technique

0RKDPDG +RVHLQ 5DVKPDQHVK 3LURXWLQL\D 0DVDVR 0DQXHO /XLV 0DVDQD (QULTXH 0iUTXH] 6HJXQGR *XDUGR 0DUFRV *DUFtD &yUFROHV $ &5X]]]

[1] Group of Radio Frequency, Circuits, Antennas and Systems (RFCAS), Department of Electronics and Communication Technologies, Universidad Autonoma de Madrid, 28049, Madrid, Spain, {mohamad.rasekhmanesh, asrin.piroutiniya }@estudiante.uam.es, {joseluis.masa, eduardo.garcian, juan.corcoles, jorge.ruizcruz }@uam.es

[2] Telecommunication Research Institute (TELMA), E.T.S. Ingeniería de Telecomunicación, Universidad de Málaga, 29016 Málaga, Spain {ems}@ic.uma.es

Abstract: This study focused on a double stacked array antenna with patch elements disposed linearly and circularly. Using the inkjet printing method, the single patch antenna was created for the 5 GHz band. The goal is to print conductive silver ink on a thin Kapton film to produce microstrip lines. High impact polyester (HIPS) is utilized as a substrate to secure the Kapton layers, which increases the impedance bandwidth while also enhancing mechanical stability.

Antenna design

Fig. 1 shows the suggested method for introducing a double stacked patch antenna that is described in [1]. Although this technique increases overall thickness, it improves antenna width in terms of impedance matching, which makes it worthwhile to use. As per the manufacturer [2], the electric constant of the HIPS and Kapton substrates are 2.4 and 3.4 respectively.

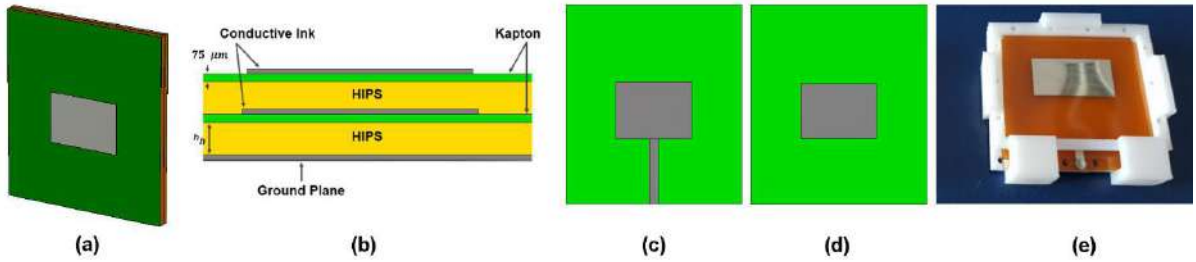

Fig. 1) Stacked patch antenna configuration a) Perspective view, b) side view of the antenna including ground plane, conductive ink, Kapton and HIPS substrate, c) front view of the bottom layer and d) top layer, e) manufactured antenna.

In a subsequent step, the idea of designing a stacked linear array antenna was discussed based on the proposed design principles. The proposed antenna's ultimate design is displayed in Fig. 2. As shown in this figure, the first layer includes the feeding network, which is intended to excite eight radiating patches. In order to obtain a compact design and enhance the impedance matching, double quarter-wavelength (λ/4) transmission lines with a corner cut T-junction power divider were used in each step of this feeding network.

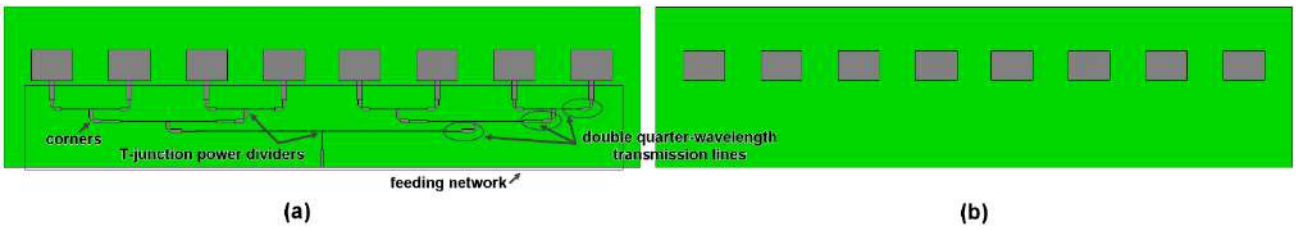

Fig. 2) Front view of the stacked linear array antenna including the a) bottom and the b) top layers.

So far, the concept of a directional stacked antenna design employing a combination of the inkjet printing method to put the silver conductive ink on Kapton films and the 3D printing method to manufacture the HIPS has been presented. This approach has a lot of potential, so it might be used to include more complex structures. An example is the omnidirectional antenna design, which is covered in more detail in this section.

It has always been fascinating to think of conformal array antennas as small, inexpensive structures. The orientation of the elements, as the primary distinction between conformal and linear array antennas, makes it feasible to obtain an omnidirectional radiation pattern in the azimuth plane with this arrangement of the radiating elements. The formulation for an N-placed prism is taken from [3] and is as follows:

$$E_{total}(\theta,\phi) = E_{element}(\theta,\phi) \sum_{n=1}^{N} A_n e^{j(kr\sin\theta\cos(\phi-\phi_n)+\alpha_n)}$$

Where $E_{total}(\theta,\phi)$ shows the conformal array antenna's radiated field, $E_{element}(\theta,\phi)$, A_n, and α_n represent, respectively, the radiated E-field, feeding amplitude, and phase of the n^{th} single radiating element, and N is the radius of the circle, which also points to the distance between the center of the circle and the center of each element. Accordingly, an initial idea of presenting a conformal array antenna by bending the concept that is presented in Fig. 2 based on designing a linearly stacked array antenna with eight elements has been shown in Fig. 3.

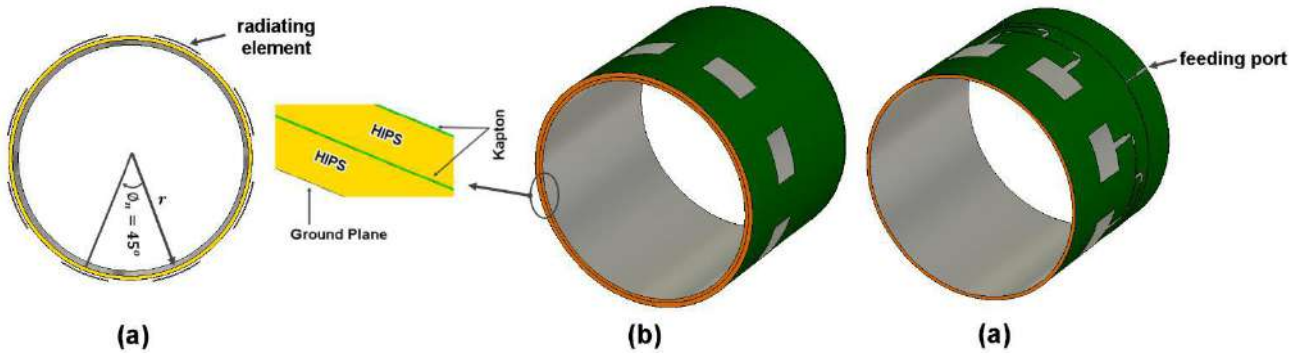

Fig. 3) Stacked conformal array configuration. a) front view, b) perspective view of the top layer and c) perspective view of the bottom layer.

References

1. E. García-Marín, E. Márquez-Segura, P. Sánchez-Olivares, J. L. Masa-Campos, J. A. Ruiz-Cruz and C. Camacho-Peñalosa, "Implementation of Stacked 3D Printed Antennas for Wireless Applications," 2019 International Microwave Workshop Series on Advanced Materials and Processes for RF and THz Applications (IMWS-AMP), pp. 151-153, 2019.
2. M. Pérez-Escribano and E. Márquez-Segura, "Parameters Characterization of Dielectric Materials Samples in Microwave and Millimeter-Wave Bands," IEEE Transactions on Microwave Theory and Techniques, vol. 69, pp. 1723-1732, 2021.
3. P. Sánchez-Olivares, P. P. Sánchez-Cancausa and J. L. Masa-Campos, "Circularly Polarized Omnidirectional Antenna Array Formed by Stacked Printed Dipoles," IEEE Antennas and Wireless Propagation Letters, vol. 16, pp. 2253-2256, 2017.

Stereolithography to generate OAM waves using dielectrics.

M.A. Balmaseda-Marquez[1*], S. Moreno-Rodriguez[1], ç . Palomares-Caballero[1], C. Molero, J.F. Valenzuela-ValdŽs[1], P. Padilla[1]

[1*]Department of Signal Theory, Telematics and Communications, Universidad de Granada (CITIC-UGR), 18071 Granada, Spain
*corresponding author: migbalmar@ugr.es

Abstract: Metal prototypes has always played an important role, with low tolerances and fulfilling the high standards of investigation [1]. 3D printing is emerging as an alternative with technologies such as stereolithography. In this work it will be seen the application of this technique in the fabrication of dielectric transmitarrays (TA) with the capability of producing orbital angular momentum waves (OAM).

Summary:
Orbital angular momentum waves were proposed by Allen et al in 1992 [2]. This type of wave has different modes, which are orthogonal one another when the mode differs. Since then, the generation of this modes have been pursued, being the multimodal generation the principal target. Many ways of creation have been achieved in previous years using high-cost systems as multi-arrays antennas or monolithic metallic prototypes [3]. Stereolithography emerged as a solution to create 3D printed devices in dielectric with the capability of generate OAM.

Stereolithography (SLA) emerged during the 1970s as a system that can build 3D objects by two intersecting radiation beams through both photochemically cross-linking or degrading polymers [4]. The process begins with an STL file, by slicing it the 3D model is converted to 2D slices that contain the information needed to generate each layer. The fundament of this process is the curing reaction of resins, this reaction is initiated by supplying the energy of UV light and it occurred two stages during the curing: gelation and vitrification. The [5] gelation is a transition between the liquid resin to a rubber state. Then, the vitrification occurred, being a reversible process that leads to the transition from rubber to a glassy solid [6] in

The choice of this technique to our problem is not trivial. After a careful design studying the phase shift introduce by each part of the cell, the unit cell presented in Figure 1 is developed:

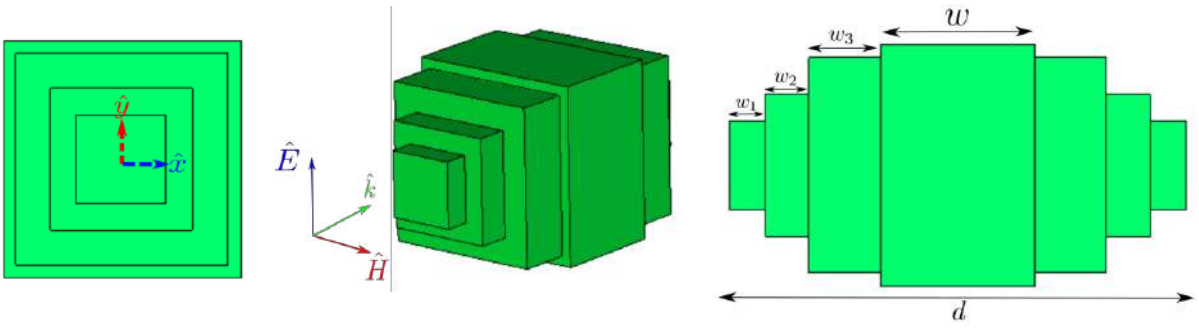

Fig.1 Front (left), perspective (center) and side (right) view of the unit cell proposed.

While the dimension & F D Q Y D U 42 mm Ut R 4.38mm (to introduce different phase shifts) G L P H Q V L R Q V & & D U H d, being [Hits function to adapt the impedance to the dielectric. The goal was to obtain four different phase shifts in order to have a 2 configuration. With this unit cell we create a transmitarray (40x40) which has the ability to generate OAMs. Our choice of material was the Grey V4 with a permittivity of Er = 2,6.

Once the final design is decided and the STL file is generated, it is used the Formlabs 3 [7] to 3D print our model. The W R O H U D Q F H R I R X U S (X Q L Q D Q W) a Q G the Layer Thickness about 50m. This kind of machine use low force stereolithography. In this type of SLA, the printer uses a flexible film which bows gradually as the part is lowered, reducing the pressure in the overall system. It is important to set a correct arrangement of supports depending on the type of geometry we have. For example, if the structure has gaps or hollow parts, it is needed to correct the possible deviations of the printing. When the printing is done, a post processing must be carried out, depending on the material used. First of all, the prototype must be washed to remove any resin residues. Then, the cured, leaving it the time needed to entangle the polymer. Some results of final results can be seen in Fig. 2. We expect to obtain a flat TA with the capability of generate a certain OAM mode.

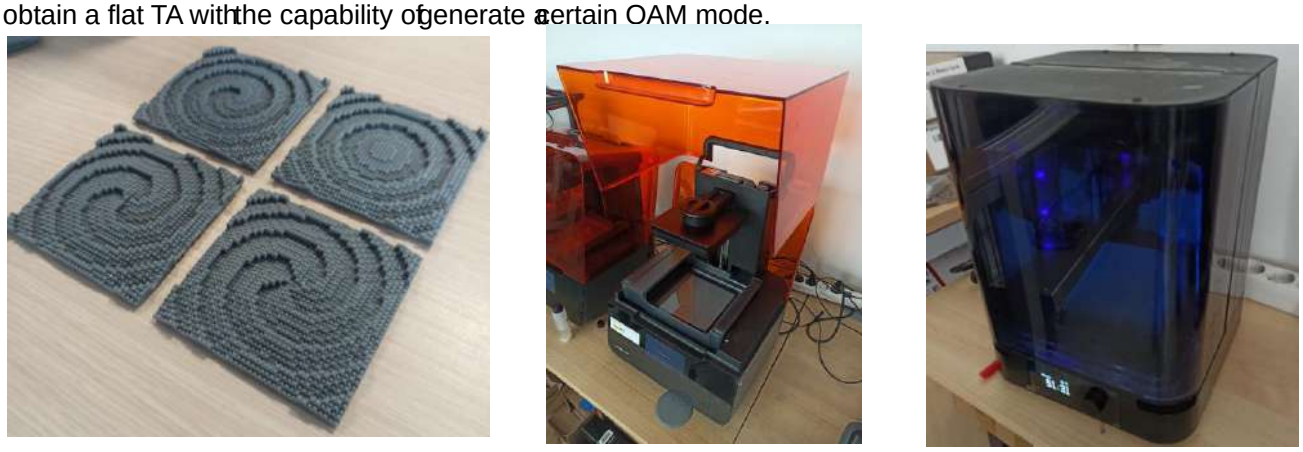

Fig. 2. Several OAMs lenses (left). Formlabs 3 (middle) and curing machine (righ

References

1. Ahmed, N. (2019). Direct metal fabrication in rapid prototyping: A review. Journal of Manufacturing Processes, 42, 167–191. doi:10.1016/j.jmapro.2019.05.001
2. / $ O O H Q 0 : % H L M H U V E H U J H Q 5 6 S U H H X Z D Q G - : R H U G H P D Q ³ 2 transformation of Laguerre-' D X V V L D Q O D V H U P R G H V ´ 3 K \ V L F D O 5 H Y L H Z $ Y R O
3. Zhang, Wang, Yuan, & Burokur (2020). A Review of Orbital Angular Momentum Vortex Beams Generation: From Traditional Methods to Metasurfaces. Applied Sciences, 10(3), 1015. doi:10.3390/app10031015
4. Huang, J., Qin, Q., & Wang, J. (2020). A Review of Stereolithography: Processes and Systems. Processes, 8(9), 1138. doi:10.3390/pr8091138
5. Olayan, H.B.; Hami, H.S.; Owen, E.D. Photochemical and Thermal Crosslinking of Polymers. J. Macromol. Sci. Part C Polym. Rev. 1996, 36, 679–719.
6. Cadenato, A.; Salla, J.M.; Ramis, X.; Morancho, J.M.; Marro, L.M.; Martin, J.L. Determination of gel and vitrification times of thermoset curing process by means of TMA, DMTA and DSC techniques. J. Therm. Anal. 1997, 49, 269–279
7. Formlabs (8 March 2023). Introducing the Form 3 and Form 3L, Powered by Low Force Stereolithography https://formlabs.com

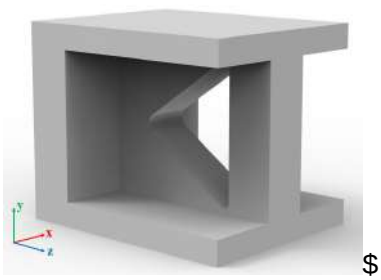
P
P
T
T/2
D
T
h
r1
r2
r1
z1
z2
x
y
z

7KH 0DQXIDFWXULQJ 0HWKRGV &RPSDULV
D .D ± %DQG 6ORWWHG :DYHJXLGH $QW

$OLFMD 6FKUHLEHU *DEOHU

0LFURZDYH DQG 5DGDU ,QVWLWXWH *HUPDQ $HURVSDFH &HQWH
$OLFMD 6FKUHLEHU#GOU GH

$EVWUDFW

7KLV SDSHU GHVFULEHV WKUHH PDQ W WKH H[DPSOH RI D VLQJOH .D ± EDQG VC P 7KH GHVLJQHG IRU DQ DLUERUQH V\QWKH G SURWRW\SH UHIHUHQFH LV PDFKLQH H ZLWK VDPSOHV RI WZR GLIIHUHQW H DQWHQQDV DUH IDEULFDWHG DQG F V ZHOO DV WKH HOHFWURPDJQHWL H PDQXIDFWXUHG DQWHQQDV DUH LC KDO UHVXOWV DUH VKRZQ DQG FRPSDU VLPXODWHG GDWD

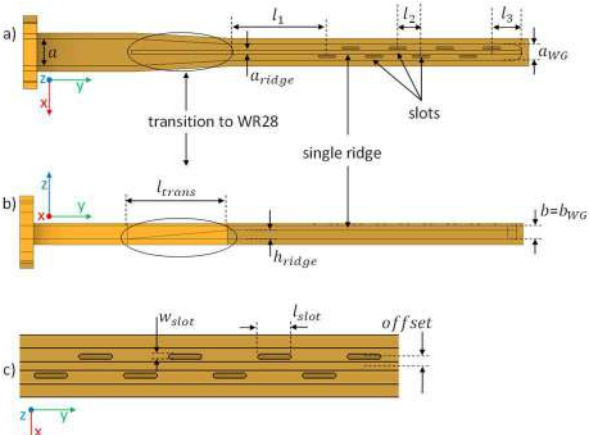

,QWURGXFWLRQ

7KHUH DUH PDQ\ GLIIHUHQW PHWKRG [illegible] DQG QHZ RQHV DUH VWLOO EHLQJ GLVFRYHUHG VLQFH WKH WHFKQLFDO SRVVLELOLWLHV FRQWLQXRXVO\ LPSURYHG LQ WKH UHFHQW \HDUV 7KHVH LQFOXGH DERYH DOO DGGLWLYH PDQXIDFWXULQJ DGYDQWDJHV RYHU FRQYHQWLRQDO PHWKRGV > @ > @ 7KLV WHFKQLTXH RIIHUV WKH SRVVLELOLWLHV RI FUHDWLQJ VRSKLVWLFDWHG JHRPHWULHV SURGXFLQJ YHU\ VPDOO VWUXFWXUHV DV ZHOO DV SRWHQWLDO PDQXIDFWXULQJ VDYLQJV DQG KDQG OLNH DQ\ RWKHU PDQXIDFWXULQJ WHFKQLTXH WKLV SURFHVV LV WKH FKDOOHQJH RI DFKLHYLQJ KLJK VXUIDFH TXDOLW\ DQG D VPRRWK VXUIDFH 7KH PDLQ SDUW VLJQL RI WKH SULQWHG FRPSRQHQWV WKDW YDU\ LQ VL]H DQG DOVR EH DFKLHYHG LVVXH VLQFH SULQWHU\ KDYH OLPLWHG DYDLODELOLW\ ZRUNVSDFH ZKLFK LV PRVWO\ VPDOOHU WKDQ WKDW LQ DGGLWLRQ WKH PDWHULDO SURSHUWLHV RI WKH GLVWULEXWLRQ ZLWK HDFK VORW SR

,Q RUGHU WR YHULI\ WKH XVDELOLW\ DQG SURSHUWLHV DQWHQQDV LQ KLJKHU IUHTXHQF\ EDQGV VORWWHG ZDYHJXLGH DQWHQQD 6:$ LV GHVLJQHG DQG IDEULFDWHG XVLQJ WKH ' VHOHFWLYH ODVHU VLQWHULQJ 6/6 SURFHVV ZLWK EROWK PHWDO DQG V\QWKHWLF PDWHULDO DQG FRPSDUHG ZLWK D EUDVV SURWRW\SH ZDYHJXLGH ZKLFK LV VHW WR WKH ZDYHOHQJWK ,Q RUGHU WR EH DEOH WUDQVLWLRQ IURP WKH VLQJOH ULGJH :5 KDV DOVR EHHQ GHYHORSHG

$QWHQQD XQGHU WHVW

7KH $87 LV DQ VORW HQG IHG VLQJOH ULGJH VORWWHG ZDYHJXLGH DQWHQQD PDGH LQ D VWDQGLQJ ZDYH FRQILJXUDWLRQ DQG GHVLJQHG IRU D FHQWUH IUHTXHQF\ RI > @ LOOXVWUDWHV WKH VLPXODWLRQ PRGHO RI WKH GHVLJQHG DQWHQQD 7 ORQJLWXGLQDO VORWV DUH DUUDQJHG LQ D EURDG ZDOO RI WKH ZDYHJXLGH LQ VXFK D ZD\ WKDW WKH FXUUHQW IORZ LV LQWHUUXSWHG UHVXOWLQJ LQ D SRWHQWLDO GLIIHUHQFH WKDW XOWLPDWHO\ FDXVHV VORWV WR UDGLDWH

7DEOH 7KH SDUDPHWHUV RI VLPXODWHG QDQWHQQD PRGHO

3DUDPHWHU	9DOXH	'HVFULSWLRQ
=	PP	6WDQGDUG :5 ZL(
>		6WDQGDUG :5 KH(
=ÐÀ	PP	:DYHJXLGH ZLGWK
>ÐÀ	PP	:DYHJXLGH KHLJKW
=åÜ×ÚØ	PP	5LGJH ZLGWK
[åÜ×ÚØ	PP	5LGJH KHLJKW
æßâç	PP	6ORW OHQJWK
Sæßâç	PP	6ORW ZLGWK
IÐÔßß	PP	:DOO WKLFNQHVV
KBB	PP	6ORW RIIVHW WR WKH PLGGOH OI
ë	PP	,QSXW OHQJWK
ê		'LVWDQFH EHWZHHQ %WZDVV VC
ì		'LVWDQFH WR WKH ZDYHJXLG(
çåÔáæ	PP	7UDQVPLVVLRQ OHQJWK

7KH GHPDQGV RQ WKH PDQXIDFWXULQJ SURFHVVHV LQFUHDVH ZLWK IUHTXHQF\ 7KLV LV EHFDXVH WKH GLPHQVLRQV RI WKH FRPSRQHQWV WR EH SURGXFHG DUH LQ WKH PLOOLPHWHU UDQJH IURP WKH OLVWHG GDWD $ UHGXFWLRQ LQ DQWHQQD SHUIRUPDQFH DOUHDG\ FDXVHG E\ VPDOO GHYLDWLRQV IURP WKH VSHFLILHG JHRPHWU\ RU VXUIDFH LPSHUIHFWLRQV LQVLGH WKH ZDYHJXLGH 7KHUHIRUH ORZ IDEULFDWLRQ WROHUDQFHV DUH DQ HVVHQWLDO UHTXLUHPHQW IRU WKH PDQXIDFWXULQJ SURFHVVHV $QRWKHU SRLQW LV WR PDNH WKH DQWHQQD IURP DV IHZ FRQQHFWLRQ LV D SRWHQWLDO VRX LQDFFXUDWH MRLQLQJ)XUWKHUPR FRQVLGHUHG GXULQJ WKH SURGXFW

$V PHQWLRQHG LQ SUHYLRXV VHFWL DLUERUQH DSSOLFDWLRQ > @ ,Q SURFHVVHV KDV WR PHHW DGGLWLRQD WRWDO ZHLJKW RI WKH DQWHQQD , RI DOO V\VWHPV XVHG LV HYHQ\ GL ZLWK DHURG\QDPLFV +RZHYHU DV UDQJH DUH UDWKHU VPDOO WKLV WKH GHVLJQ SURFHVVHV $ YHU\ LPSR DQG VWUHQJWK RI WKH PDWHULDO GLIIHUHQW IRUFHV DQG YLEUDWLRQV RI HQYLURQPHQWDO FRQGLWLRQV RI YDU\LQJ GXULQJ WKH IOLJKW DQG PLVVLRQ ,Q WKLV ZD\ WKH DQWHQQD VDPH SHUIRUPDQFH XQGHU GLIIHUHQW PXVW EH QR FRUURVLRQ RU GHIRUPDWLRQ GLIIHUHQFHV RU DLU KXPLGLW\

7HFKQRORJ\

,Q WKLV VHFWLRQ WKUHH GLIIHUHQW IDEULFDWLRQ WHFKQLTXHV DUH SUHVHQWHG IRU SURGXFLQJ WKLV DQWHQQD XQGHU WHVW

QD PLOOLQJ SURFHVV WKH PDWHUL SHFH XQWLO D GHVLUHG JHRPHWU\ URWDWLQJ WRRO ZLWK JHRPHWULFDO XVHG WR UHPRYH PDWHULDO KLJK GLPHQVLRQDO DFFXUDF\ ZLWK — P DQG SURGXFHV SDUWV ZL SURSHUWLHV +RZHYHU PLOOLQJ PDF NH\ GHVLJQ OLPLWDWLRQV LQFOXGL KROGLQJ RU PRXQWLQJ SOQWV DV Z VTXDUH FRUQHUV GXH WR WRRO JHR HYHQ LPSRVVLEOH WR PDQXIDFWXUH DV WKH WRROV DUH QRW DEOH WR DF RWKHU KDQG PLOOLQJ PDFKLQHV F VPRRWKHU VXUIDFHV WKDQ ' SULQWH IDFWRU IRU KLJK IUHTXHQF\ DSSOLFD

)LJ GHSLFWV D VDPSOH RI WKH $87 06 EUDVV XVLQJ DQ LQ KRXVH ZRUN 0DVV LV DQ DOOR\ RI FRSSHU DQG JRRG FRUURVLRQ UHVLVWDQFH GXFW 7KH YDOXH RI WKH HOHFWULF FRQGXF RI WKH DOOR\ DQG GHFUHDVH)RU WKH KHUH SUHVHQWHG DQWHQQD ê¼èÓá7=É Ô7 Ls sw Hsr 5 I :LWK WKLV WHFKQ VORWWHG ZDYHJXLGH DQWHQQD FDQ WRWDO DQWHQQD LV WKHUHIRUH PL VRQGHUHG WR HDFK RWKHU LQ DYSH SDYWH QR FQHDQ 60'47/)3 7 FHQDW WKH HOHFWULF ILHOG DW WKH DSHUWXUH RI XQZD DQWHQQD DUH MRLQHG WR RUGHU WR SURGXFH $QRWKHU SRLQW LV WKH PDWHULDO

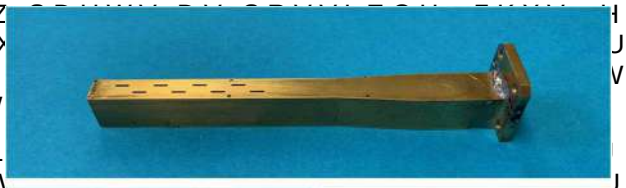

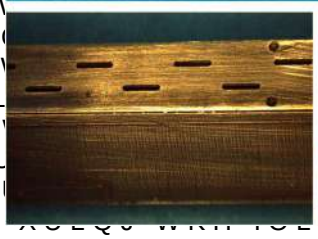

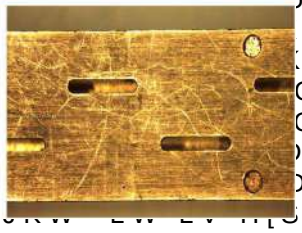

)LJXUH 7KH DLUERUQH FDPSDLJQV DUH SLFWXUHV RI WKH DQWHQQD SURWRW SDUWV OLVWHG LQ WKH 7DEOH

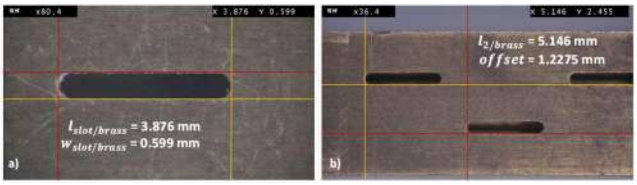

)LJXUH 7KH PLFURVFRSH YLHZV
DQWHQQD ZLWK WKHLU JHRPHWULF

+RZHYHU XQGHU WKH DVVXPSWLR
V\PPHWULFDOO\ WR WKH FHQWHUOL
EHWZHHQ WKH HGJHV RI RSSRVLWH
FRXQWV XQGHU WKH SUHUHTXLVLW
WZLFH WKH RIIVHW UHVXOWLQJ G
VLPXODWHGKSBUDPHWHU

' 6/6 0HWDO 3ULQW

7KH ' SULQWLQJ WHFKQRORJ\ LV DQ DGGLWLYH PDQXIDFWXULQJ
SURFHVV ZKHUH FRPSRQHQWV DUH EXLOW OD\HU E\ OD\HU
QXPHURXV ZD\V WR SURGXFH SDUWV XVLQJ WKLV WHFKQRORJ\
GLIIHU IURP WKH W\SH RI VXEVWDQFH IRU EXLOGLQJ FRPSRQHQWV
DQG PRUHRYHU WKH PDQXIDFWXULQJ SURFHVV LWVHOI
PDWHULDOV IRU ' SULQWLQJ DUH SODVWLFV V\QWKHWLF UHVLQV
FHUDPLFV DQG VSHFLDOO\ SURFHVVHG PHWDOV
7KH SUHVHQWHG DQWHQQDV DUH PDGH E\
6/6 SURFHVV ZKHUH D SRZGHU\ PDWHULDO LV
GHVLUHG VKDSH E\ ODVHU VLQWHULQJ
' SULQWLQJ OD\HU KHLJKW GHWHUPLQHV WKH
SULQWHG VXUIDFH DQG WKH PLQLPXP IHDWXUH VL]H
FDQ SURGXFH 7KH PLQLPXP ZDOO WKLFNQHVV RI 6/6
SDUWV LV OLPLWHG E\ WKH VL]H RI
WROHUDQFHV DUH W\SLFDOO\ “
LVVXH IRU FRPSRQHQWV RI YHU\ VPDOO JHRPHWULHV
6LQFH WKLV SURFHVV DOORZV PDQXIDFWXULQJ FRPSRQHQWV
RQH SLHFH LW LV LGHDOO\ VXLWHG IRU KLJKO\
RSWLPL]HG JHRPHWULHV +RZHYHU
UHTXLUHPHQWV RI WKH $87 GHVLJQ
LPSRVVLEOH WR DFKLHYH D WKLFNQHVV RI
FROODSVH DORQJ LWV OHQJWK 7KHUHIRUH WKH PRGHO RI WKH DQWHQQD
LV PRGLILHG EHIRUH SULQWLQJ 7KH IURQW RI WKH DQWHQQD LV
WKHUHIRUH WKLFNHQHG WR PP
FKDQJH LQ WKH LPSHGDQFH RI WKH DQWHQQD
GLPHQVLRQV RI WKH VORWV DQG WKH
WR DFKLHYH WKH GHVLUHG SHUIRUPDQFH
RI WKH ' SULQWHG DQWHQQDV DUH

7DEOH 7KH PRGLILHG SDUDPHWHUV IRU ' SULQW SURFHVV

3DUDPHWHU	9DOXH	'HVFULSWLRQ
$l_{ÐÔßß}$	PP	:DOO WKLFNQHVV
æßâç	PP	6ORW OHQJWK
$S_{æßâç}$	PP	6ORW ZLGWK
KBB	PP	6ORW RIIVHW WR WKH Ol
ϵ		'LVWDQFH EHWZHHQ VC

7KH ' PHWDO SULQWHG DQWHQQD ZK
LV PDGH IURP ,QFRQHO D SUHFLSL
FKURPLXP DOOR\

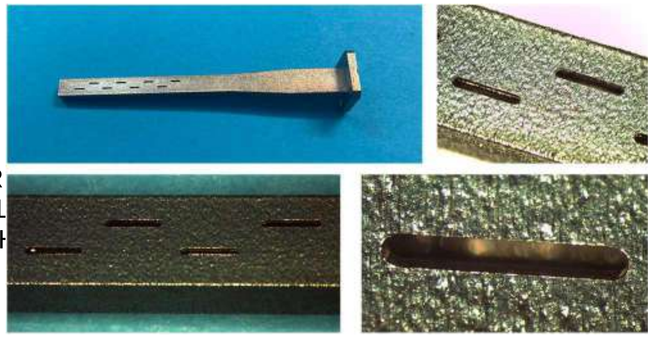

)LJXUH 7KH IDEULFDWHG ' PHWDO
HQODUJHG YLHZV

7KH ,QFRQHO KDV DQ H[FHOOHQW PHF
DQ RSWLPDO FRPELQDWLRQ RI KLJK
ZRUNDELOLW\ XVLQJ WKLV WHFKQRORJ\
PDWHULDO LV VXLWDEOH IRU EXLOGLQJ FRPSRQHQWV
KHDWHG WKH PDWHULDO IRUPV D
SURWHFWV WKH VXUIDFH +RZHYHU
YLHZ E\VXFK D OD\HU DFWV DV DQ LV
FRQGXFWLYH ORVVHV 7KH H[DFW YDOXH
RI DQ\ DOOR\ LV GLIILFXOW WR GHWHUPLQH
PDWHULDO LV EURXJKW LQWR WKH DGGLWLYH
FRPSRVLWLRQ RI WKH PHWDOV
WKLV ZRUN LV PDLQO\ FRPSRVHG RI
UHVXOWLQJ LQ DQ HOHFWULF FRQGXFWLYLW\
DQ\ XQNQRZQ VXUIDFH URXJKQHVV
DWHQQD LV VXSSRVHG WR EH RQH
VORWV ZKHUH SULQWHG DV PHWDO
7KHUHIRUH WKH VORWV DUH PDFKLQHG
RI D PLOOLQJ PDFKLQH +RZHYHU LW
WKLV SURFHVV LV D SRWHQWLDO VRXUFH
RI DQ\ PRGHO DIWHU PDQXIDFWXULQJ
HIIHFW SRVLWLRQ RI WKH VORWV ,W
LPSRVVLEOH WR DFKLHYH D IODW VXUIDFH
RI PP WKDW GHHS HQRXJK WR
FRQQHFWLRQ WR WKH PRGHO RI WKH DQWHQQD
)LJ D LOOXVWUDWHV WKH HQODUJHG
6LQFH WKLV SURFHVV UHVXOWV LQ D
PDQXIDFWXUHG PHWDO SULQWHG D
GLPHQVLRQV 7KH SRVLWLRQ RI WKH
DUH VHHQ LQ)LJ E 7KH VKDSH RI WKH
GHYLDWH VRPHZKDW IURP WKH YDOX
VXPPDUL]HG LQ 7DEOH
VSHFLILFDOO\ WKH OHQJWK RI WKH VO
FHQWHU OLQH RI WKH ZDYHJXLGH DII
ZDYH LV FRXSOHG LQWR WKH VORWV
GLPHQVLRQDO LPSHUIHFWLRQV UHVXO
GHJUDGDWLRQ

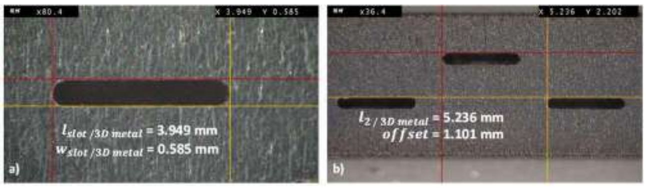

)LJXUH 7KH PLFURVFRSH YLHZV RI
SULQWHG DQWHQQD ZLWK WKHLU JHR

' 6/6 6\QWKHWLF 0DWHULDO 3ULQW 0HDVXUHPHQW YV VLPXOD

7KH ' V\QWKHWLF PDWHULDO SUL 7WHG DQWHQQD DLV DPDLQHQ IURP D FW
3$ ZKLFK LV D YHUVDWLOH VWUXFWXUH DQG GXH WR LWV KHUPRSODVWLF V\VWHP
DOVR FDOOHG 1\ORQ 7KH DQWHQQD WR HV /5 RDWHG ZLWK D JDQ GDQL,QVV
SURFHVV ZLWK D FRSSHU VKHHW RQ GLDWWHQVLDO PDG
VXIILFLHQW ZLWK UHJDUG WR VNLQ HIIHFW GHDO PDQ
FRSSHU FRDWHG DQWHQQD IRU WKH DQWHQQD EHQHILWV
HTXDO WR —P $PRQJ WKH PL
PDQXIDFWXULQJ WKH DQWHQQDV LQ
VKRZV WKH KLJKHVW YDOXH IRU
RIêL wzHsr 5 I ,Q RUGHU WR SURS
FRSSHU UHVLGXHV IURP WKH DQWH
WR WKH DQWHQQD¶V VLGH ZKLFK
WKHLU IXQFWLRQDOLW\ ,Q WKH
' WKHUPRSODVWLF DQWHQQD LV G

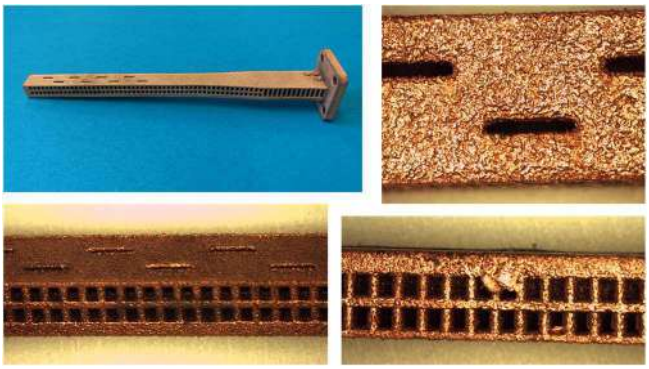

)LJXUH 7KH IDEULFDWHG ' 6/6 SULQWHG V\QWKHWLF PDWHULDO
DQWHQQD DQG LWV HQODUJHG YLHZV

$V FDQ EH VHHQ IURP WKH SLFWXUH
LQ VRPH SODFHV LQ WKH DQWHQQD
DIWHU WKH JDOYDQLF SURFHVV ZLWK
OD\HU ,Q FRQWUDVW WR PDWHULDO
SURFHVV WKDW EHFRPH EULWWOH
PHFKDQLFDOO\ VWDEOH)LJ D
D VLQJOH VORW IURP D ' WKHUPRSO
JHRPHWULFDO GLPHQVLRQV ZKLOH
GLPHQVLRQV EHWZHHQ WZR VORWV
WKH VORWV RI WKLV W\SH KDYH QR
FDQQRW HDVLO\ EH GHWHUPLQHG
WKHUHIRUH VXEMHFW WR D FHUWDLQ
1HYHUWKHOHVV WKH SDUDPHWHUV
$OO VORWV RI WKH DQWHQQD DUH
ODUJH YDULDWLRQV RYHU WKHLU
VORWV FRXOG EH GHWHUPLQHG LQ

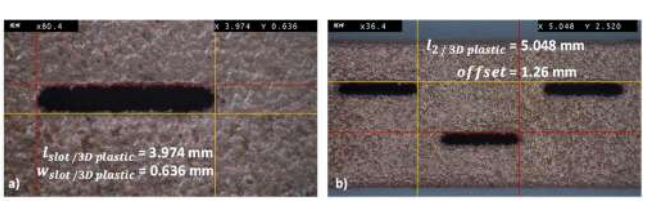

)LJXUH 7KH PLFURVFRSH YLHZV RI WKH VORWOLFRQWKH ' 6/6
SULQWHG V\QWKHWLF PDWHULDO DQWHQQD ZLWK WKHLU JHRPHWULFDO
GLPHQVLRQV

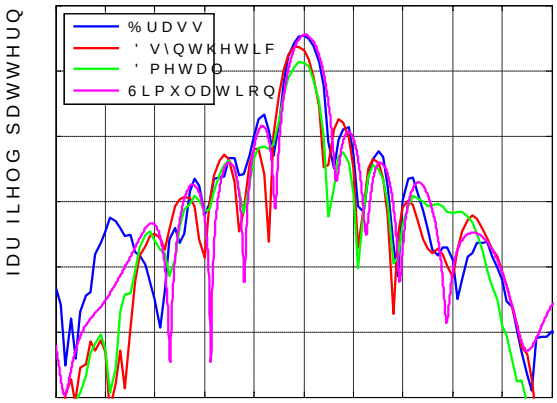

T >f @

)LJXUH 7KH PHDVXUHG FR SRODU UD
PDQXIDFWXUHG DQWHQQDV DQG WKH

&RPSDUHG WR WKH EUDVV DQWHQQD
VLPXODWLRQ UHVXOWV ERWK ' SUL
SRLQWLQJ VKLIW DV ZHOO DV D KL
ZDYHJXLGH PDWHULDO
FRQGXFWLYH ZDYHJXLGH PDWHULDO
DFFRUGLQJ WR WKH PDWHULDO
FRQGXFWLYLW\ GHSHQGV RQ
VKRZV KLJKHU FRQGXFWLYLW\ DQG
SURFHVV WKDW EHFRPH EULWWOH
DIWHU WKH JDOYDQLF SURFHVV ZLWK
OD\HU ,Q FRQWUDVW WR PDWHULDO
SURFHVV WKDW EHFRPH EULWWOH
PHFKDQLFDOO\ VWDEOH)LJ D
D VLQJOH VORW IURP D ' WKHUPRSO
JHRPHWULFDO GLPHQVLRQV ZKLOH
GLPHQVLRQV EHWZHHQ WZR VORWV
WKH VORWV RI WKLV W\SH KDYH QR
FDQQRW HDVLO\ EH GHWHUPLQHG
WKHUHIRUH VXEMHFW WR D FHUWDLQ
1HYHUWKHOHVV WKH SDUDPHWHUV
$OO VORWV RI WKH DQWHQQD DUH
ODUJH YDULDWLRQV RYHU WKHLU
VORWV FRXOG EH GHWHUPLQHG LQ
7KH VXUIDFH URXJKQHVV DOVR SOD\V
WKH ORVVHV VLQFH URXJK VXUIDFHV
FXUUHQW DQG WKXV HOHYDWHV UHV
LQFUHDVH RI ORVVHV &RPSDUHG WR
6/6 SULQWHG DQWHQQDV WKDW DUH G
UHODWLYHO\ URXJK VXUIDFH ZKLFK
SLFWXUHV DERYH 7KLV LPSOLHV W
FRQVHTXHQFH KLJKHU 7KH VLGHORE
DQWHQQDV DUH XQEDODQFHG 7KLV
LPSHUIHFWLRQ LQ WKH SKDVH ZKLFK
RI WKH VORWOLFRQWKH ' 6/6
,Q)LJ WKH UHIOHFWLRQ FRHIILFL
DQWHQQDV DUH GHSLFWHG DQG FRPS

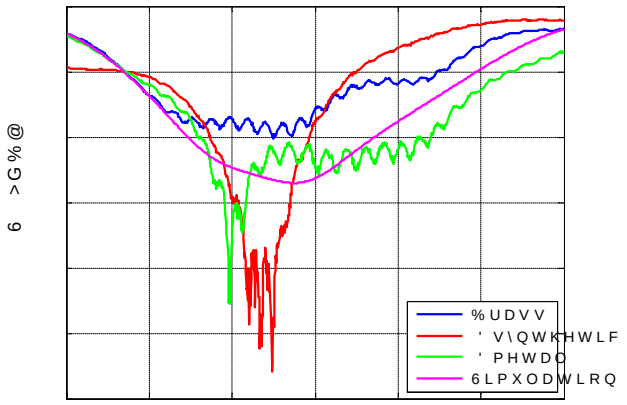

)LJXUH 7KH PHDVXUHG DQG VLPXODWHG VSHFWUD RI WKH DQWHQQD LQSXW

7KH VLPXODWHG G% EDQGZLGWK RI WKH DQWHQQD LV DERXW RI WKH PHDVXUHG *+] ZLWK WKH UHVRQDQFH DW WKH VDPH IUHTXHQF\ 7KLV GLDJUDP LW FDQ EH VHHQ WKDW RQO\ WKH ' PHWDO SULQWHG DQWHQQD FRPSOHWHO\ PDWFKHV WKH VLPXODWHG UHVXOW 7KH EUDVRQ DQWHQQD KDV D VOLJKWO\ QDUURZHU EDQGZLGWK WKDQ WKH *ROGHQ WKHLU ZRUN E\ SURYLGLQJ QXPHURXV WKH VORW ZKLFK FDXVHV WKH VKLIW RI WKH UHVRQDQW IUHTXHQF\ LQ WKH ORZ IUHTXHQF\ UDQJH

,Q)LJ WKH UDGLDWLRQ HIILFLHQF\ LV GHSLFWHG ZKLFK LV PHDVXUHG E\ PHDQV RI WKH UDGLRPHWULF KRW FROG PHWKRG > @

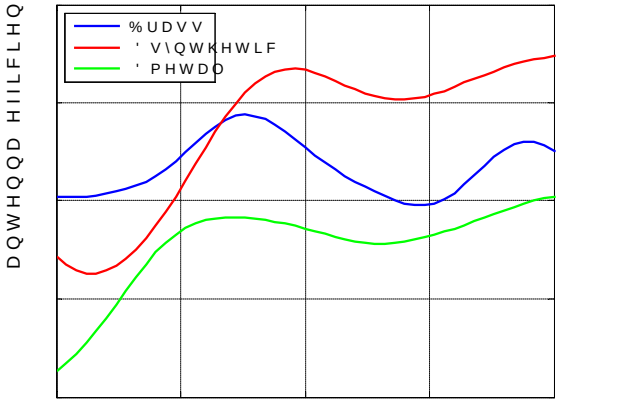

)LJXUH 7KH VLPXODWHG DQG PHDVXUHG UHILHFWLRQ FRHIILFLHQW IRU PDQXIDFWXUHG DQWHQQDV

7KH EUDVV DQWHQQD KDV D WROHUDEOH PRQVWDQW SURJUHVVLRQ RYHU WKH GHVLUHG IUHTXHQF\ EDQG ZKLOH WKH SULQWHG DQWHQQDV SURYH WR EH PRUH VWDEOH LQ [SHU\ UDGLDWLRQ HIILFLHQF\ IRU WKH ' PHWDO DQG 3&% DQWHQQDV UHODWLYHO\ ORZ HVSHFLDOO\ LQ WKH ORZHU IUHTXHQF\ UDQJH 6LQFH WKH VORW RIIVHW IRU WKLV DQWHQQD GRHV QRW FRUUHVSRQG WR WKH VLPXODWHG YDOXH WKH VORW LPSHGDQFH LV QRW RSWLPDOO\ PDWFKHG WR WKH ZDYHJXLGH LPSHGDQFH DQG WKHUHIRUH WKH PD[LPXP SRZHU LV QRW FRXSOHG LQWR WKH VORW

&RQFOXVLRQV

7R SURYH WKH DSSOLFDELOLW\ RI W PHWKRG IRU DQWHQQDV WKDW DUH R EDQGV WZR ' 6/6 SULQWHG DQWHQQ PDWHULDOV KDYH EHHQ IDEULFDWHG EUDVV DQWHQQD LQ ERWK PHFKDQLF RI YLHZ

&RPSDUHG WR FRQYHQWLRQDO IDEU PLOOLQJ RU HURGLQJ FRPSOH[PDQXIDFWXUHG LQ RQH SLHFH XVLQ +RZHYHU WKH LPSOHPHQWDWLRQ RI GXH WR WKH OLPLWHG DFFHVV IRU YL FRPSRQHQWV GHVLJQ QHHGV DQ LQ VHOHFWHG ' SULQWLQJ SURFHVV DQ VWUXFWXUHV 7KHVH DUH OLJKWHU ZKLFK LV DLUEHUQH DSSOLFDWLRQV EXW QRW HOHPHQWV DUH OLJKWHU ZHLJKW RI W GXH WR WKH UHGXFHG VWUXFWXUDO LQWHJULW\ 7KH *ROGHQ WKH ZKLV ZRUN E\ SURYLGLQJ QXPHURX WHFKQRORJ\ DQWHQQD VDPSOHV

5HIHUHQFHV

> @ +HQG $ 5DPRV 9DUX P D $QWHQQD 'HVLJQ 8VLQJ 0RGHUQ $G 7HFKQRORJ\ $QDO\VHV $SSOLFDWLRQV SS

> @ ' 1JR $ .DVKDQL * ,PEDO]DQR DQG ' +XL $GGLWLYH PDQXIDFWX UHYLHZ RI PDWHULDOV PHWKRG FKDOOHQJHV %RQG SS

> @ -RVVHIVRQ DQG 6 5 5HQJDUDMD $UUD\ $QWHQQD,QWHJUDWLRQ RI (Q 7HFKQRORJ\

> @ (QMLX 0 3 3HURWRQL 6ORWW 'HVLJQ 8VLQJ ' 6LPXODWLRQ RXU

> @ +RUQ $ 1RWWHQVWHLQHU $ 5H 6FKHLEHU) 6$5 '/5¶V QHZ PX SRODULPHWULF DQG RQ 6$5

> @) *LDFROHWWR)UHTXHQF\ DQG 7 RI 6HOI (QHUJL 9DULDWLRQV RI 9RQ 1R SULQWHG DQWHQQDV

> @ $VKUDIXO (UDQYLQH7 DQG ' 7U PHDVXUHG HQWHQQD DQG 0HDVXUHG ,QWHUQDWLRQDO 6\PSRVLXP 6HSW

Antennas, EM and Smart Sensing Technologies for Biomedical and Healthcare Applications

0LOOLPHWHU :DYHVHUR UHVHDUFKHUV FRQGXFW 3HRJHFWV WR

6 'L 0HR 0DWUL[0 3DVLDQ

'HSDUWPHQW RI (OHFWULFDO &RPSXWHU (QJLQHHULQJ DQG &RPSXWDWLRQDO
FRUUHVSRQGLQJ DXWKRU VLPRQD GLPHR#XQLSY LW

$EVWUDFW—WKLV FRQWULEXWLRQ ZH SUHVHQW WKH ILUVW WKHRUHWLFDO
D PLOOLPHWHU ZDYH LPDJLQJ V\VWHP IRU EUHDVW FDQFHU GHWHF

%UHDVW FDQFHU LV RQH RI WKH PRVW ZLGHVSUHDG GHVHDVHV DPRQJ
PDPPRJUDSK\ LV FRQVLGHUHG WKH JROGHQ VWDQGDUG WHFKQLTXH E
LQWHUHVW LQ QHZ GLDJQRVWLF PRGDOLWLHV X$HPRQWKHK HX FRVW
SURSRVHG IRU LPDJLQJ RI WKH EUHDVW E H@VZHEDVHGHDQ WGKL\HDOHGHGWG
,Q RUGHU WR LPSURYH WKH UHVROXWLRQ DQG LPDJH TXDOLW\ SDUW
3DYLD ZH KDYH EHHQ ZRUNLQJ IRU \HDUV PRQ ZDOHZULHPJLJPLHQJ ,Q\VVWD
PHDVXUHG WKH GLHOHFWULF"#$%&&$&WRSHVUXWLVH VR IWKRX PD*Q]EU%D VWDUULH
VLPXODWLYH IHDVLELOLW\ VWXG\RHIORSHG DQG PEDKJDQQDFWVWHWLH]HG &
PHFKDQLFDOO\ VHYHUDO WLVVXH PLWPHFVMLHQGJ WEWKH DLVPD JLKQDJQSWURRPWR
SKDQWRPV DOVR FRPELQLQJ PP ZDYHHOYD VXWORWJUUDVSRXQGV WKHKG IXRDOWO
WKH PDLQ DFKLHYHPHQWV DERXW WKH VRHQJVRVLHQSJV DEDQGYLQWV ZH S

'(!)%!*!+,-%+.+/0-0+,!-%10,%&2.&3./4502.6-!07,.!"#$%$&.,%774!7.

,Q FROODERUDWLRQ ZLWK WKH (XURSHDQH, QSVHWLWXWHG PW ZRQFH
FDPSDLJQV RQ P'#$%&$&KWHKDDQWK\ DQG FDQFHURXV EUHDVW\HDUPS O
0HDVXUHPHQWV ZHUH GRQH ZLWK DQUR TXHQQFQ GHDG JFHR E[LDO@S*U+R]ER
URRP WHPSHUDWXUH 7KH UHVXOWVQ RIVWKRZHMEH WV ZRL JHQ[SIHLFDRQHWQ WG D
WKH ZKROH LQYHVWLJDWHG EDQGZLGWK/VXEHWVZHHYHQQ KZHKDHQWWKHDDQWGK
ILEUR JODQGXDLUFHRUQHWGHQWUHUGHRRDQQO\ FQ@Q EH IRX

8(! 945!-%+0*.3!07%6%*%,:.7,4;:.&3.,/!.55#<0$!.%50=%2=.7:7,!5.

%DVHG RQ WKH VLJQLILFDQW GLHOHFWULFSURSHUWLHV DWWULEXWHG WZH
QXPHULFDO IHDVLELOLW\ VWXG\ RI LWQKHD PRL QZHDYH DEQG JERQ IR\VPDHC
SDUWLFXODU WKURXJK OLQN EXGRVHWLHHY DGXLDMHLURHQ WL QE UGHLDIVHWHV
DVSHFWV VXFK DV WKH RSWLPDE[LHQJ RWKHQ WLHJQQDDV WLRQ QWRKLHV HD
SHQHWUDWLRQ GHSWK DV ZHOOV DWW\SWHK RIDVF\KWHHYPD E'HMW DJLHO\RQ QXW>L@

>(! 8%#5&;0*.,%774!#5%5%+?%2=.6-!07,.@/02,&57.

7R WHVW WKH PP ZDYH LPDJLQJ SURFOWORW\SKHD UZDHF WWWXG]LHHGG VDHQYGHU
ORZ FRVW HDVLO\ KDQGOHG DQG VDIXHVFHRPSRRQHGWHV R IQ H] HEDGVH
GLVKZDVKLQJ OLTXLG DQG VROLGLU\LQJ HDJHLQHWHVFXFKLFD VSUJRHSDHUWWL
SKDQWRPV ZHUH PHDVXUHG LQ WKH IUZHHTUHHQFRP\PSUDUQHJGH Z>LWK @V
FRUUHVSRQGLQ!J#$R%X&RWDLQV VEXUHHVD VWWK RZLQJ WKH JRRG FDSDEDLOOLVE\UR D
WLVVXHV W\SHV E\ FKDQJLQJ RQ[QV\XWKM SOHRUFHHGWWDJHL ORV IRDQ LEQH W
,Q DGGLWLRQ KHDOWK\ DQG GLVHEDVHGSUWRSVNXWVLHKVD>H@GDQGHUWHR

U H D O L V W L F S K D Q W R P V W R E H X V H G K L D Q U D F P E H L Q O H J G L P D J H Q F H V \ V W H P
S K D Q W R P V X Q G H U G L I I H U H Q W H [S H U L P H Q W D O F R Q G L W L R Q V F O R V H O \ P D W F K L Q J
L Q F U H D V H G W K H S K D Q W R P V W L I I Q H V V E H \ R Q G W K H D Y D L O D E O H U H I H U H Q F H
P R Q L W R U L Q J L W V G L U H F W H Q Y L U R Q P H Q W D O E D F N J U R X Q G L Q

)(! A4*,%#5&;0*.%50=%2=.+&56%2%2=.55#<0$!7B.4*,-07&42;7.02;.4*,-07&42;7.!*07,&=-0@/:.

:H W H V W H G W K H P P Z D Y H L P D J L Q J S U R E H Z L W K P R Q R P R G D O I U H T X H Q F \ V H Q V R U
Z D Y H J X L G H V Z L W K P R Q R P R G D O I U H T X H Q F \ V H Q V R U D Q G Z H L J K W D Q D O \ V L V
U D G L D W R U V $ O O P H D V X U H P H Q W V Z H U H P D G H X V L Q J D G H G L F D W H G Z D W H U W D Q N
S R V V L E L O L W \ R I U H D F K L Q J P R W L R Q Z L W K V O R Z V Z L U O V S H H G V X S W R Y H O R F L W L H V
,Q D G G L W L R Q D W U L S O H P R G H V F D Q Q L Q J S U R E H Z D V D O V R X V H G W R P H D V X U H
T X D Q W L W D W L Y H O D V H U J U D S K \ L P D J L Q J W H F K Q L T X H V Z H U H D O V R X V H G W R F K D U D F W H U L]
F R P S R V H G R I Q R Q W R [L F O R Z F R Q F H Q W U D W L R Q V R I W K H D F W L Y H F R P S R X Q G
Z D W H U D Q G D J D U 7 K H V H D U H L Q W H Q G H G W R S U R Y L G H D Q R Q G H V W U X F W L Y H D Q G
Q H R S O D V W L F W L V V X H V U H V H D U F K L Q E L R P H G L F D O D Q G E L R P H G L F D O H Q J L Q H H U L Q J
T X D Q W L W D W L Y H O D V H U J U D S K \ D Q G T X D Q W L W D W L Y H O L Y H F H O O L P D J L Q J R I W K H
I R X Q G Q

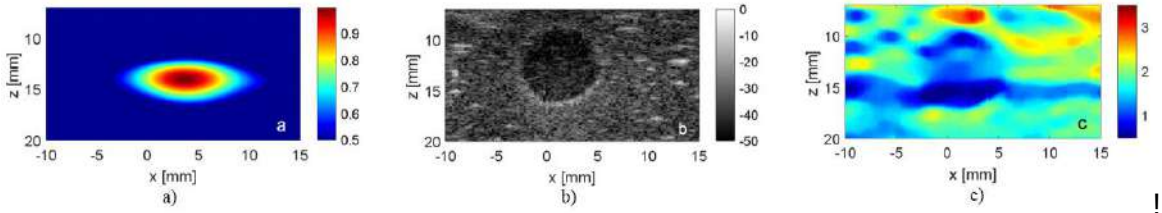

)L J X U H D P P Z D Y H E X O W U D V R X Q G J % H V P R G H W K H Q S H U I R U P H G R Q W K H D F U \ O L F S K D Q W R P D Q G U H P R Y H G W K H D V V R F L J D W H G F H O O V L Q W K H F K D U D F W H U L] L Q J L Q D G G L W L R Q W R W K H G L I I H U H Q W H [S H U L P H Q W D O G H W D L O V D Q G S U H V H Q W H G Z L W K P R Q R P R G D O I U H T X H Q F \ V H Q V R U D Q G P X O W L P R G D O I X Q F W L R Q Z L W K P R Q R P R G D O I U H T X H Q F \ D Q G D J D U 7 K H V H D U H L Q W H Q G H G W R S U R Y L G H D Q R Q G H V W U X F W L Y H D Q G Q H R S O D V W L F W L V V X H V U H V H D U F K L Q E L R P H G L F D O D Q G E L R P H G L F D O H Q J L Q H H U L Q J T X D Q W L W D W L Y H O D V H U J U D S K \ D Q G T X D Q W L W D W L Y H O L Y H F H O O L P D J L Q J I R X Q G Q

C(D2=&%2=.0+,%$%,%!7.

:H D U H F X U U H Q W O \ G H D O L Q J Z L W K H [W U D F K D U D F W H U L] L Q J W K H D V V R F L D W H G Q H X U D O S K D Q W R P D Q G U H P R Y L Q J W K H D V V R F L D W H G Q H X U D O F K D U D F W H U L] L Q J L Q D G G L W L R Q W R W K H G L I I H U H Q W H [S H U L P H Q W D O G H W D L O V D Q G S U H V H Q W H G Z L W K P R Q R P R G D O I U H T X H Q F \ D Q G P X O W L P R G D O I X Q F W L R Q Z L W K P R Q R P R G D O I U H T X H Q F \ D Q G D J D U 7 K H V H D U H L Q W H Q G H G W R S U R Y L G H D Q R Q G H V W U X F W L Y H D Q G Q H R S O D V W L F W L V V X H V U H V H D U F K L Q E L R P H G L F D O D Q G E L R P H G L F D O H Q J L Q H H U L Q J T X D Q W L W D W L Y H O D V H U J U D S K \ D Q G T X D Q W L W D W L Y H O L Y H F H O O L P D J L Q J I R X Q G Q

5 H I H U H Q F H V

1 . 1 L N R O R Y D ³0 L F U R Z D Y H L P D J L Q J D Q G U H P R W H V H Q V L Q J R I E L R P H G L F D O W L V V X H V ´ ± ' H F
$ 0 D U W H O O R V L R H W D O ' L H O H F W U R P D J Q H W L V P L Q E L R P H G L F D O U H V H D U F K ´ L Q 3 U R F 6 3 ,((O H F W U R Q L F 6 W D W H 2 I W K H $ U W 2 I 0 H G L F D O ,P D J L Q J 9 R O 1 R SS 0 D U F K
6 ' L 0 H R H W D O ' L H O H F W U L F S H U U R L S P H H U Q W L D O U H V H U Y R L U E X U D F K P D W F K L Q J L Q E L R P H G L F D O L P D J L Q J 9 R O 1 R SS 0 D \
8 . $ S U L O
6 ' L 0 H R H W D O 2 Q W K H) H D V L E L O L W \ R I W K H) U H H K D Q G 0 L U U R U W H F K Q L T X H I R U E L R P H G L F D O L P D J H U H J L V W U D W L R Q 9 R O 1 R SS 0 D \
6 ' L 0 H R H W D O 7 L V V X H P L P L F N L Q J E D V H G G H I R U P D E O H U H J L V W U D W L R Q I R U % U H D V W & D Q F H U ' H W H F W L R Q ( ) H E
$ 6 D P D Q L H W D O ³(O D V W L F P R G X O L I R U E U H D V W W L V V X H G H I R U P D W L R Q D Q G V W U D L Q L Q Y H V W L J D W L R Q 2 I 3 K \ W L F P V D Q G 0 H G L F L Q H % L R S R O J
6 ' L 0 H R $ & D Q Q D W j 6 0 R U J D Q W L 2 Q ' W O K H W G E R K H H F D W Q G L E D 3 D Q G V L P H Q F K D Q L W L V V X H P L P L F N L Q J E U H D V W S K D Q W R P V O R J 2 3 9 R O V L F V L Q 0 H - O D F L Q H D Q G
6 ' L 0 H R H W D O ([S H U L P H Q W D O 9 3 D K O D L G W R P V L R Q I R Q L 7 D V L P X H W H U P L F Y N H L Q & D Q F H U ' H W H F W L R Q 6 9 R O 1 R SS -
6 ' L 0 H R H W D O & R P E L Q L Q J 0 L O O L P H W H U (D Y H W R F D J D L S Q J \ 3 Q W D U D W L R Q I R U % U H D V W & D Q F H U ' H W H F W L R Q (, 2 L % & D O ([S H U L P H Q W D W L R Q & D Q F H U W - X O

A systematic study of the electromagnetic occupational exposure in healthcare applications

S. D'Agostino[1], M. Colella[1], M. Liberti [1] and F. Apollonio[1]

[1]Department of Information Engineering, Electronics and Telecommunications (DIET), Sapienza University of Rome, Italy
*corresponding author: simona.dagostino@uniroma1.it

Abstract: This paper aims to study how to improve occupational health and safety conditions in the healthcare environment; in particular we will focus on a systematic evaluation of the exposure to the variable magnetic field produced during a transcranial magnetic stimulation (TMS) treatment. Four exposure conditions are provided based on two virtual human body models, in the case of a circular coil applicator. Results of the induced electric field inside the human body models show that in some cases exposure limits are exceeded and lead us to possible safety suggestions.

Introduction

The study began by carefully reviewing real exposure scenarios of clinicians, as the reference material used is company user manuals, websites, papers, and measurement campaigns[1]. We collected approximately 70 images of these scenarios to identify all the possible positions assumed by clinicians during TMS treatments. Furthermore, since the coil must be held in place in proximity of the patient's head, the operator often uses hands to hold it during treatment. This can potentially introduce critical issues on operator's limb exposure that were confirmed by some results obtained in a previous study[1,2]. To reduce these local risks, a dosimetric approach to provide useful suggestions is carried out, as no technical standard devices are currently available for TMS.

Models and methods

As a source model, it is considered a circular coil model 9784-00 of Magstim powered with Magstim 200 and BiStim system, at the maximum stimulator output (100% MSO). The two systems deliver current pulses assimilated to pure sinusoids at equivalent frequencies of 3 kHz (5.6 kA) and 1 kHz (9.7 kA), respectively. The Human models used to reproduce the operator, are two posable versions of the male models, called Duke (34-year-old, 1.77 m, 70.2 kg) and Jeduk (33-year-old, 1.62 m, 64.5 kg), both members of the Virtual Population (ViP., v.3.0)[3]. Concerning the exposure scenario, in order to conduct a local analysis of the exposure of the clinician's hands, two different way of gripping the coil are considered for each human model. For Duke, the clinician is assumed to hold the coil with one hand (right and left assessed separately) with two different ways of gripping (defined as Closed and Open). For Jeduk model, a more realistic conditions are evaluated, with both hands involved in the exposure, as well as two different holding modes (related to the orientation of the right hand and named defined as "Alfa" and "Beta"). Finally, the 99th percentile of the induced electric (E-) field in the human model was assessed by comparing it with the limit of ICNIRP 2010[4] guidelines (i.e., 1.13 V/m for these frequencies).

Results

First, we have evaluated the local maps of the induced E field due to the TMS exposure of the hands, considering the four conditions described before (Figure 1).

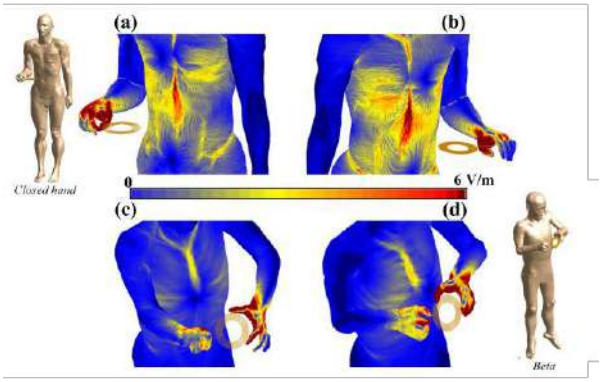

Figure 1. E-field maps (a) Duke right Closed hand, (b) Duke left Open hand, (c) Jeduk Alfa with coil handle perpendicular to the body surface, and (d) Jeduk Beta with the handle parallel to the body surface.

These distributions of the E-field show how, in all the cases, a large portion of the hand exceeds the limit confirming the criticality of the proximity in use of the device. The extent of the exposure becomes clearer by analyzing the 99th percentiles of the E-field evaluated in the hand and forearm, as reported in Table I.

Table 1. 99th percentiles of induced E-field (V/m)

	Duke		Jeduk			
	Closed	Open	Alfa		Beta	
Hand	right	left	right	left	right	left
70% MSO	21.36	15.17	7.33	15.88	6.97	21.67
50% MSO	15.26	10.84	5.23	11.34	4.98	15.48
30% MSO	9.15	6.50	3.14	6.81	2.99	9.29

Discussions

For all the exposure conditions here considered, the circular coil causes an induced E-field that exceeds the suggested limits, also considering the lowest level of MSO used in practice in clinics (30% MSO). Excluding the implausible 100% MSO[5], the percentage variation respect the limits ranges between +164.6% up to +179.0%. These results indicate the need to explore new method for shielding the hand by using for example a dedicated glove. In conclusion, we demonstrate how risk assessment in healthcare workplace can be effectively approached using computational methods with ultimate goal to identify possible flaw of knowledge and suggesting new protocol for assessing exposure to devices such as TMS, which currently lack standardizations.

References

1. D'Agostino S, Colella M, Liberti M, Falsaperla R, Apollonio F. Systematic numerical assessment of occupational exposure to electromagnetic fields of transcranial magnetic stimulation. Med Phys. 2022;49(5):3416-3431. doi:10.1002/mp.15567
2. D'Agostino S, Colella M, Liberti M, Falsaperla R, Apollonio F. Dosimetric assessment of clinical staff exposed to magnetic field produced by a transcranial magnetic stimulation circular coil. 2021 34th Gen Assem Sci Symp Int Union Radio Sci URSI GASS 2021. 2021;(September):2022-2024. doi:10.23919/URSIGASS51995.2021.9560280
3. Gosselin MC, Neufeld E, Moser H, et al. Development of a new generation of high-resolution anatomical models for medical device evaluation: the Virtual Population 3.0. Phys Med Biol. 2014;59(18):5287-5303. doi:10.1088/0031-9155/59/18/5287
4. ICNIRP. Guidelines for limiting exposure to time-varying electric and magnetic fields (1 Hz TO 100 kHz). Health Phys. 2010;99(6):818-836. doi:10.1097/HP.0b013e3181f06c86
5. Groppa S, Oliviero A, Eisen A, et al. A practical guide to diagnostic transcranial magnetic stimulation: Report of an IFCN committee. Clin Neurophysiol. 2012;123(5):858-882. doi:10.1016/j.clinph.2012.01.010

! "#$%$&"!'%"($)*&$ +,$-*%"(.// +0*--'!'%" ($ 01,&$213'&**"4033%"5&*--.&*" 6-21)$213"7*283%"

$

43"9$': [4];"<81"<8*': [4];"=$321$">81[2];"$'%"@3': A1'"B.3[45]"

[4].6789:6;$3:8<=>?87@$9A$#8$B8C3C<9$=
[5]D9>>=?C9:E8:B$6F7G$BH9$@IJ:F?K=EF$K?B

$

!,-2&$C2D!" $DFA/A??$D6;8L>6789:=$M,$=?78N6789:EO87G$AF?89:$A>9N6>6E6>$6:E$6$D6N=>6$8?$C
PG=$D6<=A9>N$A=67F>=?$6:E$G=6;7G$8:A9>N6789:$6>=$D9><E$6?8$C$7=?79:=7O$>Q$RN9E=;?$
79$=?78N67=$M,?K$PG=$N9E=;?$6>=$A8>$7=E$8$6>=$A9>N6789:$(6>7$A9>$-:7=:?8<=$S6>=$---$R(-(-S
E676L6$:E$7G=:$7>6:?A=>>=E$79$D9C76$D9$?=7FCK$PG=$C>9C9?=E$N=7G9E$C>9<8E7$6$2U=6$8L;=$O
D6;8L>6789:==DF/AM,$=?78N6789:K

$

$

M;99E$C>=??F>=$RM,T$8?$6:$8NC9>76:7$<876;$?8B:$N@$?=E$D6;8L>6789:EO87G$AF?89:$A>9N6>6E6>$6:E$6$D6N=>6$8?$C6C7F>=$7G=$
V4W$D6:$>=6;8U=$D=?$M,$=?78N6789:'$LF7$@?$E=L@$?=E$D6;8L>6789:EO87G8?$C6C$>'$6
DFA/A??'$D6;8L>6789:=$M,$=?78N6789:$?@?7=N$8?$E=?8B:=E$O87G$AF?89:$A>9N$6$>6E6>$6:E6D6N=
79$ D6C7F>=$ 7G=$ 7G9>6I$ G=6>7L=67$?8B:6;'$ 6:E$ 6$ D6N=>6$ N9:879>?$ 7G=$ CF;?=$ A>9N$ 7G=$ C6;N
C>9C9?=E$D=?$N=6?F>=N=:7$N=7G9E$8?$6CC;8D6L;=$79$E8AA=>6:$7G=$C>9A9?$8$E7$6>=$
?G9O:$8Y8BF>4#$

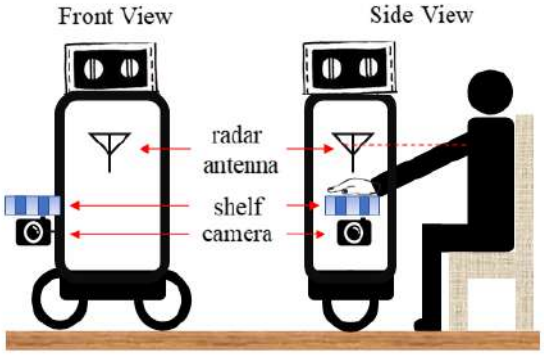

$

Y8BF>4#$Q=7DG$N6C$9A$7G=$?@?7=N$?=$7FC$9:6>9L97

PG=$C>9C9?=E$N=7G9E$D=?$M,$=?78N6789:$E$O87G$AF?89:$A>9N$6$>6E6>$D6C7F>=$?=$7G=$
G=6>7L=67$?8B:6;$@$?=:?8:B$7G=$DG=?7$O6;;$N9<=N=:7?$D6F?=E$L@$?=E$D6;8L>6789:$E$O87G8?$C6C$>'$6
A>9N$7G=$6;@U8:B$7G=$?Q8:$D9;9>$DG6:B=$D6F?=E$L@$?=E$7G=$>9L97$?=7FC'$7G=$?FLX=D7$9:
:==E?79?87$8:$A>9:7$9A$7G=$?=E$D6;8L>6789:EO87G$AF?89:$A>9N$7G=$C6;$D6C7F>=$?=$7G=$
/&$?=D9:E?$6>=$>=D9>E=E$8:$7G=$=IC=>8N=:7K

!$D9:<9;F789:$:=F>6;$:=7O9>Q$RS..T$8?$F=E$6?$8:CF7?$79$7G=$N9E=;K$PG=$C>9C9?=E$N=7G9E$D=?$M,$=?78N6789:$E$O87G$AF?89:$A>9N$6$>6E6>$6:E6D6N=>6$8?$C6C7F>=$7G=$
8:A9>N6789:$6:E$O6<=A9>N$A=67F>=?$6>=$F?=E$6?$8:CF7?$79$7G=$N9E=;K$PG=$C>9C9?=E$N=7G9E$D=?$M,$=?78N6789:EO87G$AF?89:$A>9N6>6E6>$6:E$6$D6N=>6$8?$C6C7F>=$7G=$
G@C=>7=:?89:$G8?79>@'$O=8BG7$G=8BG79A$A=67F>=?'$8:D;E6:B$7G=NA=67F>=?'$6>=6$A=67F>=?'
6:E$,PP$A=67F>=?'$6>=$=I7>6D7=E$A>9N$7G=$B9$?=$C>9;8N8$9A$.FNL=>$9A$E676$?6NC;=?79
7>68:$7G=$N9E=;$7>6:?A=>$?DG=N=$8?$6E9C7=EK$PG=$N9E=;$7G=$C>9C9?=E$N=7G9E$D=?$M,$=?78N6789:EO87G$AF?89:$A>9N$

(=E8D6;$-:A9>N6789:$(6>7$A9>$-:7=:?8<=$S6>=$+---$E676$?=7'$6:E$7G=:$7>6:?A=>>=E$79$7G=$O6<=A9>N?$N=6?F>=E$L@$7G=$'$6:E$7G=:$7>6:?A=>>=E$79$7G=$O6<=A9>N?$N=6?F>=E$L@$"S*T$6:E$CG979C;=7G@?N9B>6CG@$
-:$7G=$(-(-S+---$E676$?=7'$6:E$7G=:$7>6:?A=>>=$D6C7F>=E$L@$D6>E89B>6N$R"S*T$6:E$CG979C;=7G@?N9B>6CG@$
#8:D=$6;;$N=6?F>=7N$6>=$N9E8A8=E$L@$D6>E86D$6D67=A97=?$N=6?F>=E$L@$"S*$6:E$,,*$D6:$L=$
7>6:?A=>>=E$79$7G=$O6<=A9>N?$N=6?F>=E$L@$7G=$'$6:E$7G=:$7>6:?A=>>=E$79$7G=$O6<=A9>N?$N=6?F>=E$L@$"S*$6:E$,,*$D6:$L=$A=6?8L8;87@$9A$7G
7>6:?A=>$?DG$?=N=K?G9O:$6:E$;=$7G=$=IC=>8N=:7$?=$?G9O$7G67$7G=$C>9C9?=E$N=7G9E$C>9<8E=?$6
O6@79>=6;8U=$7G=$DA8L>6A9:=$M,$=?78N6789:K
$

P!M)"$-$"?78N6789:$,=>A9>N6:D=

*>9FG$	.9K$9A$?FLX=D$	#@?79;8D$M,$RN$N[BT			\86?79;8D$M,$RNN$[BT		
		(=6:$ ">>9$	(=6:$!<=>6B=$ ">>9$	#76:E6>E \=<86789$	(=6:$ ">>9$	(=6:$!<=>6B=$ ">>9$	#76:E6>E \=<86789$
#FLX=D7?$O87G$G@C$=	]^ $	%_K4$]	%_K`$	%&K$&	4&K%$]	4]Ka/$	bK`$
#FLX=D7?$O87G$G@C$9	%&$	+_Kb$4	44Ka$	bK%$/	+4^K$	4]K_$	bKb$
#FLX=D7?$O87G$M,$8: :9>N6;$>6:B$=	4%$	aKa$	4%K^$\	4%K%$4	/Kb`$	aK`/$	^K^$
P976$	4`] $	4&K]$	4_Ka$	4_K&$4	/K4^$	4&K%$/	aK`/$

$
$
#*/*&*'C*- "
V4$W SK$SK$0K$,99:$6:E$0KPKcG6+$'$6:E$A:9:8:<6?8<=$N=6?F>=N=:7?$9A$6>7=>86;$L;99E$C>=??F>=$L@$CF
78N='e$#$%&'"$%()"*$%&+++%+",$%-./$%01)$%9;K$a$fg)#'$:9K$(6@$%&4]'$CC1K$b$&a%&$_K
V%$W hK$#G>8>6N'$!K$i6Q6:Q6>'$.K$\6NEKh6NE6?8'$dS9:78:F9F?$DFAA;=??$L;99E$C>=??F>=$N9:879>8:B$L6
,PP'e$&(007%89:9$%9:9%&'"$%()"*$%01)1"*)5;<$%01);./$%7$C)2$1_4'$%&4$&K
$

!"#$%&'(&)'*+,$-$.(,$/&'/0'12(&#-$##$/&'3/$4#'0/2'5(%&",$6'7"#/&(&6'"3/8+4$&%' 98-(&':/);'3/--8&$6(,$/& '

$

<4(&%'"=$>?8+"$'<@"&%'>:$&%@"&%'3@>"8"-$&%'A(/ 78'>?()/&%'?$& 7>'B$"C$"'?(&%' D$/'9(&%'E8&'(&) '5(&%'F'G($' '

7$19:;<=><?@B$$-?D:9?E:9C$:F$;B?@$.=HE9IJB=E$?=G$1K?9J?>BIE<>?@$9BHKI$@<L;B9H(KEC<=?
%#E?EBABC-?D:9?E:9C$:F$!=?@:L$?=G1$;?@BG-#.($6=<;B9H<EC$:F$,?>$I($OK<=?
8>:99BHR:=G<=L$?IEKI9LS$T LJ?<@U>$J

$

HI#,2(6, J')K<H$HIJJ?9C$9BHB=EH$?=$:RE<J<N?E<:=$?RR9:?>K$F:9$GBH<L=<=L$>:<@H$:F$J?L=BE<>$9B
KIJ?=$D:GC$>:JJI=<>?E<)KB:RE<J?@$>:=F<LI9?E<:=$:F$;?9<:IH$>:<@H$<H$BP?J<=BG$?=G$?EE?<=B
B@B>E9:J?L=BE<>$ H<J$@DEKHVIHJ=E@C($ BPRB9$J9BB$ >:=GI>EBG$ E:$;?@<G?EB$ EKB$ FB?H<D<@<EC
BFFB>E$K;BKBJ$KB$9BHI@EG$>?EB$EK?E$EKB$HE9:=LBHE$&9BZ?@?E<FIWG$DBEZBB=$EKB$<==B9$G<
?=G$<EH$<=GI>E9B>B9($<E$B<$>B$EK?E$?=>9B?H$BG@$GI>E?=>B$9BHI@EI<E$9?=HJ<HH<:=$@:HHU

$

)KB$BJB9LB=>B$:F$KIJ?=$D:GC$>:JJI=<>?E<:=$EB>K=:@:LCEKB9B=<=BG$J?=?LBJB=E$:F$
JBG<>?@($9BK?D<@<E?E<:=$?=G$RKCH<>?@$>?9B$EK?E=B$QCHR@<=L$[IJ?=$\:GC$O:JJI=<>?E<:=
W,+O$[\OY$<H$?=$<==:;?E<;B$EB>K=:@:LC$EK?E$B=?D@B$H9BFB9$>BJ$H?EL@($?=G$<H$?=E<><R?E
E:$<=E9:GI>B$=BZ$R9:HRB>EH$?=G$>K?@@B=LBH$<=EKB9B?@J$:F$ZB@@$D@B$GB;E<>BH$7($G$=B?
.=$,+O [\O($H<L=?@H$?9B$EBGDC$9BH:=?E<=L$EKB$HCHEBJ($ZK<>K$>:=H<HEH$:F$E9?=H>B<;B9$>:<
D:GC($?E$EKB$H?JB$F9BVIB=>CU$)KB9BF:9B($EKB$GBH<L=$?=G$:RE<J<N?E<:=$:FEKBE9?=H>B<;B9
EKB$,+O [\O$ HCHEB$ [ZB;B9($ BP<HE<=L$ 9BHB?9>K$ K?H$ R9<C$9BE?EB$?EEB=E<:=$ E:$ EKB$ GB;B@
E9?=HJ<HH<:=$U$$?EKBE"?$BPR@:9BG$EKB$G<HE<=>E<:=H$?=G$?HH:><?E<:=H$DBEZBB=EKBJ
[\O$?=G$ EKB$ "O$ EK9:ILK$ H<JI@?E<:=H$?=G$ <@$ BPRB9<JB=EHBE ?@U$]a^$ >:JR?9BG$ KIJ?
>K?==B@$>K?9?>EB9<HE<>H$JB?HI9BGDCEKB$\@IBE::EK$?RR9:?>K$?=G$EKB$>:<@$?RR9:?>K$E:
FB?H<D<@<EC$:F$J?L=BE<>$>:IR@<=L$?@BE$?@$BPR@<>BGEKB>:IR@<=L$JB>K?=<HJ$DBEZBB=EKB>
?=GEKBKIJ?=$D:GC$EK9:ILK$?=$BVI<;?@B=E$>:9<=E$H=EGEBGEKB$>:EB=E<?@$EKB$
?9JU$=$HIJJ?9C(EKBJ?c:9<EC$:F$>I99B=E$GBH<L=H$K?;B$J:=HE9?EB$EKB$FB?H<D<@<EC$:F$J?L=BE<>
[\O$:9$BPR@?<=EKB>:=GI>E<:=$JB>K?=<HJ$:F$B@B>E9:J?L=BE<>$ZK<>K$9B$K$K?H$DBB=$GBG<
?$ >:JR9BKB=H<;B$ GBH<L=$:F$ E9?=HJ<HH<:=$ HEIGC$ R9:R:HBH$?$ >:<@$:RE<J<N?E<:=$ JBE
J?P<J<N<=L$<=GI>E?=>B$K<H$HIDHBVIB=E@C$BPRB9<JB=E?@@C$;?@<G?EBG$F:9$<=H$BFFB>E<;B=
)KB$<=GI>E?=>B$:FEKB>:<@$<H$<=G<>?E<;B$:F$EKB$BPEB=E$:F$;?9<?E<:=$<=$J?L=BE<>$F@
>I99B=EH$ RBEKB GBF<=<E<:=$:F$ <=GI>E?=>B$?=G$ M??9$GBHH$EK?E$K?$LKB$:<@$ <=GI>E?=>B$
<=G<>?E<:=$9B$J?L=BE<>$F<B@G$<=EB=H<EC$LB=B9?EBG$DCEKB>:<@U$%:9B$DBK<=GEKB<=GI>E?=>B
B=B9LC$ HE:9?LB$?=G$ E9?=HJ<HH<:=$ <=$ EKB$ R:HHBH$?=$ EKB$@:<@$ >:=F<9J<=L$ E:$ ZB?9?D@B$ HB=H:9$
R:HHBHHEKBL9B?EBHE$R:HH<D@B$<=GI>E?=>B$ZK<@B$?@H:$DB<=L$?H$J<=<?EI9<NBG$?H$R:HH<

$ #$ $ $ $ $ $ $ $ 3) G $ W$ $ $ $ $ $
!

1(I4"KL"*+,$-(4' 3/-I$&(,$/&'/0' !>" '(&)' #$%(&)' 3/22"4(,$/&'H&(4;#$#

$	.=GI>E?=$B	O:99B@?E<:=$>:BFF<	#<L=<F<>?=>B$@
!&	&U2JJ$	&U7e$%	.X&U$7
" &	&U2JJ$	&U&2$2	.X&U$2
#$%&	7'U2JJ $	&U'2$	.X&U$7

1(I4"MLF&)86,(&6"#0/2'! $00"2"&A"/-",2$"# '/0'3/$4#

$	+B>E?=LI@	[BP?L:=?@	* >E?L:=?@	O<9>I@?=
#<JI@?E<$=	gU7 +$	2U47 +$	2Uga +$	2U'2 +$
, B?HI9BJB$I	gU7% +$	2Ug7 +$	2Ua' +$	2U% +$
"99:9$	' U7 7 $	' U2a $	' U4 7 $	%U% 7$

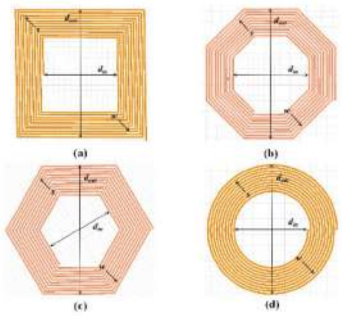

(a)
(b)
(c)
(d)

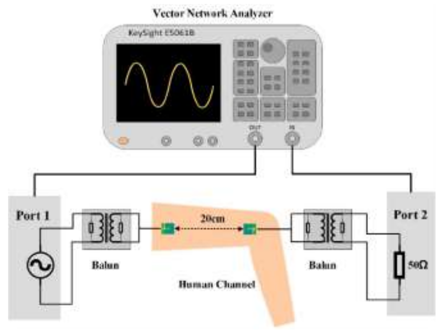

Vector Network Analyzer
KeySight E5061B
Port 1
Port 2
Balun
Balun
20cm
Human Channel
50Ω

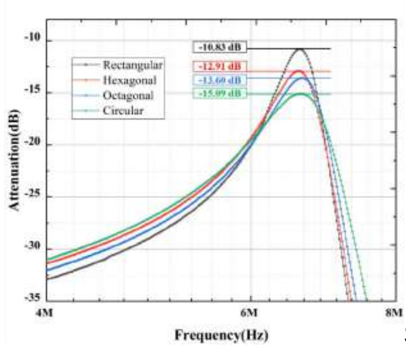

Rectangular
Hexagonal
Octagonal
Circular
-10.83 dB
-12.91 dB
-13.60 dB
-15.09 dB
Attenuation(dB)
Frequency(Hz)
4M
6M
8M
-10
-15
-20
-25
-30
-35

%LRLP SHGDQFH EDVHG0 XVFOH$FWLYLW0 RQLWRULQJ

3DQ; X : DQJQJ+H : HL0 D 7LQJ/LX <LSHQJ/LDR äHOMD/ XpHY9DVLü 0 DUR&LLUHN DQG<XHP LQJ* DR

&RQHJHRI 3K\VLFVDQG,QRUP DWRQ(QJLQHULQJ)XJKRX8QLYHUVLW\ &KLQD
6FKRRORI $GYDQFHG0 DQXIDFWXULQJ)XJKRX8QLYHUVLW\ &KLQD
)DFXOW\ R(OHFWURQLF QJLQHULQJ DQG&RP SXWLQJ 8QLYHUVLW\ RI =DJUHE &URDWLD
FRUUHVSRQGLQJ DXWKRU I]XJ\P# JP DLOFRP

$EVWUDFW 7KLV VXP P DU\ SURSRVHG D QHZ P HWKRG IRU FRQWQXRXV P RQLWRULQJ RI ILQJHU IOH[RU DFWLYLW 7KH ELRP SHGDQFH P HDVXUHP HQW WFKP H IRUP XVFOHG\ QDP LF P RQLWRULQJ LV GHVLJHG E\ DQDO\VLV RI ILQJHU HOEP HQW HOHFWURP DJQHWF VLP XODWRQV Z LWK DQ XSSHU DUP P RGHO ,Q YLYR H[SHUP HQW Z HUH FRQGXFWHG VR Y HUL\ WKH DFFXUDF\ RI WKH VLP XODWRQ IRGBZ HG E\ FRQWUDFWQJ D BRQJ DQG VKRUWWUP P HP RU QHWZRUN WR FKDUDFWUL HWKH P XVFOH DFWLYLW OHYHOE\ ELRP SHGDQFH 7KH UHVXOWV LQGLFDWH WKDW WKH ELRP SHGDQFH WFKQLTXH KDV WKH SRWHQWLDO WR P XVFOH DFWLYLW FRQWQXRXVO

0 XVFOH DWXH LV D SK\VRJLFDOSKHQRP HQRQ FKDUDFWUL HG E\ DGHFQH LQ P XVFOH WUHQJWK DQG DQ LQDEL OLW WR P DLQWLQ HWDEOLVKHG P RYH P HQW> @,WRFF XUV FRP P RQ) LQ\SRUW ILWQHW DQGUHKDELOLWDWRQ WDUJHW > @$ SSURSULDW H[HUFLVH SURP RWHV KHDOX EXWUH UDGLFDO SURGXFHG E\ H[FHVVLYH H[HUFLVH Z LOO FDXVH DQ LP EDODQFH LQ WKH ERG\ V R[LGDWLYH DQG DQWR[LGDQWFDSDFLW > @&RQWQXRXV P RQLWRULQJ RI P XVFOH DFWLYLW LV DQ HIHFWLYH P HWKRG RI DYRLGLQJ P XVFOH LQMU DQG GHYHORSLQJ SURPRWLQJ SDQV 6KLQHWDO > @XVHG ELRP SHGDQFH % GDW DWP XQWSOH IUHTXHQF\ VR WDFN P XVFOH FKDQJHV LQ SDWHQW Z LWK VWRNH / L HWDO > @P HDVXUHG OBFDO% FKDQJHV GXULQJ WKH SURJUHVVRQ RI P XVFOH DWXH WR YHUL\ WKDW% FDQEHD ELRP DUH RI P XVFOH VWDWV 1RQH RI WKH DERYH VWXGLHV KDYH

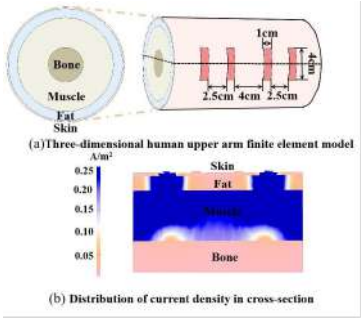

) LJ 7KH) (0 PRGHO

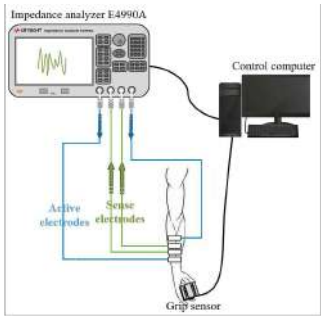

) LJ ([SHUP HQWDO GLDJUDP

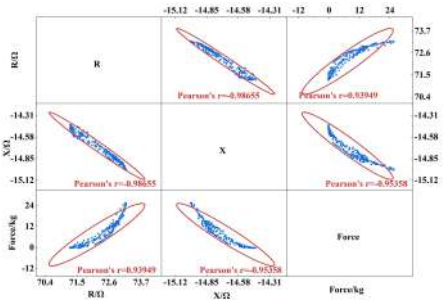

) LJ &RUUHODWRQ$QDO\VLV

YDOLGDWLQJ ZKHWKHU% KDV WKH SRWHQWLDO WR P XVFOH DFWLYLW FRQWQXRXVO 7KLV VXP P DU\ GHWLQJV P XVFOH VXWDLQHG FRQWUDFWLRQ H[SHUP HQWVEDVHG RQ HDFWRP DJQHWF VLP XODWRQV WR DFKLHYH HP DSSLQJ IURP % WR P XVFOH DFWLYLW

7KH HDFWRGH FRQLJXUDWQ LV DQ LP SRUWDQWQLQIXHQFH RQ P HDVXULQJ VXUDFH % ,WLV QHFHVDU WR FRQGXFWDQ HDFWRP DJQHWF VLP XODWRQ RI WKH HDFWRGH DUDQJHP HQWWR GHWHUP LQH WKH DYLODEELOW RI WKH VFKP H) LWWZ HXHG 9,112 SRWDEOH XOWDRXQG4 / 6X]KRX &KLQD WR FRDFWWKH WKLFNQHV RI HDFK WXXXH OD\HUI WKH VXEMHFW IRUHDUP IURP WKH ZULWWRQ WR WKH HDEZ NRLQW DQG FDBXODWG WKH DYHUDJH YDOXH DV D EDVLV IRUP PRGHOQJ : H FRQWKFWWG DKXP DQ IRUHDUP ILQLWH HDP HQW) (0 HDFWF ILHG P RGHOLQ &20 62/ 0 XQWSK\VF 7KH IRUHDUP ZDV HTXDWG WR DIRXUOD HUF\ OQGHU Z KHUH WKH WKLFNQHV RI HDFK WXXXH OD\HUZ DV VHWDV IROBZ V \NLQ FP IDW FP P XVFOH FP DQG ERQH FP 7KH GLHDFWF SDUDP HWUV RI HDFK WXXXH OD\HUZ HUH REWDLQHG IURP WKH GDWDEDVH> @ @7KH) (0 PRGHOLV VKRZQ LQ) LJ D 7R WDFN WKH FKDQJHV LQ ILQJHU IOH[RU XVFOH JURXS DFWLYLW

FDXVHG E\ ILQHUHQW[LRQDQG H[WUDFWLRQ HDFKRGHVZHUHSDVVHG WKURXJK WKH ILQHUHQW[LRUP XVFOH ZLWK WKH VZR H[WUDFWHG HDFKRGHV DVH[FLWDWLRQ HDFKRGHV DQG WKH VZRLQWLDODFHDFKRGHV DV VHQVLQJ HDFKRGHV 7KHHDFKRP DJQHWF VLP XODWLRQ IRFRBZ VWKHIRCBZLQJ SULQFLSOHV 0DNHWKH H[FLWDWRQ FXUHQWVCBZ WKURXJK WKH VDJHWDUHDEXWQRWDIHFW WKH VHQVLQJ HDFHVRHV ZRUN 0DNHWKH H[FLWDWRQ VJQDOCBZ WKURXJK WKHP XVFOHDUHDV PXFK DV SRVLEOH : H ILQDOO GHVLJQHG WKH HDFWRGHDUDQJHP HQWDV VKRZQ LQ)LJ D ,Q WKH HDFWRP DJQHWF VLP XODWLRQ WKH H[FLWDWRQ FXUHQWVLJQDOP SDWWHUQ HDFHVRHV WKH H[FLWDWRQ FXUHQWV DQG WKH P XVFOHDUHDV ZKLOH DDP RWVQR FXUHQWSDWWHUQ WKURXJK WKH ERQHDUHU 7KHUHRU-WKLV HDFWRGHFRQLJXUDWRQ VFKHP HP HHWV WKH H[SHUP HQWDO DQG WKH P HDVXUHG LP SHGDQFHILQRUP DWRQ P DQG RUJLQDWV IURP WKHP XVFOHDUHDV

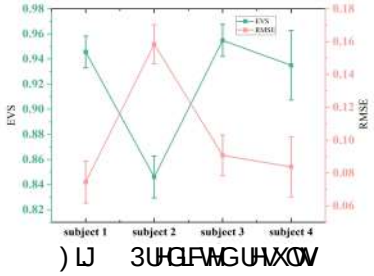

: H FRQGXFWHG LQ YLYR H[SHUP HQWV EDVHG RQ WKH VLP XODWRQ UHVXOW 7KI)LJ 3UHGLFWHG UHVXOW . H\ VJKW$JLDHQW($ LP SHGDQFH DQDO]HU . H\ VJKW7HFKQRORJLHV 86$ ZDV XVHG WR REWDLQ WKH LP SHGDQFH SDUDP HWHU RI WKH ILQJHUIORP XVFOH : H XVHG D WKUHHIRUFH WDQGXFHU ' </ <)UHG &KLQD WR VLP XODQHRXV FRQWUDFWLRQ GHWHFWLRQ DQG WKH GLIHUHQWLDWLRQ XVFOHDFWLYLW\ )RUUVXEMHFWZHUH DVNHG WR SHUFRUP ILQJHUIORP DQG H[WHQVLRQ P RYHP HQWV DQG WKH H[SHUP HQWDOGLDJUDP LV VKRZQ LQ)LJ : H FRQGXFWHG DFRUHDWRQ DQDO\VLEHWZHHQ WKH HLJHQFHILQHUHQW; DQG WKH JUSIRUFH 7KHUHXOW DUH VKRZQ LQ)LJ WKH UHG HOOSVHLQ WKH ILJXUH UHSUHVHQWV WKH FRQGHQFHILQHWWKH UHVXOW DQG; ZHUH KJKO FRUUHODWHG ZLWK JUSIRUFH DQG WKH DEVROXWH VRI 3HDWRQ VUZHUHDOJUHDWUDQ ,WYDOGDWHG WKH UHXOWVRI WKHHDFWRP DJQHWF VLP XODWRQV DQG GHP RQWUDWHG WKH DELOLW\ RI %, WR WDFNFKDQJHVLQP XVFOHDFWLYLW\ 7RIXUWKHUYHUI\ LP SHGDQFHSDUDP HWUV FDQEH XVHG WR FKDUDFWHUL]H WKH GHJUHHRI P XVFOHDFWLYLW\ ZHUHWRUHG WKHP XVFOHDFWLYLW\E\ LP SHGDQFHSDUDP HWUV XVLQJ DQRJ DQG VKRUWWUP P HP RU QHZRUN 7KH HIIFWVHYDOXDWHG E\ H[SDQGLQG YDULDQFH VFRUH (96 ZLWK URRWP HDQ VTXDUH HUURU 506($IWHUQRUP DO]LQJ WKH GDW5 ; ZDV XVHG DV WKHLQSXWWR WKH QHWZRUN DQG IRUFH ZDV XVHG DV RXWSXW RI WKH GDWZDV XVHG DV WKH WUDLQLQJ VHWDQG ZDV XVHG DV WKH WHVWVHW7KH SUHGLFWRQ UHXOWV IRUWKH IRXUXEMFWV DUH VKRZQ LQ) LJ 7KHDYHUDJH (96 RI WKH UXEMFWV ZDV f DQG506(ZDV f ,Q WKLV SDSHU ZHGHVLJQHG DQ H[SHUP HQWDOVFKP HEDHG RQ WKH VLP XODWRQ UHXOWV DQG DFKLHYHG WKH DFFXUDWH UHGXFWRQ IURP %, WR P XVFOH DFWLYLW\ ZLWK WKH KHSS RI DUWLFLDO LQWHOOLJHQH ,WSURYLGHV P RUHOJKWHJKWDQG VLP SOHGHVLJQ\RXWRQ IRUZHDUDEOHP XVFOHFRQWURO IURP

5HIHUHQFHV

: DQ - - = 4LQ DQG 3 < : DQJ HWDO ³0 XVFOHIDWXH JHQHUDWLQJ DQG WUDQVODWLQJ DQG WUDQVODWLQJ ([S 0RO 0HG 9RO 1R H " H

$SSHO+ - - 0 & 6RDUHVDQG- $ 5 ' XDUWH ([HUFLVH P XVFOHGDP DJHDQGIDWXH´ 6SRUWV0HG 9RO 1R "

/L; / /L DQG+ 6KLQHWDO ³(OHFWURFDOLP SHGDQFHP\RJUDSK\ IRUHYDOXDWQJ SDWHQF P XVFOHFKDQJHV DWWUVWRH´ ,(((7UDQV1HXUDO6\VW5HKDELO(QJ 9RO 1R "

/L/ + 6KLQ DQG; /LHWDO ³/RFDO[HG HDFWUFDOLP SHGDQFHP\RJUDSK\ RI WKH ELFHSV EUDFKL P XVFOHGXULQJ GLIHUHQWHYHQWV RI LVRP HWUF FRQWUDFWRQDQG IDWXH´ 6HQVRUV 9RO 1R

* DEUHO6 5 : /DX DQG& * DEUHO ³7KHGHDFWUF SURSHUWHV RI ELRGRJLFDOWXHV ,,, 3DUDP HWUF PRGHOV IRUWKH GLHDFWUF\SHFWUP RI WXWXHV´ 3K\V0HG %LRO 9RO 1R "

$QGUHFFHWW' 5)RVL DQG& 3HWUFFL ³$Q,QWHJUDWHGRUHIRUWKHFDSDXQDQRI WKHGLHDFWUF SURSHUWHV RI ERG\ WXWXHVLQWKHIUHTXHQF\ UDQJH +] * +] ´ ,QW$SSO3K\V

Space Division-Based Stroke Classification and Localization Using Wearable Microwave Sensing Technique

Zheng Gong[1] and Yifan Chen[1,2]*

[1]University of Waikato, New Zealand
[2]University of Electronic Science and Technology of China, China
*corresponding author: yifan.chen@uestc.edu.cn

Abstract: A novel microwave medical sensing method is proposed for fast stroke classification and localization, which utilizes space division of the region under examination (i.e., the head). The space division is enabled by the generalized scattering matrix theory and incorporates the brain anatomy. Then a novel decision tree learning method is proposed, which facilitates efficient stroke feature identification for classification. The classification accuracy and localization efficiency are shown to be greatly improved compared to the traditional method.

In microwave medical sensing (MMS), signals scattered from a region under examination (RUE) such as the human head generally carry information about its geometric shape, internal structure, and electromagnetic properties. A wearable MMS system is shown in Fig. 1(a). The RUE structure is often highly complex, and it is difficult to characterize the spatial property of an anomaly without reconstructing the image. To solve this problem, we propose a novel space-division-based stroke classification and localization method. As shown in Fig. 1(b), the RUE is an enclosed area A, whereas the receiving antennas are outside A. Assume that there is an anomaly in the RUE; this feature will influence the electromagnetic responses at the receiving antennas. According to medical knowledge and anatomical structure, RUE is divided into multiple subareas by spatial partitioning. The generalized scattering matrix (GSM) theory is utilized to conduct an electromagnetic analysis on space division, merging some of the subareas. The merging aims to ensure that the electromagnetic responses of different subareas are independent of each other. Thus, any anomaly present in a certain subarea will introduce highly location-selective signatures. Subsequently, if the RUE A is divided into several subareas, as $A = \{A_1, \ldots, A_i, \ldots, A_I\}$. Each subarea separately satisfies the electromagnetic independence requirement based on GSM [11]. When an anomaly occurs in a certain A_i, this feature will produce a specific electromagnetic response. Based on this response, we can obtain the location information of the disease.

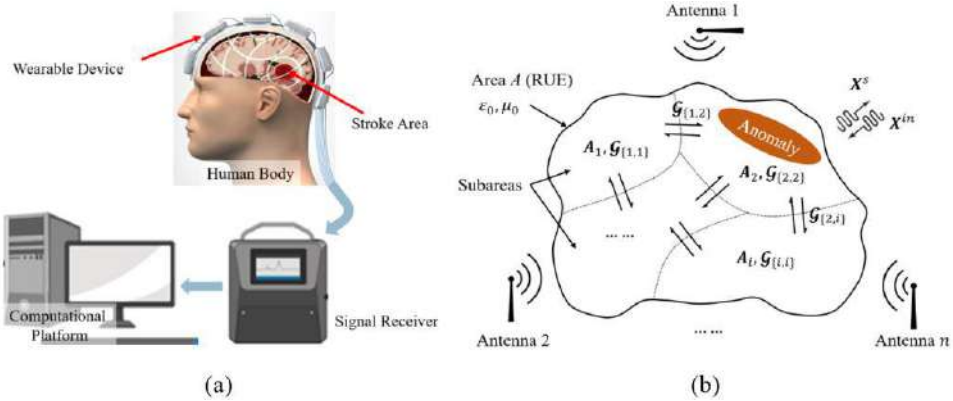

Fig. 1. (a) Architecture of the proposed system. (b) Pictorial illustration of the space-division-based method.

For each A_i, a stroke incidence probability p_i is assigned according to expert knowledge, where the risk set of A is $P = \{p_1, \ldots, p_i, \ldots, p_I\}$. Without loss of generality, let us assume that the subareas are sorted in risk so that A_1 has the highest risk in A and $p_1 \geq p_2 \geq \cdots \geq p_I$. We now proceed to construct a decision-tree-based classifier. The criterion for decision-making is the incidence probability, where the highest-risk subarea should be selected.

Thus we first check A_1 for stroke classification. In this case, the root node has two branches, which are $\{A_1\}$ and $\{A_2, ..., A_i, ..., A_I\}$. If the stroke area is not in A_1, we would continue to the subarea with the second highest incidence probability A_2. As such, the detection sequence is obtained based on the incidence rate. Next, as there are two types of stroke, intracranial haemorrhage (ICH) and ischemic stroke (IS). Linear discriminant analysis is utilized to distinguish ICH from IS due to its efficiency.

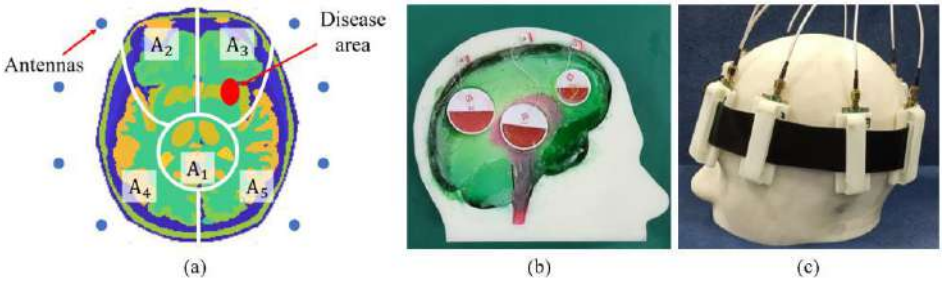

Fig. 2. (a) Brain structure and space division (b) Head-mimicking phantom (c) Wearable antenna array.

The brain area is divided into five subareas based on GSM brain anatomy: basal ganglia region (BGR) A_1, left forebrain A_2, right forebrain A_3, left hindbrain A_4, right hindbrain A_5, as shown in Fig. 2(a). Then we define the incidence probabilities of these subareas as $_1 = 46\%$, $_2 = 20\%$, $_3 = 20\%$, $_4 = 7\%$, $_5 = 7\%$ [2]. The disease area is randomly introduced to these subareas according to their corresponding incidence probabilities. Half of the manufactured human brain is shown in Fig. 2(b), and the experimental system setup with the wearable antenna array is shown in Fig. 2(c).

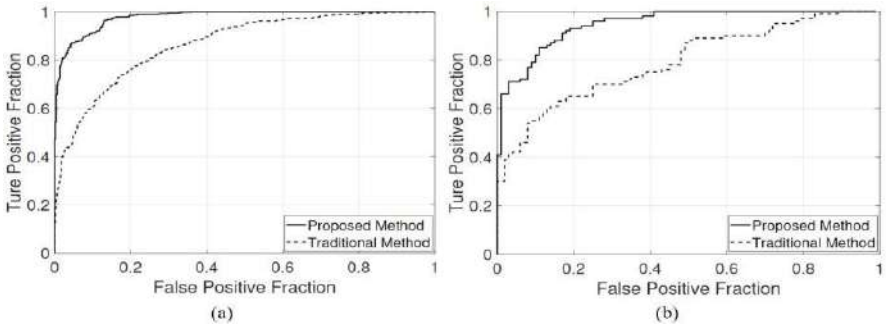

Fig. 3. (a) Simulation and (b) experimental results for proposed and traditional methods.

There are 1000 and 200 groups of simulation and experimental results in the database, respectively, and half of those are IS and the other half are ICH. The training set accounts for 70% of the database, whereas the test set accounts for 30%. For the classification performance, the receiver operating characteristic (ROC) curves of the proposed and traditional methods are shown in Fig. 3. For simulation results, the areas under the curve (AUCs) for the proposed and traditional methods are 0.97 and 0.85, respectively, which exhibits a 14% performance improvement. The localization accuracy of the proposed method is 94.2%. For experimental results, the AUC for the proposed and traditional methods are 0.93 and 0.78, respectively, which exhibits a 19.2% performance improvement. The localization accuracy of the proposed method is 90.5%. In addition, due to the decision tree learning method, the diagnosis time is significantly reduced, with a 21.1% efficiency improvement.

References

1. & :DQ DQG - $ (QFLQDU ³(IILFLHQW FRPSXWDWLRQ RI JHQHUDOL]HG V W U X FHEEE Trans. Antennas Propag., vol. 43, no. 11, pp. 1238–1242, 1995.
2. C. Nag, K. Das 0 *KRVK DQG 0 .KDQGDNDU ³3UHGLFWLRQ RI FOLQLFDO RXW single CT scan on admiVL RNQ North Amer. J. Med. Sci., vol. 4, no. 10, p. 463, 2012.

Advances in Sensor Technologies Involving Electrodynamics and Magnetism

*LDQW 0DJQHWRLPSHGDQFH (IIHFW LQ DPRUSKRXV F WR QRQ GHVWUXFWLYH FRPSRVLWHV PR

$ =KXNRY3 &RUWH /0HRQDWR %ODQFR 9 =KXNRYD
'SWR GH 3ROtPHURV \ 0DWHULDOHV $YDQ]DGRV 8QLYHUVLW\ RI %DV
'SWR GH)LVLFD $SOLFDGD (,* 8QLYHUVLW\ RI %DVTXH &RXQWU
,.(5%$648(6DQ 6HEDVWLDQ DQG %LOEDR 6SDLQ
(+8 4XDQWXP &HQWHU 8QLYHUVLW\ RI WKH %DVTXH &RXQW
FRUUHVSRQGLQJ DXWKRU DUNDGL MRXNRY#HKX HV

$EVWUDFW ,Q WKLV SDSHU H[WHQVLYH VWXGLHV RI WKH IDFWRUV DIIHFWLQ
DQG PDJQHWLF ILHOG GHSHQGHQFH LQ DPRUSKRXV PDJQHWLF PLF
VRIWQHVV KDYH EHHQ REVHUYHG LQ &R ULFK PLFURZLUHV +RZHY
LPSURYH VXEVWDQWLDOO\ WKH *0, HIIHFW DQG PDJQHWLF VRIWQH
GHSHQGHQFH RI WKH *0, HIIHFW LV DOVR VXEVWDQWLDOO\ DIIHF
UHSRUWHG LQ WKLQ PLFURZLUHV LQ WKH *+] IUHTXHQF\ UDQJH $
VSDFH PLFURZDYH VSHFWURVFRS\ XVLQJ IHUURPDJQHWLF PLFURZ
IUHTXHQFLHV IRU VWUHVV WHPSHUDWXUH DQG PDJQHWLF ILHOG
FDUERQ ILEHUV FDQ EH DYRLGHG E\ DSSO\LQJ D ORZ IUHTXHQF\
PLFURZDYH VLJQDO IURP WKH FRPSRVLWHV FRQWDLQLQJ FDUERQ

6WXGLHV RI WKH *0, HIIHFW KDYH DWWUDFWHG FRQVLGHUDEOH
VXLWDELOLW\ IRU YDULRXV WHFKQRORJLFDO DSSOLFDWLRQV > @
RI WKH FODVVLFDO VNLQ HIIHFW RI D PDJQHWLF FRQGXFWRU DV
FXUUHQW IORZLQJ WKURXJK WKH PDJQHWLFDOO\ VRIW FRQGXFWR
*0, HIIHFW LV GHVFULEHG DV WKH PDJQHWRLPSHGDQFH UDWLR û=

′= = >= + PD[@ + PD[+

EHLQJ + WKH D[LDO PDJQHWLF '& ILHOG

&\OLQGULFDO VKDSH DQG KLJK FLUFXPIHUHQWLDO SHUPHDELO
IDYRUDEOH IRU DFKLHYHPHQW RI KLJK *0, HIIHFW > @ :LWK LQF
VKLIWHG WR ODUJHU ILHOGV ZKHUH VDPSOH LV PDJQHWLFDOO\ VD
RI WKH VDPSOH V LPSHGDQFH KDYH EHHQ GLVFXVVHG LQ WHUPV R
5HFHQWO\ PDMRU DWWHQWLRQ LV IRFXVHG RQ KLJK IUHTXHQFLHV
GHYHORSPHQW RI WKLQQHU PDJQHWLFDOO\ VRIW PDWHULDOV DQG
ILHOG VHQVRUV > @ 7KXV WKLQ PLFURZLUH LQFOXVLRQV ZLWK
IRU WKH GHYHORSPHQW RI WXQDEOH FRPSRVLWHV WKDW DOORZ Z
PDJQHWLF ILHOG > @

7KH SXUSRVH RI WKLV SDSHU LV SUHVHQW ODVW UHVXOWV RQ

IUHTXHQFLHV DQG H[SORUH WKH DSSOLFDWLRQ RI VXFK PLFURZL
ZLWK WKLQ PLFURZLUHV LQFOXVLRQV

:H PHDVXUHG PDJQHWLF ILHOG + GHSHQGHQFHV RI LPSHGDQ
PDJQHWLF PLFURZLUHV SUHSDUHG E\ WKH 7D\ORU8QJHUXS1RPH
IUHTXHQFLHV ,Q DPRUSKRXV PDWHULDOV FKDUDFWHUL]HG E\ WKH
WKH PDLQ VRXUFHV RI PDJQHWLF DQLVRWURS\ DUH
E\ WKH PDJQHWRVWULFWLRQ > @

.H\ 1L

9DQLVKLQJ 0DJQHWLF)LHOG DQG EHWWHU PDJQHWLF
0 0 V\VWHPV DW "[" > @)URP û= = + GHSHQGHQFHV
ZLWK§ ZLWK EXW ZLWK GLIIHUHQW GLDPHWHUV G G —P DQ
PLFURZLUHV SUHVHQW KLJKHU û= = UDWLR DW I 0+] +RZHYHU
IRU WKLQQHU PLFURZLUH $FFRUGLQJO\ WKHUH LV DUHODWLRQV
SHUIRUPDQFH DQG WKH ZLUH GLDPHWHU D WUDGH RII EHWZHHQ ZL
7KH GLDPHWHU UHGXFWLRQ PXVW EH DVVRFLDWHG ZLWK WKH LQF
0DJQHWLF VRIWQHVV DQG *0, RI)H UHLF PLFURZLUHV
VXEVWDQWLDOO\ LPSURYHG E\ VWUHVV DQQHDOLQJ DOORZLQJ LQ

7KH LQWHJUDWLRQ RI VXFK IHUURPDJQHWLF PLFURZLUHV LQWR
HIIHFWLYH PLFURZDYH UHVRQVH DOORZLQJ WR REWDLQ WXQDE
FRPSRVLWHV FRQWDLQLQJ FDUERQ ILEHUV WKH VXUURXQGLQJ
PLFURZDYH VLJQDO JHQHUDWHG E\ IHUURPDJQHWLF PLFURZLUHV
PRGXODWLRQ DOORZV WR GHWHFW WKH PLFURZDYH VLJQDO IURP
UHVXOWV GHPRQVWUDWH WKH FDSDELOLW\ IRU WKH LQWHJUDWLRQ
FDUERQ FRPSRVLWH SDUWV IRU ZLUHOHVV PRQLWRULQJ RI H[WHU
RU PDJQHWLF ILHOG

5HIHUHQFHV

> @ =KXNRY $ &RUWH /HQ 3 *RQ]DOH] /HJDUUHWD / ,SDWRY 0
³$GYDQFHG IXQFWLRQDO PDJQHWLF PLFURZLUHV IRU WHFKQRORJLFDO DS

> @ 3KDQ 0 + 3HQJ + ; ³*LDQW PDJQHWRLPSHGDQFH PDWHULD
3URJ 0DWHU 6FLHQFH YRO ±

> @ 3DQLQD / 9 DQG 0RKUL . ³0DJQHWR LPSHGDQFH HIIHFW LQ DPR

> @ 0pQDUG ' %ULWHO 0 &LXUHDQX 3 DQG <HORQ $ ³*LDQW PDJ
- $SSO 3K\V YRO ±

> @ 0DNKQRYVNL\ ' =KXNRY $ =KXNRYD 9 DQG *RQ]DOH] - ³7
FRPSRVLWH PDWHULDO LQFRUSRUDWLQJ IHUURPDJQHWLF PLFURZLUHV ´

6HQVLQJ FDUERQ ILEHU FRPSRVLWHV ZLWK FRQWL
HOHFWURPDJQHWLF DQG PHFKDQLFDO FKD

5 % *DUFLD ('W3DLEHH%G D0XQLR]-XU0HQ&-RKDQVVRQ
9 =KXNRYD,SDWQRY $ =KXNRY

*$,.(5 7HFKQRORJ\ &HQWUH %DVTXH 5HVHDUFK DQG 7HFKQORJ
5,6(5HVHDUFK ,QVWLWXWHV RI 6ZHGHQ 'LJLWDO 6\VWHPV
'HSW $GYDQFHG 3RO\PHUV DQG 0DWHULDOV DQG 'HSW $SSO 3K\
6DQ 6HEDVWLDQ
,.(5%$648(%DVTXH)RXQGDWLRQ IRU 6FLHQFH %LO

FRUUHVSRQGLQJ DXWKRU HW[DEH#JDLNHU HV

$EVWUDFW $ JODVV FRDWHG IHUURPDJQHWLF PLFURZLUHV KDYH G
IRU VWUXFWXUDO FRPSRVLWH SDUWV 2Q WKH RWKHU KDQG FRQ
QRQ FULPS IDEULFV DQG WKH DXWRPDWLRQ RI WKH HPEHGGLQJ S
ERWK FDUERQ ILEHUV DQG PLFURZLUHV LQFOXVLRQV KDYH EHHQ V
H[SHULPHQWDO UHVXOWV RQ VWXGLHV RI WKH FRPSRVLWHV ZLWK
FDUERQ FRPSRVLWHV 7KLV ZRUN IRFXVHV RQ WKH IUHH VSDFH PL
WKH FDUERQ ILEHUV DQG IHUURPDJQHWLF PLFURZLUHV LQFOXVLR
SURSHUWLHV RI FRQWLQXRXV JODVV FRDWHG &R ULFK IHUURPDJQ

Kv }(šZ }uu}v ‰Œ} o u•]v }u‰}•]š u š Œ] o•]• Á]Œ o •• u}v]š}
h•µ ooÇU šZ }u‰}•]š • u}v]š}Œ]vP]• ‰ Œ(}Œu Ç]((Œ vš • v•}Œ•
• v•}Œ• }Œ šZ}µPZ šZ ‰] Ì} o šŒ] (] Œ• Á]šZ] u š Œ• }(íì š} íìì ..
v}š Á]Œ o •• }Œ Œ ‹µ]Œ ‰o š • (}Œ •µ‰‰oÇ]vP o šŒ] o (] o U } µ
‰Œ}‰}• •}oµš]}v• (}Œ }u‰}•]š • u}v]š}Œ]vP]• v Á • v•]vP u šZ}
•‰ šŒ}• }‰Ç µ•]vP]v oµ•]}v• }((ŒŒ}u Pv š] u] Œ}Á]Œ • ‰Œ • vš]v
Z]PZ • v•]š]À]šÇ š} ‰‰o] •šŒ ••U š u‰ Œ šµŒ v u Pv š] (] o €î
Á]Œ •U u] Œ}Á]Œ • Á]šZ u š oo] vµ o µ•] u š Œ• }(ìXî r íìì …u }À Œ
v šZ Œ (}Œ ‰Œ • vš]vP Æ oo vš u Z v] o v }ŒŒ}•]À ‰Œ}‰ Œ
u}v]š}Œ]vP }(•šŒ •• • v š u‰ Œ šµŒ }(}u‰}•]š • €ï•X
dZ]vš PŒ š]}v }(•µ Z (ŒŒ}u Pv š] u] Œ}Á]Œ •]vš} }u‰}•]š u š
u] Œ}Á À Œ •‰}v• U u l]vP]š ‰}••] o š} } š]v v Á šµv o v • o(r
u Z v] o •šŒ •• ‰ v v }(šZ u Pv š] •Á]š Z]vP (] o]v Po •• }
À o}‰u vš }(• v•}Œ• (}Œ v]vP }Œ •šŒ]v u}v]š}Œ]vP €ð•X D Pv
u] Œ}Á]Œ • v]š• Œ •‰}v• š} o šŒ}u Pv š] (] o • v µ• š}
}u‰}•]š u š Œ] o• €ñ•X ' v Œ ooÇU Z]PZ •š D/ ((š]• } • ŒÀ]v }r
}voÇ u] Œ}Á À Z À]}Œ }(}u‰}•]š • Á]šZ }šZ Œ }v (] Œ• v & rŒ]
À ŒÇ (Á ‰ ‰ Œ• €ó•X
/v šZ]• ‰ ‰ ŒU Á ‰Œ • vš v Á Æ‰ Œ]u vš o Œ •µoš• }v Á]Œ o ••

0DJQHWLF SURSHUWLHV DQG DSSOLFDWLRQV RI JO

9 =KXNRYD &RUWH /HRQDUGR %ODQFR $ =KXNRY
'SWR GH 3ROtPHURV \ 0DWHULDOHV $YDQ]DGRV 8QLYHUVLW\ RI %DV
'SWR GH)LVLFD $SOLFDGD (,* 8QLYHUVLW\ RI %DVTXH &RXQWU
(+8 4XDQWXP &HQWHU 8QLYHUVLW\ RI WKH %DVTXH &RXQWU
,.(5%$648(6DQ 6HEDVWLDQ DQG %LOEDR 6SDLQ

FRUUHVSRQGLQJ DXWKRU YDOHQWLQD]KXNRYD#HKX

$EVWUDFW 7KH WLPSDFW RI SRVW SURFHVVLQJ RQ VRIW PDJQHWLF SURS
HIIHFW RI)H DQG &R EDVHG JODVV FRDWHG PLFURZLUHV LV HYDO
DQG *0, HIIHFW LV REVHUYHG LQ)H ULFK JODVV FRDWHG PLFU
GHSHQGHQFH RI *0, UDWLR RI VWUHVV DQQHDOHG)H ULFK PLFU
GHSHQGHQFH RI WKH VNLQ SHQHWUDWLRQ GHSWK / DV ZHOO DV F
$QQHDOHG DQG VWUHVV DQQHDOHG &R ULFK PLFURZLUHV SUHVHQ
ZDOO SURSDJDWLRQ +RZHYHU &R EDVHG VWUHVV DQQHDOHG PLF
VWUHVV LQGXFHG DQLVRWURS\ DQG UHODWHG FKDQJHV RI PDJQH
UHOD[DWLRQ DQG ³EDFN VWUHVVHV´

'HYHORSPHQW RI PDJQHWLF VHQVRUV LV IRFXVHG RQ WKH PLQLDW
IHDWXUHV DQG RQ ILQGLQJ RI QHZ PDWHULDOV $PRQJ QHZ PDJQ
UHGXFHG GLPHQVLRQV UHFHQWO\ JDLQHG FRQVLGHUDEOH DWWH
SUHSDUHG XVLQJ WKH 7D\ORU 8OLWRYVN\ WHFKQLTXH ZLWK WKLQ
P FRYHUHG E\ IOH[LEOH LQVXODWLQJ DQG ELRFRPSDWLEOH JO
DSSOLFDWLRQV > @ 7KLV WHFKQLTXH DOORZV SUHSDUDWLRQ R
DPRUSKRXV RU FU\VWDOOLQH VWUXFWXUH RI PHWDOOLF QXFOHXV
LQ FU\VWDOOLQH RU LQ DPRUSKRXV PDJQHWLF ZLUHV EXW DP
DGYDQWDJHV VXFK DV VXSHULRU PHFKDQLFDO SURSHUWLHV WKH
ERXQGDULHV FU\VWDOOLQH WH[WXUH GLVORFDWLRQV SRLQW GH
QRW UHTXLUHG 3DUWLFXODUO\ DPRUSKRXV PLFURZLUHV FDQ S
PDJQHWLF EVWDELOLW\ ,Q WKH FDVH RI JODVV FRDWHG PLFURZL
EHFRPHV UHOHYDQW VLQFH WKH SUHSDUDWLRQ SURFHVV LQYROY
VLPXOWDQHRXV VROLGLILFDWLRQ RI WKH PHWDOOLF QXFOHXV VXU
GLIIHUHQW WKHUPDO H[SDQVLRQ FRHIILFLHQWV > @

7KH SXUSRVH RI WKLV SDSHU LV SUHVHQW ODVW UHVXOWV RQ
HIIHFW LQ JODVV FRDWHG PLFURZLUHV SD\LQJ VSHFLDO DWWHQW
RSWLPL]DWLRQ RI GRPDLQ ZDOO G\QDPLFV

6WXGLHG &R ULFK DQG)H ULFK DV SUHSDUHG PLFURZLUHV SUHV
KHQFH *0, HIIHFW)H ULFK PLFURZLUHV SUHVHQW SHUIHFWO\ UHF

ELVWDELOLW\ DQG RFFXUUHQFH RI +\VWHUHVLV ORRSV ZLWK DQ RUGHU RI PDJQLWXGH +RI $P ,Q FRQWUDVW &R ULF
K\VWHUHVLV ORRSV ZLWK DQ RUGHU RI PDJQLWXGH ORZHU +

6WUHVV DQQHDOLQJ RI)H EDVHG PLFURZLUHV DW G RZ HDVRQHV LQGXFHG
LQGXFLQJ RI WUDQVYHUVH PDJQHWLF DQLVRWURS\ 0DJQHWLF SUR
1P DSSOLHG GXULQJ WKH VWUHVV DQQHDOLQJ LQGXFHG WUDQV
QRWLFHDEOH ZLWK LQFUHDVLQJ DQLVRWURS\ UHPDUNDEOH LPSURYH
LQ VWUHVV DQQHDOHG &R)H PLFURZLUHV LPSURYHPHQW LQ RUG
PDJQLWXGH LV DFKLHYHG

$V UHFHQWO\ UHSRUWHG HOVHZKHUH > @ XSRQ DQQHDOLQJ W
EHFRPHV UHFWDQJXODU SUHVHQWLQJ FRQVLGHUDEOH PDJQHWLF
PLFURZLUHV &R6L & PLFURZLUHV SUHVHQW ORZHU FRHUFLYLW\
ZLWKRXW VWUHVV &R ULFK PLFURZLUHV

+\VWHUHVLV ORRSV RI &R ULFK PLFURZLUHV REVHUYHG DIWHU V
RP ±YDOXHV SUHVHQW IHDWXUHV VLPLODU WR WKDW RI)H ULFK
L H UHFWDQJXODU VKDSH WKDW PXVW EH UHODWHG WR SUHVHQ
LQGXFHG PDJQHWLF ELVWDELOLW\ 7KHUHIRUH VLPLODUO\ WR DQ
DQQHDOHG &R ULFK PLFURZLUHV SUHVHQW VLQJOH GRPDLQ ZDOO

&RQVHTXHQWO\ VWUHVV DQQHDOLQJ RI IHUURPDJQHWLF PLFU
FRPELQDWLRQ RI PDJQHWLF SURSHUWLHV ,Q WKH)H ULFK PLFU
LPSURYHPHQW RI PDJQHWLF VRIWQHVV DQG *0, HIIHFW 6WUH
VLPXOWDQHRXO\ SUHVHQW VLQJOH DQG IDVW GRPDLQ ZDOO ': S
5HIHUHQFHV

> @ =KXNRY $ &RUWH /HQ 3 *RQ]DOH] /HJDUUHWD / ,SDWRY 0
³$GYDQFHG IXQFWLRQDO PDJQHWLF PLFURZLUHV IRU WHFKQRORJLFDO DS

> @ +HU]HU * $PRUSKRXV DQG QDQRFU\VWDOOLQH VRIW PDJQHWV
,QVLWXWH RQ 0DJQHWLF +\VWHUHVLV LQ 1RYHO 0DWHULDOV 0\NRQRV
1$72 $6, 6HULHV 6HULHV ($SSOLHG 6FLHQFHV 9RO SS
'RUGUHFKW %RVWRQ /RQGRQ

1RQ SODQH 6XUIDFH 0DJQHWLF 6WUXFWXUHV LQ &

$ &KL]KL3N &RUWH 9HRQXNR-YD*RQ]DOH]URQDVQG $ =KXNRY

'HSDUWPHQW RI 3RO\PHUV DQG $GYDQFHG 0DWHULDOV 3K\VLFV &KHPLV
GHO 3DtV 9DVFR 839 (+8 6DQ 6HEDVWLDQ 6SDLQ
'HSDUWPHQW $SSOLHG 3K\VLFV , (83'6 839 (+8 6DQ 6HE
$*+ 8QLYHUVLW\ RI 6FLHQFH DQG 7HFKQRORJ\ )DFXOW\ RI 3K\VLFV DQG
,.(5%$648(%DVTXH)RXQGDWLRQ IRU 6FLHQFH %LOEDR
FRUUHVSRQGLQJ DXWKRU ROHNVDQGU FK\]K\N#HKX H

$EVWUDFW WXGLHG WKH PDJQHWR RSWLFDO DQG PDJQHWLF EHKDY
VWUHVV DQQHDOHG DW WHPSHUDWXUHV GLVWULEXWHG DORQJ W
PDJQHWLF VWUXFWXUH DFURVV]RQHV VXEMHFWHG WR GLIIHUHQW DQQHDO
JUDGHG PDJQHWLF DQLVRWURS\ LQ D PDJQHWLF PLFURZLUH

:H UHSRUW WKH PDJQHWR RSWLFDO DQG PDJQHWLF VW
VWUHVV DQQHDOHG PDJQHWLF DQLVRWURS\ DORQJ WKH JUDGHG
PDJQHWLF DQLVRWURS\ KDV EHHQ REWDLQHG E\ VWUHVV DQQHDO
7KH WUDQVIRUPDWLRQ RI WKH PDJQHWLF VWUXFWXUH ZDV I
DQQHDOLQJ DW GLIIHUHQW WHPSHUDWXUHV)LJ &KDQJH
WZR W\SHV RI WKH LQYHVWLJDWHG PLFURZLUHV 7KH IORUPD
ZDV REVHUYHG GHSHQGLQJ RQ WKH W\SH RI PLFURZLUH)R
PDJQHWLF V\VWHP ZDV UHFRUGHG DW D VXIILFLHQWO\ ORZ D
7KH PDJQHWRVWULFWLRQ FRHIILFLHQW WKDW GHWHUPLQHV WKH I
DQG &R ULFK PLFURZLUHV 7KHVH WZR FODVVHV RI FRPSOHPHQW
PDJQHWLF VHQVRUV $ FRPSDUDWLYH DQDO\VLV RI VXUIDFH DQ
VXSSOHPHQWDU\ REMHFWLYH RI WKLV VWXG\
$ VSDWLDO GLVWULEXWLRQ RI FLUFXODU HOOLSWLF VSLUDO DQ
&R ULFK PLFURZLUHV WKH H[LVWHQFH RI WZR GLIIHUHQW W\SHV R
KHOLFLW\ ZDV IL[HG E\ WKH 02.(PLFURVFRS\

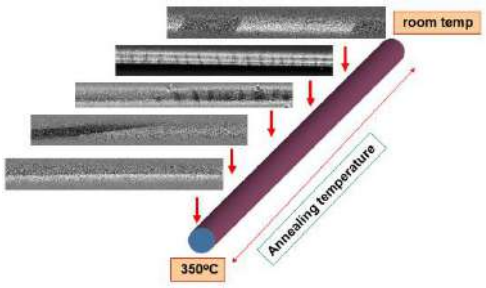

)LJ 0DJQHWLF VWUXFWXUH GLVWULEXWLRQ DORQJ WKH PLFUR
$ WKHRUHWLFDO DQDO\VLV ZDV SHUIRUPHG RQ WKH EDVLV RI WKH
F\OLQGULFDO V\PPHWU\ RI WKH ZLUH OLPLWV WKH VWUHVV WR UD

VWUHVV DORQJ HDFK D[LV 7KH UHVXOWV RI FDOFXODWLRQ DUH
EOXH FRUUHVSRQG WR WZR RSSRVLWH D[LDO PDJQHWL]DWLRQ RU
7KLV DQDO\VLV KDV GHPRQVWUDWHG WKDW WKH GRPDLQ VWUXFW
GRPDLQV RI WKH W\SH , UHG FRORXU FRQVLVW RI LQQHU SDUW
VXSHUILFLDOO\ ORFDWHG GRPDLQV RI WKH W\SH ,, KDYH D KLJK
PDJQHWL]DWLRQ UHYHUVDO SURFHVV LQ PLFURZLUHV

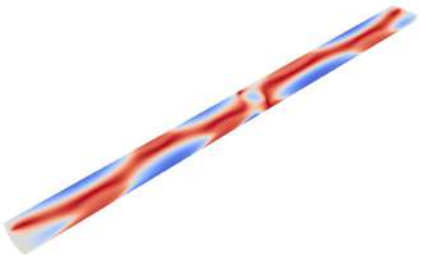

)LJ &DOFXODWHG LPDJHV RI GRPDLQ VWUXFWXUH LQVLGH WKH

7KH REVHUYHU YDULHW\ RI PDJQHWLF VWUXFWXUHV FRXOG EH XV
V\VWHP LQ WKH VHDUFK IRU RSWLPDO PDJQHWLF VWUXFWXUHV LQ

5HIHUHQFHV

3 &RUWH /HyQ 3 9 =KXNRYD - 0 %ODQFR $ &KL]KLN 0 ,SDWRY -
³(QJLQHHULQJ RI GRPDLQ ZDOO SURSDJDWLRQ LQ PDJQHWLF PLFURZLU
7RGD\ 9RO

Smart Electromagnetic Skins and their Applications

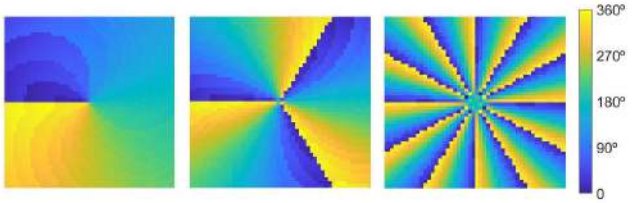
360°
270°
180°
90°
0

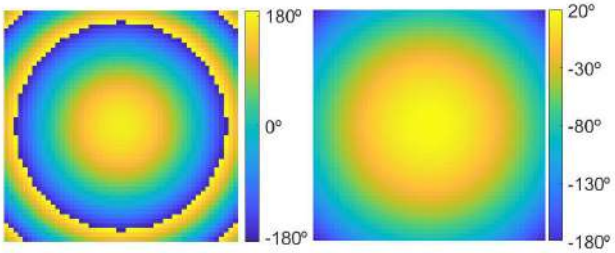
180°
0°
-180°
20°
-30°
-80°
-130°
-180°

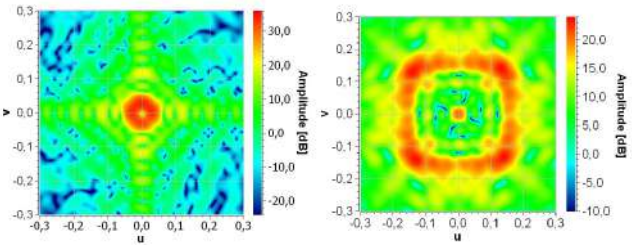
v
u
Amplitude [dB]
30,0
20,0
10,0
0,0
-10,0
-20,0
20,0
15,0
10,0
5,0
0,0
-5,0
-10,0

Reflection Loss Assessment of Reflecting Intelligent Surfaces

F. Costa[1], M. Borgese[2]

[1]Dipartimento di Ingegneria dell'Informazione, Università di Pisa, Italy
[2]Research and Development Department, SIAE MICROELETTRONICA, 20093 Cologno Monzese, Italy
*corresponding author filippo.costa@unipi.it

Abstract: Reconfigurable Reflecting Intelligent Surfaces represent a valid solution for future 6G communications but face practical implementation challenges such as limited tuning range of diodes and losses caused by their presence. The paper focuses on the impact of diode series resistor on RIS performance, highlighting the importance of minimizing losses.

In recent years, Reflecting Intelligent Surfaces (RISs) have become a highly investigated solution for wireless communication systems [1]. The concept behind RISs is to manipulate the phase and amplitude of incident signals by adjusting the impedance of the surface [2], [3]. This can be achieved by using reconfigurable RISs, which allow for dynamic changes to the impedance and reflectivity in real-time [4], [5].

The reconfigurable nature of RISs brings numerous benefits to wireless communication systems, such as improved spectral efficiency, increased coverage, and reduced interference [6]. There are various methods to achieve reconfigurability in RISs, including using Varactor Diodes [7] – [9], PIN Diodes [10], [11], and MEMS [12].

By applying a varying bias voltage to varactor diodes, the impedance of the surface can be adjusted, resulting in a range of reflection coefficients for incident signals. However, there are also challenges associated with reconfigurable RISs. One of these challenges is the limited tuning range of varactor diodes, which restricts the range of impedances that can be realized by the RIS [13]. Additionally, the high series resistance of the diodes can result in substantial reflection losses, which can negatively impact the overall performance of the RIS.

In addition to losses caused by the presence of diodes, there are other factors that affect the efficiency of Reflecting Intelligent Surfaces (RISs). For example, the use of materials such as glass-reinforced epoxy laminate (FR4), which are cost-effective but also have high loss properties, can result in losses. Furthermore, the flow of current on imperfect conductors and losses in the active components can lead to ohmic losses. Minimizing the effect of these losses is critical, and it has been found that a small periodicity of the lattice is an effective way to achieve this [14]. In fact, designing the pattern with a small period not only reduces losses but also leads to a wider bandwidth for the RIS, thus improving its overall performance [15], [16].

Studies in the literature have investigated the behavior of varactor diodes, the key components of RISs, at microwave frequencies. However, it has been discovered that the actual resistor value of the diodes is significantly different from the one specified in the data sheet, and the series resistance is often much higher than expected [17]. Given these findings, it is critical to assess the reflection losses of RISs when the series resistor exceeds 2 ohms.

This paper aims to provide a comprehensive evaluation of the reflection losses of RISs, focusing on the impact of the diode series resistor on the performance of the RIS.

References

[1] 4 :X DQG 5 =KDQJ µ7RZDUGV 6PDUW DQG 5HFRQILJXUDEOH (QYLURQP 1HW ZRUNV IEEE Commun. Mag., vol. 58, no. 1, pp. 106–112, Jan. 2020, doi: 10.1109/MCOM.001.1900107.

[2] S. Abeywickrama, R. Zhang, Q. Wu, and &<XHQJLQ µ,QWelligent Reflecting Surface: Practical Phase Shift Model and %HDPIRUPLQJ 2SWLPL]DWLRQ,¶ IEEE Trans. Commun., vol. 68, no. 9, pp. 5849–5863, Sep. 2020, doi: 10.1109/TCOMM.2020.3001125.

[3] ' 'DUGDUL µ&RPPXQLFDWLQJ with Reconfigurable Intelligent Surfaces: Analysis of Received Signal,¶ IEEE J. Sel. Areas Commun., vol. 38, no. 11, pp. 2526–2537, Nov. 2020, doi: 10.1109/JSAC.2020.3007036.

[4] C. Pan et al., µ5HFRQILJXUDEOH ,QWHOOLJHQW 6XUIDFHV IRU * 6\VWHPV¶ 3U IEEE Commun. Mag., vol. 59, no. 6, pp. 14–20, Jun. 2021, doi: 10.1109/MCOM.001.2001076.

[5] (%M|UQVRQ g g]GRJDQ DQG (*/DUVVRQ µ5HFRQILJXUDEOH ,QW 4XHVWLRQV,¶ IEEE Commun. Mag., vol. 58, no. 12, pp. 90–96, Dec. 2020, doi: 10.1109/MCOM.001.2000407.

[6] &+XDQJ $=DSSRQH *&$OH[DQGURSRXORV 0 'HEEDK DQG &< (QHUJ\ (IILFLHQF\ LQ :LUHOHVV &RPPXQLFDWLRQ,¶ IEEE Trans. Wireless Commun., vol. 18, no. 8, pp. 4157–4170, Aug. 2019, doi: 10.1109/TWC.2019.2922609.

[7] A. Araghi et al., µ5HFRQILJXUDEOH ,QWHOOLJHQW 6XUIDFH Based Wideband Design, Implementation, and Real-:RUOG 'HPRQVWUDWLRQ,¶ IEEE Access, vol. 10, pp. 26462–26655, 2022, doi: 10.1109/ACCESS.2022.3140278.

[8] R. Fara, P. Ratajczak, D. Phan-+X\ $2XULU 0 'L 5HQ]R DQG - GH 5RVQ\ µ$ 3 ,QWHOOLJHQW 6XUIDFH ZLWK &RQWLQXRXVO\ Tunable Local Wireless Channel,¶ IEEE Wireless Commun., vol. 29, no. 1, pp. 75–81, Feb. 2022, doi: 10.1109/MWC.007.00345.

[9]) &RVWD DQG 0 %RUJHVH µ(OHFWURPDJQHWLF Compliant Deployment of Reconfigurable Intelligent Surfaces,¶ IEEE Open J. Commun. Soc., vol. 2, pp. 1577–1589, 2021, doi: 10.1109/OJCOMS.2021.3092217.

[10] J.-B. Gros, V. Popov, M. A. Odit, V. Lenets DQG * /HURVH\ µ$ 5HFRQILJXUDEOH ,QWHOOLJHQW 6XUIDFH RQ D %LQDU\ 3KDVH 7XQLQJ Unit Cell,¶ IEEE Open J. Commun. Soc., vol. 2, pp. 1055–1064, 2021, doi: 10.1109/OJCOMS.2021.3076271.

[11] H. Yang et al., µ$ 1Bit 10×10 Reconfigu UDEOH 5HIOHFWDUUD\ $QWHQQD 'HVLJQ 2S IEEE Trans. Antennas Propag., vol. 64, no. 6, pp. 2246–2254, Jun. 2016, doi: 10.1109/TAP.2016.2550178.

[12]) <DQJ 3 3LWFKDSSD DQG 1 :DQJ µ7HFKQRORJLHV IRU 5HFRQILJXUDEOH , /LQN Micromachines, vol. 13, no. 2, Art. no. 2, Feb. 2022, doi: 10.3390/mi13020285.

[13] F. Costa and M. Borgese, Circuit Modelling of Reflecting Intelligent Surfaces, 2021, p. 550. doi: 10.1109/SPAWC51858.2021.9593104.

[14]) &RVWD DQG $ 0RQRUFKLR µ&ORVHG5HIOHFWLRQ /RVVHV LEEE Trans. Antennas Propag., vol. 60, no. 10, pp. 4650–4660, Oct. 2012, doi: 10.1109/TAP.2012.2207318.

[15] ' 0 3R]DU µ:LGHEDQG 0LFURVWULS 3DWFK $QWHQQDV for 24 GHz,¶ in IEEE Antennas and Propagation Society International Symposium 1997. Digest, Jul. 1997, pp. 1948–1951 vol.3, doi: 10.1109/APS.1997.630282.

[16]) &RVWD 6 *HQRYHVL DQG $ 0RQRUFKLR µ$:LGHEDQG 'XDO-Frequency Double Square Ring Frequency Selective Surface (FSS),¶ IEEE Antennas Wireless Propag. Lett., vol. 8, pp. 1341–1344, 2009, doi: 10.1109/LAWP.2009.2038346.

[17] .2PRWR 7 7RPXUD DQG -LConcept and Prototyping of a Reconfigurable Intelligent Surface for 5.8 GHz-Band 5HIOHFWDUUD\ $QWHQQDV IEEE Access, vol. 9, pp. 154401–154408, 2021, doi: 10.1109/ACCESS.2021.3071090.

$(6 7255(02/,12663$,1± -81(

Preliminary Results on Conformal Reflective Surfaces for Urban Scenarios

M. Beccaria[1*], A. Mazzinghi[2], A. Massaccesi[1], A. Freni[2] and P. Pirinoli[1]

[1]Department of Electronics and Telecommunications, Politecnico di Torino, Turin, Italy
[2]Department of Information Engineering, University of Florence, Florence, Italy
[*]corresponding author: michele.beccaria@polito.it

Abstract: In this communication, the results of a preliminary analysis on the possibility to use a curved passive smart electromagnetic skin working at millimeter waves to be mounted on street light or stop light poles are presented. In particular, the radiation properties of the curved surface are studied and compared with those of a planar solution, taking also into account the visual impact and the possibility to rotate the surface around the supporting pole.

The need for the next generation of communication systems to provide huge data rates with very low latency, ubiquitous mobile ultra-broadband connectivity, seamless coverage, and reduced power consumption has pushed research interest to find new solutions to satisfy these requirements. If, on one side, the use of the mm-wave frequencies presents several advantages, on the other, the larger attenuation and stronger interaction with obstacles along the propagation path can cause a degradation of the services in those regions that are not in the line-of-sight of the base station antennas. To limit their spread, Smart Electromagnetic Skins (SESs) can be introduced in the environment in which the propagation occurs [1-2]. They are very thin surfaces, consisting of many elements with resonant or subwavelength size, able to provide anomalous reflections. Depending on the scenario in which they are introduced, they could be passive structures [3], but, if necessary, they could also include active elements to provide coverage reconfigurability [4]. Usually, SESs are assumed planar to be integrated on walls of buildings. However, this solution is not always feasible, as for example, in historical city centers or on buildings with plenty of windows. Thus, other supporting structures must be used, such as street light or the stop light poles (see the scheme in Fig. 1a). For the latter cases, the use of a curved instead of a planar reflecting surface seems convenient to reduce its visual impact and allow the SES to be illuminated by the field arriving from different base stations.

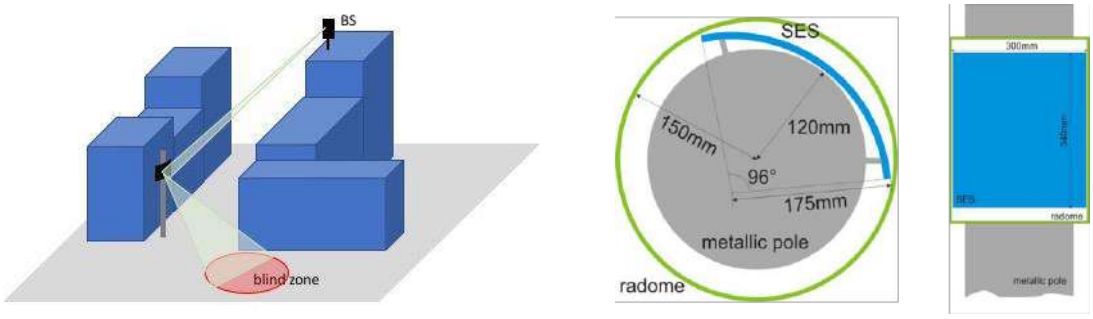

(a) (b)

Figure 1: (a) Example of the considered environment, where the SES is used to cover blind zones for the base station antenna. (b) Top and side view of the SES.

To assess the feasibility and the performance of a curved SES, a configuration as the one shown in Fig. 1b,

designed to be mounted on a tight pole with a diameter of 240 mm and protected by a radome concentric to the pole, with a diameter of 300 mm, is considered. Note that in the present analysis the effect of the radome on the performance of the SES is assumed negligible, but it is used to have an indication of the size of the reflecting surface that can be introduced between it and the pole.

Even if SESs can be realized either with resonant sub-wavelength unit-cells, here the first choice is adopted. Moreover, since the required bandwidth is less than 1.0%, a simple non-radiating element is selected, i.e., a square patch printed on a single layer of Dicald 527, with thickness $h = 0.8$ mm, relative dielectric constant $\varepsilon_r = 2.4$ and losses characterized by $\tan\delta = 0.0009$. The unit-cell has a size equal to $0.4\lambda_0$ at the upper bound of the considered frequency range, $f = 27.5$ GHz. The surface, that has size of 300 mm × 340 mm, is therefore discretized with 55 × 62 elements.

The performance of the curved SES is compared with that of two different planar reflecting surfaces with the same height of the curved one. The first one has a width of 180 mm, to stay between the pole and the radome. The width of the second configuration is instead fixed in such a way that the reflected main beam has the same HPBW of the curved SES, and it is equal to 266 mm. In Fig. 2a the top and side views of the two planar SESs are shown. The three configurations are designed to provide a reflection in the direction ($\theta_r = 20°$, $\varphi_r = 0°$) with respect to the coordinate system indicated in Fig. 2a when an incident plane wave is impinging on the surface with angles ($\theta_i = 20°$, $\varphi_i = 0°$) and then their radar cross section (RCS) is evaluated. The obtained patterns in the plane $\varphi_s = 0°$ are plotted in Fig. 2b. It is worth noting that the curved SES has a maximum RCS comparable to that of the larger planar SES, which however is too large to stay behind the radome.

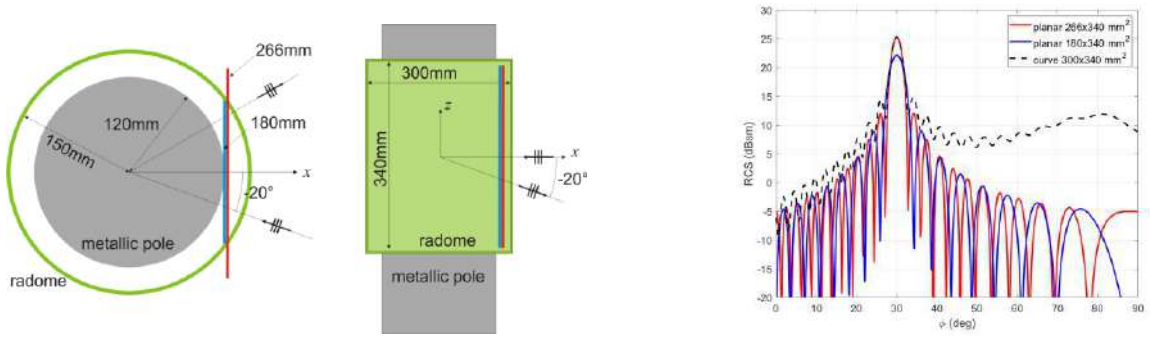

(a) (b)

Figure 2 (a) Top and side view of the planar SESs. (b) Evaluated RCS in the $\varphi_s = 0°$ plane.

References

1. Erricolo D., Rajo-Iglesias E., Sabouni A., Uduwawala D., Gandhi P., "Effect of Periodicity on Mutual Coupling of Antennas Embedded in a Lossy Dielectric Half-Space," IEEE Trans. Antennas Propag., vol. 54, no. 4, pp. 1382–1390, Apr. 2006.
2. Oliveri G., Gregori M. A., Poli L., Rocca P., Massa A., "Load-Network-Oriented Powers Matching Optimization for Multiport Receiving Antennas," IEEE Trans. Antennas Propag., vol. 62, no. 4, pp. 1676–1684, Apr. 2014.
3. Oliveri G., Rocca P., Massa A., "Reliable Diagnosis of Large Linear Arrays—A Bayesian Compressive Sensing Approach," IEEE Trans. Antennas Propag., vol. 60, no. 10, pp. 4627–4636, Oct. 2012.
4. Oliveri G., Rocca P., Massa A., "A Bayesian-Compressive-Sampling-Based Inversion for Imaging Sparse Scatterers," IEEE Trans. Geosci. Remote Sens., vol. 49, no. 10, pp. 3993–4006, Oct. 2011.

B. 8$.)3.4 &

Some Notes on the Electromagnetic Field Processing in the Deep Physical Layer

Marco Donald Migliore

DIEI,
University of Cassino and Southern Lazio
*corresponding author, E-mail: mdmiglio@unicas.it

Abstract

Antennas and Electromagnetic Þeld Processing Devices (EPD) are discussed, considering their role in the OSI stack of the next generations of personal communication systems. The physical layer is divided into two layers, the ÔSurface Physical LayerÕ, which will be called simply the Physical Layer (PL), and the ÔDeep Physical LayerÕ (DPL). According to this Ôextended OSIÕ model, antennas are Ôcross-layer devices, while EPDs are Ôsignal processingÕ devices operating at the DPL, wherein the ÔsignalÕ is the electromagnetic Þeld conÞguration.

1. Introduction

The challenging objectives of the next generation of personal communication systems require extremely aggressive use of the communication channel with active control of it. In this new vision, the communication channel becomes a resource that can be dynamically optimized, with a great impact on the performance of the communication system. Radiating systems interact intelligently with the environment, playing an active role in the communication system.

The starting point of the analysis carried out in this presentation is to use a physical approach to information theory [1] for the analysis of such structures. The basic idea is to split the Physical Layer, introducing a layer below the physical layer, called the Deep Physical Layer, wherein information is not yet an abstract quantity, but a physical quantity, deÞned as the number of distinguishable conÞgurations of the observable (in the speciÞc case the electromagnetic Þeld) in the presence of noise at the receiver side [2].

This opens new challenges in the study of the physical processing of information in the communication channel and the analysis of the impact of these systems on the communication process.

2. The Deep Physical Layer

The OSI model (Fig. 1) gives a complete view of the communication process. In the OSI model the data stream is divided into seven layers starting from the highest level, the ÓapplicationÓ layer, down to the lowest level, the Óphysical layerÓ (PL), which describes the implementation of the transmission of bits through the communication channel. Each intermediate layer represents a conceptual Ôdiscontinuity Õ in the complex procedures required for communication.

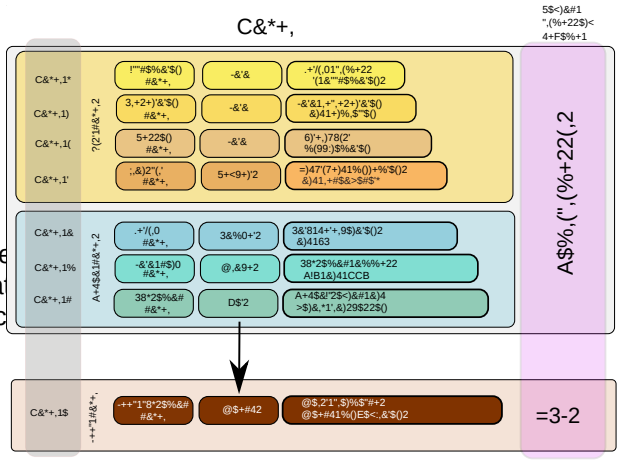

Figure 1: In the extended OSI layer, antennas are Ôcross layerÕ devices, while RISs (Reßecting Intelligent Surfaces) are special EPDs (Electromagnetic Þeld Processing Devices) able to perform signal processing at the Deep Physical Layer level

If we look at the physical layer, we can note that the analysis of the communication process at this level is performed using statistical models. This is a well-established approach, routinely applied by the signal processing community with great success.

However, the Þrst step that any communication system does before starting the communication is to identify the channel state. In practice, this changes the perspective of the communication systems from a statistical approach to a deterministic approach, ÔobservingÕ the actual state of the channel. This indicatedn that inside the physical layer, there is a ÔconceptualÕ discontinuity.

Loosely speaking, in the physical layers two ÔworldsÕ coexist. In a world, information is an abstract concept related to the Shannon mutual information. This is the world of the mathematica theory of information. However, there is a further world where information is encoded in a physical observable, that obeys the rule of physics. Loosely speaking, this is the world of the physical theory of information. Here, limitations are Þxed by the laws governing our universe and hence are unbreakable.

All this suggests dividing the physical layer into two parts, an upper part, the Òsurface physical layer,Ó which in the following will be called simply the Physical Layer (PL)

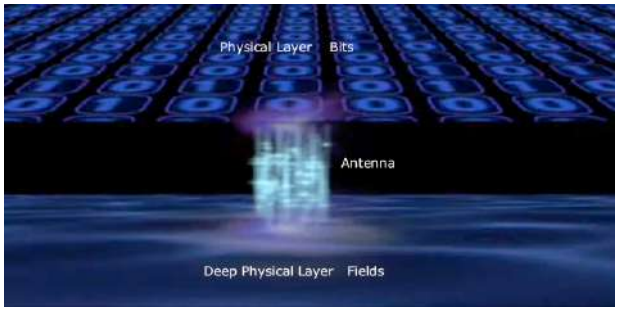

Figure 2: A prictorial view of the roel of the antennas in the extended OSI layer; antenna is the ÕgateÕ between the Physical Layer (PL) and the Deep Physical Layer (DPL). In this sense, antennas can be seen as Õcross-layerÕ devices.

Figure 3: A pictorial view of an EPD; it consists of an array of electromagnetic controllable scattering elements optimized to maximize the capacity of the wireless system. The DPL contains all the resources regarding space/time/polarization degrees of freedom of the electromagnetic Þeld that the communication system can use to encode information while EPDs allow the maximization of these resources by increasing the number of possible distinguishable Þeld conÞgurations by the receiver, acting as ÕlensesÕ for physical information.

for the sake of simplicity, and a lower part, the ÒDeep Physical LayerÓ (DPL) [1]. While in the upper part, information is represented by abstract quantities, at the DPL, information is associated with physical observables. In particular, the amount of information is deÞned as the number of distinguishable electromagnetic Þeld conÞgurations on the receiver.

In this ÔextendedÕ OSI model the DPL is treated the same way as the other layers of the stack. In particular, as in the other layers, also in the DPL it is possible to do some Ôsignal processingÕ to optimize the communication process [4]. The only difference is that at the DPL the ÔsignalÕ is the electromagnetic Þeld conÞguration, and the devices at the DPL directly modify the electromagnetic Þeld conÞguration. We will call these devices Electromagnetic Þeld Processing Devices (EPDs) [3]..

3. The role of Antennas in the DPL

As discussed above EPDs directly modify the electromagnetic Þeld conÞguration in the DPL. In this view, antennas can be seen as quite special EPDs.

Indeed, the role of the antennas is to ÔconnectÕ the PL with the DPL (Fig. 2). In this sense, they ÔtranslateÕ bits in different electromagnetic Þeld conÞgurations and vice-versa [4].

All this also suggests a bottom-up vision of the communication systems.

The DPL contains all the resources regarding space/time/polarization degrees of freedom of the electromagnetic Þeld that the communication system can use to encode information [1]. EPDs allow the maximization of these resources by increasing the number of possible distinguishable Þeld conÞgurations by the receiver.

The different distinguishable conÞgurations of the Þeld must be converted into ÔbitsÕ to be processed by the layers above the DPL. The antenna does this conversion.

As a consequence, while before the use of EPD the propagation channel was the bottleneck, the use of EPD shifts such a bottleneck toward the antennas. It is worth noting that this view also suggests a Ôcross-layerÕ approach for antenna synthesis, in which the radiating system is designed considering a double goal: controlling the distribution of the radiated power density in the space and maximizing the channel capacity [4].

4. The role of EPDs in the DPL

As noted above, the role of the EPD is to maximize the resources the DPL makes available to the upper layers [3].

An EPD consists of several electronically controllable scattering elements. The general architecture is similar to the one used in the Reßecting Intelligent Surfaces (RIS) [5]. However, there are some differences.

The goal of EPDs is the maximization of the channel capacity, and their synthesis is driven by information-based goals [6]. The solution maximizes the number of MIMO spatial subchannels [7], giving quite complex Þeld conÞgurations on the EPD. Instead, the main goal of the RIS is extending the wireless connection to overcome the limitations of the high-frequency communication systems, as in 5G FR2 or in the THz band that will be used in the next-generation 6G communication systems. RIS is based on reßection, allowing more classic synthesis methods to be used.

Also, the Þeld of application of EPDs and RISs is different. RISs are highly effective in mmW and THz frequencies, where their use at lower frequencies, where scattering mitigates the coverage problems, is more attractive at the lower frequencies, where increasing the MIMO spatial subchannels allow increasing the capacity balancing the narrower bandwidth available, while is less appealing. at very high frequencies, where extremely large bandwidth allows very high bit rates.

EPDs and RISs share the use of controllable devices. Indeed, EPDs can also be obtained as an array of RISs, i.e.,

of reßecting controllable surfaces [7] organized to maximize the capacity of the wireless system [3] (Fig. 3).

Loosely speaking, RIS devices give optimal Þeld processing when Þeld conÞgurations have only one spatial degree of freedom, [4]. More complex Þeld elaboration must be carried out to maximize the channel capacity if more than one degree of freedom is available.

5. Conclusions

Introducing the Deep Physical Layer in the OSI model allows for quantifying the amount of information transmitted by the communication systems in terms of electromagnetic Þeld conÞgurations. Put simply, in the DPL, information is physical

In this model, the role of the antennas is to ÔconnectÕ the upper layer of the physical layer with the DPL, ÕmappingÕ bits in different conÞgurations of the electromagnetic Þeld and vice-versa.

Processing at the DPL is made by devices called Electromagnetic Field Processing Devices (EPDs), which consist of arrays of controllable reßecting devices organized to maximize the capacity of the wireless system [3]. They act as ÔlensesÕ instead of Ômirrors,Õ as in RIS devices, for information.

A simple Óproof of conceptÓ of EPD is the ADAM architecture, in which several controllable scattering elements are placed in proximity of a MIMO antenna, obtaining a 6 bits local controllable environment [6]. Experiment tests conÞrmed the effectiveness of the use of EPD. In particular, the prototype allowed almost half the transmitted power without reducing the performance in terms of channel capacity, with a positive impact not only on the communication network, reducing energy consumption, but also on the environment, lowering the level of the electromagnetic Þeld [7]. The ADAM architecture is the starting point for developing new devices under investigation in the microwave laboratory of Cassino University.

References

[1] Migliore, M. D. ÓOn electromagnetics and information theory.Ó IEEE transactions on antennas and propagation 56.10 (2008): 3188-3200

[2] Migliore, M. D. ÓThe world beneath the physical layer: An introduction to the deep physical layer.Ó IEEE Access 9 (2021): 77106-77126.

[3] Migliore, M. D. ÓInformation Flows at the Deep Physical Layer Level.Ó A Glimpse Beyond 5G in Wireless Networks. Cham: Springer International Publishing, 2022. 59-87.

[4] Migliore, M. D. ÓHorse (electromagnetics) is more important than horseman (information) for wireless transmission.Ó IEEE Transactions on Antennas and Propagation 67.4 (2018): 2046-2055

[5] Martini, E., and S. Maci. ÓTheory, analysis, and design of metasurfaces for smart radio environments.Ó Proceedings of the IEEE 110.9 (2022): 1227-1243

[6] Migliore, M.D., D. Pinchera, F. Schettino. ÓImproving channel capacity using adaptive MIMO antennas.Ó IEEE Transactions on Antennas and Propagation 54.11 (2006): 3481-3489

[7] Pinchera, D., Wallace, J. W., Migliore, M. D., Jensen, M. A. ÒExperimental analysis of a wideband adaptive-MIMO antennaÓ, IEEE transactions on antennas and propagation, (2008). 56(3), 908-913

!!

"#$%$&'(%)*$')+,!$,-!./')0)*$')+,!+1!2,'(33)4(,'!5(13(&')6(!78%1$&(9!),!00 :;$6(!<$,-!),&38-),4!'#(!5(13(&')+,!=%+-8&(-!>?!'#(!<8)3-),4!7'%8&'8%(!

!
@A!BA!C$D8(%E!FA!G$%'),(*(:5)+H$E!GA!I%%(>+3$$,-! JA!IA!F,&),$%'

7:;<=>?@;A?!BC!#D;E?>FE=D!#AGFA;;>FAG(!3AFH;>IFJ=J!J;!*HF;JB(!$<=FA
%AI?F?K?B!J;!);D;EB@KAFE=LM;I(!3AFH;>IFJ=J;!J;!-FINB±(!1B>?KG=D
':;<O!BC!$FGA=D!)P;B>Q!=AJ!RB@@KAFE=?FBAI!=AJ!);D;@=?FE!$QI?;@I!=AJ!RB@<K?FAG(!3AFH;>IFJ±J!+;Q!2K=A
9.ACB>@=?FBA!1>BE;IIFAG!=AJ!);D;EB@@KAFE=?FBAI!R;A?;>(!3AFH;>IFJ=J!1BDF?SEAFE=!J;!,=J>FJ(!$<=
8RB>>;I<BAJFAG?PB>T!;NBD±KAFBH±O;I

!

!

I>9'%$&!

)PFI!VB>W!<>;I;A?I!?P;!J;IFGA!=AJ!B<?F@FX=?FBA!BC!=
.A?;DDFG;A?!+;CD;E?FH;!$K>C=E;!Y.+$Z!N=I;J!BA!=!>;C
?;EPABDBGQ! ?B! F@<>BH;! ?P;! EBH;>=G;!=HBFJFAG!4\! @@
IE;A=>FBO! "! <>;DF@FA=>Q! J;IFGA! FI! <;>CB>@;J! ?B! =
VFJ;!N;=@!FA!=XF@K?P!=AJ!;D;H=?FBAO!)P;!.+$!FI!<D=E
NKFDJFAG! C=L=J;! =AJ! FE?!! ;CC;;D;E?>B@=GA;?FE=I
EP=>=E?;>FX;J! CB>! JFCC;>;A?! @=?;>F=DIO!)P;! J;IFG
F@<>BH;J!NQ!B<?F@FXFAG!?P;!.+$!EBAIFJ;>FAG!?P;!V
F?!FI!<D=E;JO

KA 2,'%+-8&')+,!

.A! ?P;! >;E;A?! Q;=>I(! $@=>?! #D;E?>B@=GA;?FE! BV
P=H;!N;;A!<>B<BI;J!CB>!NB?P!K>N=A!=AJ!FAJBB>!IE;A=>FBO!)P;!
<>B<=G=?FBA! N;E=KI;! BC! ?P;! <PQIFE=D! N=>>F;>I
J;<DBQ@;A?! BC! ABH;D! VF>;D;II! A;?VB>W!Q[=FA!4\! @@
IE;A=>FBO! "! <>;DF@FA=>Q! J;IFGA! FI! <;>CB>@;J! ?B! =
=>;! KI;J! ?B! ;AP=AE;! 4\! _+%! EBH;>=G;! =HBFJFAG! EBH;DJ!
FAI?=DBA!BC!@KD?F<D;!N=I;!I?=?FBAI!Y`$ZO!"A!.+$!FI!<D=E
IK>C=E;! @=J;! K<! BC! <DF=C?FAG! ;D;@;A?I! ?P=?! >;CD;E?FH;!
F@<FAGFAG!IFGA=D!>=JF=?;J!C>B@!?P;!`$!FA?B!=!J;IF>;BJ!B=E?FBA!
Y<;EKD=>!B>!=AB?P;>!JF>;E?FBAZO!)P;!>;CD;E?;J!CF;D=DBK?JJN;J!
;F?P;>!=!N;=@BFA?FAG!B>!;H;A!=!IP=<FAG!N;=@O!"E?B<?FB@FX=?FBAI!<>BE;IIO
<=IIFH;! <P=DPFC?FAG! ;D;@;A?I! E=A! N;! KI;J! FA! ?P;! <=A;D(!
@=FADQ! J;<;AJFAG! BA! ?P;! >;EBACFGK>=?FBA! >;aKF>;J! NQ!?P;!
EBH;>=G;O!,B>;BH;>(!.+$!P=I!N;;A!=DIB!<>B<BI;J!?B!FA?>BJKE;!
N;=@!?FD?FAG!FA!=!<BFA?FAGBH;>EBK@;A?DB;!=DD;J!
NDFAJ!XBA;I(!VPFEP!=>;!J;CFA;J!=I!=A!=>;=!BC!<BB>!B>!)P;!A?DD!
EBH;>=G;O!QP;A!?P;!.+$!FI!N=I;J!BA!<=IIFH;!;D;@;A?I!F?!FI!
E=DD;J!$,#O
.+$!P=H;!N;;A!<>B<BI;J!CB>!NB?P!K>N=A!=AJ!FAJBB>!IE;A=>FBO!)P;!
]' ^(!P^O!.A!NB?P!E=I;I(!?P;!V=DDI!=>;!KIK=DDQ!?P;!@BI?EBH;>=G;!
<D=E;@;A?I!CB>!FAI?=DDFAG!?P;!>;CD;E?FH;!IK>C=E;@DA!=!<BFA?!
IE;A=>FB(!?P;!`$!FI!C=>!=V=Q!C>B@!?P;!.+$(!?P;>;CB>;!@BI?!
I@=DD!C>=E?FBA!BC!?P;!>=JF=?;J!<BV;>!<>BHFJ;J!NQ!?P;!
E=<?K>;J!NQ!?P;!O!)PFI!I@=DD!C>=E?FBA!@KI?!N;!<>BHFJ;J!
@=A=G;J!?B!;AP=AE;!?P;!EBH;>=G;O!*VFAG!?B!?P;!`$!?B!C=>!
=V=Q(!?P;!IK>>BKAJFAGI!BC!?P;!.+$!=>;!=DIB!I?>BAG=DQ!
FDDK@FA=?;J!IB!?P=?!?P;!<FDDBH;>!BA!?P;!NKFDJFAG!<BJKE;!
N;!A;GDFGFND;O!
)P;!>;CD;E?FBA!<>BJKE;J!NQ!?P;!IK>>BKAJFAG!V=DD!
EP=>=E?;>FX;J!=AJ!EBAIFJ;>;J!CB>!=A!=EEK>=?;!@BJ;DI!
EBH;>=G;!<>BHFJ;J!?B!?P;!J;HFE;I!BC!?P;!KI;>I!=!_FGK>;!7O!,=FADQ(!?P;!<=A;D!BA!?P;!
)PFI!VB>W!<>;I;A?I!?P;!J;IFGA!=AJ!B<?F@FX=?FBA!BC!=
.A?;DDFG;A?!+;CD;E?FH;!$K>C=E;!Y.+$Z!N=I;J!BA!=!>;C
?;EPABDBGQ! ?B! F@<>BH;! ?P;! EBH;>=G;!=HBFJFAG!4\! @@
IE;A=>FBO! "! <>;DF@FA=>Q! J;IFGA! FI! <;>CB>@;J! ?B! =
VFJ;!N;=@!FA!=XF@K?P!=AJ!;D;H=?FBAO!)P;!.+$!FI!<D=E
NKFDJFAG! C=L=J;! =AJ! FE?!! ;CC;;D;E?>B@=GA;?FE=I
EP=>=E?;>FX;J! CB>! JFCC;>;A?! @=?;>F=DIO!)P;! J;IFG
F@<>BH;J!NQ!B<?F@FXFAG!?P;!.+$!EBAIFJ;>FAG!?P;!V
F?!FI!<D=E;JO

KA 2,'%+-8&')+,!

.A! ?P;! >;E;A?! Q;=>I(! $@=>?! #D;E?>B@=GA;?FE! BV
P=H;!N;;A!<>B<BI;J!CB>!NB?P!K>N=A!=AJ!FAJBB>!IE;A=>FBO!)P;!
<>B<=G=?FBA! N;E=KI;! BC! ?P;! <PQIFE=D! N=>>F;>I
J;<DBQ@;A?! BC! ABH;D! VF>;D;II! A;?VB>W!Q[=FA!4\! @@
IE;A=>FBO! "! <>;DF@FA=>Q! J;IFGA! FI! <;>CB>@;J! ?B! =
=>;! KI;J! ?B! ;AP=AE;! 4\! _+%! EBH;>=G;! =HBFJFAG! EBH;DJ!
FAI?=DBA!BC!@KD?F<D;!N=I;!I?=?FBAI!Y`$ZO!"A!.+$!FI!<D=E
IK>C=E;! @=J;! K<! BC! <DF=C?FAG! ;D;@;A?I! ?P=?! >;CD;E?FH;!
F@<FAGFAG!IFGA=D!>=JF=?;J!C>B@!?P;!`$!FA?B!=!J;IF>;BJ!B=E?FBA!
Y<;EKD=>!B>!=AB?P;>!JF>;E?FBAZO!)P;!>;CD;E?;J!CF;D=DBK?JJN;J!
;F?P;>!=!N;=@BFA?FAG!B>!;H;A!=!IP=<FAG!N;=@O!"E?B<?FB@FX=?FBAI!<>BE;IIO
<=IIFH;! <P=DPFC?FAG! ;D;@;A?I! E=A! N;! KI;J! FA! ?P;! <=A;D(!
@=FADQ! J;<;AJFAG! BA! ?P;! >;EBACFGK>=?FBA! >;aKF>;J! NQ!?P;!
EBH;>=G;O!,B>;BH;>(!.+$!P=I!N;;A!=DIB!<>B<BI;J!?B!FA?>BJKE;!
N;=@!?FD?FAG!FA!=!<BFA?FAGBH;>EBK@;A?DB;!=DD;J!
NDFAJ!XBA;I(!VPFEP!=>;!J;CFA;J!=I!=A!=>;=!BC!<BB>!B>!)P;!A?DD!
EBH;>=G;O!QP;A!?P;!.+$!FI!N=I;J!BA!<=IIFH;!;D;@;A?I!F?!FI!
E=DD;J!$,#O
.+$!P=H;!N;;A!<>B<BI;J!CB>!NB?P!K>N=A!=AJ!FAJBB>!IE;A=>FBO!)P;!
]' ^(!P^O!.A!NB?P!E=I;I(!?P;!V=DDI!=>;!KIK=DDQ!?P;!@BI?EBH;>=G;!
<D=E;@;A?I!CB>!FAI?=DDFAG!?P;!>;CD;E?FH;!IK>C=E;@DA!=!<BFA?!
IE;A=>FB(!?P;!`$!FI!C=>!=V=Q!C>B@!?P;!.+$(!?P;>;CB>;!@BI?!
I@=DD!C>=E?FBA!BC!?P;!>=JF=?;J!<BV;>!<>BHFJ;J!NQ!?P;!
E=<?K>;J!NQ!?P;!O!)PFI!I@=DD!C>=E?FBA!@KI?!N;!<>BHFJ;J!
@=A=G;J!?B!;AP=AE;!?P;!EBH;>=G;O!*VFAG!?B!?P;!`$!?B!C=>!
=V=Q(!?P;!IK>>BKAJFAGI!BC!?P;!.+$!=>;!=DIB!I?>BAG=DQ!
FDDK@FA=?;J!IB!?P=?!?P;!<FDDBH;>!BA!?P;!NKFDJFAG!<BJKE;!
N;!A;GDFGFND;O!
)P;!>;CD;E?FBA!<>BJKE;J!NQ!?P;!IK>>BKAJFAG!V=DD!
EP=>=E?;>FX;J!=AJ!EBAIFJ;>;J!CB>!=A!=EEK>=?;!@BJ;DI!
EBH;>=G;!<>BHFJ;J!?B!?P;!J;HFE;I!BC!?P;!KI;>I!=!_FGK>;!7O!,=FADQ(!?P;!<=A;D!BA!?P;!

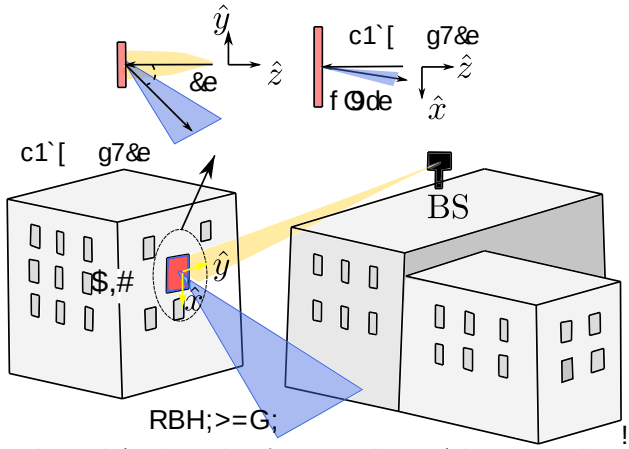

!

_FGK>;!7O!$W;?EP!BC!=A!=FB!KIFAG!=A!.+$!?B!;AP=AE;!?P;!EBH;>=G;O!
)P;!`$!FDDK@FA=?;I!?P;!.+$(!?P;!EBH;>=G;!?B!BH;>EB@;!=!NDFAJ!
=>;=O

L'ÀK7&(,$%)+!$,-!70$%'!F3(&'%+0$4,(')&!7M),!./')&9!

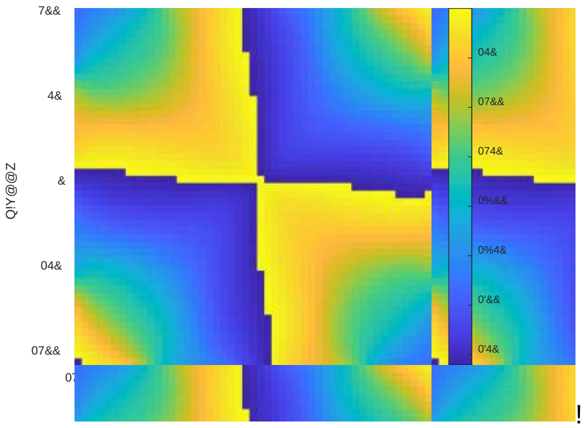

_FGK>;!%O!1P=H;!PFC?!JFI?>FNK?FBA!BC!?P;!;D;@;A?I!BC!?P;!A$,J#!
=C?;>!?P;!1*$O

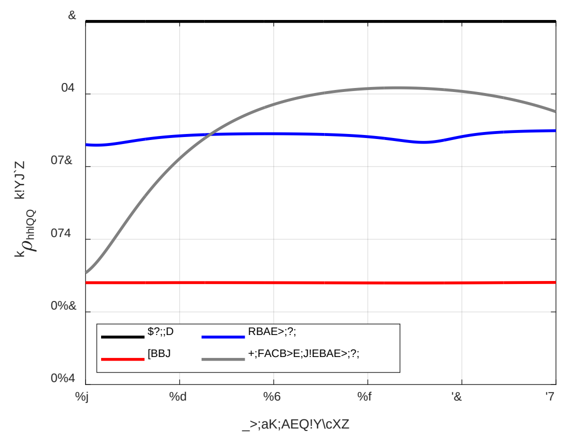

Y=IZ

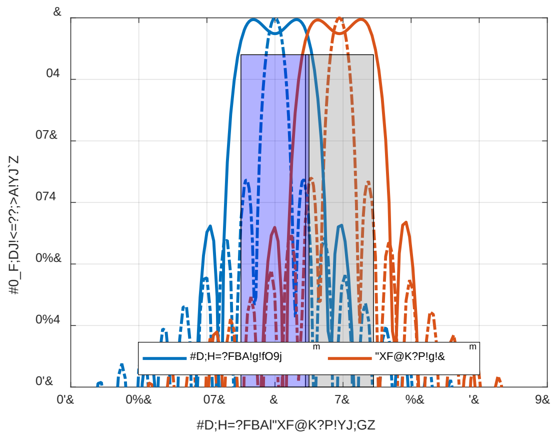

_FGK>;!'O!B>@=DFX#JCF;DJ!<=??;>A!EB@<K?;J!FA!?P;!@=FA!EK?I!BC!?P;!
EBH;>=G;!CB>!?P;!<BD=>FX=?FBA!YJB??;J!DFA;Z!=AJ!C>BYIBDFJ!DFA;Z!
?P;!IOA?P;IFI!6/?!4789O

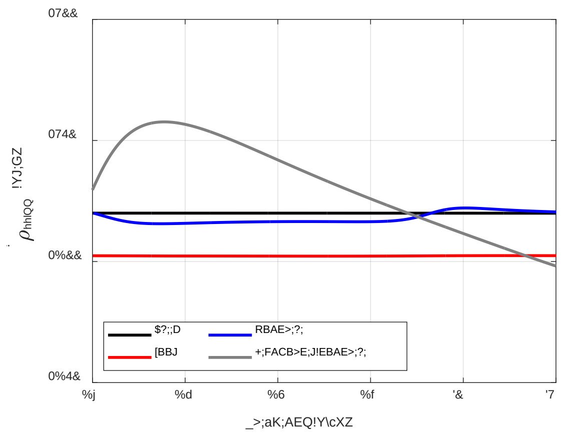

YNZ

_FGK>;!9O!CD;E?FBA!EB;CCFEF;A?!BC!?P;!=A=DQX;J!@=?;>F=DI!=?!I;H[illegible]
C>;aK;AEF;I!EBAIFJ;>FAG!AB>@=D!FAEFJ;AE;!Y=Z!=@<DF?KJ;!YJ`Z!YNZ!
YJ;GZO

FAEFJ;A?!V=H;!FI!>;CD;E?;J!FA!?P;!I<;EKD=>(!?P;!BK?GB[illegible]
=>;!fO9de!FA!;D;H=?FBA!=AJ!&e!FA!=XF@K?PO!

)P;! <=A;D! FI! JK@DFA;=>DQ! <BD=>FX;J! EBAIFJ;>FAG! ?P;! [illegible]
PB>FXBA?=D!<BD=>FX=?FBA!YcZ!J;CFA;J!=I!EB>>;I<BAJFAG!?B!?P;! [illegible]
VPFD;!?P;!H;>?FE=D!<BD=>FX=?FBA!YiZ!FI!B>?PBGBA=D!FA!?P;! [illegible]
)B!=EPF;H;!?P;!J;IF>;J!I<;EFCFE=?FBAI!?P;!>;CD;E?FH;!$,#!FI! [illegible]
EB@<>FI;J! BC! 4&! h! 4&! ;D;@;A?I! BC! <;>FBJFEF?Q! 9O%f! h! 9O%f! [illegible]
@@O!

LAL!A!N(9)4,!/%+&(-8%!(

"I!=!CF>I?!=??;@<?(!?P;!$,#!FI!J;IFGA;J!?B!>=JF=?;!=!<;AEFD! [illegible]
N;=@!FA!?P;!J;IF>;J!JF>;E?FBA!CBDDBVFAG!Y7Z!?B!EB@<K?;!?P;! [illegible]
<P=I;!0PFC?!BC!?P;!;D;@;A?I!T!

ö! Tß" Uß#$ G4!%Šß%F! Tß&'(î 4) Uß(*+ î 4#(*+ à4#! Y7Z

VP;>;! G4!FI! ?P;! V=H;AK@N;>! FA! H=EKK@!(! ?P;! [illegible]
<BFA?FAG!JF>;E?FBA!BC!?P;!<;AEFD!N;=@!(!/0A!=AJ!1!E=! [illegible]
10 (! >;I<;E?FH;DQO!FI! ?P;! JFI?=AE;! C>B@! ?P;! C;;J! [illegible]
! T» ¡" U» ¡" V» ¡#$! F2" 1"31#45 !=AJ! ?P;!H?P! ;D;@;A?(! =AJ! [illegible]
YTß" UßZ!=>;!?P;!EBB>JFA=?;I!BC!?P;!;D;@;A?!>;C;>>;J!?B!?P;! [illegible]
E;A?>!BC!?P;!$,#!O

)PFI! IBDK?FBA! <>BHFJ;I!=!>>BV! N;=@! VPBI;! 0<BD>! [illegible]
N;=@VFJ?P!FI!=>BKAJ!%O9!;>;CB>;(!?PFI!EBACFGK>=?FBA!?B;I! [illegible]
AB?!<>BHFJ;!=!IKEE;IICKD!IBDK?FBA(!>;aKF>FAG!VFJ;>!N;=@! [illegible]

N;=@! FA! NB?P! =XF@K?P! =AJ! ;D;H=?FBA! ?B! CKDCF[illegible]
I<;EFCFE=?FBAI
)B!BN?=FA!?P;!N>B=J;A;J!N;=@(!?P;!<P=I;!0PFC?!JFI?>FNK?FBA!BC! [illegible]
?P;!$,#!EB@<K?;J!KIFAG!Y7Z!FI!IQA?P;IFX;J!KIFAG!=!1P=I;! [illegible]
*ADO!$QA?P;IFI!Y1*$Z!?;EPAFaK;O!)P;!=IQ@@;?>FE!?P;! [illegible]
<P=I;!BC!?P;!>;CD;E?FBA!EB;CCFEF;A?I!BC!?P;!;D;@;A?I!?B! [illegible]
CFA=J!<>B<;!JFI?>FNK?FBA!?P=?!>=JF=?;I!?P;!J;IF>;J!<=??;>A[illegible]
JB! IB(! ?P;! ED=IIFE=D! ?;EPAFaK;! N=I;J! BA! ?P;! .A?;>I;E?F[illegible]
"<<>B=EP!]4^(!jFI!KI;J!?B!>;=EP!?P;!N>B=J;A;J!N;=@!VF?P!=!
>F<<D;!DBV;>!?P=A!'!J`O!/B?;!?P=?(!JK>FAG!?P;!(PP!<>BE;II
;D;@;A?I!=>;!@BJ;D;J!=I!FJ;!;D;@;A?I!=AJ!?P;!BK?<K?!BC!?P;!
IQA?P;IFI!FI!?P;!<P=I;!0PFC?!JFI?>FNK?FBA!?P=?!<>BJKE;I!?P[illegible]
J;IF>;J!EB<BD=>!<=??;>AO
)P;!IQA?P;IFI!<>BE;JK>;!FI!N=I;J!BA!=!@?KD?F<>BE;II!?B!
F@<>BH;!?P;!EBAH;>G;AE;!BC!?P;!=DGB>F?P@O!)PFI!<>BE;[illegible]
EB@@BADQ! KI;J! VP;A! J;=DFAG! VF?P! =! D=>G;! AK@N;>[illegible]
;D;@;A?I! YFA! ?PFI! E=I;! %4&&Z(! IFAE;! ?P;! ;D;@;A?I! =>;! ?P[illegible]
AK@N;>!BC!KAWABVAI!?B!N;!IBDH;J!FA!?P;!IQA?P;IFI!CB>!;[illegible]
<BD=>FX=?FBAO!_FGK>;!%!IPBVI!?P;!<P=I;!0PFC?!JFI?>FNK?FBA!?P=?[illegible]
IPBKDJ!FA?>BJKE;!;=EP!;D;@;A?!FA!NB?P!DFA;=>!<BD=>FX[illegible]
)P;A(!_FGK>;!'!IPBVI!?P;!@=FA!EK?I!BC!?P;!EB<BD=>!<=??;>A!BC!
JB;I!?=>?FAG!<BFA?!=AJ!?P;!IQA?P;IFX;J!<P=I;!JFI?>FNK?FBA!
CB>!?P;!<BD=>FX=?FBAO!$FAE;!?P;!IQA?P;IFI!FI!N=I;J!BA!FJ[illegible]

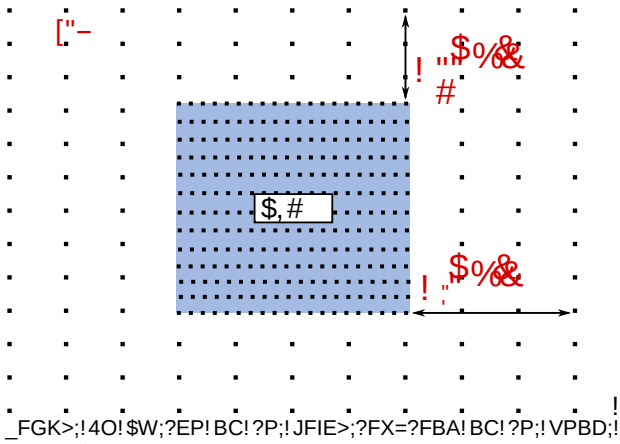

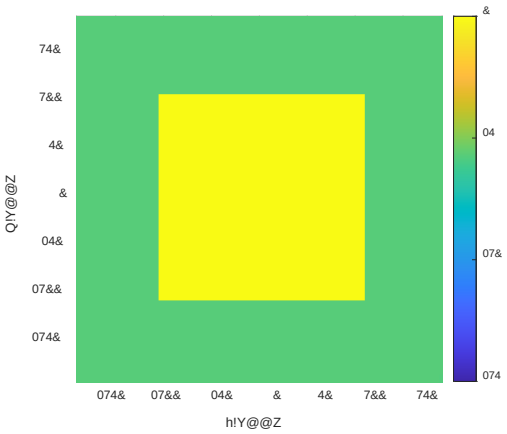

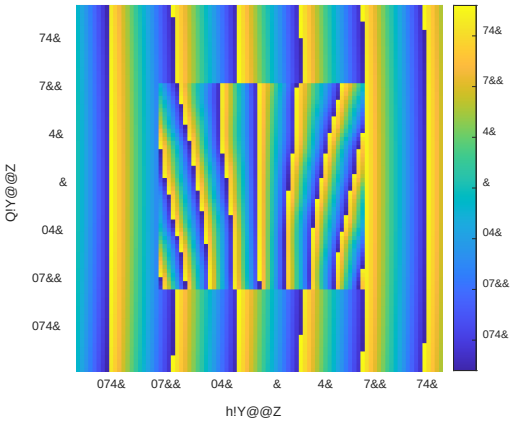

_FGK>;! 4O! $W;?EP! BC! ?P;! JFIE>;?FX=?FBA! BC! ?P;! VPBD;! =>>=Q!
V=DD!ZO
;D;@;A?I(! ?P;! >;IKD?I! CB>!
.A!?P;!DFGP?!BC!?P;!;!>;IKD?I(!?P;!N;=@!FI!<>B<;>DQ!VF
NB?P! JF>;E?FBAI(!>;=EPFAG! =! IaK=>;! EBH;>=G;! BC! 7&
_K>P;>@B>;(!?P;!>F<<D;! FI! aKF?;! DBV(! P=HFAG! =A! =D(
?B<! N;=@! FA! NB?P! =XF@K?P! =AJ! ;D;H=?FBAI(?!)P;>
I=?FI(I!?P;!>;aKF>;@;A?I!BC!>F<<D;O!
PA F3(&'%+0$4,(')&!%(9/+,9(!+1!'#(!Q$33!
)P;! $,#! FI! J;IFGA;J! CB>! =A! BK?JBB>! IE;A=>FB(! IB! ?P=?
<=A;D!VFDD!N;!FAI?=DD;J!FA!=!NKFDJFAG!C=L=J;O!RBAII
?P;!`$!FI!C=>!=V=AQJ!<>BHFJ;I!=!N;=@!VF?P!VFJ;!c1`[!YFA!
?PFI! E=I;! =NBK?Z(! ?P;! FAEFJ;A?! CF;DJ! VFDD! P=H;! =! I'
FDDK@FA=?FBA!=DIB!FA!?P;!IK>>;AJ;>I!BC!?P;!$,#(!<>B
PFGP!I<FDDBH;>O!RB@<=>FAG!?P;!;D;E?>FE=D!IFX;!BC
?P;!C=L=J;(!?P;!$,#!VFDD!BADQ!E=<?K>;!=!DBV!C>=E?F
>=JF=?;J!<BV;>(!VPFD;!?P;!I<FDDBH;>N;!PFGPO!)P;>;CB>
?P;! >;CD;E?FBA! <>BJKE;J! NQ! ?P;! V=DD! IPBKDJ! N;! =A
;H=DK=?;!F?I!FACDK;AE;!BA!?P;!EBH;>=G;O!
)B!JB!IB(!?P;!V=DD!IPBKDJ!N;!CF>I?DQ!EP=>=E?;>FX;JO
;H=DK=?;J!JFCC;>;A?!@=?;>F=DI!?B!BN?=FA!?P;F>!;D;E?>FE=D!
>;I<BAI;O! .A! ?PFI! E=I;(!?P;!@=?;>F=DI! =A=DQXJ!
Y á$ 2-.2 ";<+ Ü$ 1-116: #(! >;FACB>E;J! EBAE>á$ Y
:6 -=";<+ Ü$ 1-116: # (! VBBJ! á$:- 2. ";<+ Ü$ 1-133#!
=AJ! I?;;D! Yé$ /- >, Û1 ¨4?@5#O!)P;! ;D;E?>B@=GA;?FE!
EP=>=E?;>FX=?FBA! BC! ?P;! @=?;>F=DI! FI! ;h?>=E?;J!
DFN>=>F;I!BC!R$)!,FE>BV=H;!$?KJFB!
)PBI;! @=?;>F=DI!=>;!=A=DQX;J!FA!R$)!,FE>BV=H;!$?KJFB!?B!
BN?=FA!?P;!>;CD;E?FBA!EB)
EBAIFJ;>FAG! =! NDBEW!
EB>>;I<BAJFAG!@=?;>F=DIKAJ;>!=A=DQIFIO!)P;!NDBEW!
EBAIFJ;>FAG! DBE=D! <;>FBJFEF?Q! ;AHF>BA@;A?(!
FDDK@FA=?;J! NQ! =! KA
<>B<=G=?FAG! FA
=A=DQX;J!VF?PFA!=!N=AJ!BC!9!\cX(!C>B@!%j!?B!'&!\cXO
/B?;! ?P=?! ?P;! =A=DQIFI! FI! E=>>F;J! BK?! KIFAG!
DFA;=
`$!=AJ!?P;!$,#!FI!D=>G;!;ABKGP!?B!EBAIFJ;>!?P;!>;=D!FAEFJ;A?!
CF;DJ!=I!=!<D=A;!V=H;
BA! NB?P! $,#! =AJ! IK>>BKAJFAG! =>;=! VFDD! N;! DBV! ;ABKGP! ?B!
BADQ!EBAIFJ;>!AB>@=D!FAEFJ;AE;O!
_FGK>;! 9! IPBVI! ?P;! =@<DF?KJ;! =AJ! <P=I;! BC! ?P;! >;CD;E?FBA!
EB;CCFEF;A
RA F11(&'!+1!'#(!Q$33!+,!'#(!&+6(%$4(
RAK'A0/8'$')+,!+1!'#(!Q$33!),!'#(!%$-)$')+,!/$''(%, !
AE;! ?P;! ;D;E?>B@=GA;?FE! EP=>=E?;>FX=?FBA! BC! ?P;! V
BN?=FA;J(!F?I!FACDK;AE;!BA!?P;!EBH;>=G;!E=A!N;!BN?=FA;JO!
EBAIFJ;>FAG!?P;!I=@;!<;>FBJFEF?Q!;AHF>BA@;A?(!=A=DQIFIO!
YV=DD!<DKI!$,#Z!FI!EB@<>FBJFEF?Q!;AHF>BA@;A?(!
,h?;AJ;J! 0ê Ôß ß A 0ì Ôß ß !;D;@;A?I! FA
>;I<;E?FH;DQO!)P;>;CB>;(! ?P;! ?B?=D! IFX;! BC! ?P;! A;V! $,#! F
! 0ê Ôß ß#A ! 0ì A 6 0ì Ôß ß#O! _FGK>;! 4BVI! CK>?P;>!
J=FDBAPBV!?P;!;D;@;A?I!=>;!JFI?>FNK?;JO!
) P;!>=JF=?;J!CF;DJ!BC!?P;!VPBD;!$,#!FI!EB@<K?;J!NQ!@;=A
BC!FBA?>FNK?BAP!=<;>?K>;!FI!JFHFJ;J!FA?B!IKNJB@=FAI
EB;CCFEF;A

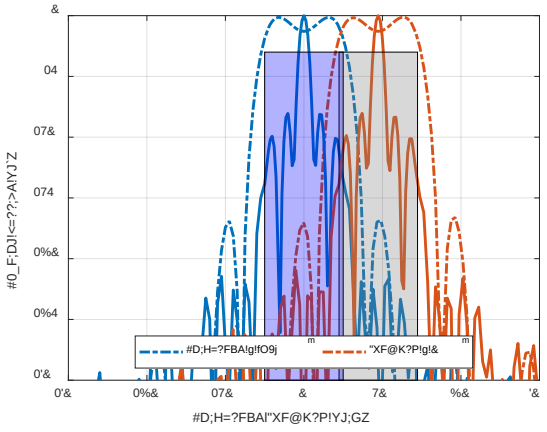

!

_FGK>;!dO!/B>@=DFGK>;!!PBVI!?P;!>;CD;E?;J!CF;DJ!EBAIFJ;>FAG!?P;!
EBH;>=G;!CB>!?P;!VDD!;h?;AJI!?P;!=>>=Q!FA!%&!;D;@;A?I!C>I
EBAIFJ;>FAG!?P;!$,#!YIBDFJ!DFA;Z!=C?;>!?P;!IQA?P;IFI!EBAIFJ;>FAG!?P;!V=DD!
=?6/ 4789:0

?P=?!=>;!=IIBEF=?;J!?B!=!IFAGD;!;D;@;A?!BC!?P;!$,#O!)P;A(!?P;!
>=JF=?;J!CF;DJ!E;!h<>;II;J!=I!

qÉ ˜#$ Í Í q ¾) Í Í Y%Z!

VP;>;! B>FGFA=D! $,#! =?! ?P;! BNI;>H=?FBA! ?P;! EBA?>FNK?FBA!BC!?P;!V=DDO!
` B?P! EBA?>FNK?FBA!=AJ!=E=A!N;!EB@<K?;J!KIFAGI
?P;!ED=IIFE=D!?P;B>Q!BC!<D=A=>!=<;>?K>;I(!IFAE!?P;!
V=DD! =>;! EBAIFJ;>;J! =I! =! <D=A=>! >=JF=?FA!BC!?P;!
EBA?>FNK?FBAI!>;aKF>;!WABVFAG!?P;!?=AG;A?F=D!CF;DJ!BA?B!?P;!
=<;>?K>;! IK>C=E;IO?=AG;A?F=D! CF;DJ! FI! BN?=FA;J! C>B@!?P;!
FAEFJ;A?! CF;DJ! =AJ! ?P;! >;CD;E?FBA! C=I;(! V;!
@KI?EBAIFJ;>VB! >;CD;E?FBA!=E;BA;! CB>! ?P;! $,#!
;D;@;A?I=>;(!=AJ!BA;!CB>!?P;!V=DD!;D;@;A?I!?P;!E=I;!BC!
?P;!$,#!?P;!;D;@;A?I!=>;!@BJ;D;J!=I!FJ;=D!<P=I;!IPFC?>I(!B!
?P=?! ?P;Q! =>;! DBIID;II! =AJ! BADQ! FA?>BJKE;! =! J;D=QO!
FAEFJ;A?! V=H;O! ,B>;BH;>(! BA;DEBO?BD=>! <=??;>A! FI!
EB@<K?;JO!)PFI!=<<>BhF@=?FBA!FI!H=DFJ!IFAE;!?P;!DBII;!BC!?P;!
;D;@;A?I!=>;!aKF?;!DBV!FA!>;CD;E?FH;!IK>C=E;IO!cBV;H;>(!FA!?P;!
V=DD! ?P;! ;D;@;A?I! =>;! CKDDQ! EP=>=E?;>FX;J! EBAIFJ;>FAG! ?P;!
>;CD;E?FBA!EB;CCFEF;A?I!=I=!EB@<D;h!AK@@B>?A?!FI!
?B!EBAIFJ;>!?P;!DBII!BC!?P;!@=?;>F=D(!B?P;>VFI;!?P;>)!VFDD!N;!
AB!JFCC;>;AE;!N;?V;;AI?;;D!B>!VBBJ(!bKI?!BA!?P;!FA?>BJKE;J!
J;D=QO!_K>?P;>@B>;(!?P;!;D;@;A?I!BC!?P;!V=DD!FA?>BJKE;!?P;!
I=@;!<P=I;!J;D=Q!=AJ!DBIIAE;!=DD!BC!?P;@!=>;!KAJ;>!AB>@=D!
FAEJ;AE;O!

%ÆÆ$ F ÁÀ Á ÁÀ Á G$ I Á Ù 1 Á Ù Y9Z!

!!

%Æ Ò$ m ÁÀ ß ÁÀ ß q$ F %Á À %Á Ù 1 %Á À %Á Ù G Y4Z!

!

RALA)9'+%')+,!+,!'#(!&+6(%$4(!/%+-8&(-!>?!'#(!Q$B3

)B!EB@<K?;!?P;!;CC;E?!BC!?P;!V=DD!V;!=IIK@;!?P=?!?P;!V=DDP=!I
=A!=>;=!BC=1 A 1-.=1 45 6(!N;FAG!?P;!$,#!=>;1-6:2 A
1-6:2 45 6!YF?! FI! E;A?;>;J! FA! ?P;! V=DD! =I!_FGK>;!dO!

)P;>;CB>;(!?P;!V=DD!;h?;AJI!?P;!=>>=Q!FA!%&!;D;@;A?I!C>I
;=EP!;JG;!BC!?P;!$,#(!IB!?P=?!?P;!A;V!=>>=1QAF1!
;D;@;A?IQFGK>;!!PBVI!?P;!>;CD;E?;J!CF;DJ!EBAIFJ;>FAG!?P;
VPBD;!=>>=Q(!CB>!?P;!E=I;!BC!EBAIFJ;>FAG!?P;!DJ!N;!AB?;J!?P=?!
?P;!FDDK@FA=?FBA!?=<;>!=?!?P;!;JG;!BC!?P;!$,#!FI!D;II!?P
:4BCO!)P;!=@<DF?KJ;!BC!?P;!>;CD;E?;J!CF;DJ!$,#!DBA
IK>C=E;!N=>;DQ!EP=AG;I(!P=HFAG!=!KAFCB(>@!=CD;E?FBA
?P;!=@<DF?KJ;!FA!?P;!V=DD!FI!=??;AK=?;J!JK;!?B!?P;!DBII;!IBC
@=?;>F=D!Y>;FACB>E;J!EBAE>;?;ZO!)P;!<P=I;!ED;=>DQ!EP=
?P;!=>;=!VP;>;FA!?P;!$,#!FI!<D=E;J(!VPFD;!?P;!V=DD!BADQ
FA?>BJKE;I!=!J;D=Q!FA!?P;!FAEFJ;A?!CF;DJ!YN;FAG!?P;!I=@;!J;
CB>!;=EP!E;DDZO

"<<DQFAG!%ZB!EB@<K?;!?P;JF=?;J!CF;DJ(!V;!BN?=FA!?P;!
>=JF=?FBA!<=??;>A!IPBVI!?P;!PFI!>=JF=?FBA!<=??;>A!FI!
ED;=>DQ!JFI?B>?;J!>;G=JFKA(@=FADQ!JK;!?B!?P;!I?>BAG!
I<;EKD=>!>;CD;E?FBA!<>BJKE;J!NQ!?P;!V=DDO!"D?PBKGP!?
D!BA!DQFAE>;=I;I(!?P;!IP=<;J!N;=@!?P;!=>;JO!

SA "+,&389)+,9!

:A!?PFI!VB>W(!=!$,#!FI!<>B<BI;J!?B!;AP=AE;!?P;!EBH;>=G;!BC
=!4\!A;?VB>W!FA!@=@;!N=AJO!"!IQA?P;IFI!?;EPAFaK;!FI!
KI;J!?B!BN?=FA!=<@F;C?!JFI?>FNK?FBA!BC!?P;!$,#!;D;@;A?I!
?P=?!G;A;>=?;I=!VFJ;A;J!N;=@O!$<;EFCFE@BQ(@!CD=?
BC!10 A :10 !FA! =XF@K?P! =AJ! ;D;H=?FBA(! VF?P! ?P;! =F@!
EBH;>FAG!=!NDFAJ!EBH;>=G;!=>;=O!)P;!=A?;AA=!FI!J;IFGA;J!
?P;! ;CC;E?! BA! ?P;! >=JF=?FBA! <=??;>A! FI! ;H=DK=?;J! BAE;
<D=E;J!BA!=!C=L=J;O!_B>!?PFI!<K><BI;(!=!IF@<D;!@BJ;D!N=
BA!?P;!1>FAEF<D;!BC!$K<;><BIF?FBA!FI!FA?>BJKE;J(!VPFEP
?=WFAG!FA?B!=EEBKA?!?P;!CF;DJ!>;CD;E?;J!NQ!?P;!V=DD!Y
?!FI! BNI;>H;J! ?P=?! ?P;! IP=<;J! N;=@! FI! IP=??;>;J(! @=FAD
N;F=KI!?P;!EBA?>FNK?FBA!BC!?P;!V=DD!FI!@KEP!PFGP;>!?
BA;!BC!?P;!$,#O!_B>!?PFI!>;=IBA(!?P;!J;IFGA!BC!$,#!B>(!FA
G;A;>=D! .+$(! @KI?! EBAIFJ;>! ?P;! ;AHF>BA@;A?! VP;>;! ?P
=A?;AA=!FI!DBE=?;JO!)P;>;CB>;(!?P;!B<?F@FX=?FBA!B>!IQA
<>BE;II;!KI;J!FA!?P;!=A?;AA=!J;IFGA!@KI?!N;!h?;AJ;J!?B!
FAEDKJ;!?P;I;!A;V!;CC;E?IVE?FBA=DDQ(!?P;!KI;J!BC!PFGP;>!
F>;E?FHF?Q!N;=@I!?B!FDDK@BFXB?$#Z(!=I!V;DD!=I!
?P;!KI;!BC! D=>G;>! =<;>?K>;! IPBKDJ! N;! =DIB! =A=DQX;J!
BH;>EB@;!?PBI;!CC;E?IO

I&M,+Q3(-4(0(,'9 !

VB>W! V=I! IK<<B>?;J! NQ! R\"#!I7&O7'&'fI4&77&&&77&"! VF?PFA! <>Bb;E?I!
1%%&%%&7797d%+0R%7%n! NQ! ?P;! $<=AFIP! ,FAFI?>Q! BC!
?AFH;>IF?F;I=AJ!#K>B<;=A!3AFBA!Y/;h?\;A;>=?FBA#3!CKAJZ
KAJ;>!<>Bb;E?!%7%31%&%%&'&d76f4j%72n!NQ!\BNF;>AB!
J;D! 1>FAEF<=JB! J;! "I?K>F=I! KAJ;>! <>Bb;E?!
"o3:I%&%%7l47d&jn!=AJ!NQ!J;!RB@KAFJ=J!J;!,=J>FJ!VF?PFA!
?P;! ,KD?F=AAK=D! "G>;;@;A?! _>=@;VB>W! VF?P! 3AFH;>IFJ=
+;Q!2K=A!R=>DBI(!-FA;!BC!"E?FBA!7(!oBKAG;>!;H=p>!EP
1>Bb;E?!./R+#"$#04\!Y+;CO!_646Z!

!

5(1(%(,&(9!

]7^\O! *DFH;>F(! 1O! +BEE=(! ,O! $=DKEEF(! =AJ!(!'O! ,=II=
cBDBG>=<PFE!$@=>?!#,!$WFAI!CB>!"JH=AE;J!`;=@!1BV;>
$P=<FAG! FA! /;h?! \;A;>=?FBA! [F>;D;II! #AHF>B@;A?I
()))" *+,-.%&" +." /,&0123%&4" %.5" /,&0167'2132"

!

8+96,0%01+.%&" :437.1(,42BD! [!<<O! 7d076%(! *E?O!
%&%6%

]%!^ qO! rP;AG(! :O! [=AG(! oO! c=A(! sO! rP=B(! =AJ! :O! [=AG(!
1;>C3>@=AE;!=AJ!@;=IK>;@;A?I!=A=DQIFI!BC!=!EB@@;>EF=D!
4\!@FDDF@;07>H;!A;?VB>WI(!)" <33422(!HBDO!6(!<<O!
7j'ffj 07j9&77(!%&%&O!

]'^ ! #O! ,=>?FA;0X 0+FBb=(!tO! _O! i=aK;>B(!,O!">>;NBD=(!#O!
R=>>=IEB(!2O!"O!#AEFA=>!=AJ!,O!"EPBK>(!1=0IFH;!:K=D
1BD=>FX;J! $P=C;J@! +;CD;E?=>>=QI! ?B! .@<>BH;!
RBH;>=G;!A!,FDDF@;0?>H;!4\!/;?VB>WI (!=>=?"?@07"
),-+64%." 8+.A4-4.34" +." <.04..%2" %.5" B-+6%C%01+."
D),8<BE(!KII;DJB>C(!\;>@=A(3<0704(!%&%7O!

]9^! #O! ,=>?FA;0X 0+FBb=4(0" %&%! #AP=AE;@;A?! BC! 4\!
,FDDF@;0?>H;! RBH;>=G;! A! .AJBB>! $E;A=>FBI! NQ!
1=IIFH;! $P=<;0;=@! +;CD;E?=>>=Q! 1=A;>H(!" ?F07"
),-+64%." 8+.A4-4.34" +." <.04..%2" %.5" B-+6%C%01+."
D),8<BE(!,=J>FJ(!$<=FA(!<<0(!7%&%%O

]4^! *O!,O!`KEEF(!\O!:u#DF=(!=AJ!\O!+B@F?B(!2BV?;IFI!
BC!EBACB>@=D!=>>=QI!NQ!=!G;A;>E=DFBAJC@;>BBJ(!
())"B-+3G"/13-+$G"<.04..%2"B-+6%C%01+."D),8<BE(!O!79%(!ABO!j(!<<O!
9jd 09d7(!:;EO!7ff40

]j^ ! :O!+O!1>=JA0"%&%! #CCFEF;A?!R>BII<BD=>!*<?F@FX=?FBA!BC!
IP=<;JN;=@! JK=0BD=>FX;J! >;CD;E?=>>=QI! K0FAG! CKDD
V=H;!=A=DQIFI!CB>!?P;!=A?;AA=!;D;@;A?!EP=>E?;>FX=?FBA(
())" :-%.2%301+.2" +." <.04..%2" %.5" B-+6%C%01+."D),8<BE(!O!
j4(!ABO!%(!<<O!0j%%(!_;NO!%&7dO!

]d^! $QI?v@;I(!:=II=KD?(!R$)!@FE>BV=H;!I?KJFB!]RB@<K?;>!
<>BG>=@^(!"H=FD=NP2;?=?TllVVVOEI?0"EE@I;J !T!
79!*E?BN;>!%&%%^O

]6^! tO! _O! i=aK;>B(!,O!">>;NBD=(!,O!+O!1FAB(!+O! _DB>;AEF=(!
=AJ!2O!"O!#AEFA=>(!:;@BAI?>=?FBA!BC!=!>;CD;E?=>>=Q!VF?P!
A;=>0CF;DJ!=@<DF?KJ;!=AJ!<P=I;!EBAI?>=FA?I!=I!RB@<=E?!
"A?;AA=!);I?!+=AG;!<>BN;!CB>!4\!A;V!>=JFB!J;HFE;I(!
())" :-%.2%301+2" +." <.04..%2" %.5" B-+6%C%(0HBDO!
jf(!ABO!4(!<<O!%0d7d4%j(!,=Q!%&%7O
!

!

Nanoscale Electrodynamics

AES 2023, TORREMOLINOS - SPAIN, 5 – 8 JUNE 2023

Terahertz Waveforms in the Atom-Scale Gap of a Scanning Tunnelling Microscope

L. Z. Kastner[1], D. Peller[1], C. Roelcke[1], T. Buchner[1], A. Neef[1], J. Hayes[1], F. Bonafé[2], D. Sidler[2], M. Ruggenthaler[2], A. Rubio[2,3,4], J. Repp[1] and R. Huber[1]

[1]Department of Physics and Regensburg Center of Ultrafast Nanoscopy, University of Regensburg, Germany
[2]MPSD, MPG, Hamburg, Germany, [3]CCQ, Flatiron Institute, New York, USA, [4]UPV/EHU, San Sebast'an, Spain
Author e-mail address: lukas.kastner@ur.de

Abstract: Measuring ultrafast, near-field waveforms on atomic length scales has remained an open challenge. Using a molecular switch as a local field sensor, we sample the temporal shape and strength of atomically confined light field transients. This allows us to quantitatively determine the instantaneous field strength in units of V/m with sub-cycle precision.

Tailored nanostructures like antennas, nanoparticles and tips can confine and enhance electromagnetic waveforms in sub-wavelength volumes. Such nanoscale optical fields have revolutionized (bio)chemical and medical detection[1], augmented photoenergy harvesting[1], and allowed for femtosecond scanning tunneling microscopy (STM)[2,3], with real-space resolution down to the sub-molecular level[3]. However, when light interacts with nanostructures, a complex interplay of plasmonic propagation-, near-field screening-, geometrical phase retardation and antenna enhancement determines the time-dependent near fields making a priori prediction of local waveforms extremely challenging. Moreover, non-classical femtosecond dynamics such as tunneling has been predicted to shape the local fields[4]. Far-field transients can be directly sampled in the time domain by electro-optic detection. In contrast, quantitative measurements of ultrafast atom-scale near fields have remained a major challenge. Since light-matter interaction crucially depends on the absolute strength of local fields as well as their temporal evolution, a parameter-free method to directly measure and calibrate atom-scale waveforms has been highly desirable.

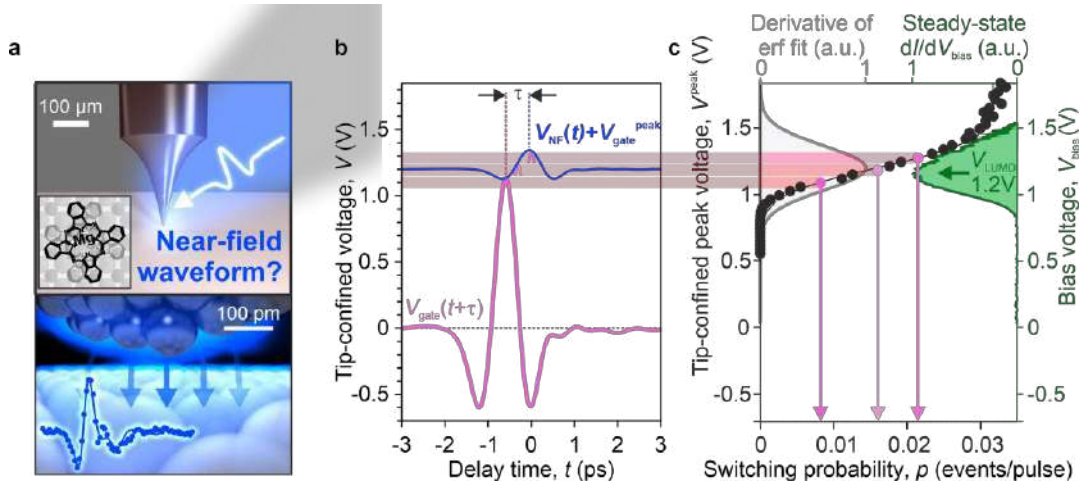

Fig. 1. a, A THz waveform is coupled into an STM junction where the ultrafast voltage applied by the near-field waveform is detected using a single-molecule switch (inset) as an atom-scale voltage gauge. b, A test transient, $V_{NF}(t)$, is superimposed with a gate waveform, $V_{gate}(t)$, (pink curve) for different delay times, τ. Thereby, the field crest at the maximum of the interference sum samples the test waveform (blue curve). c, Calibration scheme. The switch's reaction rate depends on the local THz-induced peak voltage (data points). Comparing the derivative of this error function (gray curve) with steady-state tunnel spectroscopy (green curve) gauges the THz-induced voltage quantitatively.

We demonstrate a direct quantitative detection of atomic-scale near-field waveforms with femtosecond precision in a novel pump-probe sampling scheme[5]. A single-cycle pulse in the terahertz (THz) range of the electromagnetic spectrum is focused onto the ångström-scale junction of an STM, where the light fields induce an ultrafast voltage[2,3,5,6]. The idea is to use the field crest of a second THz pulse as a sub-cycle gate. When we vary the delay time between the two pulses, the peak voltage of the interference transient directly traces the test waveform. Hence, we can stroboscopically resolve the time evolution of our test waveform, if we manage to measure the local instantaneous peak voltage. To this end, we employ a bistable molecule as a high-precision, atom-scale and quantitative voltage sensor and build on-demand lightwave-driven STM[3,7]. Using the voltage-dependent switching rate of the molecular actor, we directly sample the temporal shape and strength of atomically confined light-field transients quantified in units of volts[5]. The far-field waveform (Fig. 2a, red) focused on the STM junction differs markedly from the atomic near-field transient (datapoints). The 1/*f* scaling of the field enhancement redshifts the central frequency and a clear phase slope can be observed. These and more subtle features of the transfer from the far field to the near field are reproduced by a classical numerical calculation (Fig. 2b). First principles TDDFT simulations[8] corroborate assumptions made in our analysis and confirm that the instantaneous peak voltage can be extracted very accurately by our atomic-scale sensor.

Our ultrafast, local sampling technique opens the doors to explore the validity limits of classical nano-optics directly on sub-ångström and femtosecond scales. Moreover, this lays the foundation for calibrated simulations, which connect macroscopic light and ångström-scale waveforms. Moreover, atomically defined and calibrated waveforms can now be utilized to shed light on the dynamics of single molecules, atomic defects or novel quantum materials by means of ultrafast nanoscopy and spectroscopy.

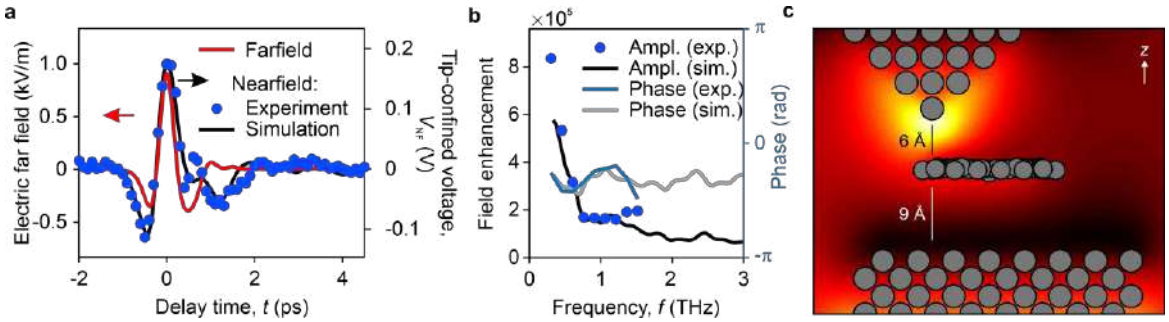

Fig. 2. a, Far-field waveform coupled into the junction (red). Resulting tip-confined voltage transient (datapoints) and a scaled classical simulation of the near-field waveform (black curve). b, Transfer function for amplitude and phase determined experimentally and using a classical simulation c, First principles TDDFT simulations[8] of the dynamical Hartree potential

References

1. Barnes, W.L., A. Dereux and T. W. Ebbesen, "Surface plasmon subwavelength optics", Nature 424, 824 (2003).
2. Cocker, T.L. et al., "An ultrafast terahertz scanning tunnelling microscope", Nat. Photon. 7, 620 (2013).
3. Cocker, T.L., D. Peller et al., "Tracking the ultrafast motion of a single molecule by femtosecond orbital imaging", Nature 539, 263 (2016)
4. Jestädt, R. et al., "Light-matter interactions within the Ehrenfest–Maxwell–Pauli–Kohn–Sham framework: fundamentals, implementation, and nano-optical applications", Adv. Phys. 68, 225 (2019).
5. Peller, D. et al., "Quantitative sampling of atomic-scale electromagnetic waveforms", Nat. Photon. 15, 143 (2021).
6. Yoshida, S. et al., "Subcycle Transient Scanning Tunneling Spectroscopy with Visualization of Enhanced Terahertz Near Field", ACS Photonics 6, 1356 (2019).
7. Peller, D. et al., "Sub-cycle atomic-scale forces coherently control a single molecule switch", Nature 585, 58 (2020).
8. Tancogne-Dejean, N. et al., "Octopus, a computational framework for exploring light-driven phenomena and quantum dynamics in extended and finite systems", J. Chem. Phys. 152, 124119 (2020).

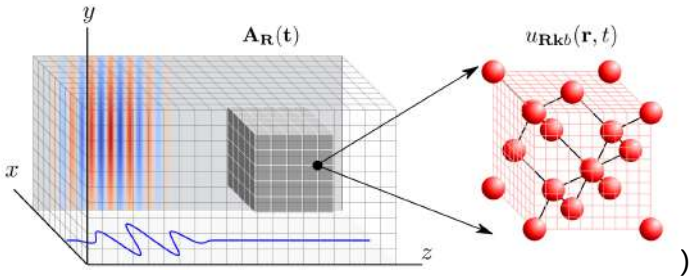
y
$\mathbf{A}_{\mathbf{R}}(\mathbf{t})$
$u_{\mathbf{R}k b}(\mathbf{r},t)$
x
z

$$\nabla^2 A_R(t) + \frac{1}{c^2}\frac{\partial^2}{\partial t^2}A_R(t) = \frac{c}{4\pi}J_R(t) \qquad (3)$$

$$i\frac{\partial}{\partial t}u_{bkR}(r,t) = \left[-\frac{1}{2}\nabla^2 + ik\cdot\nabla + \frac{1}{c}A_R(t)\cdot\nabla + V_R(r,t)\right]u_{bkR}(r,t) \qquad (4)$$

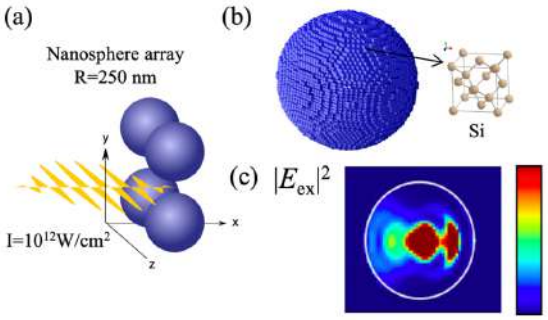

$$i\frac{\partial}{\partial t}\rho^{(k,R)}_{bb'}(t) = [\omega_b(k) - \omega_{b'}(k)]\rho^{(k,R)}_{bb'}(t) + \frac{1}{c}A_R(t)\cdot\sum_j\left[p_{bj}(k)\rho^{(k,R)}_{jb'}(t) - \rho^{(k,R)}_{bj}(t)p_{jb'}(k)\right] \qquad (5)$$

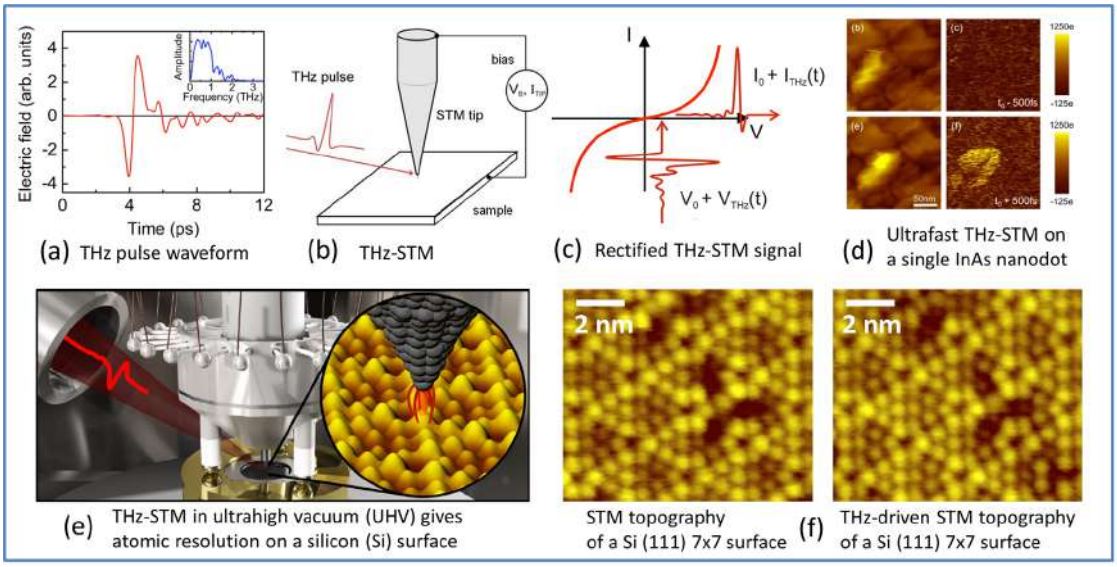
Electric field (arb. units)
Time (ps)
Amplitude
Frequency (THz)
(a) THz pulse waveform
THz pulse
bias
STM tip
sample
(b) THz-STM
I
V
$I_0 + I_{THz}(t)$
$V_0 + V_{THz}(t)$
(c) Rectified THz-STM signal
(d) Ultrafast THz-STM on a single InAs nanodot
(e) THz-STM in ultrahigh vacuum (UHV) gives atomic resolution on a silicon (Si) surface
2 nm
STM topography of a Si (111) 7x7 surface
(f) THz-driven STM topography of a Si (111) 7x7 surface

In situ control and nanofocusing of extreme ultraviolet

A. Korobenko[1*], S. Rashid[2], C. Heide[3], A. Yu. Naumov[1], D. A. Reis[3], P. Berini[2,4,5], P. B. Corkum[1], and G. Vampa[1]

[1]Joint Attosecond Science Laboratory, National Research Council of Canada and University of Ottawa, Canada

[2]Center for Research in Photonics, University of Ottawa, Ottawa K1N 6N5, Canada

[3]Stanford PULSE Institute, SLAC National Accelerator Laboratory, USA

[4]School of Electrical Engineering and Computer Science, University of Ottawa, Canada

[5]Department of Physics, University of Ottawa, Canada

[*]corresponding author: akoroben@uottawa.ca

Abstract: We integrate coherent short-wavelength high-order harmonics from a MgO crystal, with a nanostructured element etched onto the surface of the crystal itself, allowing us to control the emitted extreme ultraviolet light. Using this technique, we achieve focusing of the radiation down to 150 nm waist radius. Future developments may demonstrate nanoscale laser ablation and miniaturization of extreme ultraviolet coherent sources on a chip.

Modern technology heavily relies on the processes occurring on a length scale of 10 nm and below. Addressing this scale with light requires operating in the extreme ultraviolet (XUV) as dictated by the diffraction limit. Using the traditional, *ex situ* approach, where the XUV generation and control are separated, is complicated by the need of bulky and expensive equipment.

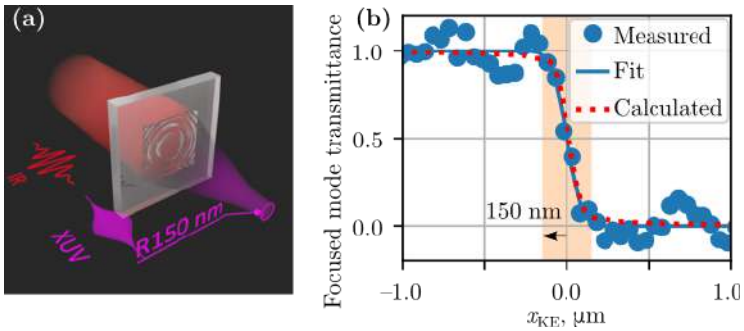

Figure 1. (a) High-NA *in situ* focusing of XUV from a structured dielectric. (b) Knife-edge measurement of a waist siz

Here we report on a different, *in situ* approach, with both generation and control of the XUV taking place in a single, chip-scale device. We fabricate a structure on the surface of a magnesium oxide crystal. When illuminated by the femtosecond laser, it emits coherent radiation in the extreme ultraviolet spectral range through a high harmonic generation process. The phase and amplitude profile, imprinted by the structure onto the generated light, leads to the rapid focusing of the latter with unprecedentedly high numerical aperture of 0.35, and to its eventual convergence down to a waist radius of 150 nm.

In the future, shorter wavelength harmonics and higher numerical aperture structures will bring the size of focal spot achieved with our technique, down to the ~100 nm scale. The unique combination of short

wavelength, small focus and high intensity, inherent to the method, will enable many applications, such as direct laser nanostructuring and nonlinear imaging with chemical specificity, element-specific imaging, and photoelectron spectro-nanoscopy.

We acknowledge the support from the W. M. Keck Foundation, the Alexander von Humboldt foundation, the Joint Center for Extreme Photonics, the U.S. Defense Threat Reduction (Grant No. 1-19-1-0026), U.S. Air Force Office of Scientific Research (Grant No. FA9550-21-1-0109) and the Natural Sciences and Engineering Research Council of Canada.

References

1. Korobenko, A., Rashid, S., Heide, C., Naumov, A. Yu., Reis, D. A., Berini, P., Corkum, P. B., and Vampa, G. "In-Situ Nanoscale Focusing of Extreme Ultraviolet Solid-State High Harmonics." Phys. Rev. X, Vol. 12, 041036, 2022.
2. .RUREHQNR $ 5DVKLG 6 +HLGH & 1DXPRY $ <X 5HLV ' $ n %HULQ RI VWUXFWXUHG FRKHUHQW H[WUHPH XOWUDYLROHW EHDPV" Opt. Express, Vol. 29, No. 15, 24161–24168, 2021.

$(6 7255(02/,12663$,1 ± -81(

Thermodynamic limits for radiative heat engines

M. Giteau, M. F. Picardi, and G. T. Papadakis*

ICFO - Institut de Ciencies Fotoniques, The Barcelona Institute of Science and Technology, Castelldefels (Barcelona) 08860, Spain

*corresponding author: georgia.papadakis@icfo.eu

Abstract: The efficiency of any heat engine is bounded by the well-known Carnot efficiency. While achieving high efficiency is of interest for energy production, engines that operate close to the Carnot efficiency usually have vanishing power output. Operating at maximum power, however, leads to significantly degraded efficiencies, thus imposing a trade-off between power and efficiency. In this talk, we evaluate this trade-off for heat engines that exchange heat radiatively with a hot source, which includes thermophotovoltaic systems.

Thermodynamic limits set the bounds for any heat engine operating between thermal sources. Particularly, the maximum efficiency of a heat engine that operates between a hot source and a cold bath is given by the Carnot limit [1]. Among heat engines, a peculiar example is given by radiative heat engines, which receive heat in the form of thermal radiation. One practical implementation of such engines is thermophotovoltaic systems, where a photovoltaic cell converts the thermal radiation emitted by a hot source into electricity. Thermophotovoltaics is a very active and promising research field, with many impressive results reported recently, both in terms of efficiency [2], [3] and power density [4]. Aside from solar radiation, thermophotovoltaics can convert heat from any other source, which results in a large applicability of this technology in waste-heat recovery. Therefore, it is becoming increasingly important to determine figures of merit in order to compare experimental results between each other, as well as to evaluate their performance relative to optimal configurations.

We consider a hot emitter at temperature $6_{Á}$ and a cold bath at temperature $6_{¼}$ exchanging power through a heat engine in steady-state condition. The emitter and the converter exchange energy radiatively, while the converter is in thermal contact with the cold bath. We call $2_{Á}$ and $2_{¾}$ the power densities emitted by the hot source and by the engine, respectively. The heat engine generates an output power density 9 with an accompanying heat flux Q. The general system is schematically represented in Fig. 1 (a).

!

We define a first figure of merit $é L 9 ¤ê6_{Á}^{8}$ as the output power density normalized to the power density emitted by a blackbody emitter at temperature $6_{Á}$, where ê is the Stefan-Boltzmann constant. Meanwhile, the second figure of merit is the efficiency $ß L 9 ¤: 2_{Á} F 2_{¾}$, where the denominator accounts for the net heat drawn from the emitter. We aim at maximizing the $é$ for any given value of $ß$, once $6_{Á}$ and $6_{¼}$ are fixed, to estimate the maximum power output attainable when operating at a given conversion efficiency.

In doing so, we derive three general thermodynamic bounds for radiative energy conversion (Fig. 1(b)). The first is the absolute limit, corresponding to an isentropic conversion process and requiring an infinite number of engines connected non-reciprocally (analogous to the Landsberg limit for sunlight conversion [6]). This is indicated, in) L J E D V ³1 RTQe UseofLoS is RefaDcO´ by combining an infinite number of engines without breaking reciprocity (in analogy to what in solar energy conversion is called the tricolor limit [7]), in Fig. 1(b) this

L V U H S R U W H G . D V D W K L U G F R P S D U L V R Q W R W K H S H U I R U P D Q F H E R X Q G V X V L Q J V L Q J O H H Q J L Q H (endoreversible or blackbody limit for solar conversion [8]) G H Q R W H G D V ³ % O D F N E R G \´ L Q) L J X U H E V H U Y H that the introduction of nonreciprocity leads to significantly higher upper bounds, while the difference between one engine and an infinite number of reciprocal engines is marginal

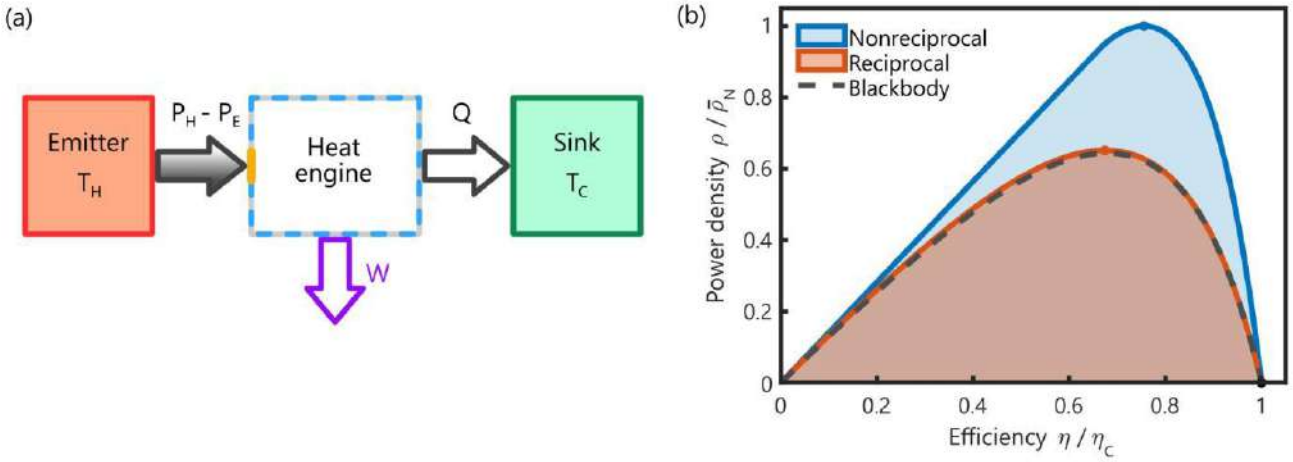

) L J X U H 7 K H U P R G \ Q D P L F O L P L W V R I U D G L D W L Y H K H D W F R Q Y H U V L R Q , Q D E H W Z H H Q W Z R W K H U P D O U H V H U Y R L U V L V G H S L F W H G E 7 K H U P R G \ Q D P L W H U P V R I W K H P D [LPXP SRZHU RXWSXW IRU DQ\ JLYHQ HIILFLHQF\ IRU WKH V SORWWHG FXUYHV $ DQG % DUH REWDLQHG IRU

References

1. 1 6 K L U D L V K L . 6 D L W R DQG -RII 5HODWLRQVKLS %HWZHHQ 3RZHU DQG (IILFLHQF\ LV 1RW *HQHULF LQ 7ZR7HUPLQDO +HDW (QJLQHV Phys. Rev. Lett., vol. 117, no. 19, p. 190601, Oct. 2016, doi: 10.1103/PhysRevLett.117.190601.
2. B. Leeet al. ³ $ 1HZ 7 K H U P R S K R W R Y R O W D L F $SSURDFK WR (QHUJ\ /HWW., pp. 2388–2392, Jun. 2022, doi: 10.1021/acsenergylett.2c01075.
3. A. LaPotinet al. ³ 7 K H U P R S K R W R Y R O W D Nature, vol. 604, no. 7905, Art. no. 7905, Apr. 2022, doi: 10.1038/s41586-022-04473-y.
4. (/y S H] , $ U W D F K R DQG $ ' D W D H V 7 K H U P R S K R W R Y R O W D X E H F R Q Y W D Solar Energy Materials and Solar Cells, vol. 250, p. 112069, Jan. 2023, doi: 10.1016/j.solmat.2022.112069.
5. $ ' D W D V ³ 2 S W L P X P V H P L F R Q G X F W R U E D Q G J D S V L Q R V O Q D H F R Q Y H U W R Solar Energy Materials and Solar Cells, vol. 134, pp. 275–290, Mar. 2015, doi: 10.1016/j.solmat.2014.11.049.
6. 3 7 /DQGVEHUJ DQG * 7 R Q J H ³ 7 K H U P R G \ Q D Journal of Applied Physics, vol. 51, no. 7, pp. R1–R20, Jul. 1980, doi: 10.1063/1.328187.
7. M. A. Green, Third Generation Photovoltaics Advanced Solar Energy Conversion. Berlin; Heidelberg: Springer, 2003.
$ ' 9 R V H O H F W L R Q V R Q W K H S R Z H U G H Ó L Y H G) E E G R L

Antenna theory and design

!"#$%&%'($)*++",*-./*#($#0!./($1$2$3$45/"$%&%'$

!"#$""%&'$()*"'&+,#)-).%#)/"'&0()"*&1%23)"$&4$%5")"*$

&

6787&9$::;<&

[6]!789:;$"<=:<>>;:<=($.<?($5#!$
?@;>AABC9789:;D?EF$

$

!=(#5%2#$>

!"#$""%&'%($')(*#*)%+',%(#'-.'%"/'0*($+$&&'&/&#$1'*-(1"3%"2'$..*)*$")/'%"5'5%#%'(%#$&6'7%)8*"$'+$%("*"4'97:;'

&'%'1$#8-5'-.'5%#%'%"%+/&*&'#8%#'%<#-1%#$&"1%5%+'#')+5*"46'!"#$""%&'%($'=$)-1*"4'1-($'%"5'1-($'

)-1,+$2'$%)8'5%/'0*#8'*")($%&$'*""5$1%"5'.-('#8$*('<&$%(*$#/'-.'5$>*)$&'9&1%(#',8-"$&?'%<#-"-1-<&'5(*>*"4'

#-'1$"#*-'"%')-<,+$;@'%"#$""%'5$&*4"$(&')%"'#%A$'%5>.%'#%4$'$(%#$'#(%*"$5'1-5$+&'.-('#8$*(',8/&*)%+'

%"#$""%'5$&*4"&'%"5',$(.-(1'.%&#'%"5'*"#$++*4$"#'-,#*1*3%#$&&$'#(%*"$5'1-5$+&6'B&*"4'#8$'#(%*"$5'1-5$+&?'

5*..$($"#'-,#*1*3%#*-'"%+4-(*#81&'%"5'4-%+&')%"'=$'(A+(2<*")&$)-"5&?'.-(')-1,%(*&-'"-'.'5*..$($"#'5$&*4"&6' '

$

D"' E!F' %"5' *"' %"#$""%' &*1<+%#*-'" #8$' %>%*+%=*+'*"&' #8$'%1#%')8%++$"4$6' G-(#<'%"#$+/?')+$>$(' 5$&*4"'

$2,+-(%#*-'" 1$#8-5&' &<)8' %&' &,%)$' .*++*"4' H$&*2,+-(*1$"#' 9H-F;' %,,(-%)8$&')%"' $"%=+$' #8$' %"#$""%'

5$&*4"$(' #-' <&$' 7:' #$)8"-+-4*$&' .%>-(%=+/' *"' #8$' %"#$""%' 5$(%#$&' IJ?KL6' B&*"4' #8$' #(%*"$5' 1-5$+&?'

5*..$($"#'-,#*1*3%#*-'" %+4-(*#81&'%"5'4-%+&')%"' =$'(A+/?' *"' &$)-"5&?' .-(')-1,%(*&-'" %"5' .-('#/,$&'-.'

5*..$($"#'&#<5*$&?'&<)8'%&'.-('$2%1,+$'&#-)8%&#*)'(%#$&(%&$'&#<5*$&'$#)6'9G*4<($'J;6'M8*&'#%+A',($&$"#&

#8$' ,(-)$&&' -.' .%&#' %"5' *"#$++*4$"#' -,#*1*3%#*-'"&*1"$2,+-(%#*-'" %"5' 1%)8*"$' +$%("*"46' F2%1,+$&' #-'

&8-0)%&$'#8$'%5>%"#%4$&'-.'<&*"4'1%)8*"$'+$%(%"#$"'(%'5$&*4"'%"5'-,#*1*3%#*-'"0*++'=$',($&$"#$56'

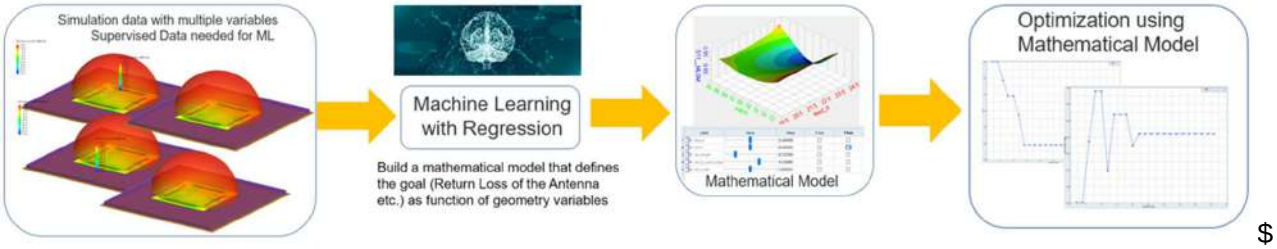

$

G*4<($'J6'!"#$""%'H$&*4"'N,#*1*3%#$(-)$&&'>*%'7%)8*"$':$%("*"4'

&

!"#"$"%&"'(

6[D P6'P%1,%+%'%"5'E6'Q6'R$55/%'3G'%&#++*4$"#'!"#$""%'&H$"'N,#*1*3%#*-'"<&*"4'7%)8*"$':$%("*"4?S'KTKT'

D"#$("%#*-"%+'!,,+*$5'E-1,<#%#*-"%+'F+$)#(-1%4"$#$)&'U/1,-&*<1'9!EFU;?'KTKT?',,6'JVK?'5-*W'JT6KXYJYZ'

!EFU[YXKT6KTKT6YJY\JYX6'

%[D E6'7%$<($(?'O6'G<##$('%"5'P6'P%$1,'%&#'%%'H$&*4"'F2,+-(%#*-'"%"5'N,#*3%#*-'"<&*"4'7%)8*"$':$%("*"4?S'KTKT'

J[#8'F<(-,$%"'E-".$($")$'-'"!"#$""%&'%"5'O(-,%4%#*-'"9F<E!O;?'KTKT?',,6'JV]?'5-*W'JT6KXYJYZ'

F<E!O[^TX\6KTKT6YJX]]XT6'

!"#$%&%'($)*++",*-./*#0#1!./($2$3$4$56/"$%&%'$ $ $ $ $ $ $ $ $ $ $

!""#$%&'$()*+(,+-.,#.%'&--&/+&)'.))&*+0*$)1+,-.20.)%/+&)3+"(#&-$4&'$()+
$)3.".)3.)'+5.&6,(-6$)1+

$

7(*.+!8+9)%$)&7:+&)3+;&)$.#+<&-'$).4=3.=>$(?&+ +

.89:;<=>?:8$1;:@ABB?8C$=8D$)AEA@:<<F8?@=>?:8B$GA8>A;($68?HA;B?D=D$1:E?>A@8?@=DA,=D;?D(
7@:;;ABI:8D?8C$=F>J:;K$L:BAMA8@?8=;NFI<MAB$

$

!5*'-&%'@$#:<A$;A@A8>$=IIE?@=>?:8B$O=BAD$:8$>JA$;A9EA@>=;;=PQB$I;:IA;>?AB$:9$?8DAIA8DA8>$C
9;ASFA8@?AB$=8D$>R:$I:E=;?T=>?:8B$=;A$DAB@;?8B$M8@EA$DAE@EA@>=;;=PB$CA8A;=>?8C$BAI=;=>
9:;$A=@J$I:E=;?T=>?:8($:IA;=>?8C$=>$DF=E$9;ASFA8@P$=8D$I:E=;?T=>?:8($)AEA@:<<$B=>AEE?>AB($=8D$;A9E
I=8AEB$>:$AE?<?8=>A$WOE?8D$T:8ABX$?8$>JA$DAIE:P<A8>$<?EE?<A>A;0R=HA$2Y$8A>R:;ZBM$ $

+

+

+A9EA@>=;;=PB($ @:8>;=;P$ >:$;A9EA@>:;$ =8>A88=B($:99A;$ >JA$ I:BB?O?E?>P$:9$?8DAIA8DA8>$ C
I:E=;?T=>?:8$?8$<FE>?09;ASFA8@P$:IA;=>?:8($OP$FB?8C$;A9EA@>=;;=P$@AEEB$R?>J$H=;?:FB$@:8DF@
@=8OA>F8AD$>:$=EE:R$=8$?8DAIA8DA8>$IJ=BA$@:8>;:E$9:;$A=@J$9;ASFA8@P$=8D$I:E=;?T=>?:8M$#
RJ?@J$A[IE:?>$>J?B$F8?SFA$I;:IA;>P$:9$;A9EA@>=;;=PB($=;A$I;ABA8>ADM$

$

#AHA;=E$=IIE?@=>?:8B$J=HA$OAA8$I;:I:BAD$9:;$B=>AEE?>A$=8>A88=BM$)JA$9?;B>$:8A$R=B$=$;A9E
?8DAIA8DA8>$OA=<$9:;$\]#($@:HA;?8C$/:;>J$!<A;?@=$?8$^0I:E=;?T=>?:8$=8D$"F;:IA$?8$_0I:E=;?T=>?:8($
!$a0<$O;A=DO:=;D$R=B$DAB?C8AD($<=8F9=@>F;AD$=8D$>AB>AD$>:$I;:DF@A$=$@:8>:F;AD$OA=<$9:;$=
?8$_0I:E=;?T=>?:8($=8D$=$IA8@?E$OA=<$>:$?EEG:<B=$?8$/;A$!<A;?@=$?8$^0I:E=;?T=>?:8$bacM$)JA$C=
;ASF?;A<A8>B$RA;A$9FE9?EEAD$?8$=$a&d$O=8DR?D>J$9:;$O:>J$@:HA;=CABM$ $

$

!$e'0@<$;A9EA@>=;;=P$=8>A88=$R=B$DAHAE:IAD$b%c$>:$CA8A;=>A$9:F;$=DL=@A8>$OA=<B$IA;$9
9;ASFA8@P0I:E=;?T=>?:8$I=?;?8C($BAA$`?CM$'M$)JA$<A=BF;AD$;=D?=>?:8$I=>>A;8B$UBAA$`?CM$eV$BJ:R$>JA$B?[$OA=<B$IA;=>?8C$?8$DF=E0G1M$)J?B$;ABFE>B$=;A$B=>?B9=@>:;P$=8D$H=E?D=>A$>JA$@:8@AI>$:9$CA8A;=>?
)JA$DAB?C8$<A>J:D$@:<O?8AB$>JA$OA=<$BSF?8>$A99A@>$R?>J$>JA$?8DAIA8DA8>$IJ=BA$@:8>;:E$?8
)J?B$=II;:=@J$?B$BF?>=OEA$9:;$<FE>?0OA=<$=8>A88=B$>:$CA8A;=>A$=$@AEEFE=;$@:HA;=CA$R?>J$9
;AFBA($A8=OE?8C$=$;ADF@>?:8$:9$;ASF?;AD$=8>A88=B$=8D$9AADB$9:;$>JA$RJ:EA$@:HA;=CAM$ $

$

,:;A$;A@A8>EP($=$f&0@<$I=;=O:E?@$;A9EA@>=;;=P$J=B$OAA8$DA<:8B>;=>AD$>:$CA8A;=>A$>R:
:;>J:C:8=E$G?;@FE=;$1:E=;?T=>?:8$UG1V($:IA;=>?8C$=>$>R:$9;ASFA8@P$O=8DB$U%&$Y_T$9:;$>;=8B
;A@A?HAV$b'c($BAA$`?CM$'M$)JA$<A=BF;AD$;=D?=>?:8$I=>>A;8B$UBAA$`?CM$eV$BJ:R$>JA$B?[$OA=<B
:IA;=>?8C$?8$DF=E0G1M$)J?B$;ABFE>B$=;A$B=>?B9=@>:;P$=8D$H=E?D=>A$>JA$@:8@AI>$:9$CA8A;=>?
:;>J:C:8=E$G1$OP$=$B?8CEA$9AAD($@J=8C?8C$>JA$I:E=;?T=>?:8$:9$>JA$OA=<$?8$)[$=8D$+[M$)J?B$@
9:;$<FE>?BI:>$B=>AEE?>AB$?8$g=0O=8D($A8=OE?8C$>:$;ADF@A$>JA$8F<OA;$:9$:8O:=;D$=8>A88=B($
;A9EA@>:;B$>:$>R:$;A9EA@>=;;=PBM$

$

`?8=EEP($;A9EA@>=;;=P$I=8AEB$J=HA$OAA8$8;?8DA$<BA$@AEE?CA8>$#F;9=@AB$U+.#V$>:$=DD
I;:OEA<$:9$WOE?8D$T:8ABX$?8$>JA$DAIE:P<A8>$<?EE?<A>A;0R=HA$2Y$8A>R:;ZB($BAA$`?CM$2M$1=E
>:$?EEF<?8=>A$>JA$OE?8D$T:8AOP;AD?;A@>?8C$=8D$BJ=I?8C$>JA$;A9EA@>AD$OA=<$;A@A?HAD
U]#V(OPFB?8C$=$IJ=BA0:8EP$I=>>A;8$BP8>9EA@$bc=M$)AAD+.#$@=8$OA$DAIE:PAD$=>$;ADF@AD

E:R$H?BF=E$?<I=@>$U?8B>=EEAD$:8$R=EEB$:;$@A?E?8CBV$=8D$R?>J:F>$;ASF?;?8C$=8P$A8A;CP$
DAB?C8AD$?8$DF=E0E?8A=;$I:E=;?T=>?:8$>:$@:<IA8B=>A$>JA$D?99A;A8>$;A9EA@>?8C$I;:IA;>?AB$F8D
>:$=IIEP$I:E=;?T=>?:8$D?HA;B?>PM$)JAP$@=8$=EB:OADAB?C8AD$>:$CA8A;=>A$D?99A;A8>$@:HA;=CA
=B$%4$Y_T$=8D$'4Y_TM`?8=EEP($;A@:89?CF;=OEA$;A9EA@>=;;=P$I=8AEB$O=BAD$:8$E?SF?D$@;
DP8=<?@=EEP$;A@:89?CF;A$>JA$@:HA;=CA($=@@:;D?8C$>:$>JA$FBA;BQ$DA<=8DM$
$

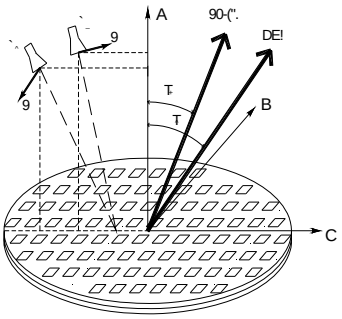

$

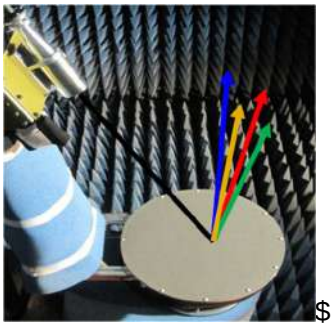

$

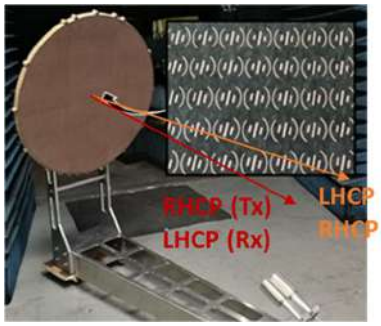

$

!"#$%&'()'*&+,&-./%%/0'1".2'3"++&%&4.' !"#$%&'=)'*&+,&-./%%/0' !"#$%&'?)'*&+,&-./%%/0'#&4&%/."4#'='5&/67'
5&/67'+8%'9'/43':';8,/%"</."84) #&4&%/."4#'>'5&/67';&%'+&&3) ;&%'+&&3'/.'@A'/43'*A'+%&B$&&$-"&7)'

$

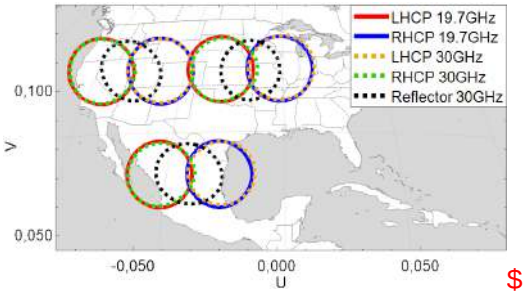

$

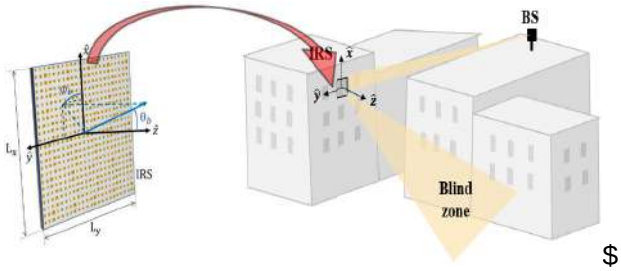

$

!"#$%&'>)'C"A'5&/67'#&4&%/.&3'50'?'+&&37'"4'3$/,DEF!)'#$%&'G)'*&+,&-./%%/0';/4&,7'/7'*HC'+8%'66D1/I&$GJ)'

)J?B$R:;Z$J=B$OAA8$BFII:;>ADOP>JA$#I=8?BJ$,?8?B>;P$:9$#@?A8@A$=8D$.88:H=>?:8$=8D$>JA$
!CA8@P$ R?>J?8$ I;:LA@>B$ 1.\%&%&0aaeah%=8]D$1a0%&%a0a%&f2f0G%a!".ia&Ma'&'fi2&aa&&&aa&"($
=8DOP>JA$#I=8?BJ$,?8?B>;P$:9$"@:8:<?@$!99=?;B$=8D$\?C?>=E$);=8B9:;<=>?:8$R?>J?8$>JA$I;:LA@>$
&j'&&&0%&%a04%M$)JA$E=B>$>R:$C;=8>ADOP>JA$/A[>YA8A;=>?:8"6$F8DA;$>JA$+A@:HA;P$IE=8$9
+A@:HA;P$=8D$+AB?E?A8@A$`=@?E?>PM$ $
>.,.-.)%.*+
aM "8@?8=;($5M!M$A>$=EM($k\F=E01:E=;?T=>?:8$\F=E0G:HA;=CA$+A9EA@>=;;=P$9:;$#I=@A$!IIE?@=>?:8B(k$."""$);
!8>A88=B$=8D$1;:I=C=>?:8($H:EM$2e($8:M$a&(IIM%4%h0%4'h($*@>M$%&&jM$
%dM,=;>?8AT0\A0+?:L=($\M($"M$,=;>?8AT0\A0+?:L=($5M$!M$E8@8?:($=8D$YM$):B:($k+A9EA@>=;;=P$>:$YA8A;=>A$`:
!DL=@A8>$]A=<B$IA;$`AAD$9:;$,FE>?BI:>$#=>AEE?>A$!8>A88=B(k$?8$."""$);=8BM$:8$!8>A88=B$=8D$1;:I=C=>M$
IIM$a%j20a%jf($`AOM$%&afM$
'M ,=;>?8AT0DA0+?:L=($\M$A>$=EM($W);=8B<?>3+A@A?HA$1=;=O:E?@$+A9EA@>=;;=P$>:$YA8A;=>A$)R:$]A=<B$IA
#=>AEE?>A$!8>A88=B$?8$g=0]=8D(X$."""$);=8BM$:8$!8>A88=B$=8D$1;:I=C=>M($H:EM$jf($8:M$2($IIM$%jh'0%j42($
eM ^=SFA;:(lM`M$A>$=EM($k+A9EA@>=;;=P0O=BAD$.8>AEE?CA8>$+A9EA@>?8C$#F;9=@A$>:$.<I;:HA$<<0m=HA$
B@A8=;?:B(k$%&%%%$."""$.8>EM$#P<IM$:8$!8>A88=B$=8D$1;:I=C=>?:8$U!10#i6+#.V($\A8HA;($G*($6#!($%&%%($II
2M YF?;=D:($+M$A>$=EM($k\P8=<?@$,:DAE?8C$:9$-?SF?D$G;PB>=E0]=BAD$,A>=BF;9=@AB$=8D$.>B$!IIE?@=>?:8$
+A@:89?CF;=O?E?>P$)?<AB(k$?8$."""$);=8BM$:8$!8>A88=B$=8D$1;:I=C=>M($H:EM$h&($8:M$a%(IIMaa4eh0aa42

Multiband Substrate Integrated Waveguide Dielectric Resonator Antenna for 4G and 5G Applications

I. K. C. Lin [1] and M. H. Jamaluddin [1*]

[1]Wireless Communication Centre, Faculty of Electrical Engineering, Universiti Teknologi Malaysia, 81310 Johor Bahru, Johor, Malaysia
[*]corresponding author: haizal@fke.utm.my

Abstract: In this work, Substrate Integrated Waveguide with a Dielectric Resonator Antenna is introduced in a more compact size to operate in the 4G bands for LTE Band 3 (1.8 GHz), LTE Band 7 (2.6 GHz) and covers 5G Band n77 (3.7 GHz). A U-shaped slot cut is introduced in order to produce multiple frequency of operation. Simulation is done using Ansys HFSS (High Frequency Structure Simulator) version 2019. Simulated impedance bandwidths are 21.51% (1.67-2.07 GHz) at 1.8 GHz, 4.43% (2.53-2.65 GHz) at 2.6 GHz and 7.57% (3.56-3.84 GHz) at 3.7 GHz and good radiation pattern performance were obtained.

I. Introduction

A compact multiband antenna is favored to DV ZLUHOHVV FRPPXQLFDWLRQ V\VWHPV [1]. A multiband performance can be obtained by the multiple slots [2] using Substrate Integrated Waveguide (SIW). In this paper, a rectangular Dielectric Resonator Antenna (DRA) excited by a U-shaped slot using Substrate Integrated Waveguide is proposed in this paper for 4G and 5G applications to have higher bandwidth and higher gain.

II. Research Methodology

The 3D model view of a single port SIW fed DRA is shown in Fig. 1. A FR4 substrate with a permittivity of 4.6, a loss tangent of 0.019 and with a thickness of 1.6 mm is used. ' 5 4 ¶V SHUPLWWLYLW\ LV W\SLFDOO\ WDNHQ DV 4.6 and loss tangent of 0.0019 is used in this work. Its dimensions for 1.8 GHz are calculated in [1]. It is excited in respective mode by the U-shaped cut configuration, located in the top wall of SIW operating in TE10 mode. The SIW and microstrip transition design parameters are calculated from a conventional waveguide WR 430 in [3], [4], [5].

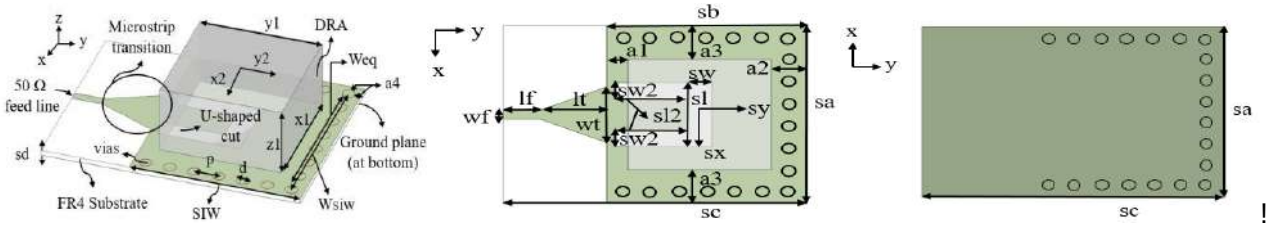

(a) (b) (c)

Fig. 1 Single port SIW with a DRA geometry (a) Overall 3D view (b) Top view (c) Back view

Table 1 Optimised design parameters

Parameter	sa	sb	sc	sd	x1	y1	z1	x2	y2	lf	lt	wf	wt	sw
Value (mm)	64	56	85	1.6	40	40	21	0	-2	10	19	2.95	20	7

Parameter	sl2	sw2	sx	sl	sy	d	p	a1	a2	a3	a4	Weq	Wsiw
Value (mm)	20	6	0	23	-2	4	8	6	10	12	2	52	56

III. Result and Discussion

The simulated results of the proposed antenna are discussed. The simulated impedance bandwidths are 21.51% (1.67-2.07 GHz) at 1.8 GHz, 4.63% (2.53-2.65 GHz) at 2.6 GHz and 7.57% (3.6-3.84 GHz) at 3.7 GHz, as shown in Fig. 2(a). Less than 22 dB of return loss is found within the bands of interest. Simulated normalised radiation patterns of E-plane and H-plane for each frequency is depicted in Figs. 2(b), 2(c) and 2(d).

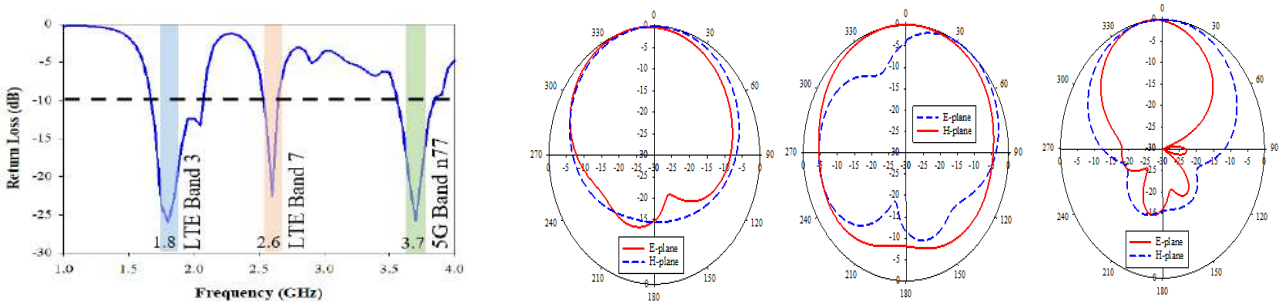

(a) (b) (c) (d)

Fig. 2 Simulated antenna performance (a) return loss (b) normalised radiation patterns at 1.8 GHz (c) normalised radiation patterns at 2.6 GHz (d) normalised radiation patterns at 3.7 GHz

IV. Conclusion

A multiband SIW singly fed with a DRA and a U-shaped cut is presented in this paper. The antenna exhibits good characteristics where impedance bandwidths are 21.51% at 1.8 GHz, 4.63% at 2.6 GHz and 7.57% at 3.7 GHz. More than 4.5 dBi of gain and at least 74% of antenna efficiency are found within the bands of interest. The proposed antenna can be a good candidate for 4G and 5G applications.

Acknowledgements

This study was supported by the Fundamental Research Grant Scheme (FRGS) awarded by the Ministry of Education of Malaysia (Investigation of Low Cost Substrate Based Antenna Using Three-Dimensional Printing Technology for Fifth Generation Wireless System, FRGS/1/2021/TK0/UTM/02/60).

References

1. Lin, I. K. C., M. H. Jamaluddin, A. Awang, R. Selvaraju, M. H. Dahri, L. C. Yen, and H. A. Rahim, "A Triple Band Hybrid MIMO Rectangular Dielectric Resonator Antenna for LTE Applications," IEEE Access, Vol. 7, 122900-122913, 2019.
2. $VKUDI 1 2 +DUD] 0 $ $VKUDI 1 2 +DUD] 0 $ "Quad-band millimeter-wave SIW array antenna with (%* VWUXFWXUHV IRU * DSSOLFDWLRQV ´ LQ ,QWHUQDWLRQDO &RQIHUHQFH RQ ,QWHUJUDWHG :DYHJXLGH 6 , :) LO, Vol. 8, 232-237, 2015, 2015 Research (ICTRC), 58, 2015.
3. Iqbal, A., J. J. Tiang, S. K. Wong, M. Alibakhshikenari, F. Falcone, D Q G (/LPLWL "0LQLDWXUL]DWLRQ RI ,QWHJUDWHG :DYHJXLGH 6 , :) LO, Vol. 8, 232-237, 2015, 2015 Research (ICTRC), 58, 2015.
4. Kumar, P., S. Dwari, S. Singh, D Q G 1 . $JUDZDO "'HVLJQ ,QYHVWLJDWLRQ RI Dual-Band DRA for Mil LWDU\ $SSOLFDWLRQV ´ 2, 7HFK, 2018]RO 1R
5. Kumar, H., R. Jadhav, D Q G 6 5DQDGH "$ 5HYLHZ RQ 6XEVWUDWH ,QWHJUDWHG :DYHJXLGH IOSR J Electron Commun Eng, Vol. 3, No. 3, 35-40, 2012.

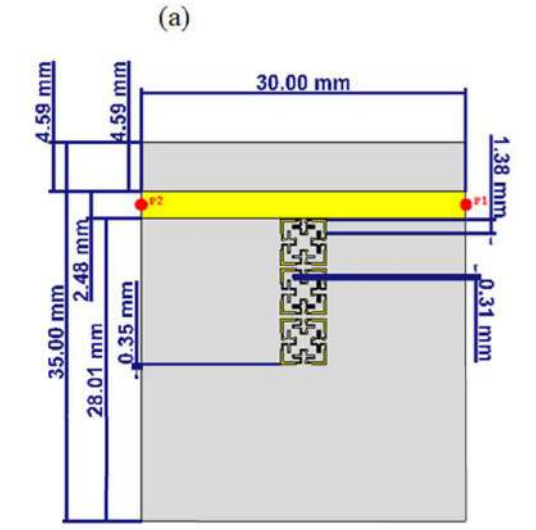
(a)
30.00 mm
4.59 mm
4.59 mm
1.38 mm
2.48 mm
35.00 mm
28.01 mm
0.35 mm
0.31 mm
P2
P1

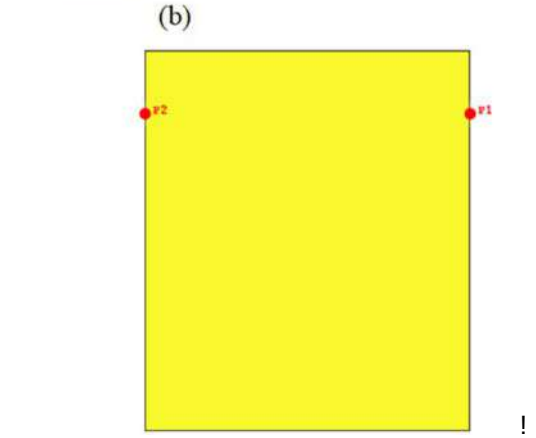
(b)
P2
P1

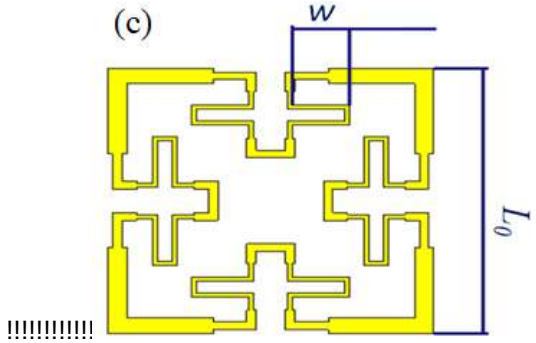
(c)
w
L_0

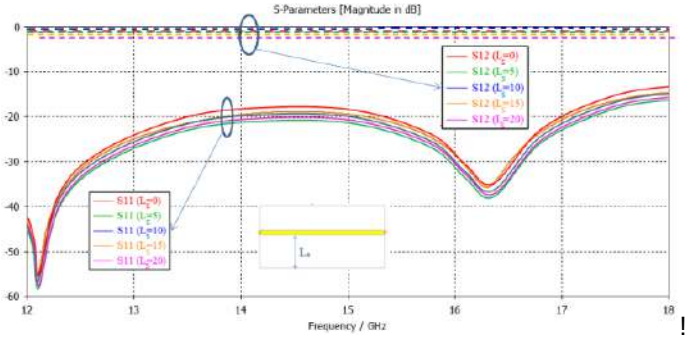
S-Parameters [Magnitude in dB]
Frequency / GHz

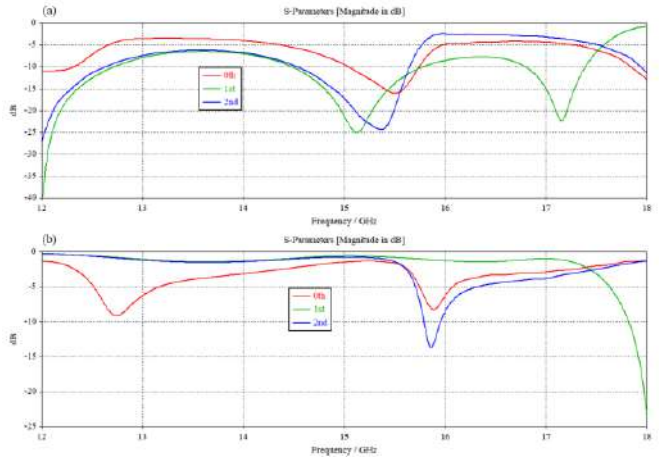
(a)
S-Parameters [Magnitude in dB]
dB
Frequency / GHz
(b)
S-Parameters [Magnitude in dB]
dB
Frequency / GHz

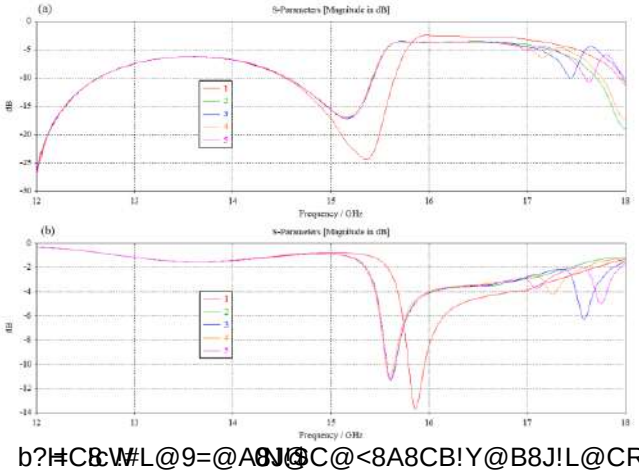
(a)
S-Parameters [Magnitude in dB]
dB
Frequency / GHz
(b)
S-Parameters [Magnitude in dB]
dB
Frequency / GHz

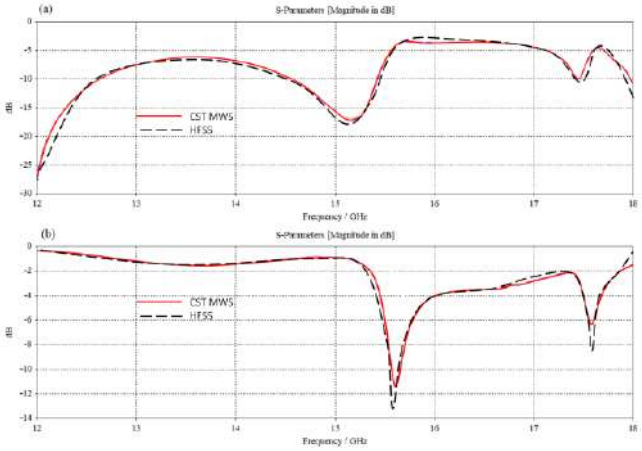
(a)
S-Parameters [Magnitude in dB]
CST MWS
HFSS
dB
Frequency / GHz
(b)
S-Parameters [Magnitude in dB]
CST MWS
HFSS
dB
Frequency / GHz

C8B=9AB!?>!A8C<B!;Q!$77!@>J!$%7!N@C@<8A8CB!@A!AD8!NC;N;B8J!C8B;>@A;C!
C8B;>@A;C!N@C@<8A8CB!@A!AD8!NC;N;B8J!C8B;>@A;C!Y98!7G

!

)@Y98!7W!N@C?B;>!Y8AZ88>!AD8!NC;N;B8J!C8B;>@A;C!
C8B=9AB!@>J!;AD8C!N=Y9?BD8J!C8B=9AB

!

6&)#	G>Q;:#	G>Q;:#	)(QKR#
f7g	07G!	074!	%G7
f%g	0%G4	0&!	4Gh
f'g!	04G&	0c&	%Gi4
fcg	0G]!	0%&	%
fcg	07G!	074!	7Gc
f4g	0%G	06 !	cG&4
f] g	0cG4	07%	'G4
fhg	0%G	07'e0%7	&Gh4e7G
f6g	07G!	07i !	%G7c
fig!	07G!	07] !	'Gh4
f7&g	07G7	0&!	cG7
f77g	07G!%	0c&	&G6
f7%g	0%G'	0%%	7G7
f7'g!	0G&	076!	%Gi
f7cg	07G6	07i !	%G%'

!

!

SA T*"-582/*" #

)D8! NC;N;B8J! Z;C[! ?B! J8B?H>8J! Y@B8J! ;>! @! NC?>A8J!
<?:C;Z@L8!C8B;>@A;C!ZD?:D!?B!J8L89;N8J!Q;C!=>?A!.A!?B!
J8B?H>8J!Y@B8J!;>!@!B?>H98!:;9=<>!@CC@R!;Q!'!=>?A!:899B!;Q!
,?>[;ZB[?!QC@:A@9!J8B?H>G!)D8C8Q;C8(!AD8!NC;N;B8J!J8B?H>8J!
Q;=>J! A;! NC;L?J8! @! N@BB! Y@>J! @C;=>J! 74G]^_`! Z?AD!
@Y;=A@7%JTG!)D8! NC;N;B8J! Z;C[! ?B! J8B?H>8J! P$)!
,a$! A;! ;NA?<?`8! AD8! C8B;>@A;C! Y@>JZ?JAD! N@C@<8AC!
)D8! NC;N;B8J! C8B;>@A;C! ;::=N?8B!@>!@C8@!@Y;=A!'4d'&<<%!
ZD8>!NC?>A8J!;>!+;H8C!644&!B=YBAC@A8!;Q!&G6<<!AD?[8BBG!
)D8! NC;N;B8J! Z;C[! ?B! Q;=>J! A;! BD;Z! @>! 8\:8998>A!+8;>Q?H=C@Y98!
N8CQ;C<@>:8!?>!:;<N@C?B;>A;?:@9!C8B;>@A;CB!AD@A!Z8!8*&5%1!
N=Y9?BD8J! ?>! AD8! 9?A8C@A=C8G! b;C! L@9?J@A?;>B(! A!
C8B;>@A;C! N8CQ;C<@>:8B! @C8! 8L@9=@A8J!=B?>H!
AD8!C8B=9AB!QC;<!P$)!,a$!@>J!_b$$!@C8!Q;=>J!A;!@HC8!A
8@:D!;AD8C!8\:8998>A9RG

6&)&(&"-&2#

f7g $G!"C@?>(!1G!=C8B(!,G!"G!TG!"YY@B?(!"G!U=JJ?;=B(!
,G! "G! ">A;>?@J8B! @>J! $G! /?[;9@;=(! m+8:;>Q?H=C@Y98!
T@>JZ?JAD! T@>JN@BB! b?9A8C! a?AD! #+8Q@>:8J! *=A
T@>J! +8n8:A?;>B?>H! C=0$8:A?;>;@J8J! +?>H!
+8B;>@A;C!(#"!$%&'()*+,!*-.!/%',0,11!2(34(-,-51!
6,55,'1(!L;9G!%6(!>;G!7(!NNG!&&!2(6>G!%&76G

f%g)G! PD8>H! @>J! $G!)@<(! m"! a?J8Y@>J! T@>JN@BB!
b?9A8C!a?AD!+8:;>Q?H=C@Y98!T@>JZ?JAD!T@B8J!;>!P$)!
$D@N8J! +8B;>@A;C!(#"!$%&'()*+,! *-. ! /%',0,11!
2(34(-,-51!6,55,'1 (!L;9G!%h(!>;G!7&(!NNG!7(!:AG!
%&7hG

f'g! oG!XG!T?(!oG!pD@>H(!$Ga;>H(!$G!_G!^=;!@>J!)G!
q=@>(!mO8B?H>!;Q!/;A8B!Y@>J!T@>JN@BB!b?9A8C!a?AD!
Z?AD+8:;>Q?H=C@Y98!T@>JZ?JAD!T@B8J!;>!)8C<?>@A8J!
6,55,'1(!L;9G!'c(!NNG!7(!:AG!%&7%G

!

c!

!

D8C8B8>A8J! +8B;>@A;C!(#"!$%&'()*+,! *-. ! /%',0,11!
'hc7] 0hc%h(!%&%&G

fcg ,G! "G! $@>:D8`$;C?@>;(! +G! ^;<8`^@C:?@(! ^G!
);CC8HC;B@ 18>@9L@(r+8:;>Q?H=C@Y98!
Y@>JN@BB! Q?9A8C! Z?AD! ;::>?=;=B! ::>AC;99@Y98!
7-5,--* (!L;9G!h(!NNG!&&!/;LG!%&7%G

f4g "G! -G! T;Cn@(! 2G! P@CY;>899(! 2G! -G! r,"@CA?>8`(
:;>AC;99@Y98! Y@>JZ?JAD! Q?9A8C! Z?AD! ::>A?>=;=B!
<8A@<@A8C!QC8S=8>:R! @>J! Y@>JZ?JAD! AC@>B<?BB?;>!
7-5,-- *1! /%',0,11! 9' (4*:*5%(-;! L;9G! 7&(! NNG! 74h4
74h6(!,@RG!%&7'G

f]g! /G! PD8>(! $G! XG! 28>H(! r+8:;>Q?H=C@Y98! Y@>JN@BB!
Z?AD! B8N@C@A89R! C89;:@A@9!Y98H!8N@BBY@>!
$%&'()*+,! /%',0,11! 2(34(-,-51! 6,55,' (! L;9G! %%(! NNG!
44i 54]7(!$8NG!%&7%G

fhg oG!,G!a@>H(!oG!XG!T?(!$G!_G!^=;G!r$R>AD8B?B!J8B?H>
8S=@C?NN98! @>J! B9@BA?:! Z?J8Y@>J! T1bB! Z?AD!
?>J8N8>J8>A9R! C8:;>Q?H=C@Y98! 9;Z8C! N@BBY@>J!
"###!7&&,11!L;9G!(!NNG!h]6]](!*:AG!%&%&G

f6g +G! ^;<8`0^@C:?@(! "G! PG! ^=R8AA8(! OG! 1BR:D;H?;=
rU=@B899?NA?:!<9@?J!Q?9A8CB!Z?AD!C8S=8>:R!
@>J! Y@>JZ?JAD! A8:t@*#9!$%&'() *+,! /%',0,11!
2(34(-,-51!6,55,'(!L;9G!%](!NNG!7i%(O8:G!%&7iG

fig! TG! PG! _=@>H(! /G! aG8>(! $G! XG! 28>H(! r
C8:;>Q?H=C@Y98! Y@>JN@BB! Q?9A8C! Z?AD!
N8CA=CY8J(BD@N8J! J<@9! C8B;>@A;C "###!
$%&'()*+,! /%',0,11! 2(34(-,-51! 6,55,'1(! L;9G! %c(! NNG!
%i!5%ii(!2=>G!%&7hG

f7&g $G!"C@?>(!1G!=C8B(!,G!"G!TG!"YY@B?(!"G!U=JJ?;=B(!
,G! "G! ">A;>?@J8B! @>J! $G! /?[;9@;=(! m+8:;>Q?H=C@Y98!
T@>JZ?JAD! T@>JN@BB! b?9A8C! a?AD! #+8Q@>:8J! *=A
T@>J! +8n8:A?;>B?>H! C=0$8:A?;>;@J8J! +?>H!
+8B;>@A;C!(#"!$%&'()*+,!*-.!/%',0,11!2(34(-,-51!
6,55,'1(!L;9G!%6(!>;G!7(!NNG!&&!2(6>G!%&76G

f77g $G!"C@?>(!1G!=C8B(!,G!"G!TG!"YY@B?(!"G!U=JJ?;=B(!
,G! "G! ">A;>?@J8B! @>J! $G! /?[;9@;=(! m+8:;>Q?H=C@Y98!
T@>JZ?JAD! T@>JN@BB! b?9A8C! a?AD! #+8Q@>:8J! *=A
T@>J! +8n8:A?;>B?>H! C=0$8:A?;>;@J8J! +?>H!
+8B;>@A;C!(#"!$%&'()*+,!*-.!/%',0,11!2(34(-,-51!
6,55,'1(!L;9G!%6(!>;G!7(!NNG!&&!2(6>G!%&76G

f7%g)G! PD8>H! @>J! $G!)@<(! m"! a?J8Y@>J! T@>JN@BB!
b?9A8C!a?AD!+8:;>Q?H=C@Y98!T@>JZ?JAD!T@B8J!;>!P$)!
$D@N8J! +8B;>@A;C!(#"!$%&'()*+,! *-. ! /%',0,11!
2(34(-,-51!6,55,'1 (!L;9G!%h(!>;G!7&(!NNG!7(!:AG!
%&7hG

f'g! oG!XG!T?(!oG!pD@>H(!$Ga;>H(!$G!_G!^=;!@>J!)G!
q=@>(!mO8B?H>!;Q!/;A8B!Y@>J!T@>JN@BB!b?9A8C!a?AD!
Z?AD+8:;>Q?H=C@Y98!T@>JZ?JAD!T@B8J!;>!)8C<?>@A8J!
6,55,'1(!L;9G!'c(!NNG!7(!:AG!%&7%G

!

c!

!

,QYHVWLJDWLRQ RI &RPSDFW $QWHQQD

0 'LUL[DQG 6) *UHJVRQ

$QWHQQD 6\VWHPV 6RROXWLRQV 6SDLQ
1H[W 3KDVH 0| 86$4XHHQ 0DU\ 8QLYHUVLW\ /RQGRQ 8.
FRUUHVSRQ PGLUL[#DV\VRO FRP

$EVWU7DKFHWRSWLPDOFBHPSOLFQV RDIQDVHQQD LV FRQVWDUQ\LQDHGWEU\HOHFWULFDO SHUIRUPDQFH DYDLDEDEOH7KVLSDWWKUDWGHLGRSOLFDWLRQV IRU WKH ORF ZKLFK LQFUHDHGHHFWWKRHU DQWHQC DQG IHHG 7KRLWLVSDSHUHUSUHVHUHFHQW VWXG\ WKDW H[DPLQHG WKH HIIHXWLOLVLQJ WKUHH FRPPRQO\ XV IHHG SRSLWLRQ QDPHQG\ IHOGRRUHEUWRLUSXHUU DWWHQWLRQ LV SDLC PHDVXUHG WHVW DQSWRHQQD FR DQG FURVV

:KLOH RYHU WKH DLLVU S2H7USRUWHHVGWDQJLQ W GLUHFW IDU ILHOG LEQDQWGW VWXEH &$7)5G H IDF VWDQGDUG WHVW PZHDWKRRGRVOVRLJ\HIRPXOPWLSC 0DVVLYH 0,02 DQWHQQDV IRU \DWLRQ V\VW 7KLV LV HSHFLDOO\5WU2XSH WRHUVWPDZSDYHLFDW JUHDWO\ LQWHQVLILHG WKSG SHHDQGXORDUU&$7WK RVH KDYLQJ VPDOO)LJXUHD\RX RI D FF TXLHW]RQH 4JUDQJLQVJ MURPP LQ GLDPHWHU 7KLV FRXSOHG ZLWK WKH IUHTXHQWXOWLSOHWRQHHGGHFDPWH SURGXFWXRQHDWWWLQWH GHV KLJKO\ VSDFH HIILHFHQWWKGHHVLJQRI WKH IHHG ZLWKLQ D & IDFWRU LQ WKHVH FRQVLRUQHU IHGSU&RSY5GH DQ HDV\ RYHUDOO OHQJWK VHWXS ZKLOVWDLHRFXSUDUPLQJRQDOO\ LPSDFWVRQVWLKHOXWWRWHG LQ) IORRU FRQHHG &SQG FRQGHLJXUDWLRQV SODFH GLIIHUHQW FRQVW WKH UHSHFWLYH V\VWHPV ZKLOVW DO\UHVXOWLQJSVFRXGLZDYHHS @

,Q WKLV SDSHPSUDUZH DQG FRQWUDVW WKH HOHFWULFDO SHUIR FRQILJXUDWLRQV E\ PHDQV RI DQ DFFXUDWH QXPHULFDO VLPXOD &$75 DQG $87 SDLU VLHPXWDWHG7KRILTXHH WRJHWKHUOZHLWWKWLRWVWKHUL ILFDWL @ IORRU IHG EOHQGHGVLQJOH RIIVHW SDZUWKRDLF PUHHZDHVFGRUVLJQHG D RSWLPLVHG XVLQGHWKHHOFWHFKQLTX@HV7KH &$75 GKHVQJIORRU FRQHU DQ ZLWKH HGJH WUHDWPHQWV E WKUHH FDVHV ZLWK WKHL&SC7G GXLVHWUL]RQWL SUHGLFWHG DW+H*U+] IRUUHDTXHQF\ WRZDUGV WKH ERWWRP RI WKH WKLV LV WKH UHJLRQ LQ ZKLFK WKH KHWHH UHIOHFWRU LV7KHVH FDQ EH VHHQ SUHVHQWHG OLQH WKJHXUHPPHWUL\ RI WKH FRSRODU ILHOG GL RQGHLPHQVLRQDO OLQH WKH RYHUDOO FURVV\SRODUL\SDWWHUQ GQG LWV WZGRLPHQVLRQDO IDOVH FRO G DQG I ,QVLGHZRWKLHV4=XOEWGG WHVW D DUH FRQVLGHUHG 7:KH ISUVDPLDQDWHQQDQL ZKLFK ZDV WKHHFFHQWZLWKGLWV FHQWUH RI URWDWSLRQL I7KVLKH UBHSHVHQWV D YHU\ JRLFPESDYHHFLDQH IRQGXS HYDOXDWLRQ RI WKHKHDRQRUDWKPDOKRZDHQYGHU\SRLFDWKEH\4=SLWLRFEXSRUWLRQ GXULQJ DQ DFTXLVLDWQWRF7KHL³WHGFRQKH VDPH S\UDPLGZDKRGULQSRQHHGK P LQ WKH SRVLDWZDYHU|GRUVHWLRQHUZKRWFKWPLHDQRUWKHQ FURVV D ODUJ

SRUWLRQ RI WKH 4= GXULQJ LWV PHI V V URWDWH
IURPq WRq LQ D]LPXWK 7KLV LV WKH QO
DFTXLVLWLRQ PRGH ZLWK HYHQ ID I O ZHU´
RYHUW\SH SRVLWLRQLQJ V\VWHP XW VI QWDO
PRWLRQ > @ 7KHQ IRU HDFK RI WKH WKUHH &$75 FRQILJXUDWLRQV
WKH 506 G% GLIIHUHQFH OHYHO ZDV FDOFXODWHG EHWZHHQ WKH LGHD
³UHIHUHQFH´ IDU ILHOG SDWWHUQ R QG ODWHG
³PHDVXUHG´ SDWWHUQ WR SURYLGH QV PHDVXU
VLPLODULW\ > @ $ IXUWKHU WHVW IUI IOLS WH
RQ HDFK RI WKH SDWWHUQV WR REW JH \ ZLWKL
WKH PHDVXUHPHQW ZKLFK UHSOLFDWHV WKH LQ
LQ DQWHQQD WHVW V\VWHP YDOLGDWLRQ FDPSDLJQV > @)LQDOO\ W
ORZHU ERXQG VHQVLWLYLW\ IRU WKH) RXQG W
EH DW FLUFD G% IRU WKH FRSROD QO QWO\ OF
IRU WKH FURVV SRODU SDWWHUQ ZL HG QDWLQJ
$87 ZLWK D SHUIHFW SODQH ZDYH ' SL ZLWK
WKH UHIHUHQFH IDU ILHOG SDWWHUQ WKH VHQVLWLWLW\ RI W
VLPXODWLRQ WHFKQLTXH ZDV HVWDEOLVKHG DV PRUH WKDQ G% EHOR
WKH SDWWHUQ OHYHO IRU DOO FDVHV FRQVLGHUHG)LJXUH %5(&$75 4XLHW =RQH)LHOG 'LV

,Q 7DEOH WKH 506 G% GLIIHUHQFH OHYHOV DUH VKRZQ IRU FRPSDUL
WKDW WKH SDWWHUQ DFFXUDF\ RI WKH H RU D W SU P WK H F KQ W H D K RU H
E\ WKH ODUJHU SDUW RI WKH 4= WKDW WKH RIIVHW KRUQ WUDYHUVHV WK
WKH GLIIHUHQFHV EHWZHHQ WKH &$75 VHWXSV UHPDLQ ZLWKLQ G% IR
RI WKH KRUQ)XUWKHU LQYHVWLJDWLRQ RI 7DEOH VKRZV WKDW IRU
SDWWHUQV LV YHU\ VLPLODU HYHQ WKURXJK WKH IOLS WHVW FOHDUO\ VK
HVVHQFH WKLV MXVW PHDQV WKDW WKH OHIW DQG ULJKW KDQG VLGHV R
DW WKH IXUWKHVW ULJKW WKH FRQV PQ DW 7DEOH H SHFWHG IURP WKH ILHOG GLV
IHG FDVH SHUIRUPV WKH ZRUVW LQ WHUPV RI FURVV SRODU
DFFXUDF\ DQG WKH VLGH IHG FDVH VKRZV WKH 2IIVHW \UDPLGDO +RUQ
SHUIRUPDQFH IRU DQWHQQD FHQWUHG RQ WKH 4= DQG 3 RYHU
SRVLWLRQHU ,W VKRXOG EH QRWHG KHUH WKDW WKH &$75 RQO\
EH WUXH IRU DQ D]LPXWK VFDQQLQJ ZKLFK DV QRWHG DERYH
LV WKH PRVW FRPPRQO\ XVHG VHWXS LQFOXGLQJ XVLQJ D
FRQYHQWLRQDO RPQL DQWHQQD SHWDO

,Q VXPPDU\ WKLV SDSHU KDV XVHG DQ HQG WR HQG

&HQWUHG				

7DEOH 0HDVXUHPHQW DFFXUDF\ SUHVHQWHG D

PHDVXUHPHQW VLPXODWLRQ WR FRPSDUH WKH PHDVXUHPHQW
DFFXUDFLHV RI VHYHUDO FRPPRQ &$75 IHHG FRQILJXUDWLRQV ,W ZDV
WKUHH FRQILJXUDWLRQV LV FRPSDUDEOH ZKHUH UDQJH V\PPHWU\ LV R
HUURUV 7KXV ZH KDYH HVWDEOLVKHG WKDW FRQYHQWLRQDO IOLS WHV
LQWHUSUHWHG FRUUHFWO\ 7KLV SDSHU KDV EHHQ DEOH WR FRQILUP WK
VLGH IHG &$75 DUUDQJHPHQW ZKHQ WKH $87 LV QRW ORFDWHG DW WKH R

5HIHUHQFHV

> @ +X 6 :DQJ DQG 6 $Q 2YHU WKH $LU 7HVWLQJ DQG (UURU $QDO\
&RPSDFW $QWHQQD 7HVW 5DQJH 3KRWRQLFV (OHFWURPDJQHV
;LDPHQ &KLQD SS GRL 3,(56)DOO

> @ ' 2OYHU &RPSDFW DQWHQQD WHVW UDQJHV 6HYHQWK ,QWH
,&$3 ,((<RUN SS YRO

> @ 3DULQL 6 *UHJVRQ - 0F&RUPLFN ' -DQVH YDQ 5HQVEXUJ DQ
$QWHQQD 5DQJH 0HDVXUHPHQWV QG ([SDQGHG (GLWLRQ HG YRO

> @ 3DULQL 5 'XEURYND DQG 6 *UHJVRQ ³&RPSDFW 5DQJH 4XLHW =
9DULHW\ RI (OHFWURPDJQHWLF 6LPXODWLRQ 0HWKRGV ´ LQ /RXJKE
/RXJKERURXJK

> @ 3DULQL 5 'XEURYND DQG 6 *UHJVRQ ³&$75 4XLHW =RQH 0RGHO
3DWWHUQ (UURUV &RPSDULVRQ XVLQJ D 9DULHW\ RI (OHFWURPDJ
0HHWLQJ 6\PSRVLXP /RQJ %HDFK &DOLIRUQLD

> @ *XSWD DQG : %XUQVLGH ³$ 0HWKRG WR 'HVLJQ %OHQGHG 5RRH
6WDWH 8QLYHUVLW\ (OHFWUR6FLHQFH /DERUDWRU\ &ROXPEXV

> @ *UHJVRQ 0 'LUL[DQG 5 'XEURYND ³(IILFLHQW 2SWLPL]DWLRQ
6LQJOH 2IIVHW)HG &RPSDFW $QWHQQD 7HVW 5DQJH 5HIOHFWRU 8VL

> @ 'LUL[6 *UHJVRQ DQG 5 'XEURYND ³*HQHWLF (YROXWLRQ RI WKH
&RPSDFW $QWHQQD 7HVW 5DQJH IRU * 1HZ 5DGLR $SSOLFDWLRQV
'D\WRQD %HDFK)ORULGD

> @ 'LUL[6 *UHJVRQ DQG 5 'XEURYND ³*HQHWLF 2SWLPL]DWLRQ R
&RPSDFW $QWHQQD 7HVW 5DQJHV ´ LQ 07 $QQXDO 0HHWLQJ DQG 6

!"#$%&%'($)*++",*-./*#0#1!./($2$3$4$56/"$%&%' $$$$$$$$$$

!"#$%&'()&'*"'+*,+&-$+&$.&'/$+&$0-"*/*(1+'23)0&4%+*"'+&-$+56+3$7,*72)"0$%+*,+)+,8//1
&$.&'/$+*,,%$&+3)7)9*/'0+)"&$"")+:$%'("

;<+=>5?!>5 @ABC A+D<+EFGHI@N+J<+K>5L@S"':+I+<?E55EI M+

7#8."/)"!,!($%9$:;<$=<>$?@<ABC::DCA>($7EF7&$GD@@HA>$@<>$I;D>>HA>($J:CAK<
%!),*#L.1#-($6G#M$6ADN<:>DOP$1C:D>0#CK@CQ($#H:IHAA<$6ADN<:>DOP($8/+#($J:CAK<
J.-.R$#!#($+;<$#CDAO0!N<AODA($J07&72&$8:<A<Q0S:P>0):HQ<$[CCAUK<C$:C>V$WD@DXUW:
Y$-PC$,"+8."+Z$@<CU[<:KD<:V>KD<AO<C[CUW:

E9%&7)0&+O-'%+3)3$7+:$&)'/%+&-$+)")/1%'%+*,+)+,8//1+&$.&'/$+*,,%$&+3)7)9*/'0+)"&$"")+&-)&+*3$7)&$%+)7
FKQ<+O-$+3$7,*72)"0$%+*,+&-$+&$.&'/$+:$%'("+)7$+0*23)7$:+&*+&-)&+*,+)+7$,7"0$+0*8"&$73)7&+)"&$
37*#':$:+91+?G>I<+O-$+*9R$0&'#$+*,+&-'%+%&8:1+'%+&*+*9%$7#$+&-$+'23)0&+*,+&-$+&$.&'/$+&$0-"*/*(1
:$&$7'*7)&'*"'+*,+&-$)+7S,7$T8$"01+3$7,*72)"0$%+*,+&-$+)"&$"")+)":+&*+-'(-/'(-&+&-$+7)&'*+9$&U$$"+&-$
$,,$0&'#$+()"'+*,+&-$+)"&$"")+)":+&-$+U$'(-&+*,+&-$+:$%'("<+

.A$OT<$KHA>OCAO@Q$<NH@NDAB$>SCK<$><KOH:($A<\$O<KTAH@HBD<>$TCN<$I<<A$DAO:H=;
@DBTO\<DBTO$CA=$:<>D>OCAO$[CO<:DC@>$\TD@<$=<C@DAB$\DOT$>SCK<$KHA=DODHA$C>$NCK;
C@>H$>THK]$CA=$NDI:CODHA>$=;:DAB$OT<$@C;AKTU$">S<KDC@@Q$DA$OT<$=<>DBAHWA<
=<S@HQCI@<$CA=$:<KHAWDB;:CI@<$WH:$KH[[;ADKCODHA>$H:$S@CA<OC:Q$>KD<AODWDK$HI_<K
1<ACO:CODAB$+C=C:UUUa$CKKH:=DABOHOT<$A<<=>$HW$OT<$BDN<A$[D>>DHAU$!O$OT<$[<CAOD
DAK:<C><=$O:<[<A=H;>@Q$DA$:<K<AO$Q<C:>($\TDKT$TC>$DAK:<C><=$OT<$DAO<:<>O$CA=$OT<$DA
\DOT$W@<XDI@<$>O:;KO;:<DA=DWW<:<AO$><KOH:>$>;KT$C>$>[C:O$K@HOTDAB$H:$[<=DKC@$DA
=<N<@HS>$;@O:C$@DBTO$CA=$W@<XDI@<$<@<KO:HADK$=<NDK<>$;>DAB$O<KTAH@HBQ$IC><=$
IQ$J.-.Rb$KH[SCAQ$c7dc%dc'dU$)T<><$O<XOD@<$[CO<:DC@>$TCN<$I<<A$=<>DBA<=$DA$OT<$KHAO<
HA$DAAHNCODN<$O<XOD@<($J.-$e!+,*/.M6"$DADODCO<=$DA$%&79$c7dc%dU)<XOD@<$CAO<AAC>$;
C@:<C=Q$I<<A$:<C@Df<=$CA=$O<>O<=DA+J$`+C=DH0J:<g;<AKQa$:C=DCODHAU$.A$.*)$H:$h-!/$`h
/<O\H:]a$KHAWDB;:CODHA>$c'd$I;O$AHO$Q<O$WH:$>SCK<$CSS@DKCODHA>U$

.A$H:=<:$OH$<NC@;CO<$OT<$S<:WH:[CAK<$HW$>;KT$C$O<KTAH@HBQ$CA=$DO>$SHO<AODC@
DA=;>O:Q(CKH@@CIH:CODHA$TC>$I<<A$DADODCO<=$I<O\<<A$#8."/)"!,!$CA=$8/"#U$hDOT$C>$C$S:
KH[SC:<$OT<$+J$S<:WH:[CAK<>$HWC:<W<:<AK<$CAO<AAC$S:HND=<=$IQ$8/"#cEd\DOT$]AH\A$KT
<XCKO$>C[<$=<>DBA$\DOT$D=<AODKC@$SC:C[<O<:>$[C=<$\DOT$H;:$[CO<:DC@>U$!A$HWW><O$S
I<O\<<A$4(&%2$?ef$CA=$4(E$?ef$TC>$I<<A$><@<KO<=$IQ$8/"#$WH:$OT<$CAC@Qf<($\DOT$C$%&
=DC[<O<:U$)T<$[CDA$HI_<KODN<>$C:<OHC>><>>$OT<$D[SCKOHWO<XOD@<$O<KTAH@HBQ$I;O$
S:H[D>DAB$A<\$O<KTAH@HBQDAO<:[>HW[C>>LBCDA$:CODHU

)\H$=DWW<:<AO$N<:>DHA>HWOTD>$CAO<AAC$TCN<$I<<A$[C=<$\DOT$S:HK<>><=$O<XOD@
>O:;KO;:<>DAH:=<:OH>O;=Q$C@>H$OT<D:$<WW<KO$HA$+J$S<:WH:[CAK<>U$!@>H($OT<Q$[
O<[S<:CO;:<$:CABDAB$I<O\<<A$042j8$CA=$k42j8U$)T<$>H@;ODHA$;><=$WH:$OT<$CAO<AAC>$KHAK
KHA=DODHA>$OTCO$KH[S@Q$\DOT$+J$>S<KDWDKCODHA>($\TD@<$[CDAOCDADAB$@DBTO\<DBTO$
D>$A<DOT<:$C$\<CNDAB$AH:C[<[I:CA<($S:HND=<>$:C=DCODHA$S:HS<:OD<>$WH:$+J$=<NDK<>U$
<ACI@<>$OT<$CAO<AACOHI<$WH@=<=$CA=$;AWH@=<=$;>DAB$>TCS<$[<[H:Q$\D:<>$<[I<==<=DAC

lHOT [$H=<@> $ TCN< $ I<<A $ O<>O<= $ \DOT $ OT< $ >C[< $ >H;:K< $ CA= $ W<<= $ SH>DODHA<: $ C> $ OT< $
KTC:CKO<:DfDAB$OT<$CAO<AAC>$;A=<:$OT<$<XCKO$>C[<$KHA=DODHA>$IQ$8/"#$cEdU$)T<$\<DBTO$
CA=$%mU'$B($=<S<A=DAB$HA$OT<$CSS@D<=$O<XOD@<$>O:;KO;:<$CA=$OT<D:$OTDK]A<>>$`C:H;A=$
CAC@Qf<$OT<$<XS<:D[<AOC@$=COC$HIOCDA<=HWIHOT$O<XOD@<$>O:;KO;:<$CA=$OT<D:$OTDK]A<>>$`C:H;A=$:<W<:<AK<

E0V"*U/$:($2$"&%N[k]AH\@<=B<[<AO$D>$[C=<$OH$OT<$8/"#$WH:$DO>$KHAO:DI;ODHA($<>S<KDC@@Q$
O<>O$S@COWH:[$CA=$OT<$:<C@DfCODHAHWOT<$CAO<AAC>$KTC:CKO<:DfCODHAU
h<$C:<$B:CO<W;@OHOT<$J.-.Rb$KH[SCAQ$WH:$S:HND=DAB$OT<$O<XOD@<$[CO<:DC@>$:<g;D:<=$V
CAO<AAC$CA=$OT<$J:CAK<$/H:[CA=Q$+<BDHA$>;SSH:O$WH:$OTD>$:<><C:KT$\H:]U

5$,$7$"0$%

7U #U$8C::C>($lU$!BA;>($lU$+CA$lQ$H[($n"XS<:D[<AOCODHAHWCA$![ID<AO$,DK:H0"A<:BQe1N<O$:$1D@@H
8HAB:p>$J:CAqCD>$=<$,PKCADg;<$%&7m($l:<>O($J:CAK<($%F0'&$!HrO$%&7m($SSU$704U

%U iU$R;($lU$+CN<@H($lU$!BA;>$CA=$#U$8C::C><$[DK:HB:D=$WDI<:$<WW<KO>$H(a$[EKU$%&7m@DA<
>Q[SH>D;[($:H;A=0O:DS$[C:><D@@<$K:;D><($_;A<$%E$3$_;@Q$7($%&74

'U lU$!BA;>($#U$8C::C>($lU$+CN<@H($s.[S:HN<[<AOHW)<XOD@<$!AO<AAC$#Q>O<[$hD:<@<>>$-DA]$l;=B<O$\DC
+<W@<KOH:s($1:HKU$!"#$%&7m($OT<$9OT$!=NCAK<=$"@<KO:H[CBA<ODK>$#Q[SH>D;[($-D>IHA($1H:O;BC@($%

EU tU$"@D>($,U$+H[D<:($-U$J<CO($U$J<$&=M,e($CAO<AA<$w$SHDAOCB<$[PKCADg;<$<A$ICA=<R;OD@D>CAO$
KH;=P$AHA0=PSH@C:D>CAOo(RR.p[<>$5H;:AP<>$/CODHAC@<>$,DK:H0HA=<>$7E079$[CD$%&7m$3$8C<A

Review on Dual BP-NGD Phase Shifter Application for Beam Steering Antenna Design

(Invited talk)

B. Ravelo[1*], S. Ngoho[2], F. Wan[1], T. Gu[1], F. Haddad[3], M. Guerin[3], and W. Rahajandraibe[3]

[1]Nanjing University of Information Science & Technology (NUIST), Nanjing 210044, Jiangsu, China
[2] $ V V R F L D W L R Q) U D Q o D L V H G H 6 F L H Q F H G H V 6 \ V W q P H V $) 6 & (7
[3]Aix-Marseille University, CNRS, University of Toulon, IM2NP UMR7334, 13007 Marseille, France
[*]Corresponding author: blaise.ravelo@yahoo.fr

Abstract: Recent study reveals an application of dual band pass (BP) type negative group delay (NGD) circuit for beam steering antenna array (BSAA) design. The innovative BSAA is based on frequency independent microwave phase shifter. The operation principle in function of the BP-NGD center frequency and bandwidth is described. An illustrative recent result showing simultaneous steering in two different directions by means of NGD value in dual-band frequency is reviewed. The proposed dual BP-NGD microwave function is particularly useful in the future for 5G and 6G communication system.

1. Introduction of BP-NGD description for microwave signal synchronization

An unfamiliar electronic circuit susceptible to operate with NGD effect was investigated [1]. Thanks to the behavioral analogy with filter theory, a BP type NGD microwave function was identified [1]. The NGD can be analytically understood by means of GD definition from f-frequency dependent transmission coefficient S_{21} associated to PS expression $\varphi(f) = \arg[S_{21}(jf)]$:

$$GD(f) = -\frac{d\varphi(f)}{d\omega} \quad (1)$$

The outstanding BP-NGD circuit can be used to synchronize microwave signals for 5G communication system [2]. The proposed dual BP-NGD can be potentially employed for WSN Tx-Rx system performance improvement owing to the principle illustrated by Fig. 1. In this scenario, a tri-band NGD circuit having center frequency and bandwidth $(f_k, \Delta f_k)_{k=\{1,2,3\}}$ is expected to synchronize signals transmitted by WS_k by reducing propagation from distance d_k.

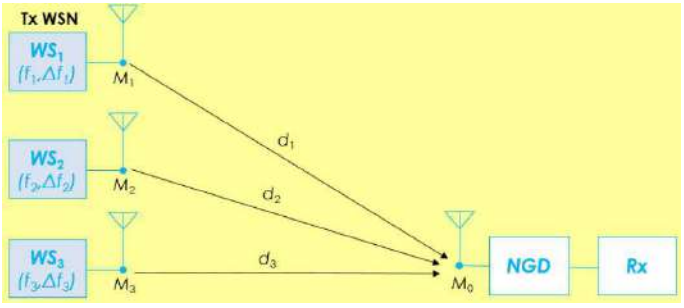

Fig. 1: Illustrative Tx-Rx multi-WSN scenario of synchronization by using BP-NGD circuit [2].

By assuming that $GD(f = [f_k - f_k/2]) = 0$, the following equation explains how the synchronization can be performed:

$$t_k \approx d_k / \text{velocity} \approx GD(f_k) \quad (2)$$

2. BSAA design principle with dual BP-NGD frequency independent PS

The unfamiliar BP-NGD circuit was also used for frequency independent PS design [3-4]. We remind that the classical BSAA operating through bandwidths B_1 and B_2 at two frequencies f_1 and f_2 which are associated to PS values $\varphi_1 = \varphi(f_1)$ and $\varphi_2 = \varphi(f_2)$, respectively, can be represented by Fig. 2(a). The BP-NGD PS was recently exploited to design BSAA with outstanding control of radiation center frequencies and bandwidths as illustrated by Fig. 2(b) [5].

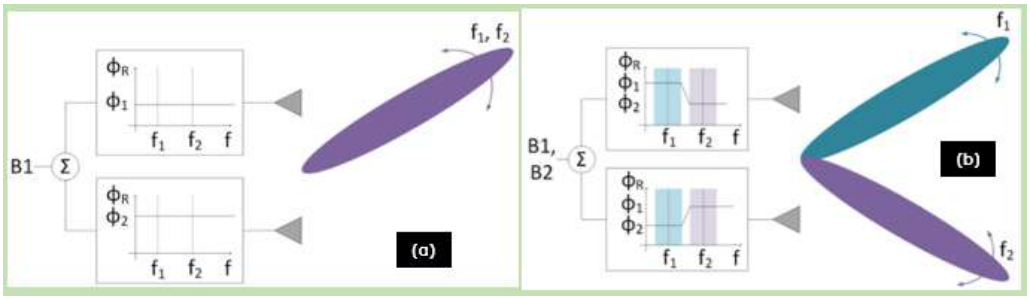

Fig. 2: Illustration of (a) classical and (b) dual band NGD BSAA [5].

The BSAA BP-NGD design principle of the multi-beam phased array is described. The design feasibility is illustrated with dual BP-NGD circuit. A proof-of-concept (PoC) of BP-NGD circuit is simulated and analyzed. Based on the PoC, simulations with separate beam steering positions at different frequencies are also analyzed. The innovative SBAA behavior is discussed.

3. Conclusion

An innovative application of dual BP-NGD circuit for BSAA design is reviewed. After description of BP-NGD unfamiliar microwave function, the design principle is illustrated. Simulations with dual BP-NGD PoC explain the feasibility of the SBAA design. The developed concept is useful in the future for designing SAA-NGD system of innovative multi-beam antenna for the improvement of RF and microwave system.

References

1. Ravelo, B., "Study on the NGD function versus conventional group delay," International Journal of Microwave and Wireless Technologies, Vol. 6, No. 3-4, pp. 363-370, 2014.
2. Lallechère, S., L. Rajaoarisoa, L. Clavier, R. Sanchez Galan, and B. Ravelo, "Broadband NGD function for microwave signal delay synchronization application," ACES, Tome 22, no. S1, 53-71, 2021.
3. Ravelo, B., G. Fontgalland, H. S. Silva, J. Nebhen, W. Rahajandraibe, M. Guerin, G. Chan, and F. Dong, "2.4 GHz Application of Stop-Band Negative Group Delay Microwave Passive Circuit for Two-Step Stair Phase Shifter Design," Progress In Electromagnetics Research C, Vol. 119, No. 1, 1493-1508, 2022.
4. Ravelo, B., M. Guerin, J. Frnda, F. E. Sahoa, G. Fontgalland, H. S. Silva, S. Ngoho, F. Haddad, and W. Rahajandraibe, "Design Method of Stair Microwave Passive Integrated Circuit in 180 nm BiCMOS Technology with Bandpass Response," Progress In Electromagnetics Research C, Vol. 123, 93-108, 2022.
5. Ravelo, B., G. Fontgalland, A. P. B. Dos Santos, H. S. Silva, N. M. Murad, F. Haddad, M. Guerin, and W. Rahajandraibe, "Dual-band type XNGD network design for true time-delay based multi-beam phased array system," PIER B, Vol. 98, 107-123, 2023.

Optimizing a pyramidal horn together with a dielectric lens for an airborne X-band transmitter

J.Kuster[1*], F.Christophe[2], A.Penarier[1], and P.Nouvel[1]

[1]IES, CNRS- Montpellier University, France
[2]Aresia, France
corresponding author, E-mail: !"#$%&$#'()%+,-)."#%/+001+,'2, 3
3
3

Abstract

The design of a pod-mounted transmitter is subject to specific radiation pattern constrains, to be fulfilled in a strongly limited volume. The step-by-step definition of the antenna is described.

1. Introduction

The antenna will be housed in a pod of internal diameter 250 mm and protected by a radome to be optimized separately. The antenna to be designed has to cope with radiation pattern requirements as indicated below:

Table 1: Radiation pattern requirements

Frequency band (GHz)	Beamwidth horizontal	Beamwidth vertical	Gain (dBi)	Near SLL (dB)	Far SLL (dB)
8.5-9.6	<10¡	>30¡	>20	<-15	<-25

The horizontal beam width requires the width of the antenna to be close to the pod diameter. A further requirement is the capability of the main beam to be mechanically scanned from the axis of the pod up to at least 40¡ laterally, which adds a constrain to the length of the antenna, see figure 1. Due to power handling capability, the antenna has to be fed by a waveguide, chosen to be flexible to avoid rotary joint issues.

First, in terms of antenna selection, a pyramidal horn of thickness smaller than width is close to a sectoral horn appears to approach the radiation pattern requirements [1]. Nevertheless, the criteria of quasi-plane wave front at the D S H U W X U H G R H V Q ¶ W D S S H D U D F K L H Y H G Z L W K R X W D Q H Q J W K R I W K horn prohibiting wide enough angular scan, (figure 1a) [1]. Therefore, compensating the spherical wave front of a reduced length horn through a plan-convex dielectric lens was selected [2]. Secondly, since mechanical scan remained still insufficient (figure 1b), the next improvement was to add a dielectric prism to deflect the main beam out of the plane of symmetry of the horn (figure 1c). Numerical simulations with a 3D electromagnetic commercially available code implementing Finite Integration Method with the Perfect Boundary Approximation were performed

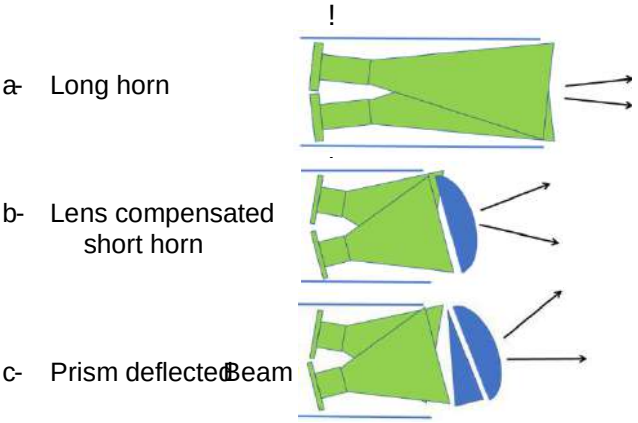

Figure 2 : Principles for mitigating the size limited angular scan (radome not shown)

This article presents the different steps to achieve an antenna that meets the different constraints imposed by the specifications.

2. Preliminary antenna selection

Without taking into account the size of the antenna, a pre-selection of several kinds of antennas has been made. For the realization of this project, high peak power was considered, to be generated by a magnetron. This leads to feed the antenna through a waveguide. In the literature [1], several types of antennas can be found which meet this criterion. From radiation pattern and footprint considerations, sectoral horn antennas were first selected.

Because of its simplicity of construction and dimensioning, the horn antenna is the most widely used antenna for microwaves [1], fed by a waveguide. At the end of this waveguide, the edges are flared to obtain a larger opening. The angle, cross-section and length of the flare play an important role in the radiation pattern. This gradually increasing aperture also prevents mismatch from guided to free space propagation.

2.1. Sectoral E plane

The sectoral horn in E plane corresponds, on the one hand, to the flaring of the guide sections perpendicular to the E field. On the other hand, the edges of the guide parallel to the E field keep the same dimension, as shown below.

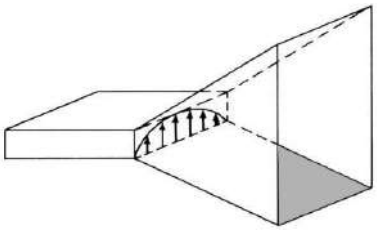

Figure 3 : Geometry of a sectoral E horn antenna [1]

Thanks to this aperture, the radiation in the E plane is thin and wide in the H plane. We have dimensioned a sectoral E plane horn from a WR112 guide (12.63 x 28.50mm). First, we considered that the horn will be installed in a 250 mm diameter cylinder. this leads us to choose an aperture width of 240 mm. In a second phase, following the main laws of illumination for a rectangular aperture and assuming that the plane E follows a uniform and equiphase law [2], we obtain :

$$* 2 \$ 9 L w \frac{\lambda z}{a} \quad (1)$$

With the wavelength, the aperture width of the horn and $* 2 \$ 9$ is the half-power beamwidth in degrees. Taking an average frequency of 9 GHz, we obtain HPBW = 7°, with a peak side lobe at -13.2 dB. We are now interested in the distance Re from the center of phase of the horn to the center of its aperture. We seek the smallest possible length, while having secondary lobes lower than -15 dB. From the universal E-plane radiation pattern [1], for an E-plane sectoral antenna, we derive a parameter s of one eighth and side lobes less than -15 dB for angles greater than 15°. This parameter corresponds to a coefficient given in the literature[1].

$$OL \frac{o \cdot}{< \ddot{E} \emptyset} \quad (2)$$

Thus, depending on this parameter, and using relationship (2) we obtain a length Re of 172 cm.

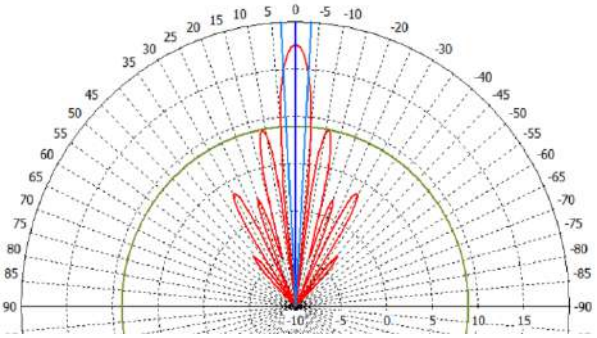

Figure 3 : Radiation diagram in E-plane (in blue the half-power beamwidth, in green the peak side lobe level)

We carry out a simulation with the dimensions determined previously, the result is presented in figure 3. The simulation results show parameters in agreement with those obtained analytically. Nevertheless, the side lobes are too high (-8 dB peak value) and do not meet the specifications. In addition, the length of the horn does not allow for the expected angular deflection.

2.2. Sectoral H plane

The H-plane sectoral horn is defined by flaring the guide sections parallel to the E-plane, with constant dimension in the perpendicular plane, resulting in a wide beam in the E plane and a thin beam in the H plane

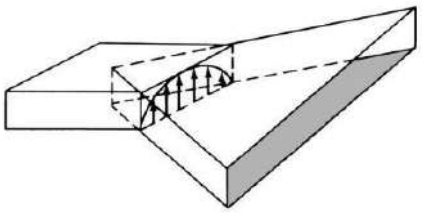

Figure 4 : Geometry of a sectoral H horn antenna [1]

We start from a WR112 guide to shape the horn and we keep an aperture width of 240 mm. Since the illumination now follows a cosine law [2], we obtain in a first step a -3 dB beamwidth of 9.6°, as well as a peak side lobe equal to -23dB for a frequency of 9 GHz. In a second step, reference is made to the universal H-plane radiation pattern for an H-plane sectoral antenna: a parameter s of one quarter is determined for same conditions as in E-plane, this parameter s is also obtained from the literature [1]. A length Re of 86 cm is now required to reduce the side lobes below -15 dB. The simulation of the horn is shown in figure 5. The cross

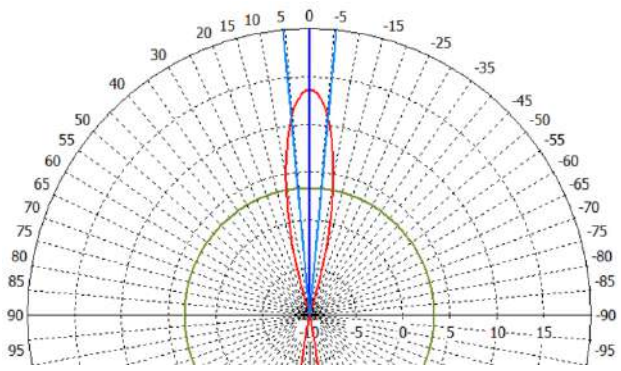

Figure 5 : Radiation diagram in H plane (In blue the half power beamwidth, in green the peak side lobe level)

sectional plane is this time quite conclusive at the level of the side lobes. It also matches the data obtained theoretically. Nevertheless, the vertical aperture has to be adjusted, which is performed in the next section.

It is now clear that H-plane sectoral horn is preferred to E-plane not only for side lobes level but also for horn length consideration.

2.3. Transition from a sectoral horn to a pyramidal horn

In parts 2.1 and 2.2 we studied the radiation pattern in the horizontal plane parallel to the flared sides of the horn. But the above defined H-plane sectoral horn has a gain of only 13.7 dBi due to its very wide but unnecessary beamwidth of 111° in the vertical plane. We therefore have to consider increasing the vertical aperture to increase the gain, i.e. turning the sectoral into a pyramidal horn. Following [1], the gain equation for a non-equiamplitude aperture is given by:

$$G = \frac{8}{\pi} \cdot S \cdot B_0 \quad (3)$$

With G the gain of the antenna, S the aperture surface, B_0 the gain factor depending on the illumination law of the aperture (in our case, this coefficient is 0.81). Thus, for a gain of 20.72 dBi at 9 GHz and an horizontal aperture of 240 mm, a vertical aperture of 155 mm is obtained. The simulation figure 6 shows the resulting vertical radiation pattern with 32° of half power beamwidth.

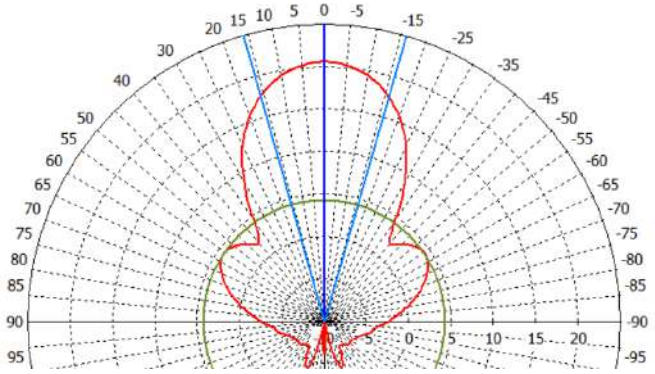

Figure 6 : Section of the radiation pattern in E-plane

3. Reduction of the length of the horn

As seen in the previous section, the length of the horn becomes our main problem to meet the specifications. To reach the angular deflection, a shortening of the horn length is necessary. We first performed a simulation by reducing the length of the horn down to 200 mm, while keeping the same aperture. The degradation on the beam in the horizontal plane is such that the main lobe widens to 16.9 degrees: this leads to a loss of 4 dB on the gain of the antenna. In order to compensate for these degradations, we now add a lens. The objective of this lens is to compensate the spherical phase front at the aperture, therefore thin the beam and increase the gain. By pure geometric rule, if we place ourselves in the H plane and look in the direction of propagation, we determine that the wave at the center of the aperture travels 17.6 mm further than on the edges of the horn. This distance difference generates a phase shift of 190° at a frequency of 9 GHz. We consider using rexolite (refractive index 1.59) for the lens, for its low loss at microwave frequencies and high resistance to environmental constraints. With these different data, geometrical considerations show that a plano-spherical lens of radius Rh = 332.3 mm and as center, the center of phase of the horn, is able to achieve the required phase front compensation at the aperture of the horn. To avoid reflections generated by the refractive index of the lens, matching layers a quarter wavelength thick and refractive index 1.26 are also included in the overall simulation presented in the figure below.

The results are quite satisfactory: when we look at the line-of-sight section, the compensation of the phase shift by the lens is obvious. This compensation is reflected in the radiation diagram, with a thinning of the main beam and a gain greater than 21 dBi.

To conclude, the lens fulfills its objective by compensating for the shortening of the horn. With such horn dimensions, angular scanning becomes feasible. However, practical implementation of the matching layers is now to be considered.

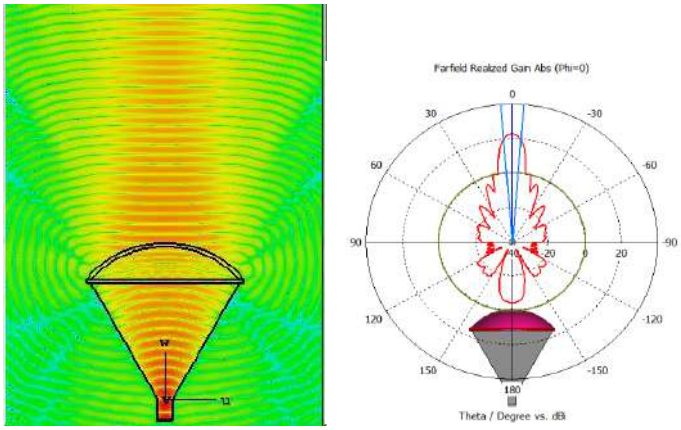

Figure 7 : Electric field inside and outside the device (left) and radiation diagram at 9 GHz for phi=0° (right)

4. Corrugated matching layers

The matching layers realized in the previous simulations are ideal, but not realizable in homogeneous rexolite. A solution is to create an artificial dielectric material, i.e. make periodic holes or grooves within the dielectric structure.

In order to be equivalent to an homogeneous medium, the period of the corrugations must not exceed the spacing p defined by the following equation

$$p = \frac{\lambda}{n_r + \sin\theta_{max}}$$

With n_r the refractive index of the rexolite, n_0=1 the refractive index in free space and θ_{max} the maximum angle of incident radiation, we find a spacing that must be less than 16 mm. There are two choices since corrugation can be achieved by periodic material substitution in 1 or 2 dimensions. For practical reasons we chose to dig cylindrical holes in the lens according to spacing p.

Following this, an optimization was made through computation of the effect of varying the diameter and

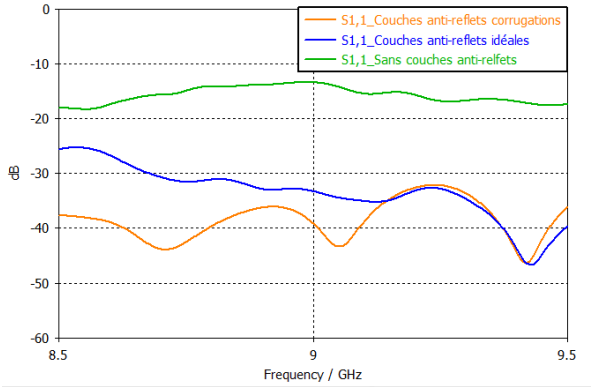

Figure 8 : Reflection coefficient without matching layer (green), with periodic holes (blue), with periodic grooves (orange)

spacing of the holes, in order to obtain the structure with the lowest reflection coefficient. Below we can see a comparison of the coefficient for a simulation without matching layers, and with layers of periodic holes or grooves.

Figure (8) confirms the advantages of the matching layers. Moreover, we observe that we obtain slightly better results with corrugated grooves

5. Beam deflection

Having achieved the design of a compact, high peak power antenna meeting the required radiation pattern, we further want to extend the potential beam deflection. Such a 15¡ beam deflection should allow a mechanical scan of +/- 25¡ of the antenna to create a beam scan -10/+40¡ with respect to the axis of the cylinder, meeting a further requirement for the system. Such beam deflection could result from the insertion of a dielectric prism into the horn. Like the lens, the prism is expected to be made of rexolite.

A representation of the antenna is given in figure 9 with lens, prism and matching layers assembled. Obviously, prism and lens may be implemented from a single piece of rexolite, with matching layers at the input of the prism and the output of the lens.

Again the sizing of the prism is done by simulation, starting with a thin prism, allowing to observe jointly beam deflection and potential radiation pattern degradation, and further increasing the thickness of the prism. The figures below shows the final result: we obtain a 15¡ beam deflection without changing the main characteristics of the radiation pattern.

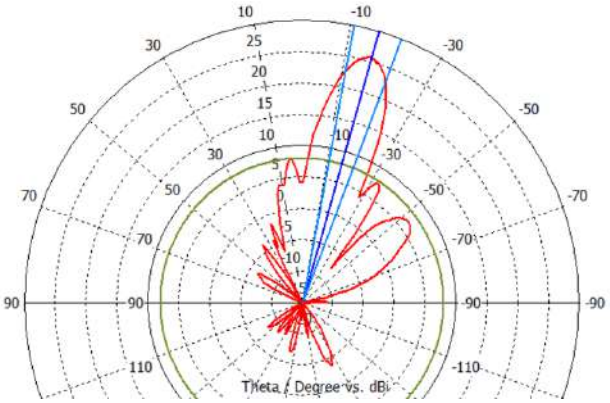

Figure 10 : Radiation diagram at 9 GHz for phi 0¡

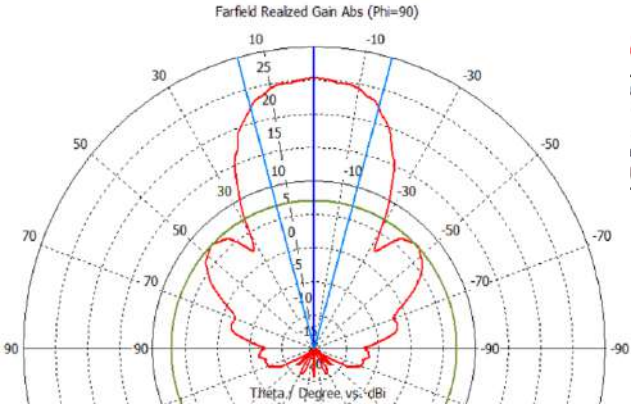

Figure 11 : Radiation diagram at 9 GHz for phi 90¡

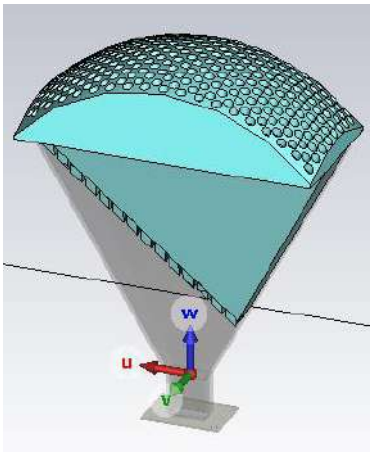

Figure 9 : Final design of pyramidal horn

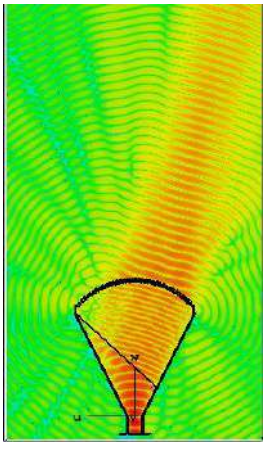

Figure 12 : Electric field inside and outside the device combining horn, lens and prism

6. Conclusion

To conclude, the step-by-step design of a horn and dielectric antenna has been shown theoretically to meet the specifications, taking into account various practical constraints. A physical realization of this antenna is underway.

Acknowledgements

The authors would like to thank RŽgion Occitanie / PyrŽnŽes-MŽditerranŽe (HERMES platform) and the European Regional Development Fund (FEDER) for partial funding of this work.

References

[1] Balanis, C. A. Antenna theory: analysis and design. Johnwiley & sons pp 639-782. 2015.

[2] Robert S.E. Antenna theory and design. Institute of Electronics & Electrical Enginneers. pp 79-99 & 482-545. 2003

[3] Wheeler, Jordan D., et al. "Antireflection coatings for submillimeter silicon lenses." Millimeter, Submillimeter, and Far-Infrared Detectors and Instrumentation for Astronomy VII. Vol. 9153. SPIE, 2014.

Array antennas, active, adaptive and reconfigurable antennas

Deep-learning-assisted reconfigurable metasurface antenna for real-time holographic beam steering

Hyunjun Ma [1], Jin-soo Kim[1], Jongho Choe[1], and Q-Han Park[1*]

[1]Department of physics, Korea University, Seoul, 02841, Korea
[*]corresponding author: qpark@korea.ac.kr

Abstract: We proposea deep-learning-based method for the control of a reconfigurable metasurface antenna. We modeled the metasurface as a collection of dipoles with states of varying polarizability and used a deep autoencoder neural network combined with a scattering equation and Born approximation to generate on-demand far-field maps. Our proposed autoencoder exhibits higher accuracy and a much faster speed compared with the conventional GA approach and allows for the real-time operation of a reconfigurable metasurface antenna for beam steering.

We propose a metasurface antenna capable of real-time holographic beam steering. An array of reconfigurable dipoles can generate on-demand far-field patterns of radiation through the specific encoding of meta-atomic states i.e., the configuration of each dipole. Suitable states for the generation of the desired patterns can be identified using iteration, but this is very slow and needs to be done for each far-field pattern. Here, we present a deep-learning-based method for the control of a metasurface antenna with point dipole elements that vary in their state using dipole polarizability. Instead of iteration, we adopt a deep learning algorithm that combines an autoencoder with an electromagnetic scattering equation to determine the states required for a target far-field pattern in real-time. The scattering equation from Born approximation is used as the decoder in training the neural network, and D Q D O \ W L F * U H H Q ¶ V is used to check the validity of the Born approximation. Our learning-based algorithm requires a computing time of only around 100 V to determine the 900 meta-atomic states, thus enabling the real-time operation of a holographic antenna.

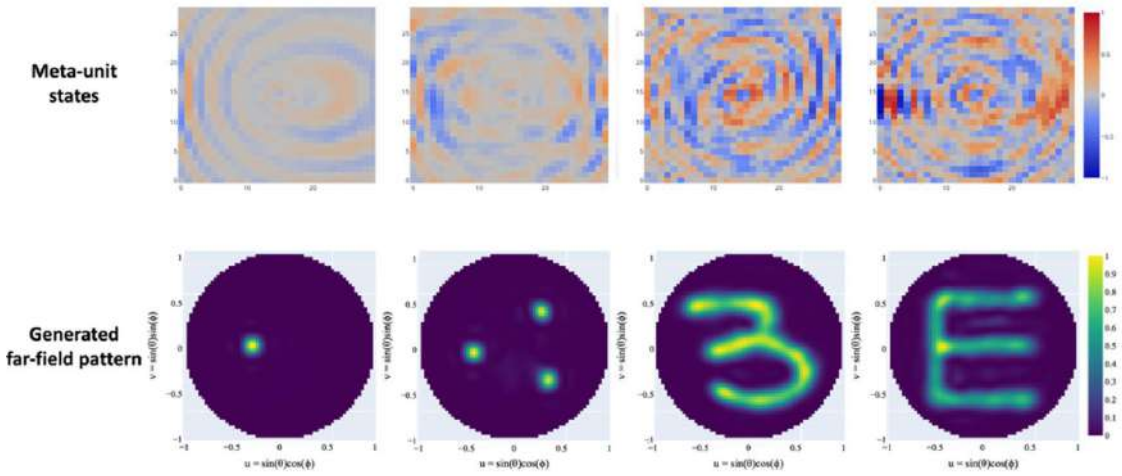

State patterns generated by the neural network, and the calculated far-field maps from the * U H H Q ¶ V I X Q F W L R Q

References

1. Ma, H. J. et al. "Deep-learning-assisted reconfigurable metasurface antenna for real-time holographic beam steering", submitted, 2023

Origami foldable and deployable reflectarray antennas for CubeSats

T. Tomura[1]

[1]Tokyo Institute of Technology, Japan
*corresponding author: tomura@ee.e.titech.ac.jp

Abstract: This paper presents origami foldable and deployable reflectarray antennas for CubeSats. To enable the reflectarray antennas, there is two key technology: creaseless reflection elements and deformation compensation reflectarray. In this paper, these technologies are shown in detail with design and measurement results.

Folding patterns are shown in Fig. 1 and are composed of mountain and valley folding lines. Array lattice is shown in the same figure and designed so that the boundaries coincide with the folding lines. Most of them match with the array lattice but some cross the array element [2]. Figure 2 shows the shape of the reflection element which does not cross the folding lines and it is composed of four triangular patches with notches. Changing the dimension of the patch and the notch reflection phase can be tuned. These reflection elements enable creaseless design of reflectarray antennas.

Figure 3 shows the deformation compensation reflectarray antennas and the reflection elements are composed of a rectangular patch and a varactor diode. Depending on the deformation amount, bias voltage to the varactor diode is controlled to compensate for the deformation. Using a solid reflectarray prototype, the gain increment is confirmed [3].

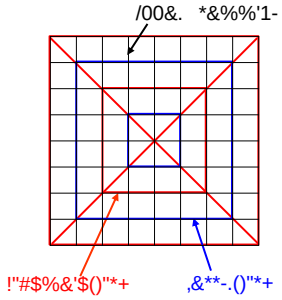

Fig. 1 Folding patterns

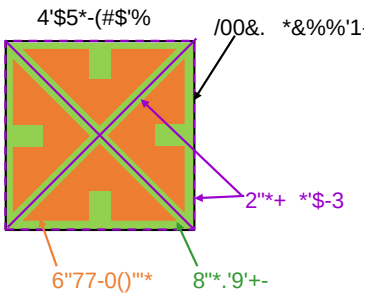

Fig. 2 Creaseless patch shap

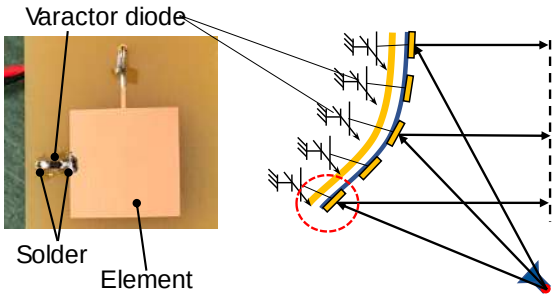

Fig. 3 Deformation compensation reflectarray

This work was supported in part by the Telecommunications Advancement Foundation, the Japan Society for the Promotion of Science (JSPS) KAKENHI under Grant JP20H00281 and Grant JP20H02146, DLab Challenge 2022 of Tokyo Institute of Technology.

References

1. K. Ikeya, et al. ³6LJQLILFDQFH RI 8 -band deployable membrane reflectarray antenna for Earth observation CubeSats´ $FWD $VWURQDXWLFD, Aug. 2020. DOI: 10.1016/j.actaastro.2020.03.038
2. T. Tomura, et al. ³7ZR-layer pop-up origami deployable membrane reflectarray DQWHQQD VWRZHG AIAA/USU Conf. Small Satellites, SSC22-WKVI-05, Aug. 2022.
3. . 2PRWR 7 7RPXUD DQG +RQJR ³Design of creaseless reflectarray antenna for CubeSats´ 3URF. 2021 IEEE Int. Symp. Antennas Propag. North. Radio Sci. Meeting (AP-S/URSI), Dec. 2021, pp. 541–542, doi: 10.1109/APS/URSI47566.2021.9703941.´ , ((($FFHVV

7KH: LGHEDQG6,: \$QWHQQD\$UUD\VIRU * 0 P ZDYH\$SSOLFDWLRQV

+XDQKXDQ+XDQJ <DQJKRQJ<X ; XHKXD/LQ -LQJ7LDQ

&RQJUHV3K\VLFV ,QVWLWXWH(QJLQHHULQJ 4XDQJKRX1RUPDO8QLYHUVLW\ )XMDQ &KLQD
6FKRRORI\GDQFHG0DWKHPDWLFV)XJKRX8QLYHUVLW\ -LQMDQJ &KLQD
\X\DQJKRQJ #FRP

\$EVWUDFW

,QWKLV SDSHU D EURDGEDQG DQWHQQD DUUD\ ZLWK KJK JDLQ LV SUHVHQWHG 7KH DUUD\ HOHPHQWVKDVREWDLQHG DJDLQRI G% DQG ZLGHUHPSHGDQFHEDQGZLGWKRI PRUHWKDQ * +] IURP * +] WR * +] \$ JDLQRI G%LVDFKLHYHG LQWKH \8 DUUD\ 7KHZRUNLQJ EDQGRI WKHIRXUHOHPHQWDUUD\ FDQ FRYHUWKH PP ZDYHEDQG 7KH SURSRVHG DUUD\ VZLWK JRRG \\PPHWU\ RI UDGLDWRQ SDWWHUQV DQG ZLGH EDQGZLGWK DUH SURSHUIRU * PP ZDYHFRP PXQLFDWLRQ

,QWURGXFWLRQ

: LWK WKH JHQHUDWLRQDO GHYHORSPHQW DQG WRFKQRORJLFDO LQQRYDWLRQ RI PRELOH FRP PXQLFDWLRQ WKHRFFXSDQF\ UDWH RI PRELOHWUP LQDOYLV JHWWQJ KJKHUDQGKJKHU ZKLFK GHDG/WR WKH UHTXLUHPHQW IRU D KJKHU FKDQQHO FDSDFLW\ DQG WUDQVPLWLRQ UDWH RI WKH PRELOH FRP PXQLFDWLRQ \\WP> @ 7KHH[WUHPHOH IUHTXHQF\ EDQGLV DOHDG\ YHU FRQJHVWHG LWLV XUJHQWWR DGRSWWKH QHZ FRP PXQLFDWLRQ IUHTXHQF\ EDQG WXFK DV PLOOLPHWUZDYH IRU * WR H[SDQG WKH CAPLWG EDQGZLGWK @ 7KHUHRH PLOOLPHWUZDYH WHFKQRORJ\ KDV DWWDFWHG PXFK DWWHQWLRQ IURP FRP PXQLFDWLRQ UHVHDUFKHV 7KH UH> @KDV SURSRVHGD î PLOOLPHWUDUUD\ ZLWK DJDLQRI G%LDQG D \\PPHWUFDO SDWWHUQ \$ FRP SDFWGXDOEDQG DQWHQQD WKDW ZRUNV DWWKHPP ZDYHIUHTXHQF\ IURP * +] WR * +] LV SUHVHQWHG LQ UH> @7R PHHWWKH UHTXLUHPHQWV RI * WKH DQWHQQD DOR QHGV WR EH ZLWK KJKHU JDLQ DQG D ZLGHU ZRUNLQJ EDQG 7KH 6,: WHFKQRORJ\ FDQ VXSSUHVV WKH GRW RI WKH VXUFFH ZDYH DQG UHGXFH ILQMUHUHQFHE\ VXSSUHVVLQJ WKH CHDNJHRI WKHHDFWRP DJQHWF VLJQDO @\$ CQHDU0 ,0 2 DQWQQD DUUD\ LV SUHSRVHG LQ WKLV DUWFOH WKH GHVLJQHG DUUD\ KDV DFKLHYHG ZLGH ZRUNLQJ EDQGZLGWK KJK JDLQ DQG JRRG SDWWHUQ FRQVLWWQF\ 6HFWRQ KDV GHVFULEHG WKH FRQWXFWRQ DQG WKH VLP XODWRQ UHVXOWRI WKH DUUD\ HOHPHQW7KH CXP HUFDOUHXOWRI WKH VZR HOHP HQW DUUD\ DQG IRXU HOHP HQW DUUD\ DUH GLVFXVHG LQ VHFWRQ 7KHFRQFOXVLRQ LVJLYHQ LQ VHFWRQ

6LP XODWRQ RI WXWXFWXUH

7KHP DWHULDORI WKH VXEWUDWH LV5RJHUV 7KHHOHP HQWV IRUP HG E\ VXEWUDWH PP VXEWUDWH PP JURXQG SDWK SDWK FRQ[LDO FDEOH FRSSHU FONGHV DQG SHF FA\ODQGHUV DVSUHVHQWHG LQ) LJXUH 7KHIHHGLQJ PHWRG FRP HQWLV FRQ[LDO FDEOH 7KH GLP HQVLRQ VRI WKHEOP HQWDUH JLYHQ LQ7DEOH

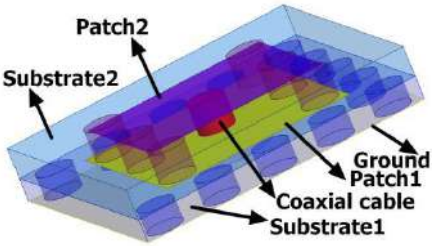

D

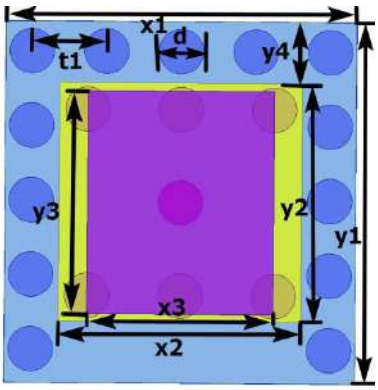

E

) LJXUH &RQLJXUDWRQV RI WKH DUUD\ HOP HQW D SHUSHFWLYHYLHZ E WRSYLHZ

7DEOH 7KH3DUP HWHUV2I 7KH(OP HQW

3DUP HWHUV	9DOXHPP	3DUP HWHUV	9DOXHPP
[		\	
[		\	
[		\	
\		W	
W		G	

7KHVLP XODWRQ UHVXOWV RI WKHHOP HQWDUH JLYHQ) LJXUH 7KH ZRUNLQJ IUHTXHQF\ RI WKH DQWHQQD HOP HQWLV IURP * +] WR * +] ZKLFK FRYHUV WKH &KLQHVH * PP ZDYHEDQG RI * +] WR * +] 7KHUHWXUQ ORVV RI WKH HOP HQWFDQ UHDFK G% DQG WKH = SDUP HWHU RI WKH HOP HQWLV LDWWKH FHQWHUIUHTXHQF\ SRLQW * +] \$ JDLQ RI G%LVREWDLQHG DWWKH FHQWHUIUHTXHQF\ RI * +] 7KH 96: 5 EDQG RI OPW WKDQ LV IRP

* +] VR * +] ZKLFK FDQ FRYHU VKH HQWLUH ZRUNLQJ EDQGZLGWK 7KH GHVLJQHG HDPHQWKDV JRRG LPSHGDQFH PDWFKLQJ DQG JDLQ

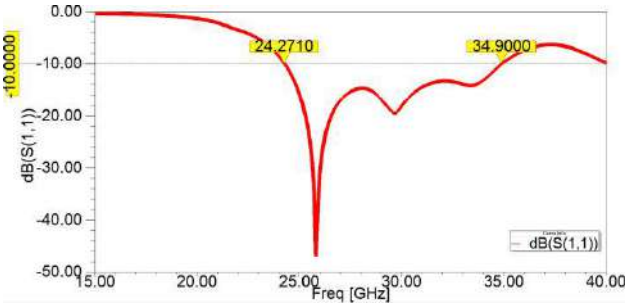

D

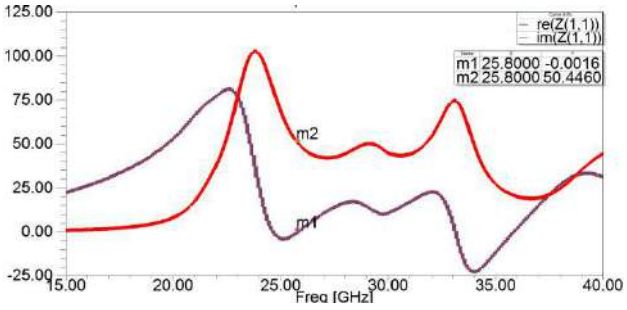

E

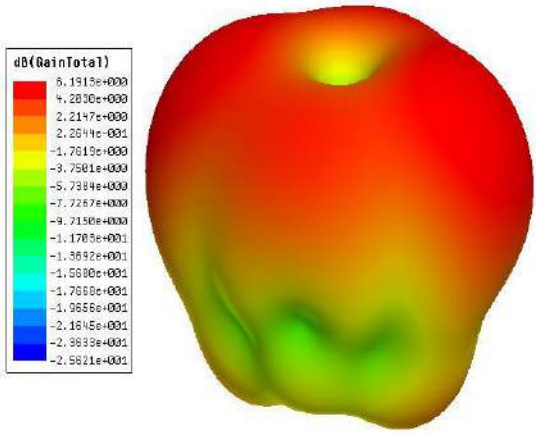

F

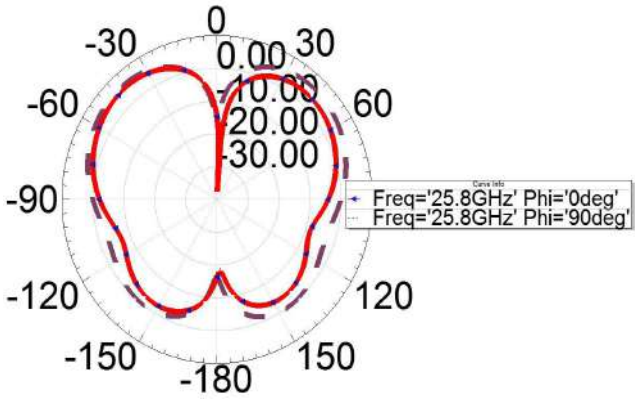

G

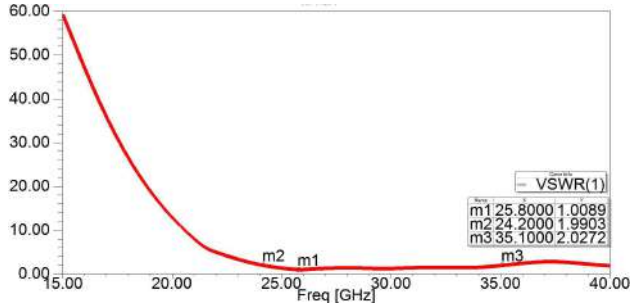

H

) LJXUH 7KH VLPXODWHG UHVXOWV RI DUUD\ HDPHQW D6 E = SDUDPHWU F ' UDGLDWRQ SDWWHUQ G (SODQH DQG + SODQH UDGLDWRQ SDWWHUQV H96: 5

1XPHULFDO5HVXOWV

7ZR NLQGV RI GLIIHUHQWLDO6,: DUUD\V DUH GHVLJHG IRU EHWWU SHUFRUP DQFH LQ WKLV VHFWRQ ,WFDQ EH VHHQ IURP) LJXUH WKDWWKH DQWQQD DUUD\V FRP SRVHG RI WKH DQWQQD HDPHQWSURSRVHG LQWKH SUHYLRXVVHFWRQ WKURXJK WKH QQ-DU DUUDQJHP HQWR \8 DQG \8

D

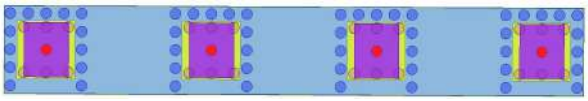

E

) LJXUH 7KH WUXFWXUHV RI WZR GLIIHUHQWDUUD\V D \8 DQWQQD DUUD\ E \8 DQWQQD DUUD\

7KH î DUUD\ KDVDFKLHYHGDJDLQRI G%ZLWKLVRDWRQRI P RUH WKDQ G% DWWKH ZRUNLQJ IUHTXHQF\ DV LOOXWUDWHG LQ) LJXUH D DQG) LJXUH E) LJXUH G DQG) LJXUH H VKRZ WKHUHVXOQ OBV DQG WKH JDLQ RI WKH î DUUD\ 7KH î DUUD\ KDVDJDLQRI G%DQG DQLVRDWRQRI P RUHWKDQ G% ZKLFK P HDQV WKH LQWUHUHQFH EHWZHHQ GLIIHUHQWHDP HQWV LV OBZ 7KH(SODQHDQG + SODQH UDGLDWRQ SDWWHUQV RI WKH î DUUD\ DQG î DUUD\ KDYH JRRG VLPP HWU

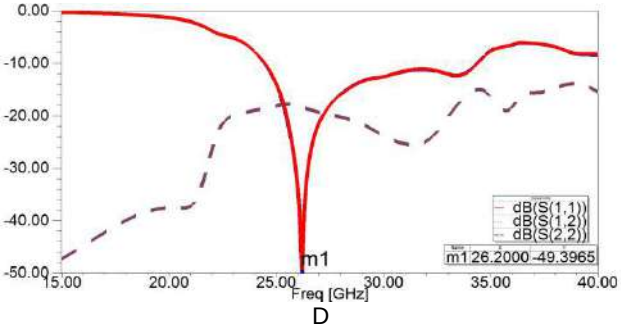

D

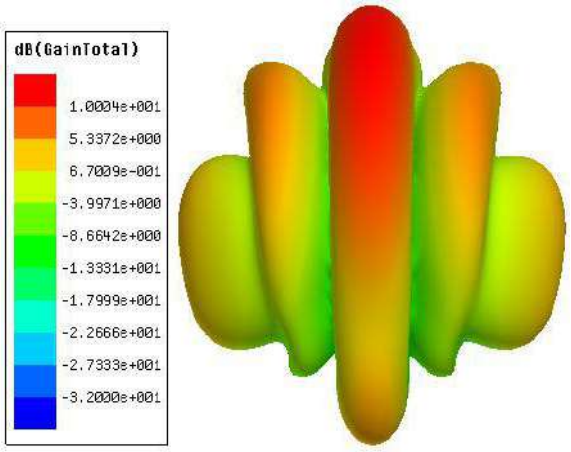

E

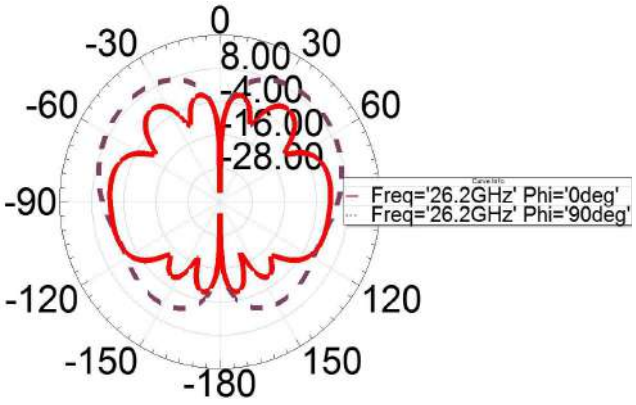

F

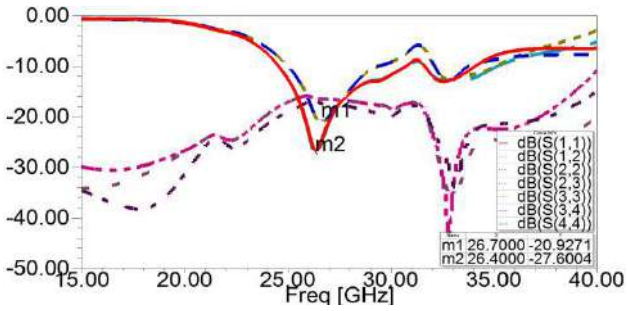

G

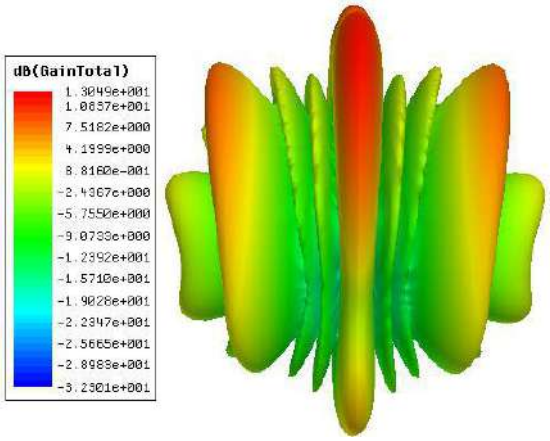

H

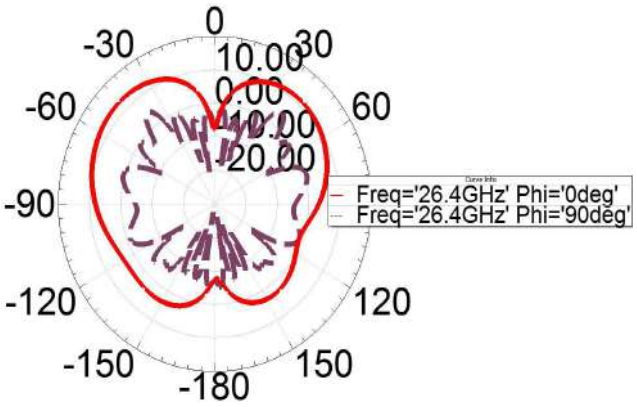

I

) LJXUH 7KH VLP XODWRQ UHVXOWV RI VZR DUUD V D5 HXOLQ GRV RI VZR HOP HQWV DUUD E ' UDGLDWRQ SDWWHUQ F(SDQH DQG + SDQH UDGLDWRQ SDWWHUQV G5 HXOLQ GRV RI IRXU HOP HQWV DUUD H ' UDGLDWRQ SDWWHUQ I(SDQH DQG+ SDQH UDGLDWRQ SDWWHUQV

&RQFOXVLRQV

6HYHUDO DQ6,: P LQLP HWUDQVPQDUUD VZ LWK KLJK JDLQ DQG VPP HWF SDWWHUQV DUH SURSRVHG LQ WKLV DUWFOH 7R LP SURYH WKH SHUFRUP DQFH RI WKH DQWHQQD HOP HQW 6,: WHFKQRORJ\ LV DSSOHG LQ WKH HOP HQWGHLJQ 7KHVLP XODWRQ UHVXOW LQIXWHG WKDW WKH GHVLJQHG DUUD KDV JRRG FKDUDFWHULVWLF $ JDLQ RI G% Z LWK WKH LVRODWRQ RI P RUH WKDQ G% EHWZHHQ GLIIHUHQW HOP HQWV DW WKH ZRUNLQJ IUHTXHQF\ KDV EH HQ REWDLQHG LQ WKH î DQWHQQD DUUD E\ VHWWLQJ WKH DSSURSULDWH DUUDQJHP HQWDQG WKH LQWHUYDOV RI DQWHQQD HOP HQWV 7KH î DQWHQQD DUUD KDV WKH DGYDQWDJHV RI EURDG EDQGZLGWK KLJK JDLQ DQG JRRG V\P P HWU\ RI WKH SDWWHUQ ZKLFK P DGH LWWXLWDEOH IRU * FRP P XQLFDWRQ DSSOLFDWRQV

$ FNQRZ OHGJHP HQWV

7KLV ZRUN LV VXSSRUWHG E\ WKH 1DWRQDO 3URMHFW RI ,QQRYDWLYH (QWHUSUHQHXUVKLS RI 8QLYHUVLGH GXDM 1R

5 H H U HQ F H V

> @0 6KDL $) 0 RDVFK DQG 3 M6P LWK ³ * $ 7XWRULDO 2 YHUYLHZ RI 6WUXFWXUH 7UDQV &KDOPHUV ' HSDUP HQW DQG 3UDFWH´ ,(((-RXUQDO RQ 6HOHFWHG $UHDV LQ &RP P XQLFDWRQV SS

> @: +RQJ . + %HN DQG 6 . R ³0 LQLP HWU: DYH * $QWHQQDV IRU6P DUWSKRQHV 2 YHUYLHZ DQG ([SHULP HQWDO ' HP RQVWUDWRQ´ ,(((7UDQVDFWRQV RQ $QWHQQDV DQG 3URSDJDWRQ

> @0 DUFXV DQG 0 - ³ * $1' ,07)25 $1' %(<21' ´ ,(((: LUHOHVV&RP P XQLFDWRQV

> @) $GEDJGDO DQG $ $\GLQ ³' XDOEDQG P P: DYH * DQWHQQ´

> @< & &KDQJ ³$ 1RYHO' XDO3RODUL]HG : LGHEDQG DQG 0 LQLDWXUL]HG / RZ 3URILOH 0 DJQHWR (OHFWUF ' LSROH

$QMQQD $UD IRUPP: DYH * $SSOFDWRQV´ ,(((
2SHQ-RXUQDOR $QMQQDVDQG3URSDJDWRQ

> @< /L ³6LPXODWRQ DQG H[SHULPHQWRQ6,: VBRVDUD
DQMQQDV´ ,(((0 LFURZDYHDQG: LUHOHVV&RPSRQHQW
/HWWHUV SS

> @0 %RǰL $ *HRUJLDGLV DQG. : X ³5HYLHZ RI
VXEVWUDWH LQWHJUDWHG ZDYHJXLGH FLUFXLWV DQG DQMQQDV´
,HHE LFURZDYHV$QMQQDV 3URSDJDWRQ SS

!"#$%&%'($)*++",*-./*#0#1!./($2$3$4$56/"$%&%'$ $ $ $ $ $ $ $ $ $ $

!"#$%&$'%()'*+,-./0.1*+#'(2#*3,45.(6*"7 1*7".8(+'(*3.(9."$3."*:(-.;+#'((
<$&"+1$*.%(&5(=0*"$83#"*,>708.%(?$8."(>"#1.88+';(

$

@7'+$A+(@#'+83+(

.789:9;9<$=>?$1@>9>7$#A:<7A<$B7C$)<A@7>D>EF($)@<$67:G<?8:9F$>=$)>HF>($5BIB7$
$HH>7:8@:J:I89K8K;09>HF>KBAKLI$

$

)&8*"$1*B(0$:8$C<MB7C<C$9>$?<C;A<$8:E7BD$D>88$C;<$9>$N?<87<D$?<=D<A9:>78$9@B9$>AA;?$>7$9@<$8

8;A@$B8$D<78<8$B7C$OBG<IDB9<8$;8<C$9?<8$B?<$MB9<?:BD$B?<$>7<$>=$9@<$B79:?<=D<A9:>7$9<A@7:R;<8$A@$B9$B?<$M;A@$9@:77<?$9@B7$9@<$OBG<D<78<8$B7C$OBG<8K$,>9@0<F<$89?;A9;?<8($O@:A@$B?<$:7$9@<$=?<R;<7AF$QB7C$Q<9O<<7$?BC:>$OBG<8$B7C$G:8:QD$B?<$>7<$>=$9@<$B79:?<=D<A9:>7$9<A@7:R;<$A>MM>7DF$;8<C$9>$=BQ?:AB9<$M:A?>89?;A9;?<8$=BQ?:AB9<C$;8:7E$DB8<?$I?>A<88:7EK$X<$B?<$C<G<D>I:7E$9<A@7>D>E:<8$B7C$:9$@B8$Q<A>M<$I>88:QD<$9?<8$B?<$M:A?>M<9<?8$8MBDD<?$9@B7$9@$$<$B9@$D7P$OBG<K$.7$9@:8$9BDH($.$O:DD$I?<8<79$9<?B@<?9P$OBG<8K$.7$9@:8$9BDH($.$O:DD$I?<8<79$9<?B@<?9P$Q?>BCQB7C$B79:0?<=D<A9:>7$M>9@0<F<$89?;A9;?<8$=BQ?:AB9<C$QF$=<$*#!$[>79:7;;M($_>D$%($%abZ3%aa%($%&U`K$

'K! +K$)BHBH;$<9$BDK($\c?>BCQB7C($M:DD:M<9<?0OBG<$B79:0?<=D<A9:G<$89?;A9;?<8$>7$8BII@:?<$BQDB9<C$5>;?7BD$>=$!IID:<C$1@F8:A8($_>D$U%4($/>K$%%($%%2'&%($%&%&K$

ZK +K$)BHBH;$ <9$ BDK($ \!$ -B?E<$ d:BM<9<?$,:DD:M<9<?0XBG<$ ->O01B88$ N:D9<?$,BC<$ >=$!D;M:7B$ O:9@$!79:0+<=D<A9:>7$[>B9:7E(^$*I9:A8$"SI?<88($_>D$%`($/>K$%2($ZUaZ20ZUab2($%&%UK$

$

A Simple mm-Wave Chipless Pressure Sensor

S. Rodini[1*], S. Genovesi[1], G. Manara[1], and F. Costa[1]

[1]Department of Information Engineering, University of Pisa, Italy

[*]corresponding author: sandra.rodini@phd.unipi.it

Abstract 3 U H V V X U H L V R I Q U H T X H Q F \ R W H O P R Q L W R U L Q J D S S O L F D W L R Q V W K D W U H T X L U H V D Q D O R J X H G S K \ V L F D O W L O W H V W V X F K D V S U H V V X U H V H Q V R U V W K D W D G D S W W K H S U R S H U W L H V R I W K H V X E V W U D W H 5) , ' W D J L V S U R S R V H G D W L K L F F R P E L Q D W L R Q R I W K H S H U L R G L F V X U I D F H Z L W K W K H V X S H U V W U D W H L V D S S O L H G W K H W D J

Introduction Pressure sensors are required in a large number of applications ranging from biomedical [1], robotics [2], aerospace industries [3]. Pressure sensors can be classified as capacitive, resistive and piezoelectric according to the characteristics of the active layer [4-5]. Many of the pressure sensors released to date are wired, difficult to install, and require active excitation. One way to make fully wireless, battery-free sensors is through RFID technology [6]. In this case it is possible to interface the sensor with the RFID chip in order to have the sensing functionality in the radio frequency system. Another possibility is to create chipless RFID sensors [7]. In chipless RFID technology the tag has no electronic components and requires no power source. In this case the sensor is based solely on the frequency response of a resonator. Hence, a chipless pressure sensor composed of a resonator working at mm-wave frequencies is proposed. The resonator operates in conjunction with a dielectric superstrate and pressure is applied to the ground of the resonator. The application of pressure causes a frequency shift of the resonance peak.

Pressure sensor design !"#$%#&'()$*+$,"#$-.*-*&#%$-.#&&/.#$&#)&*.$'&$&"*0)$')$1'(/.#$2345$6"#$&#)&*.$'&$ 74&#%$*)$4$8$9:#$;"'-<#&&$,4(6$#$,4($'&$*8-*&#%$7=$,".##$%'-*<#&$2',"$%'++#.#),$<#)(,'$&#-4.4,#%$ +.*8$4$(.*/)%$-<4)#$7$4$,"')$?*(#.$@AA@&/$7&,.4,#$3%B2CD56!"#$/)',$#<<$*+$,"#$-#.'*%';$&/.+4;# 31.#E/#);=$F#<#;,':#$F/.+4;#$1F$&$"*0)$')$1'(/.# 2375"#$-#.'*%';',=G*+$,"#$/)',$;#<<$'&$#E/4<$$$@6D 88 $H)$*.%#.$,*$7#$47<#$,*$/&#$,"#$,4($4&4-.#&&/.#$&#)&*.$4$&/-#.&,.4,#$'&$4--<'#%$,*$,"#$4#$1F$6 ');.#4&')($-.#&&/.#$'&$4--<'#%$,*$,"#$(.*/)%$-<4)#$6#$'%#4$'&$,*-<4;#$4$;*),4')#.$*)$,*-$*+$,"#$,4($4)%$+'<<$,"4,$;*),4')#.$0',"$04,#.6$I&$,"#$:*</8#$*+$04,#.$');.#4&#&>$,"#$-.#&&/.#$#J#.,#%$*)$,"#$,4($0'<<$');$#4&#6 !"#$4--<'#%$-.#&&/.#$K4<;/<4,#%$&$KB($MI>$0#.#$($'&$,"#4.,"(.4:',=$4;;#<#.4,')>$L $&$,"#$4&&$+$,"#$ 04,#.$')$,"#$;*),4')#.$4)%I'&$,"#$4.#$"#.#$-.#&&/.#$'&$4--<'#%$6#$,4($'&$;*8-*&#%$*+$2AJ2A$;#<<&$4)%$,"#.#+*.#$,"#$4.#4$0'<<$7#$C6$3@6D8"#$-.*-*&#%$&#)&*.$;4)$7#$'),#..*(4,#%$0',"$,0*$N?CO$ &,4)%4.%$(4')$1)$4),#))4&$*-#.4,')($')$,"#$+.#E/#);=$.4)(#$*+$'),#.#&,6$

Numerical results H)$*.%#.$,*$#:4</4,#$,"#$+#4&'7'<',=$*+$,"#$-.*-*&#%$&#)&*.>$)/8#.';4<$#<#;,.*84()#,';$ &'8/<4,'*)&$4.#$+'.&,$-#.+*.8#%$8'#$)/8#.';4<$&'8/<4,'*)$"4&$7##)$;4..'#%$*/,$7=$/&')($,"#$PF!$F,/%'*$ F/',#$F*+,04.#6$!"#$&'8/<4,'*)$04&$-#.+*.8#%$/&')($-#.'*%';$7*/)%4.=$;*)%','*)&$H)$.%#.$,*$#J-<*',$,"#$ 0*.Q')($-.');'-<#$*+$,"#$-.*-*&#%$&#)&*. $&#:#.4<$;4&#&$4.#$;*)&'%#&&"*0)$')$1'(/.#62 3;5$"#$,4($)<=>$,"#$,4($0',"$,"#$&/-#.&,.4,#$4)%$+')4<<=$,"#$,4($0',"#$&/-#.&,.4,#$+'<<)($,"#$&-4;#$7#,0##)$%'-*<#&$

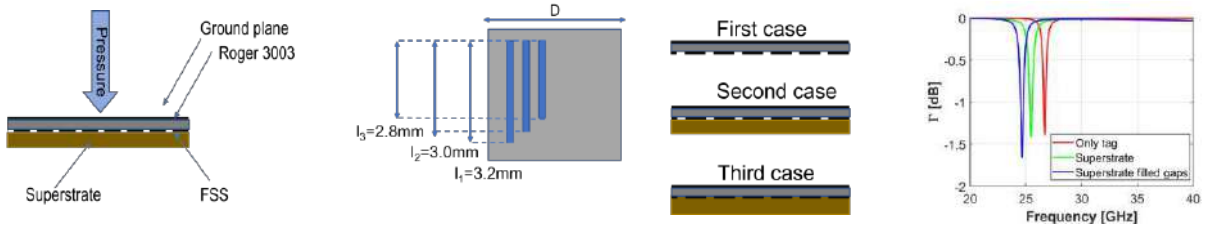

(a) (b) (c) (d)

Conclusions

Acknowledgements

Work partially supported by the Italian Ministry of Education and Research (MIUR) in the framework of both the FoReLab project and the Crosslab project (Departments of Excellence).

References

1. ?*.'U>$K6>$1.4UV*>$W
2. I<84&&.'>$I6$L6>$N4)$^4&4)>$
3. T')>$ T6>$ Z$ b/)>$ N6$ 32]]O>$ L4.,"56$ LcLF$ -.#&&/.#$ &#)&
4. ?/,">$F6$?6$I6>$1#'(>$d6$?6>$!.4)>$^6>ZX4*>$_6$3CACA56$L';.*#)(')##.')($-.#&&/.#$&#)&*.$4;,':#$<4=#.&$+*.$'8-
5. Y4:#%>$b6>$L4)&**.>$L6>$Z$F"4">$H6$I6$3CA2]56I.#:'#0$*+$-.');'-<#&$*+$LcLF$-.#&&/.#$&#)&')($0',"$',&$4#.*&-
6. X.')Q#.>$g6>$Z$_*/("'>$?6$3CAC@56$!/)47<#$P"'-<#&&$?1
7. P*&,4>$16>$`#)*:#&'>$F6>$X*.(#&#>$L6>$L';"#<>$I6>$G';4)%'4>16I6>Z

Improved Foreign Object Detection Method for Wireless Charging using Balanced and Synchronous Coils

Sehwan Choi[1*], Seungguk Nam[1], Churlseung Lee[1], and Youngkee Ryu[2]

[1]Korea Electronics Technology Institute, Korea
[2]Chungnam Display R&D Cluster Center, Sunmoon University, Korea
[*]corresponding author: shchoi@keti.re.kr

Abstract: In this paper, we propose a new foreign object detection (FOD) structure in which a synchronous coil is added to the balanced coils. The location of the foreign object can be identified by comparing the phase of the added coil with that of the two balanced coils, and using the signal processing method known as the sample and hold method. This paper presents the configuration of the FOD system and the results of the detection method.

The proposed FOD (Foreign Object Detection) method in this paper utilizes a synchronous coil added to the center of the detecting coil to obtain a transmission signal, which allows for the location of a foreign object to be determined using phase detection. The balanced coil method has been used previously, but it has limitations such as low detection rates and an inability to locate foreign objects in certain areas. The proposed method is designed to address these limitations and is applied to mobile phone charging. The location of foreign objects can be identified through simple signal processing.

The FOD structure proposed in this paper is composed of a transmitting coil and a detecting coil. The detecting coil includes two balanced coils and a synchronous coil in the center. The balanced coil generates an electromagnetic field, and when a metal object is placed in the area where the balanced coil is located, the electromagnetic field becomes unbalanced, and current begins to flow. The synchronous coil receives the transmission signal, which is synchronized with the charging signal sent by the transmitting coil, and converts it into a digital signal. This signal is then supplied to the microprocessor, where sample and hold processing is used to create a pulse. The output signal of this method changes its output level and sign depending on the location of the foreign object. The method can determine the presence or absence of a metal object and its location based on the signal change of V^1_{out} and V^2_{out}.

To verify the proposed structure, analog circuits such as filters, amplifiers, and various signal processing functions are required. By using Cypress's PSOC5 microprocessor, it can be configured relatively simply. This processor has built-in high-performance programmable analog blocks that can be configured to perform various signal processing functions. The proposed FOD method can be used to improve the safety and convenience of mobile phone charging by detecting foreign objects and preventing potential hazards.

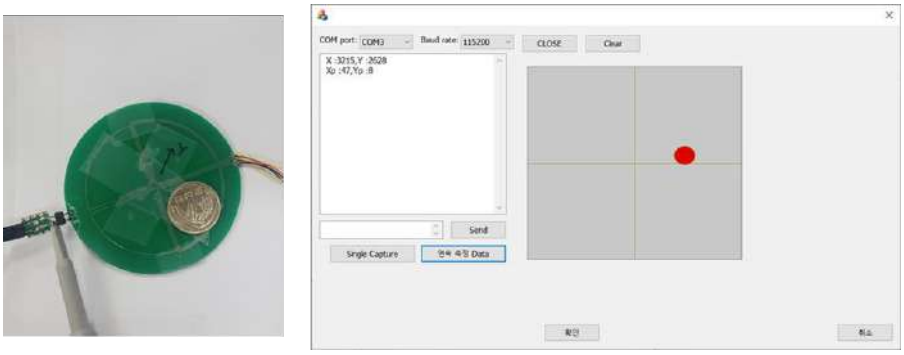

Figure 1. Experimental setup and detection result.

Acknowledgements

This work was supported by ICT R&D program of MSIP/IITP. [2021-0-00259, Development of a Fast Wireless Charging System for Portable Terminals with Improved Heat Dissipation and Shielding Performance]

References

1. L. Lan et al., "Foreign Object Detection for Wireless Power Transfer," 2018 2nd URSI Atlantic Radio Science Meeting (AT-RASC), 2018, pp. 1-2, doi: 10.23919/URSI-AT-RASC.2018.8471551.
2. < = K D Q J H W D O ³ $ U H Y L H Z R I I R U H L J Q R E M H F W W H W H F W L R Q D Q \ V L V R I U W D Volume 1, August 2019.
3. L. Xiang, Z. Zhu, J. Tian and Y. Tian, "Foreign Object Detection in a Wireless Power Transfer System Using Symmetrical Coil Sets," in IEEE Access, vol. 7, pp. 44624-44631, 2019, doi: 10.1109/ACCESS.2019.2908866.
4. https://www.philips.com/a-w/about/innovation/ips/standardization.html

Analytical, Computational and numerical techniques

!"#$%&%'($)*++",*-./*#0#1!./($2$3$4$56/"$%&%' $$$$$$$$$$$

!"#$%&'()*"%*%+%,"'+-.)*"'+%'/-."0-("'/%"),)*1#2#"-0"&(-##%.
32,)(1"4()'2,4#

56()(." 5(),%' 78"),. " 9-02":.%% 7

7 $89:;<=9$ @A;<BC$D:;<E8; ($@A;<BC$D:;<E8; $/1 ($@/+# ($

.8=>9>$D1F=GFA($H0I'$@A&$BC$D:;<<F8($H<F8G;

K GC<<;=LC8J98E$FD>MC<N$E;<F<JOE<F8;>PDGFOQ<

!"#$%&'$))!$=L;G><FA$;A;B;8>$BCJFA$B;>MCJ$>M;$C<9E98FA9>RCQSM9GM$GCB;=$Q<CB$>M;$D=;$C
TD9A>$S9>M$BCJ9Q9;J$-;E;8J<;$LCAR8CB9FA=$9=$J;:;ACL;J98>M;$E;8;<FA$GF=;CQT98F<R$G<C=
FJ:F8>FE;CQ>M;$=L;G><FA$;A;B;8#$B;>MC$$MF>$9>$GCBT98;=$>M;$E;CB;><9G$QA;W9T9A9>R$CQ$
S9>M$M9EM$L<;G9=9C8CQ=L;G><FA$B;>MCJ$OA$D=$;<F>FJ$89>M$E<F>98E=$SMC=;$LF>>;<8=$F<;$8
S9>M$>M;$TCD8JF<9;=CQ>M;$;A;B;8>F<R$G;AAO

+;G;8>ARB>FBF>;<9F$A=8JB$>F=D<QF$CM=F:;$F<CD=;J$9BB;8=;$98>;<;=>$T;GFD=;$>M;R$L<C:9J;$988C:F
=CAD>9C8=$>C$GC8><CA$;A;G><CBFE8;>9G$SF:;=O$X;$GF8$=;;$98$>M;B$LF<>9GDAF<$L;<9CJ9G$=><DG>
GAF==CQE<F>98E=O$)M;<;QC<;($>M;$8DB;<9GFA$B;>MCJ=$J;:;ACL;J$>C$GFAGDAF>;$>M;$;A;G><CBFE8;>9
98$BF8R$GF><;F8=LC=F$TA2$>FBF>;<9F$A=8JB$>F=D<QFCHC<$><F8=AF>9C8$98:F<9F8>$=><DG>D<;=($BCJFA
F8J$BCJ;$BF>GM98E$>;GM89YD;=$F<;$:;<R$98>;<;=>98E98>$M;$FWFQF8G;
/DB;<9GFA$BCJFA$B;>MCJ=$J9QQ;<$98$>M;$GMC9G;CQ;WLF8=9C8$F8J$>;=>$QD8G>9C8=O$*8;$GF8$
QD8G>9C8=$C<$=DT0JCBF98$QD8G>9C8=$FGGC<J98E$>C$SM;>M;<$>M;R$F<;$J;Q98;J$C8$>M;$SMCA;$JCBF
9>O$HC<$L;<9CJ9G$L<CTA;B=($>M;$BC=>$LCLDAF<$B;>MCJ$9=$G;<>F98AR$>M;$S;AA0[8CS$$98D<9;<$,CJ
SM9GM$;WLF8=9C8$F8J$>;=>$QD8G>9C8=$F<;$L=;DJC$L;<9CJ9G$QD8G>9C8=O$*8$>M;$GC8><F<R($D=9
S9>M98$;FGM$JCBF98$>MF>$GC8=>9>D>;$>M;$=><DG>D<;$FAACS=$>C$;WL<;==$<9EC<CD=AR$>M;$J9Q
J;>;<B98;$>M;$;9E;8:FAD;$L<CTA;B$F8J$>MD=$A;FJ=$>C$;WLC8;8>9FA$GC8:;<E;8G;$QC<$>M;$;9E;8:FAD;=$
)M;$LCAR8CB9FA$BCJFA$B;>MCJ$\%]$9=$C8;$=DGM$B;>MCJO$.>$SF=$>;$9=$J98$$Q$F8$D]$O;<QC<B$FA
C>M;<$8DB;<9GFA$BCJFA$B;>MCJ=$QC<$J9;A;G><9G$B;>FAA9G$=><DG>D<;=O$)M;$F9B$CQ$>M;$L<;=;8>$
FTC:;$LCAR8CB9FA$BCJFA$B;>MCJ$98$>;<B=$CQ$F$$#L;G><#A;$"V8$;8>$,;>MCJ$U

!"#"$"%&"'

7O ()*+$+,-.(/0/.+%1.2/3/.0+45)$1-.678##$+&98)%.+%+54'8'.)#.18"5"&9$8&.':$#+&";$"58"#.<$+98%<'-6.=/.>?9/.@)&/
A,/.A-.B)5/.CD-.EFGH! EFID-.EIGD/

%O()$#-.!/J/-.6KL?)%"%98+554.&)%M"$<"%9.+%1.%:,"$8&+554."##8&8"%9.')5:98)%.)#.(+LN"55O'."P:+98)%'.#)$.5+,"55+$
<$+98%<'-6.=/.>?9/.A,/.A-..B)5/.ED-.EQRF;EQHS-.EIIH/

'O K1""-.3/.6()1+5.,"9*)1.T+'"1.)%.':T;"'&98)%+5.0"<"%T+:"$.?)54%),8+5."L?+%'8)%.#)$.5+,"55+$.<$+98%<-6.=/
>?9/.@)&/.A,.A-.B)5/.DG-.DQQS;DQEF-.DQEE/

^O !+%1$8+,8*+U+-.(/J/-.0/.0$+%"9-.3/K1"".+%1.3/.!+%8$8*+$8%)'4-.6V)54%),8+5.,)1+5.+%+54'8'.)#.5+,"55+$
18##$+&98)%.<$+98%<'.8%.&)%8&+5.,):%98%<-6.=/.>?9/.@)&/.A,/.A-.B)5/.FF-.ESCI;ESGS-.DQES/

Exploring the Thermally Activated Delayed Fluorescence Performance for a Phenothiazine Derivative via TD-DFT

L. Cascino[1,2*], A. Maggiore[2*], I. Rivalta[3,4], G. P. Suranna[5], R. Grisorio[5], D. Conelli[5], V. Maiorano[2*] DQG 6 ' ¶$JRVWLQR

[1] 0DWKHPDWLFV DQG 3K\VLFV *UDGXDWH 6FKRRO ' ¶$SSOLFD7HFQRORJLH 1DQRWHFQRORJLH\ [3] RI 6DOHQWR /HFFH

[2]Institute of Nanotechnology, National Research Council (CNR-NANOTEC), Lecce 73100

[3] 'LSDUWLPHQWR GL &KLPLFD ,QGXVWULDOH [3]7RUR 0RQWDQDUL´ 8QL

[4]ENSL, CNRS, Laboratoire de Chimie UMR 5182, 69364 Lyon France

', &$7(&KRQWHFF GL %DUL %DUL ,WDO\

[6]Center for Biomolecular Nanotechnologies, Istituto Italiano di Tecnologia, Arnesano (LE) 73010

[*]corresponding author: lucia.cascino@unisalento.it

Abstract: To design new materials for 7KHUPDOO\ $FWLYDWHG 7LPH) DLWXUH HFUHHVFHQFH DFKLHYH D GHWDLOHG XQGHUVWDQGLQJ RI WKH UHODWLRQVKLS EHWZHHQ WKH PROHFXODU VWUXFWXUH DQG WKH SURSHUWLHV RI WKH VHQVLWL]HU PROHFXOH LV HVVHQWLDO 7KHUHIRUH ZH UHSRUW D FRPSXWDWLRQDO DQDO\VLV EDVHG RQ Time Dependent Density Functional Theory (TD-DFT) to investigate D SKHQRWKLD]LQH GHULYDWLYH 7$') RQO\ ZLWK D VLQJOH GRQRU DFFHSWRU JHRPHWU\

In classical fluorescent systems, especially at room temperature, the triplet electronic states can decay only through non-radiative pathways by vibration or phonon interaction, while radiative decay is forbidden. On the other hand, in phosphorescence metal organic complexes featuring heavy metals, the strong spin-orbit coupling enables a radiative emission from triplet excited states. In order to overcome the drawbacks of the latter (toxicity and high costs), new full organic systems that recovering triplet excitation through a delayed fluorescence mechanism have been largely investigated. Such process, namely the TADF, [1] occurs because of fast reverse intersystem crossing (rISC), which up convert triplet to singlet by thermal energy. Therefore, in order to achieve good TADF performances, besides a large transition dipole moment between excited and the ground singlet states, it is of vital importance to ensure a small enough singlet-triplet energy gap (~ 0.1 eV) [2]. In order to reduce this gap, the exchange energy (J), which is inversely proportional to the spatial separation between the highest occupied molecular orbital (HOMO) and the lowest unoccupied molecular orbital (LUMO), has to be minimized (2J = ΔE). It has been demonstrated that Donor-Acceptor (D-A) molecules presenting strong charge transfer states (CT) are among the most efficient systems to reduce the exchange coupling J.

In this work, we investigated the TADF performance of a phenothiazine derivative consisting of a strong donor (phenothiazine) and acceptor (perylene monoimide) component, adopting a quasi-equatorial D-A conformation [3] and we analyse the possibility for this molecule to activate TADF by forming aggregated electronic states (Fig. 1a). All simulations were performed by using the ORCA 5.0 package. The geometry of the ground state was optimized in the gas phase by employing the B3LYP functionals and a TZVP basis set with the def2/J auxiliary basis set for the RIJCOSX approximation to the Coulomb integrals [4]. Electronic and optical properties were calculated for the monomer in the quasi-equatorial conformation and in the non-polar cyclohexane solvent. After characterization of

the monomer properties in terms of relative positions of the first singlet (S_1) and triplet (T_3) charge transfer states, we considered three different dimer geometries, analysing their structural and electronic properties as a function of the inter-monomer separation distance (see Fig.

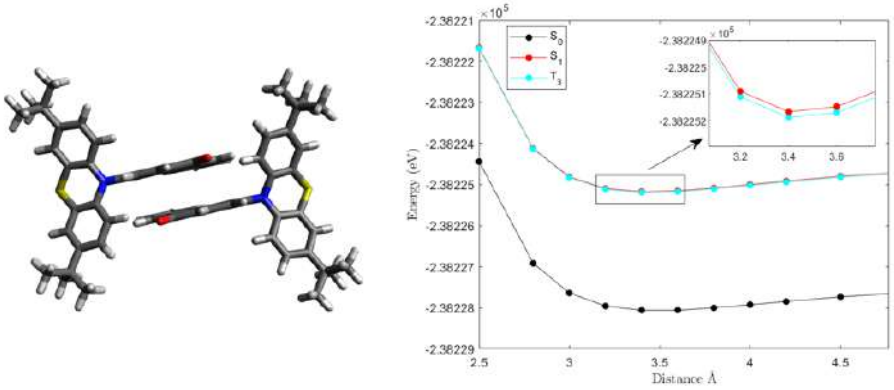

Fig. 1 (a) Sketch of a dimer of phenothiazine G H U L Y H G I U R P W K H H T X L O L E U L X P J H R P H W U L H V R E W D L Q H G Energies of S_0, S_1 and T_3 states vs separation distance between molecules (systems sketched in panel a) for the monomers relaxed to their ground state geometry

An important reconstruction in both S_1 and T_3 states was observed, resembling the typical one of dimer electronic state with one monomer in the ground state (S_0) geometry and the other one in the excited state geometry, i.e. S_1 and T_3 geometries, respectively. Moreover, fingerprints of aggregate formation were also tracked down in the nature of Natural Transition Orbitals of S_1. With respect to monomer, we registered a promising change in the relative position of the electronic states of interest for TADF. Moreover, coherently with experimental PL spectrum, we observed a red-shift of the emission peak. In addition, to what is well known about the effect of environment conditions (e.g. polarity of solvent affecting the TADF performances), this study attests a new path to activate TADF through the formation of a new aggregate electronic state. This open new perspective toward an on-demand control of the TADF response in molecules of interest for optoelectronics and nanomedicine.

7 K L V Z R U N Z D V S D U W L D O O \ I L Q D Q F H G E \ W K H 5 (& 2 1 (3 5 2 - (& 7 (8 5 2 3 ($ 8 6 5 0 H F and intelligent fibers and fabrics for TECnical clothing (CUP% &

References

1. 8 R \ D P D + . * R X V K L . 6 K L] X + 1 R P X U D D Q G & - Gating Kinetics from G H O D \ H G I O X R U H V F H Q F H ´ 1 D Vol. 8, 2012. 9 R O 1 R
2. Lv, L., K. Yuan, T. Zhao, and ' D L , Q W U L Q V L F $ Q D O \ V L V R I 7 K H U P D O O \ $ F W L Y D W H (I) Complex Based on the Path Integral Approach: Origin of the Effective Spin 2 U E L W & R X S O L Q J (I I H F W ´ - Vol. 6695, 2022. 9 R O 1 R
3. = K D Q J - 0 = K X < / X ; = K D Q J 6 ; L D R + Responsive Phenothiazine Derivatives with Triplet-Related Dual Emission and High & R Q W U D V W 0 H F K D Q R F K U R P L V P * X L G H G E \ 3 R Chem, Vol. 28, No. 29, 2022.
4. 1 H H V H) 7 K H 2 5 & $ Software, Vol. 2, Issue 1, 2012.

0RGHO7HFKQLTXH IRU)LQLWH /HQJWK 8QLIRUP-HWUL IRU 00:)LOWHUV

$ 'LYVDO'DUDQKGHNDU 6\DKNDO
5) 0LFURZDYH 5HVHDUFK /DE 6FKRRO RI &RPSXWHU 6FLHQFH D
8QLYHUVLW\ RI (VVH[8QLWHG .LQJGRP
FRUUHVSRQGLQJ DXWKRU DGLYVD#HVVH[DF XN

Abstract: A technique to analyze MMW microstrip tunable filters with finite number of unit cells is developed It uses eigen decomposition for factorization of the unit cell transmission matrix to obtain constituent parts and then canonicalize the periodic structure with N unit cells. Based on this concept MATLAB scripts have been developed to determine the dimensions of finite length MMW microstrip periodic structure filter. The results from ADS simulations uphold the validity of the technique.

With the global demands for high data rate/wider bandwidth networks, most telecommunication service providers are considering wireless MMW technology for mission-critical capabilities including superior speeds and low latencies. Due to their small sizes, development of MMW filters essential for the network transceivers are cumbersome and one promising approach is to use microstrip line periodic structures with finite number of unit cells. As such, the usual theory of periodic structures assuming infinite number of repeated cells is inaccurate In this paper an alternative approach for fast analysis of these structures is proposed.

Periodic structures are modeled based on their unit cells as shown in Fig. 1. In this technique, the reciprocal

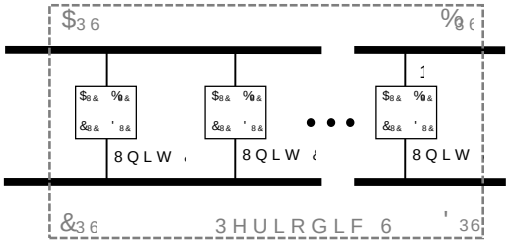

)LJ 7UDQVPLVVLRQ

transmission matrix of a unit cell is factorized into its constituent parts (i.e. canonical and eigenvectors matrix)

$$\begin{bmatrix} A & B \\ C & D \end{bmatrix} = \begin{bmatrix} A & B \\ C & D \end{bmatrix} \begin{bmatrix} \lambda_1 & 0 \\ 0 & \lambda_2 \end{bmatrix} \begin{bmatrix} A & B \\ C & D \end{bmatrix}^{-1} \quad (1)$$

Therefore, the transmission matrix of the unit cell can be expressed as a diagonal matrix. This guarantees a simpler and faster determination of the overall transmission matrix of a periodic structure with finite number of cells. The set of eigen value (EV) solutions (i.e. the spectrum of the reciprocal transmission matrix) is calculated from characteristic eigenvalue equation:

$$\det \begin{bmatrix} A-\lambda & B \\ C & D-\lambda \end{bmatrix} = 0 \quad (2)$$

Therefore, the EV and Canonical matrices can be obtained

$$\begin{bmatrix} A & B \\ C & D \end{bmatrix} = \begin{bmatrix} \frac{A-D+\sqrt{(A+D)^2-4}}{2C} & \frac{A-D-\sqrt{(A+D)^2-4}}{2C} \\ 1 & 1 \end{bmatrix} \quad (3)$$

$$\begin{bmatrix} A & B \\ C & D \end{bmatrix}^{-1} = \begin{bmatrix} \frac{A+D+\sqrt{(A+D)^2-4}}{2} & 0 \\ 0 & \frac{A+D-\sqrt{(A+D)^2-4}}{2} \end{bmatrix} \quad (4)$$

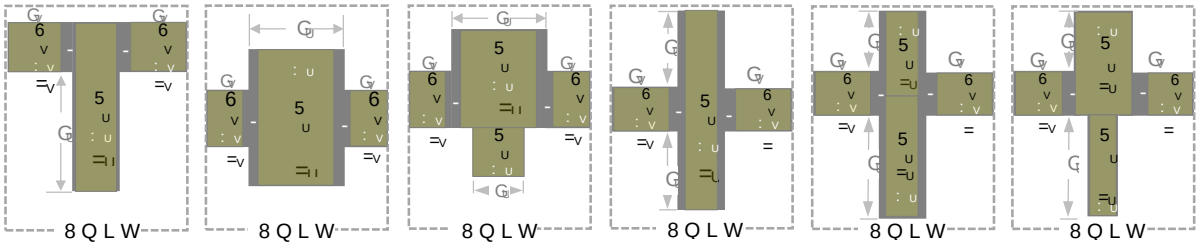

) L J ' L I I H U H Q W 8 V H G 3 R Q E W R F W R U L Q 6

Hence, for N unit cells connected in cascade, the overall transmission matrix (where PS represents the overall transmission matrix) will be obtained as follows

$$\begin{bmatrix} A & B \\ C & D \end{bmatrix} = \begin{bmatrix} A & B \\ C & D \end{bmatrix}_1 \times \begin{bmatrix} A & B \\ C & D \end{bmatrix}_2 \times \cdots \times \begin{bmatrix} A & B \\ C & D \end{bmatrix}_N \quad (5)$$

Based on the method presented, different unit cells made of microstrip structures for periodic filters are analyzed. MATLAB scripts are written to design a filter based on optimization of the periodic structure transmission matrix. The program receives basic inputs such as desired frequency, bandwidth, input impedance, number of unit cells and the microstrip lines parameters (i.e. V X E V W U D W H S H U P L W W L Y L W \ W K L F N Q H then by running different loops, it determines the physical dimensions of the microstrip unit cell. Several filters are designed using the MATLAB script. Designed filters are also simulated by ADS which verifies the validity and accuracy of the design method presented here

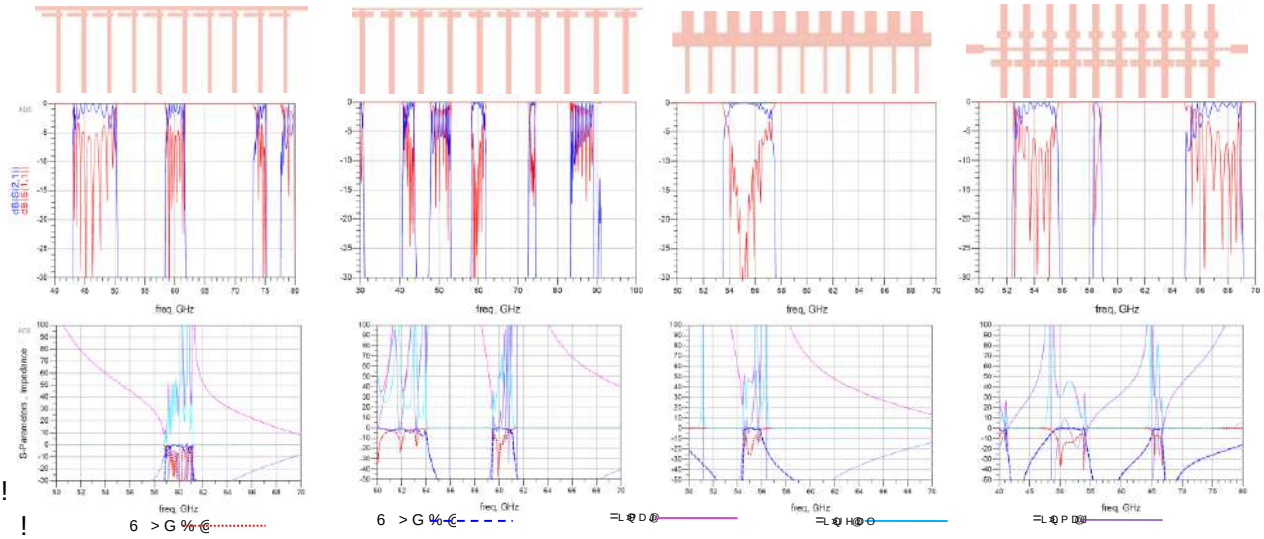

) L J ' H V L J Q H G P L F U R V W U L S U H V W U X F W X U H D U D P H W H U V D Q G

References

1. 6 %DÜVNDO < 6 .LP ³$ %&' 0DWULFHV DV 6LPLODULW\ 7UDQVIRUPDWLRQV Journal of the Optical Society of America A ! October 2009
2. $ - 3UDGR 6 .XUQDZD ³7KH -ones Matrix Approach for Power Transmission Lines and Its Application to Electricity Generation and Transmission Control´ 6 HAYHQWK &RQJUHVV RI Electricity Generation and Transmission and AGTEE 2007At: Vi–a del Mar, Chile, October 2007
3. $ 0RUFKHG % *XVWDYVHQ DQG 1. Accurate Calculation of Electromagnetic Transients on Overhead Lines and Underground Cables´ ,(((7UDQVDFWLRQV RQ 3RZHU 'HOLYHU\ YROXPH 1R -XO\ 1998
4. Hammerstad, E. and Jensen, 0., "Accurate Models for Microstrip Computer-Aided Design", 1980 IEEE MTT-S International Microwave Symposium Digest, May 1980, pp. 407-409.

A hybrid wavelet-based method to model the electromagnetic propagation above a polluted sea surface

Thomas Bonnafont[1]*, Ali Khenchaf[1]

[1]Lab-STICC, UMR CNRS 6285, ENSTA Bretagne, 29806 Brest, France
*corresponding author, E-mail: thomas.bonnafont@ensta-bretagne.fr

Abstract

Electromagnetic propagation above a rough polluted sea surface differs from one above a clean sea. Indeed, a damp effect on the waves appears. This can be used to detect a pollutant leakage. In this article, we model the propagation of electromagnetic waves above a polluted sea using a fast wavelet-based method and a two-scale model. Numerical simulations in S-band are provided.

1. Introduction

In this paper, we are interested in the tropospheric long-range propagation in the maritime environment. In this context, local phenomena such as sea waves, or the presence of a pollutant on the sea have an impact on the measured Þeld. Indeed, waves introduce diffraction for example, while the presence of oil introduces a damping effect [1]. This latter can be used to detect pollutant leakage on the sea [2, 3].

In this framework, a large part of the literature has focused on computing the radar cross section (RCS) of the sea with and without pollutant [4, 5, 6, 7, 3]. Indeed, these methods are appropriate here, since the sea spectrum (and its modiÞed version for an oily sea [1, 6]) can be conveniently introduced in the integral equation [4, 3]. Results have been obtained showing the difference between the RCS of a clean sea and a polluted sea, even leading to the detection of oil leakage from SAR images [2, 3].

Less work [8, 9] has focused on modeling the long-range propagation above a polluted sea surface. In particular, the sea geometry has been assumed to be ßat (with the roughness accounted through Ament coefÞcient [10]), and the oil to cover the whole domain. Nevertheless, the obtained results have highlighted the effect of the oil on the propagated waves and show that detection is feasible.

In this paper, we develop a fast hybrid approach for computing the propagation over a polluted sea surface. The approach is based on the one developed in [11, 12] for propagation above a clean sea, where the sea spectrum [13] is used to generate random surfaces and a roughness coefÞcient. Besides, the use of the parabolic wave equation model allows taking into account the refraction [14] (due to tropospheric ducts for example), differing from the other proposed works [8, 2, 3]. Furthermore, we show using a Principal Component Analysis (PCA) that a polluted sea can be detected from a clean one using measurements at a given vertical.

The remainder of this paper is organized as follows. Section 2 focuses on the modelization strategy. First, the parabolic wave equation is recalled. After that, both the clean and polluted sea spectra are introduced. Section 3 introduces the computational method. This latter is based on a hybrid approach to introduce the effect of the maritime environment on propagation. Section 4 shows numerical tests performed in the S-band. Besides, a PCA analysis is provided. Finally, Section 5 concludes the paper and gives some perspectives for future works.

2. The model

In the following work, a $\exp(j\omega t)$ time dependence is assumed, where j is the imaginary unit and $\omega = 2\pi f$ is the angular frequency. We also denote by n the refractive index, and this latter is assumed to be slowly varying in the propagation direction. Furthermore, from now on the Cartesian (x, y) coordinate system is used.

2.1. The parabolic wave equation

As a reminder, we want to compute the long-range propagation above a clean or polluted sea surface. A suitable model in this context is the parabolic wave equation [14] (PWE). Indeed, by only accounting for forward propagation, it allows wide steps in the propagation direction, leading to more computationally efÞcient methods. Besides, the effect of the refraction, the relief, and the terrain can be incorporated. Note that the PWE is only valid in a paraxial cone. Thus for better accuracy, we use its wide-angle PWE version here. This latter is given by

$$\frac{\partial u}{\partial x} = -jk_0\left(\sqrt{1+\frac{1}{k_0^2}\frac{\partial^2}{\partial z^2}}-1\right)u - jk_0(n-1)u, \quad (1)$$

with u the reduced Þeld [14], x the propagation direction, and k_0 the wave number. If the backward propagation is of interest, one can use the two-way PWE [15, 12].

2.2. Modeling the waves: the sea spectrum

To model the sea surface along the propagation, a common way is to use a sea spectrum, such as the Elfouhaily one [13], which is used from here on. This latter gives a statistical representation of the sea geometry with respect

to the wind speed. The spectrum S is then expressed as

$$S(K) = \frac{1}{K^3}(S_l + S_h), \qquad (2)$$

where S_l and S_h correspond to the long and short wave curvature spectrums, respectively. Note that those parameters mostly depend on the wind speed at 10 m (denoted by U_{10}) above the sea, and the interested reader is referred to [13] for more details. An example of the computed sea spectrums for different wind-speed is given in Figure 1.

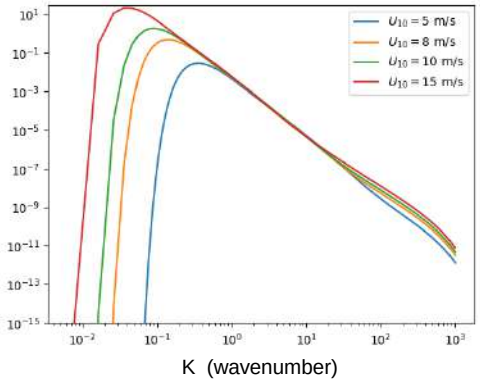

Figure 1: Computed sea spectrums [13] for different wind speeds $U_{10} \in \{5, 8, 10, 15\}$ m/s in a Log/Log scale.

Note that the wind speed has a great influence on the low wavenumber K (i.e. the large scale), thus higher waves are expected.

From this spectrum, one can derive a stochastic process to obtain sea surfaces. Indeed, S describes the statistical properties of the sea surface. The idea is to create a random surface $z_r(x)$, normally distributed with a zero-mean, $\mu = 0$, and centered ($\sigma^2 = 1$). To add the correlation with the sea surface, then z_r is convoluted to the inverse Fourier transform of $\sqrt{S}$, such that

$$z(x) = \mathcal{F}^{-1}\left(\sqrt{S}\,\mathcal{F}(z_r(x))\right), \qquad (3)$$

with $\mathcal{F}$ the Fourier transform and z the generated sea surface. Some examples of realizations are given in Figure 2 for different wind speeds.

2.3. Accounting for the pollutant: the dumped spectrum

In this section, we introduce how to model a polluted sea surface. First of all, one can consider, depending on the wind speed U_{10}, whether the oil is soluble or not, meaning that we have an emulsion or not. Here, we focus on the insoluble case, i.e. $U_{10} \geq 8 - 10$ m/s [8], where the damping model [1] can be used.

This latter is based on the following equation

$$S_{po} = S_{clean}\left(1 - F + \frac{F}{y}\right), \qquad (4)$$

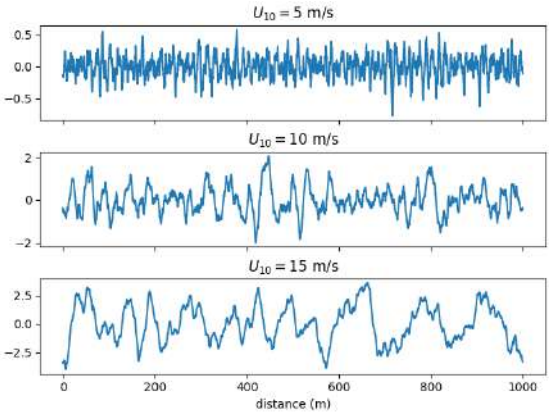

Figure 2: Generated random sea surfaces for different wind speeds $U_{10} \in \{5, 10, 15\}$ m/s using (3).

where S_{clean} corresponds to the clean sea spectrum (see Section 2.2), F to the fraction of oil covered surface, y to a damping ratio and S_{po} to the polluted sea spectrum. Here, we consider only the case where the sea is fully covered, i.e. $F = 1$. In this equation, y introduces the attenuation due to the oil film and depends on the pollutant parameters [4]. In Figure 3, an example of the clean sea spectrum and its polluted counterpart are plotted.

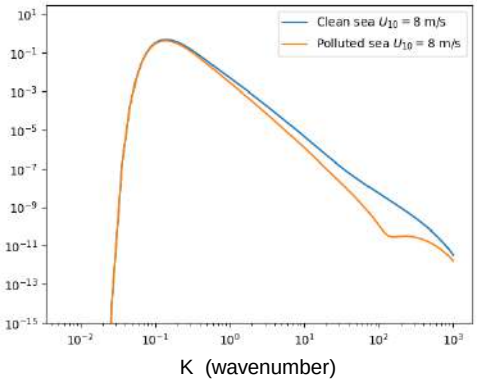

Figure 3: Computed clean and polluted sea spectrum for $U_{10} = 8$ m/s in a Log/Log scale.

One can see that the pollutant affects mainly the capillary waves, even if the maximum is reduced a little.

Using, the polluted sea spectrum S_{po}, we can use the same stochastic method to generate oil-covered sea surfaces. For a wind speed of 8 m/s, an example of the computed clean and polluted sea surface is given in Figure 4.

It should be noted that, as expected [4], the pollutant decreases the waves extremum.

3. The computational method

In this section, we describe the hybrid wavelet-based scheme proposed to solve the PWE (1), while accounting

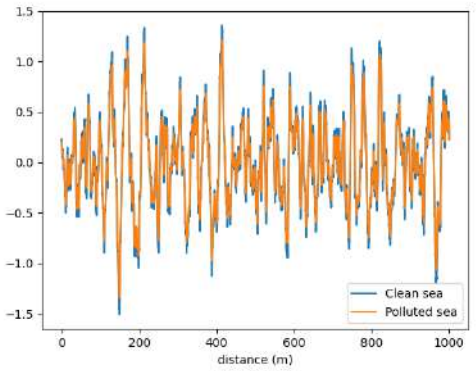

Figure 4: Generated random clean and polluted sea surface for $U_{10} = 8$ m/s.

for refraction, relief (sea surface), and ground composition.

3.1. Discretization

We denote by x_{max} and z_{max} the size of the computational domain Ω. The source is placed at $x = 0$ and we assume the field at $x = 0$ to be known. Thus, we have $\Omega = [0, x_{max}] \times [0, z_{max}]$, since the propagation above the ground is studied. For numerical reasons, Ω is discretized along z and x with N_z and N_x the number of discrete points along each direction. The mesh size is thus given by

$$\Delta z = z_{max}/N_z$$
$$\Delta x = x_{max}/N_x$$

Finally, we denote by u_x the reduced field discretized along z at position x.

3.2. An overview of split-step wavelet

In this article, the PWE is solved using the efficient iterative split-step wavelet method (SSW) [16, 17].

This latter allows computing the field marching in one distances by going back and forth in the wavelet and spatial domain. A step of propagation is thus split into two parts. First, the field is propagated in free space in the wavelet domain. Second, the effect of the refraction, the relief, and the ground composition are taken into account in the spatial domain. A step from x to $x + \Delta x$ can thus be summed up as follows

$$u_{x+\Delta x} = \mathcal{R}\mathcal{L}\mathcal{W}^{-1}\mathcal{P}_{\mathcal{C}_{V_s}}\mathcal{W}\, u_x, \qquad (5)$$

where $\mathcal{W}$ is the wavelet transform, $\mathcal{C}_{V_s}$ a compression with hard threshold, $\mathcal{P}$ corresponds to the sparse wavelet-to-wavelet propagation [17], and $\mathcal{R}$ and $\mathcal{L}$ ammount for the relief and phase-screen operators, respectively. The latter allows taking into refraction. For the relief, the staircase model is used [14]. Finally, the ground composition is accounted for through the efficient local image method [16].

To conclude on the computational method for the propagation, SSW is efficient both in terms of memory storage and computation time, with a complexity and a memory footprint lower than the conventional split-step Fourier method [16, 17].

3.3. The hybrid approach

In this section, we describe the hybrid approach [11, 12] to accurately model the effect of the sea (polluted or not) on field propagation.

The idea is that given a spatial discretization N_x of points (or a step Δx), not all the levels of the sea spectrum, S_{clean} or S_{po}, can be accounted for. Thus, we can compute the cut-off parameter K_{max}, due to the discretization, between the large-scale and low-scale waves. This latter is given by

$$K_{max} = N_x \frac{2\pi}{x_{max}}. \qquad (6)$$

Using this cut-off the effect of the sea is introduced with a two-scale model. First, the lowest part of the spectrum, with respect to K_{max}, is used to generate the random sea surfaces, as described in 2.2. Second, the highest part of the spectrum is used to compute a new roughness coefficient [11, 12] to take into account the capillary waves effect. This latter is multiplied by the Fresnel coefficient in the local image method.

Nevertheless, the geometry generation is based on a stochastic process, thus a Monte Carlo method is used to compute the mean of the propagation over N_{MC} cases. Therefore, the efficiency of SSW is very interesting here [12], in particular for large N_{MC}.

4. Numerical experiments

The objective of this section is twofold. First, we test that the method works well in different scenarios. Second, a PCA analysis is performed on the constructed database to obtain insights into the pollutant effect.

All the tests are performed in the S-band, at 3 GHz, in a domain of size $x_{max} = 5$ km and $z_{max} = 128$ m. The discretization steps are set to $\Delta x = 50$ m and $\Delta z = 0.05$ m. We also consider a surface duct, as it is frequent above the sea. A complex source point (CSP) placed at $x_s = -50$ m and $z_s = 20$ m with a width of 3 m is considered as the source. Finally, we use the following dielectric constant for the sea (resp. the oil): $\varepsilon_r = 70$ (resp. $\varepsilon_r = 2.2$) and $\sigma = 5$ S/m (resp. $\sigma = 0.0017$ S/m).

4.1. Field propagation results

In this first part, we consider two different pollutants, one with an elasticity $E_0 = 9$ mN/m and a characteristic pulsation $\omega_D = 6$ rad/s, while the other has an elasticity of 25 mN/m and a characteristic pulsation of 10 rad/s.

First, a test with a wind speed of 5 m/s, where with the given parameters, the ground is considered flat. This allows a comparison with the results of [8]. In Figure 5, we plot the field obtained with SSW, with a zoom between 0 and 56 m in altitude, at the last iteration for a clean sea and when both pollutants are considered.

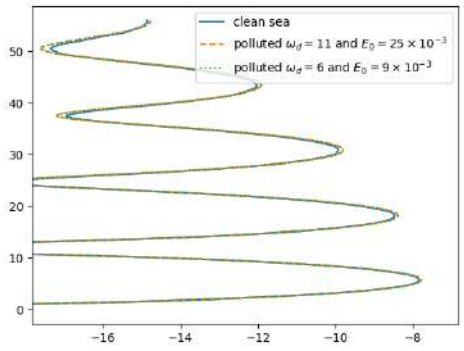

Figure 5: Field at $x = 5$ km computed with SSW for the propagation above a clean and polluted sea.

In Figure 5, one can see the effect of the pollutant on the measured electromagnetic Þeld. Indeed, the extrema are changed when an oil Þlm is considered, as expected since the ground composition is not the same. These results are in line with the one obtained in [8]. In this case, detection seems easy. Nonetheless, it should be recalled that at this wind speed, the sea is considered ßat, and one can wonder what happens with a higher U_{10} increasing, and waves appearing.

Therefore, we choose to do the same test, with $U_{10} = 7$ m/s. In this case, since the sea surface is not ßat, the mean over the 20 Monte-Carlo simulation of the Þeld computed with SSW at the last iteration is plotted in Figure 6.

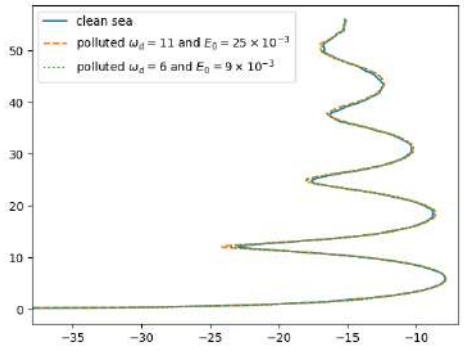

Figure 6: Field at $x = 5$ km computed with SSW for the propagation above a clean and polluted sea when $U_{10} = 7$ m/s.

In this case, we can still see the effect of the oil Þlm but it is less clear than when $U_{10} = 5$ m/s, even if all the area is covered by the pollutant (i.e. $F = 1$). This difference is due to the surface geometry, which is not ßat anymore. Note that in different cases (i.e. other surface generation), the detection can be easier or on the contrary more difÞcult. This is why we decide using a PCA analysis.

4.2. PCA analysis

Here, the goal of the PCA analysis is to obtain features that can help to detect a polluted sea surface. This method has been used in another context in electromagnetic where stochastic processes are studied, see [18].

Given the task, we still study the three cases (clean and polluted sea, with two different pollutants) for different wind speeds. Therefore, we constructed one database per U_{10} as follows. This latter is composed of 100 features per case, thus we have a total of 300 features. These latter shall represent the Þeld propagation as precisely as possible. Therefore, each feature consists of the mean of the computed Þeld at the last iteration over 20 Monte-Carlo simulations, to take into account the stochastic aspect of the surface. Example of these features are given in Section 4.1 for $U_{10} = 5$ m/s and 7 m/s.

Then, a PCA with a given number of 3 components is performed on each dataset. The goal is to Þnd one (or multiple) directions that describe the effect of the pollutant on propagation.

In Figure 7, we plot the transformed features over the Þrst two components of the PCA decomposition. Here, the wind speed is 5 m/s. Note that label 0 is for a clean sea while labels 1 and 2 correspond to the two pollutants with $E_0 = 9$ mN/m and $\omega_D = 6$ rad/s, and $E_0 = 25$ mN/m and $\omega_D = 11$ rad/s, respectively.

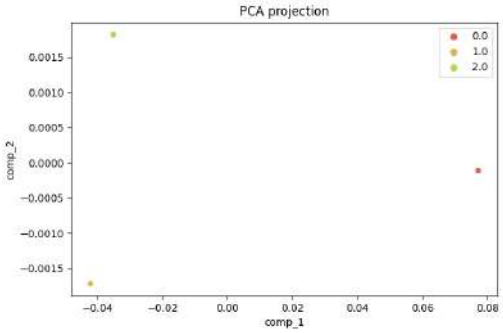

Figure 7: Features transformed onto the PCA components plotted for the Þrst two components when $U_{10} = 5$ m/s.

As expected, the three cases are fully separated, and detection is easy (using for example a logistic regression). Besides, since at this wind speed, the sea surface is ßat, all the features for each case are the same. Nevertheless, we can see that the Þrst axis here seems to relate to how close to a clean sea we are.

Therefore, the same analysis is now performed at $U_{10} = 7$ m/s. As before, we plot the transformed features over the two Þrst components of the PCA analysis in Figure 8. The labels remain the same.

In this case, since the surface is not ßat anymore, many points are plotted for each label depicting the features in the Þrst two components' axis. Nonetheless, one can see that the three cases are still separated leading to an easy

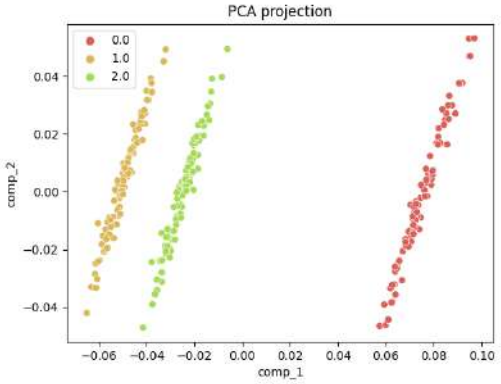

Figure 8: Features transformed onto the PCA components plotted for the Þrst two components when $U_{10} = 7$ m/s.

detection here. Besides, as before, the Þrst axis seems to refer to how close to a clean sea we are.

Other tests have been performed for wind speed upper than $U_{10} = 8$ m/s, upper than the limit for insoluble oil Þlm, and at these speeds, no separation was achieved. This is due to the dominant inßuence of the sea geometry on the electromagnetic Þeld at these U_{10}.

5. Conclusion

In this article, we studied the tropospheric propagation of the electromagnetic Þeld above a polluted sea.

The propagation model is based on a hybrid approach where the sea spectrum or its damped version to take into account the pollutant, is used to generate random surfaces and to compute a roughness factor.

A wavelet-based computational scheme is used since its efÞciency allows fast Monte Carlo simulations. Besides, we constructed a database for different wind speeds to obtain features that help to detect an oil leakage based on electromagnetic measurements.

A PCA analysis, with 3 components, has been performed on these databases, showing that the polluted and clean sea can be detected when the wind speed is below a limit of 8 m/s. Besides, we saw that the Þrst axis of the PCA decomposition could refer to how close we are to a clean see.

Thus, we are currently working on the case where the sea is not fully covered by the pollutant, i.e. $F < 1$. In this case, a new model shall introduce the position of the oil leakage. The same analysis could then be performed to assess the limit of detection. Finally, we are also working on the case where we have an emulsion of oil and water, and when a Þlm and an emulsion are considered.

References

[1] P. P. Lombardini, B. Fiscella, P. Trivero, C. Cappa, and W. Garrett, ÒModulation of the spectra of short gravity waves by sea surface Þlms: slick detection and characterization with a microwave probe,Ó Journal of Atmospheric and Oceanic Technology, vol. 6, no. 6, pp. 882Ð890, 1989.

[2] H. Zheng, Y. Zhang, A. Khenchaf, Y. Wang, H. Ghanmi, and C. Zhao, ÒInvestigation of EM backscattering from slick-free and slick-covered sea surfaces using the SSA-2 and SAR images,Ó Remote Sensing, vol. 10, no. 12, p. 1931, 2018.

[3] H. Zheng, J. Zhang, A. Khenchaf, and X.-M. Li, ÒStudy on non-Bragg microwave backscattering from sea surface covered with and without oil Þlm at moderate incidence angles,Ó Remote Sensing, vol. 13, no. 13, p. 2443, 2021.

[4] H. Ghanmi, A. Khenchaf, and F. Comblet, ÒNumerical modeling of electromagnetic scattering from sea surface covered by oil,Ó Journal of Electromagnetic Analysis and Applications, vol. 2014, 2014.

[5] C.-H. Qi and Z.-Q. Zhao, ÒElectromagnetic scattering and statistic analysis of clutter from oil contaminated sea surface,Ó Radioengineering, vol. 24, no. 1, pp. 87Ð92, 2015.

[6] T.-H. Kim, C.-S. Yang, and K. Ouchi, ÒAccuracy improvement of the radar backscatter simulation from sea surface covered by oil slick using fetch-dependent waveheight spectrum: Comparison with the 2007 Heibei Spirit Case in the Yellow Sea,Ó Ocean Science Journal, vol. 51, pp. 235Ð249, 2016.

[7] H. Ghanmi, A. Khenchaf, and F. Comblet, ÒElectromagnetic characterization of a polluted maritime surface,Ó in 2018 4th International Conference on Advanced Technologies for Signal and Image Processing (ATSIP), pp. 1Ð6, IEEE, 2018.

[8] N. Pinel, C. Bourlier, and J. Saillard, ÒForward radar propagation over oil slicks on sea surfaces using the ament model with shadowing effect,Ó Progress In Electromagnetics Research, vol. 76, pp. 95Ð126, 2007.

[9] M. Cui, H. Cha, and B. Tian, ÒA propagation model for rough sea surface conditions using the parabolic equation with the shadowing effect,Ó The Applied Computational Electromagnetics Society Journal (ACES), pp. 683Ð689, 2018.

[10] W. Ament, ÒToward a theory of reßection by a rough surface,Ó Proceedings of the IRE, vol. 41, no. 1, pp. 142Ð146, 1953.

[11] O. Benhmammouch, A. Khenchaf, and N. Caouren, ÒModelling roughness effects on propagation of electromagnetic waves in a maritime environment: A hybrid approach,Ó IET radar, sonar & navigation, vol. 5, no. 9, pp. 1018Ð1025, 2011.

[12] T. Bonnafont, O. Benhmammouch, and A. Khenchaf, ÒA two-way split-step wavelet scheme for tropospheric long-range propagation in various environments,Ó*Remote Sensing*, vol. 14, no. 11, p. 2686, 2022.

[13] T. Elfouhaily, B. Chapron, K. Katsaros, and D. Vandemark, ÒA uniÞed directional spectrum for long and short wind-driven waves,Ó*Journal of Geophysical Research: Oceans*, vol. 102, no. C7, pp. 15781Ð15796, 1997.

[14] M. Levy, *Parabolic equation methods for electromagnetic wave propagation*, No. 45, IET, 2000.

[15] O. Ozgun, ÒRecursive two-way parabolic equation approach for modeling terrain effects in tropospheric propagation,Ó*IEEE Transactions on Antennas and Propagation*, vol. 57, no. 9, pp. 2706Ð2714, 2009.

[16] H. Zhou, R. Douvenot, and A. Chabory, ÒModeling the long-range wave propagation by a split-step wavelet method,Ó*Journal of Computational Physics*, vol. 402, p. 109042, 2020.

[17] T. Bonnafont, R. Douvenot, and A. Chabory, ÒA local split-step wavelet method for the long range propagation simulation in 2D,Ó*Radio science*, vol. 56, no. 2, pp. 1Ð11, 2021.

[18] M. Haider, J. A. Russer, A. Baev, Y. Kuznetsov, and P. Russer, ÒPrincipal component analysis applied in modeling of stochastic electromagnetic Þeld propagation,Ó in*Proceedings of the European Microwave Conference (EuMC), EuMC19–2*017.

Higher-order Modes by Misalignment in Transition from Hollow Metallic Waveguides to Dielectric Waveguides

N. Xenidis[1*], S. Smirnova[1], J. Oberhammer[1] and D. Lioubtchenko[1,2]

[1]Division of Micro and Nanosystems, KTH Royal Institute of Technology, Sweden
[2]CENTERA Laboratories, Institute of High Pressure Physics PAS, Poland
[*]corresponding author: xenidis@kth.se

Abstract: In this work, we report the effects of misalignment between a dielectric waveguide and a hollow metallic waveguide in the WR-10 band. The results indicate the excitation of unwanted higher-order modes in the dielectric waveguide that are expected to degrade the performance, especially at higher frequencies.

Dielectric waveguides are a promising guiding structure for THz and sub-THz systems, owing to their low losses and fabrication simplicity. Several platforms to ease integration with standard measurement equipment have been developed, such as effective medium cladded waveguides[1] and cladded dielectric waveguides.[2] However, most dielectric waveguides are excited by a tapered transition structure inserted into a hollow metallic waveguide[3-5]. The manual insertion of the dielectric waveguide into the hollow waveguide can be a source of losses in case of misalignments. If the taper of the dielectric waveguide is not centered in the hollow waveguide, undesired higher order modes will be excited, an effect especially pronounced at higher frequencies. Fig. 1 shows different kinds of misalignments between a tapered dielectric rod waveguide (DRW) and a hollow metallic waveguide.

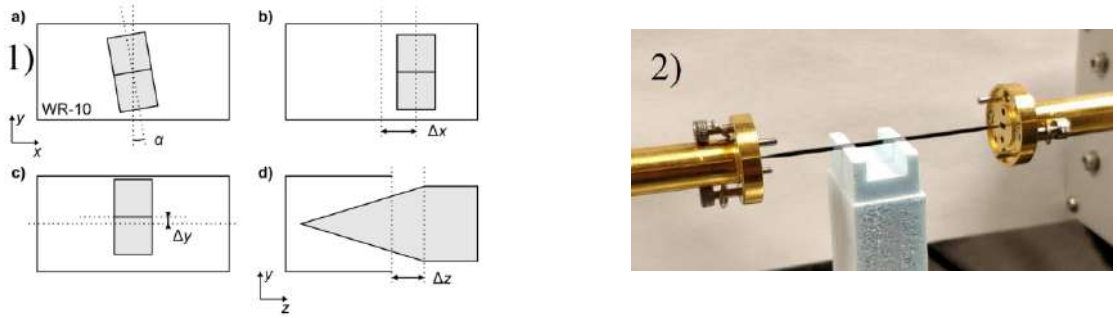

) L J X U H F K H P D W L F R I V P L V D O L J Q P H Q W H U U R U V L Q W K H W U D Q V L W L R Q U H J L R Q E H W Z H H Q Z D Y H J X L G H R X W O L Q H U H F W D Q J X O D U Z D Y H J X L G H D Q G K R O O R Z P H W D O O L F Z D Y H J X L G H D [L V D Q G \ ] D [L V U H V S H F W L Y H O \ ) L J X U H D V X U H P H Q W V H W X

A P Silicon DRW with cross section of 1 P P by 0.5 P P Q G D P W D S H U S L Q Q W K L F N Q H V V O D W H G L Q & 6 7 0 L F U R Z D Y H G 6 W U X F W X U H E X L O W E \ d e e p r e a c t i v e i o n Z D I H U etching. A WR * +] K R O O R Z P H W D O R S H U D W L Q J P R G H Z D V X V H G W R F R Q Q H F W W K H ' 5 : Z K L F K L G H D O O \ S H U I R U P V W K H V L P X O D W L R Q Z L W K O R Z P H W D O O R V V H V D Q G G L V S H U V L R Q L Q W K H V H W X S V W U X F W X U H W R F R Q W D L Q W K H P H W D O E R [D Q G S U R S H U O \ D O L J Q W K H W D S H U H G V H F W L R Q R I W K H ' 5 :) L J V K R Z V W K H V L P X O D W H G W U D Q V P L V V L R Q D Q G U H I O H F W D Q F H R I W K H W U D Q V L W L R Q U H J L R Q E H W Z H H Q W K H W D S H U H G ' 5 : D Q G W K H P H W D O O L F Z D Y H J X L G H D [L V D Q G \ ] D [L V U H V S H F W L Y H O \ W K H V H W X S V W U X F W X U H W R F R Q W D L Q W K H P H W D O E R [D Q G S U R S H U O \ D O L J Q W K H W D S H U H G V H F W L R Q R I W K H ' 5 :

Fig. shows the measured results, after TRL calibration at the metallic waveguide flanges and time gating.
, Q V H U W L R Q L Q W H U R H D V X U H H D W X S * H D Q R S W R G % D W ä / L W + W O H U P S D F
U H I O H F W L R Q O R V V L V R E V H U Y H G H V H Q W L D O I R U D F F X U D W H F D O L E U D W L R Q D Q G W K H U H O D W L Y H P H D V X U H P H Q W X Q F H U W D L Q W L H V R I W K H W H V W I L [W X U H D U H O R Z H U W K D Q G % L Q W K H P
O R Z H U I U H T X H Q F L H V G X H W R W K H P H W D O O L F Z D Y H J X L G H I O D Q J H V D Q G W K H H [S H U L P H Q W D O V X S S R U W R I P \ I D E I R U S U R Y L V L R Q L Q J R I I D F L O L W L H V D Q G H [S H U L P H Q W D O V X S S R U W R I P \ I D E L V I X Q G H G E \ W K H 6 Z H G L V K 5 H V H D U F K & R X Q F L O D V D Q D W L R Q D O U H V H D U F K L Q I U D V W U X F W X U H 7 K H Z R U N Z D V V X S S R U W H G E \ W K H (X U R S H D Q 8 Q L R Q ' V
+ R U L] R Q 2 S H Q I X Q G 3 5 2 - (& 7 7 (5 $ P H D V X U H P H Q W D J U H H P H Q W 1 R

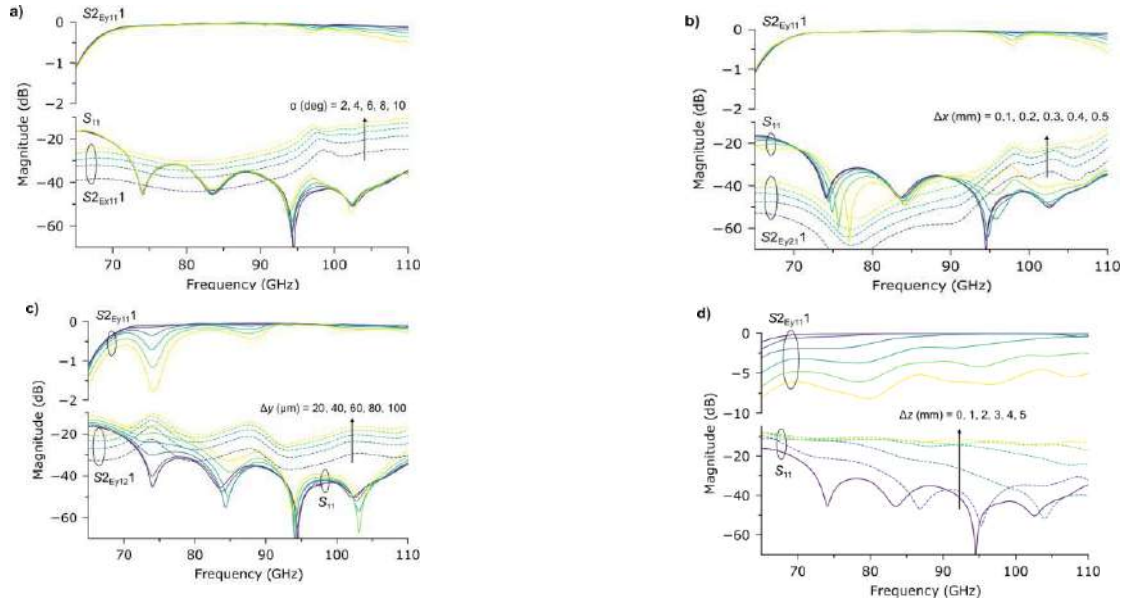

) L J X U H 6 L P X O D W H G 6 3 D U D P H W H U R Y H U W K H R S H U D W L Q J I U H T X H Q F \ U D Q J H R I W K H P H W D O O L F Z D Y H J X L G H I O D Q J H V D Q G W K H H [S H U L P H Q W D O V X S S R U W R I P \ I D E L V I X Q G H G E \ W K H (X U R S H D Q 8 Q L R Q ' V + R U L] R Q 2 S H Q I X Q G 3 5 2 - (& 7 7 (5 $ P H D V X U H P H Q W D J U H H P H Q W 1 R

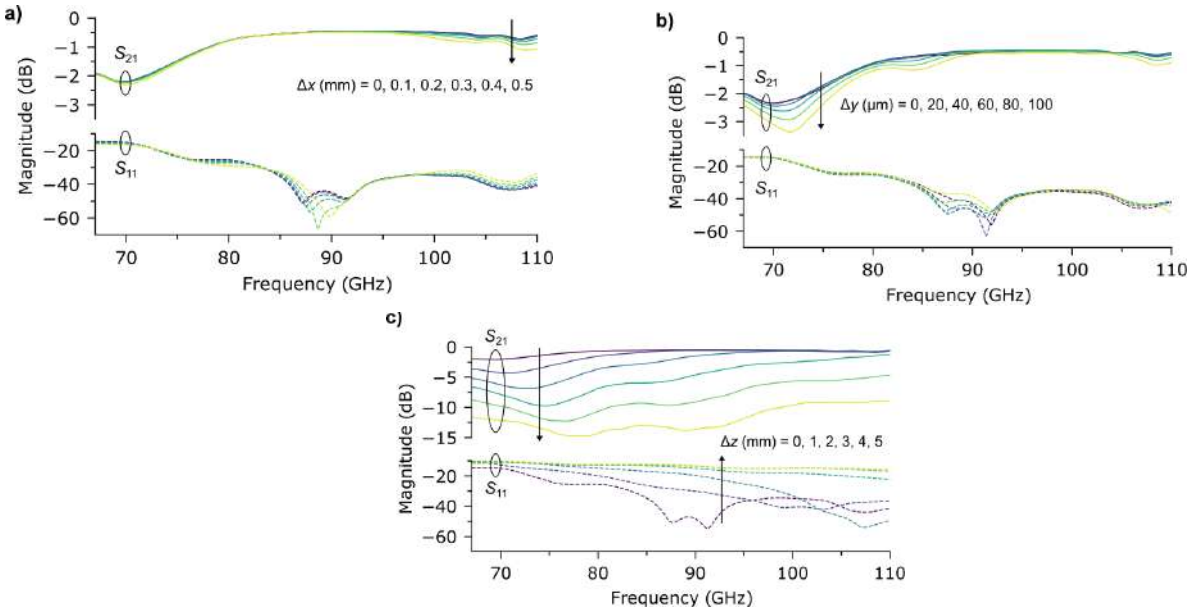

) L J X U H 6 H H D V X U H P H Q W U H V X O W V R I W K H ' 5 : ± : 5 W U D Q V P L W W L Q J I U H T X H Q F \ U H V S H F W L Y H O \

We acknowledge Myfab for provisioning of facilities and experimental support. Myfab is funded by the Swedish Research Council as a national research infrastructure. The work was supported by the European Union's Horizon 2020 FET Open project TERAmeasurand (grant agreement No 862788).